CHEMICAL FINGERPRINTING OF NAPHTHENIC ACIDS BY GC×GC/MS

CHEMICAL FINGERPRINTING OF NAPHTHENIC ACIDS BY COMPREHENSIVE TWO-DIMENSIONAL GAS CHROMATOGRAPHY MASS SPECTROMETRY AT RECLAMATION SITES IN THE ALBERTA OIL SANDS

By: DAVID THOMAS BOWMAN, B.Sc.

A Thesis Submitted to the School of Graduate Studies in Partial Fulfillment of the Requirements for the Degree Doctor of Philosophy

McMaster University

Doctor of Philosophy (2017) McMaster University

Chemistry and Chemical Biology Hamilton, Ontario

TITLE: Chemical fingerprinting of naphthenic acids by comprehensive two-dimensional gas chromatography mass spectrometry at reclamation sites in the Alberta Oil Sands.

AUTHOR: David T. Bowman, B.Sc. (McMaster University)

SUPERVISORS: Prof. Gregory F. Slater
Prof. Brian E. McCarry

NUMBER OF PAGES: xviii, 197

Abstract

The processing of bitumen in the Athabasca oil sands region (AOSR) produces extensive volumes of oil sands process-affected water (OSPW) and tailings, which are stored within tailings ponds and settling basins to promote the consolidation of solids and the recycling of water. Oil sands operators are actively investigating dry and wet reclamation strategies in order to reduce their inventory of tailings and return disturbed land back to its original state. An important component of the reclamation of tailings is understanding the environmental fate of naphthenic acids (NAs), which are considered the most toxic constituents of OSPW and tailings. However, since NAs exist as a complex mixture comprised of thousands of compounds from dozens of chemical classes, the characterization of NAs within environmental samples poses significant challenges to analytical chemists.

This dissertation is focused on the characterization of naphthenic acids by comprehensive two-dimensional gas chromatography coupled to mass spectrometry (GC×GC/MS). GC×GC/MS offers unparalleled chromatographic separation and peak capacity and has been used in recent years to resolve individual constituents within complex mixtures, including structural isomers. Since the biodegradation and toxicity of NAs is structure-specific and can vary between structural isomers, the profiling of individual NAs by GC×GC/MS is expected to enhance the monitoring of NAs within environmental samples impacted by oil sands activity. In this thesis, GC×GC coupled with time-of-flight mass spectrometry (TOFMS) was used to structurally elucidate a number of 'unknown' classical and sulfur-containing naphthenic acids by interpretation of their electron ionization (EI) mass spectra and, if available, confirmed by comparison with the spectra of references standards. GC×GC/TOFMS was also utilized as a fingerprinting tool to assess the temporal and spatial variability at two reclamation sites in the AOSR: Syncrude's Sandhill Fen reclamation site and Base Mine Lake. Lastly, a methodology was developed which coupled GC×GC with a high resolution quadrupole time-of-flight mass spectrometer (QTOFMS) for the improved profiling of NAs. GC×GC/QTOFMS is advantageous for the monitoring of NAs since it can provide useful fingerprints via isomer distributions, differentiate NAs from several chemical classes, and provide a global overview of the elemental compositions (assigned by mass accuracy) within NA mixtures.

Acknowledgements

First, I would like to thank Drs. Valbona Celo and Ewa Dabek-Zlotorzynska for my tenure as a summer student in the AAQS laboratories at Environment Canada in 2010, and for introducing me to Environmental-Analytical Chemistry. Valbona: Thank you for your mentorship and for the encouragement to pursue graduate studies following my B.Sc.

I would like to express gratitude to my supervisors, the late Dr. Brian E. McCarry (1946-2013) and Dr. Greg F. Slater. Brian: Thank you for the opportunity to join your research group. Your patience and teachings during the early days were critical to my development as an analytical chemist. Greg: Thank you for welcoming me into your lab in 2013, and for your mentorship and guidance during my studies. You not only facilitated the completion of my thesis, but also improved many aspects of it.

I would like to thank my Ph.D. supervisory committee members, Drs. Phillip Britz-McKibbin, Lesley Warren, and Kirk Green, for their valuable advice and input throughout my studies. My appreciation goes to my collaborators from the Warren lab (Tara, Michelle, Kate, Daniel, Patrick, and Florent), who contributed to my thesis by collecting samples from Sandhill Fen and Base Mine Lake. Thank you to my collaborators at the Ontario Ministry of Environment and Climate Change, Drs. Karl Jobst, Eric Reiner, and Xavier Ortiz, for the opportunities you have provided me to learn and develop as a scientist. Karl: A special thank you for your help and guidance throughout our collaboration. I would also like to thank Dr. Johan K. Terlouw for the insightful discussions regarding electron ionization mass spectrometry and for generously contributing to the edits of my first manuscript. Your critiques during our editing sessions were most valuable and significantly improved my skills in scientific writing.

To the members of the McCarry research group: Fan Fei, Sujan Fernando, Ashraf Ibrahim, Ken Chalcraft, Vi Dang, Paul Hodgson, and Roger Luckham. Thank you for your friendship over the years and for all the good times at the Phoenix, West End pub, and Mr Gao. Sujan: Thank you for your assistance and training when I first joined the group, and Fan: Thank you for lending an ear to listen to my (many) updates over the years, and for our useful discussions on multivariate statistics. I would also like to thank the members of the Environmental Organic Geochemistry group, whom I have had the pleasure to spend time with over the past few years: Kelly Martin, Corey Goad, Allyson Brady, Samantha Clay, Lauren Bradford, Caitlin Smal, Mark Belan, Sian Ford, and Mohamed El-Waraky. A special thank you to Jennie Kirby for all of your help and support over the years.

Finally, I would like to thank my parents, Rick and Irene, and my siblings, Matthew and Jacqueline, who have been extremely supportive during my studies. And to Jenn, thank you for your unwavering love and support.

Preface

This thesis consists of two published manuscripts (Chapters Two and Five), one manuscript that has been submitted to a peer-reviewed scientific journal (Chapter Three), and one unpublished manuscript (Chapter Four). Chapters Two, Three, and Four were in collaboration with Dr. Lesley Warren from School of Geography and Earth Sciences at McMaster University. Chapter Five was in collaboration with Dr. Lesley Warren from School of Geography and Earth Sciences at McMaster University, and Drs. Karl J. Jobst, Xavier Ortiz, Eric J. Reiner from Ontario Ministry of the Environment and Climate Change. All chapters were written by David T. Bowman, with editorial comments by Drs. Greg F. Slater, Lesley A. Warren, Karl J. Jobst, Xavier Ortiz, and Johan K. Terlouw.

Table of Contents

List of Figures

Chapter One:

Chapter Two:

Chapter Three:

List of Tables

Chapter Three:

Chapter Four:

List of Abbreviations

AEOs	Acid extractable organics
ANOVA	Analysis of variance
AOSR	Athabasca oil sands region
APCI	Atmospheric pressure chemical ionization
APPI	Atmospheric pressure photoionization
BML	Base Mine Lake
CI-CH_4	Chemical ionization with methane
CI-NH_3	Chemical ionization with ammonia
CT	Composite tailings
DBE	Double bond equivalence
EI	Electron ionization
EIC	Extracted ion chromatogram
EPL	End pit lake
ESI	Electrospray ionization
FFT	Fluid fine tailings
FTICR-MS	Fourier transform ion cyclotron mass spectrometry
FT-IR	Fourier transform infrared spectroscopy
FWHM	Full width half maximum
GC	Gas chromatography
GC×GC	Comprehensive two-dimensional gas chromatography
HCA	Hierarchical cluster analysis
HPLC	High performance liquid chromatography
HRMS	High resolution mass spectrometry
HRMS	High resolution mass spectrometry
IDL	Instrumental detection limit
IUPAC	International Union of Pure and Applied Chemistry
KMD	Kendrick mass defect
LRMS	Low resolution mass spectrometry
m/z	mass to charge ratio
MDL	Method detection limit
MS	Mass spectrometry
MS/MS	Tandem mass spectrometry
NA	Naphthenic acids
NAFC	Naphthenic acid fraction compounds
OSPW	Oil sands process-affected water
PAH	Polycyclic aromatic hydrocarbon
PCA	Principal component analysis
QTOFMS	Quadrupole time-of-flight mass spectrometry
RTs	Retention times
SAGD	Steam assisted gravity drainage
SFC	Supercritical fluid chromatography
SIC	Selected ion chromatogram
SRB	Sulfate reducing bacteria
*t*BDMS	*tert*-buytldimethylsilyl

TIC	Total ion current
TMS	Trimethyl silyl
TOFMS	Time-of-flight mass spectrometry
UCM	Unresolved complex mixture

Chapter One: Introduction

1.1 Oil sands overview

The Alberta oil sands represent the third largest oil reserve in the world and are estimated to contain 1.7 trillion barrels of oil. Bitumen is extracted from oil sands ore by two main processes: (a) surface mining of oil sands ore followed by caustic warm water extraction, and (b) Steam-assisted gravity drainage (SAGD). The total production of oil from both extraction processes is reported to be 2.3 million barrels per day.[1] A by-product of bitumen extraction processes is the production of large volumes of tailings. It has been demonstrated that the aqueous component of tailings, oil sands process-affected water (OSPW), has shown acute and chronic toxicity towards a variety of aquatic organisms, primarily due to a collection of persistent organic acids known as naphthenic acids (NAs).[2] Alberta's oil sands operators do not yet have approval to release treated tailings back to the environment, and therefore, all tailings-derived materials are stored on-site in tailing ponds or settling basins. In 2013, the total area occupied by tailing ponds and other containment structures was 220 km^2.[1] Following deposition within tailings ponds, the coarse solid particles within tailings settle quickly, and the fines fraction consolidates slowly to form fluid fine tailings (FFT; approximately 25 – 35 % w/w solids). The consolidation of fluid fine tailings within tailing ponds is a very slow process, reported to take between 125 – 150 years.[3] In 2013, the total volume of FFT held by mine operators in Canada was reported to be 975.6 million m^3.[1] As stated in their licensing agreement with the Government of Alberta, oil sands operators must reclaim tailings ponds, and other disturbed lands, back to self-sustaining ecosystems.[4] As a result, oil sands operators are actively researching reclamation strategies to reduce their inventory of tailings material. However, an important component of successful reclamation is understanding the source, cycling, and fate of toxic components, such as naphthenic acids, within the environmental systems.

1.2 Introduction to naphthenic acids

NAs are a complex mixture of polar organic carboxylic acids which occur naturally in petroleum and oil sands bitumen deposits. NAs accumulate within OSPW during the processing of bitumen.[4] NAs are of environmental interest because they have been linked with the acute and chronic toxicity of OSPW[2,5,6] and are known to persist within tailing ponds and other reclamation sites. Since NAs are soluble in water as salts (naphthenates), they have the potential to migrate beyond containment structures and enter the greater environment.[7–9] However, it has also been established that NAs may enter surface waters by natural processes, such as the erosion of bitumen deposits near river banks[2]. Therefore, a comprehensive understanding of NA

compositions (derived from both industrial and natural sources) is required in order to improve the specificity of methods that aim to monitor OSPW-derived NAs and differentiate sources.

According to the classical definition, NAs are a complex mixture of alkyl-substituted acyclic and cycloaliphatic carboxylic acids, with the general empirical formula: $C_nH_{2n+Z}O_2$ (where n = carbon number, Z = degree of unsaturation via ring formation). The general structures of classical NAs are presented in Figure 1. However, it is now known that the classical definition does not accurately describe the total fraction of acid-extractable organics (AEOs) within OSPW. Studies using ultrahigh resolution mass spectrometry have revealed that, in addition to classical NAs, OSPW also contains chemical species which possess sulfur and/or nitrogen heteroatoms, additional oxygen-containing substituents, and aromatic rings.[10–13] OSPW samples typically contain thousands of organic compounds, with elemental compositions belonging to dozens of chemical classes. For each chemical class, compounds possess a range of double bond equivalents (DBEs) and carbon numbers. In addition, for a given elemental composition, a large number of structural isomers may exist, as demonstrated in recent studies utilizing multidimensional chromatography[14–16]. Due to the extreme complexity of OSPW, the identities of many individual components within the mixture, particularly those linked with toxicity, are unknown.

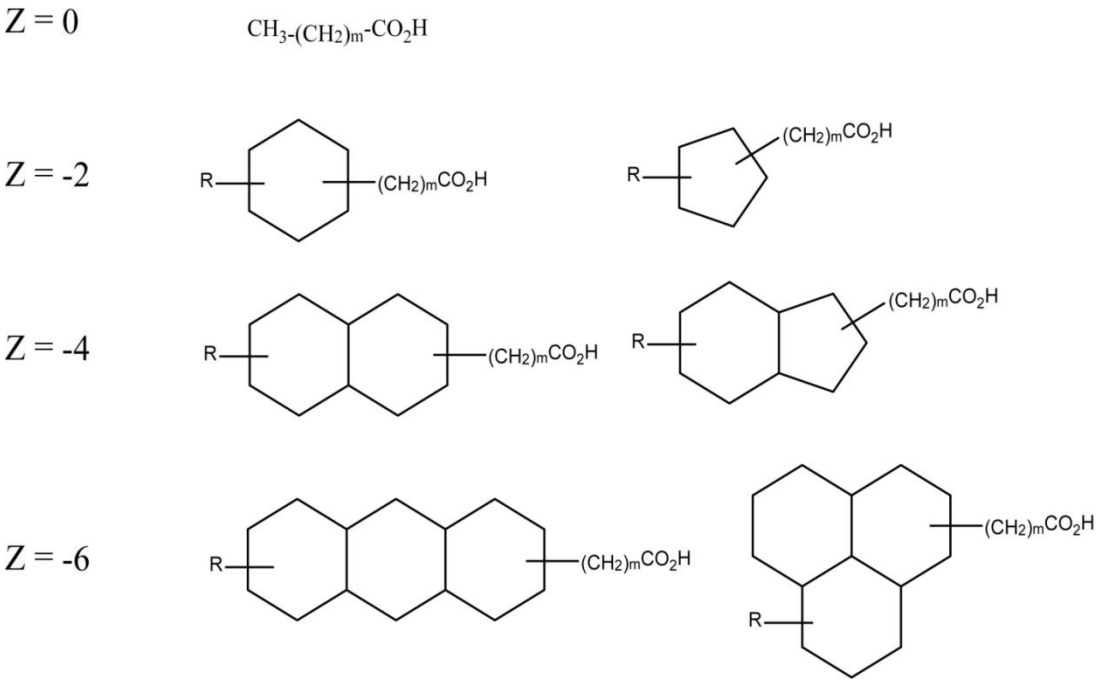

Figure 1 General structures of classical naphthenic acids ($C_nH_{2n+Z}O_2$, where n = carbon number, Z = degree of unsaturation via ring formation) for various Z-values. R represents alkyl side chains, and m represents the length of the side chain attached to the carboxylic acid group.

The composition of NA mixtures within OSPW have been shown to be heterogeneous and can vary due to local differences within bitumen deposits, bitumen extraction processes (surface mining vs SAGD)[17], oil sands producers[18] (e.g. Syncrude vs Suncor), and age of the tailings pond[19]. Furthermore, within a single tailings pond, NA profiles can vary based on depth, wind patterns, and proximity to tailings discharge points.[20] The heterogeneity of OSPW samples, in combination with the extreme complexity of NA mixtures and the sheer number of structurally similar compounds, contributes to the difficulty of monitoring NAs, differentiating sources, demonstrating biodegradation, and identifying toxic components within such mixtures.

1.3 Toxicity and biodegradation of naphthenic acids

Naphthenic acids are toxic to a variety of organisms, such as fish[21–23], plants[24], mammals[25], phytoplanktons[26,27], and amphibians[28]. Narcosis is believed to be the primary mode of acute toxicity from NAs, stemming from their surfactant characteristics. Narcosis is a non-specific mode of action, where a hydrophobic compound enters the lipid bilayer of the cell membrane causing disruption and the degradation of cell membranes.[29,30] In addition, OSPW has been reported to cause endocrine disruption; Thomas *et al.* demonstrated that NAs are weak estrogenic receptor agonists and potent androgen receptor antagonists.[31]

Due to the complexity of NA compositions within OSPW and related samples, the identification of toxic NAs has been an on-going challenge. Therefore, in order to reduce the complexity of NA mixtures, and link structure to toxicity, OSPW samples have been subjected to fractionation prior to toxicity tests. This approach, referred to as effect-directed analysis[32], has been successfully applied in a few recent studies to determine the elemental compositions, or identify NA classes, associated with acute toxicity[33,34] and endocrine toxicity[31,35,36]. Classical alicyclic NAs have been strongly associated with the acute toxicity of OSPW[33,34], while oxygenated NAs (O_3 and O_4 chemical class) are negatively correlated[33]. It has been demonstrated that the estrogenicity of OSPW is associated with the aromatic fraction of NA-containing mixtures[35,36]. Rowland *et al.*[37] identified a number of compounds with aromatic steroidal chemical structures using GC×GC/TOFMS, and, due to their structural similarities with estrone and estradiol, the authors suggested that such compounds may contribute to the estrogenic activity of OSPW.

Due to their acute and chronic toxicity, there has been much interest in understanding the degradation of NA mixtures within OSPW. It has been demonstrated in several studies that microbial biodegradation can decrease the acute toxicity of OSPW[5,19,38,39], which suggests that *in situ* biodegradation may be plausible means to remediate tailings and OSPW stored within tailings ponds and other reclamation sites in the Athabasca oil sands region (AOSR). However, it is important to note that a residual, chronic toxicity still remains following microbial

degradation, which has been attributed to the recalcitrant fraction of NA mixtures. Nonetheless, a range of indigenous and non-indigenous bacterial species have been studied to assess their potential to degrade naphthenic acids.[40–45] Alternative remediation treatments (such as ozonation[46–49], oxidation[50], photolysis[51,52], and phytoremediation[11,53,54]) have also been investigated to accelerate the degradation of NAs and remove the residual toxicity which remains in aged OSPW.

Studies on the biodegradation of model (or surrogate) NAs have been useful for elucidating degradation pathways, such as β-oxidation[44,55–59], combined α- and β-oxidation[60], and aromatization pathways[61,62]. Recent studies have revealed that increases in cyclicity and alkyl branching can decrease the biodegradation rates of NAs.[63,64] In addition, it has been shown that structural isomers can display differing levels of susceptibility to degradation.[64,65] The knowledge of NA biodegradation pathways is useful since it can aid in the identification of possible recalcitrant NAs, which is required to help to focus remediation efforts.

The composition of NA mixtures can significantly influence the extent of its degradation. Commercial NA mixtures, which are derived from petroleum, rapidly degrade under aerobic conditions, while OSPW derived NAs degrade much more slowly[41,42,63]. It is believed that the difference in recalcitrance between OSPW and commercial NA mixtures is due to the relatively high degree of alkyl branching of NAs within OSPW, which have accumulated within bitumen deposits over time via *in situ* microbial processing.[63]

1.4 Instrumental Analyses of Naphthenic Acids

1.4.1 Fourier transform infrared (FT-IR) spectroscopy

Historically, the oil sands industry standard for the quantification of naphthenic acids is by Fourier transform infrared (FTIR) spectroscopy. Briefly, extracts containing naphthenic acids are quantified by FTIR by monitoring the absorbance of the monomeric (1743 cm^{-1}) and dimeric (1706 cm^{-1}) forms of the carboxylic acid functional groups. The absorbances are then summed, and quantified by an external calibration curve of a commercial NA technical mixture. However, this technique is not deemed suitable for NA quantitation since it lacks the specificity to distinguish between NAs and other compounds which are present in natural waters and also possess carboxylic acid chemical moieties (e.g. humic acids, fulvic acids, and resin acids). Yen *et al*. demonstrated that quantitation by FT-IR leads to the overestimation of NA concentrations.[66]

1.4.2 – Gas chromatography low resolution mass spectrometry

Gas chromatography coupled to low resolution mass spectrometry (GC/LRMS) has been applied in numerous studies to improve the selectivity of NA analysis and to explore the composition of NA mixtures. NAs from OSPW must be extracted and derivatized prior to separation by GC in order to improve their volatility and chromatographic behavior. Numerous derivatization reagents have been used for NA analysis; the most commonly formed NA derivatives for GC analysis are methyl[67], trimethyl silyl (TMS)[68], and *tert*-butyldimethylsilyl (*t*BDMS) esters[69]. Although NA mixtures typically elute in unresolved complex mixtures (UCM) in the total ion current (TIC) chromatogram, mass spectrometry (MS) allows the ability differentiate NAs based on carbon number and Z-values. However, one dimensional GC generally lacks the peak capacity to resolve structural isomers within NA mixtures.

St John *et al*.[69] developed a method using GC/LRMS (election ionization, EI, mode) to analyze the *t*BDMS ester derivatives of a commercial NA technical mixture. The authors reported the *t*BDMS derivatives were useful in their study since they produced strong [M – 57] base peaks, corresponding to the loss of the *tert*-butyl group from the molecular ion. Based on the assumption that only molecules corresponding to the general NA empirical formula ($C_nH_{2n+Z}O_2$) were present in the sample, the authors reported the percent composition of each ion corresponding to the classical NA definition (n: 10 – 23, Z-value: 0 – 12). This method was later used to discover significant compositional differences between NA profiles within commercial NA mixtures and those within OSPW.[70] Notably, the authors presented the distributions of ions as a three-dimensional graph, with relative ion intensities plotted as a function of carbon number and Z-value. This representation of the data was useful for the generating NA fingerprints, and similar approaches have been performed in subsequent studies to compare NA profiles.[19,71,72] Holowenko *et al*.[19] applied the GC/LRMS method to analyze a suite of nine OSPW samples, and results appeared to link the aging of tailing ponds with the selective biodegradation of lower molecular weight NAs. However, low resolution mass spectrometry is vulnerable to possible interferences from chemical species that possess the same nominal mass as classical NAs[73], and it is now understood that some of the identifications in the previous GC/LRMS method were, in fact, oxygenated NAs (O_3 and O_4 chemical class) misclassified as classical NAs[72,74]. However, GC/LRMS methods remain advantageous due to their wide availability and ease of use, and have been recognized as being valuable for their ability to detect gross compositional differences in NA mixtures.[75]

1.4.3 High performance liquid chromatography coupled to low and high resolution mass spectrometry

High performance liquid chromatography (HPLC) is well suited to the analysis of NAs since it can be used to separate a wide range of analytes, including those which are not amenable to GC analysis (such as non-volatile, thermally labile, high molecular weight, and/or polar compounds). Furthermore, HPLC-based methods generally require shorter analysis times than

GC methods, and can be coupled to a variety of ionization techniques including electrospray ionization (ESI), atmospheric pressure chemical ionization (APCI), and atmospheric pressure photoionization (APPI). HPLC can be used to analyze aqueous samples, thus simplifying sample preparation steps, and it also allows the separation of salts from the sample matrix[76], which reduces ion suppression[77] and the generation of sodium adducts[12] (when subjected to ESI). However, HPLC generally possesses less theoretical plates than GC, and, thus, does not provide sufficient chromatographic resolution to allow the monitoring of specific isomers.

In recent years, modern HPLC/tandem MS (MS/MS) instruments have been used for the development of rapid, quantitative methods for the screening of NAs.[76–80] The aforementioned methods are advantageous since samples received minimal preparation prior to analysis, thus allowing the high throughput analysis of samples. Hindle *et al.*[77] developed the first International Organization for Standardization (ISO) accredited method (ISO17025) using HPLC/QTOF-MS for the quantitative assessment of total classical and oxygenated NAs concentrations (defined with the following empirical formula: $C_nH_{2n+z}O_{2-4}$). Prior to analysis, samples were diluted 1:10 in 50% acetonitrile, 0.1% acetic acid, with no further sample prep. The authors revealed that the response factors of 39 model NAs displayed high variabilities when ionized by ESI, and therefore, the average response factors of classical and oxygenated NAs within commercial NA mixtures was used for the determination of total concentrations within OSPW. Using the Sigma technical NA mixture, a method detection limit of 1 mg/L was obtained. However, the authors demonstrated that when samples were calibrated with two different commercial NA mixtures (Sigma vs Merichem), a 2-fold difference was observed in the total NA concentrations. The authors attributed this to the differences in NA compositions which exist within each commercial mixture. In addition, since the compositions of NAs derived from OSPW vary considerably from those within commercial mixtures, the authors stressed that analyses that quantify NAs using commercial mixtures should be considered semi-quantitative until an OSPW-derived technical mixture is established. Woudney *et al.*[80] developed a novel method for the quantitation of total NAs which used HPLC/MS/MS (positive mode ESI) to analyze naphthenic acids derivatized with *N*-(3-dimethylaminopropyl)-*N*'-ethylcarbodiimide within surface water samples. The method used MS/MS to monitor the presence of a product ion (*m/z* 129) which was characteristic of the derivatization reagent and quantitation was based on a single calibration standard, pyrene-1-butyric acid.

1.4.4 Ultrahigh resolution mass spectrometry

Ultra-high resolution MS (resolving power > 100 000) has significantly improved our understandings of NAs and other AEOs within environmental samples. Fourier transform ion cyclotron mass spectrometry (FTICR-MS) and Orbitrap mass spectrometry (Orbitrap-MS) have been used to characterize NAs within in a variety of environmental samples such as OSPW[81], ground and surface waters[82], plant tissue[83], and crude oils[84,85].

The high resolving power and mass accuracy of ultra-high resolution MS has allowed the unambiguous assignment of elemental compositions to thousands of features within the NA mixtures, revealing the presence of dozens of other compounds classes within OSPW and related samples.[10] However, the interpretation of such large mass spectral datasets can be both difficult and time-consuming. Numerous visualization methods (such as Kendrick mass defect plots, van Krevelen plots, and DBE vs carbon number plots) have been utilized to establish NA fingerprints and investigate trends within samples.[86]

Early studies using ultra-high resolution MS based techniques predominately introduced the sample into the MS by direct infusion (DI). Numerous ionization sources have been used for the analysis of NAs using ultra-high resolution MS, including ESI[81], nanospray-ESI[84], and APPI[12]. DI FTICR-MS and Orbitrap-MS techniques are advantageous since they allow the rapid, routine analyses of NAs, and do not require pre-treatment of samples prior to analysis. However, due to the absence of chromatography, DI-UHRMS techniques cannot distinguish structural isomers. Furthermore, ion suppression can arise due to competing components within the ionization source. Rowland *et al*.[87] demonstrated that offline fractionation by solid phase extraction (SPE) prior to analysis by negative ion mode ESI FTICR-MS could increase the number of unique elemental compositions detected and particularly enhance the characterization of higher molecular weight chemical species within NA mixtures.

The coupling of online chromatographic separation with ultrahigh resolution mass spectrometry detection has been performed in recent years to enhance the characterization of NAs. Ortiz *et al*.[88] and Barrow *et al*.[89] concurrently developed techniques which coupled GC with FTICR-MS for the analysis of methylated NA extracts. The technique developed by Ortiz *et al*.[88] utilized EI and chemical ionization with methane (CI-CH_4) and ammonia (CI-NH_3) as ionization sources, while Barrow *et al*.[89] used APCI. Chromatographic separation was advantageous since it allowed the characterization of compound classes as a function of time. HPLC has also been coupled to both FTICR-MS and Orbitrap-MS[17] for the characterization of NAs in recent studies. However, when NAs were separated by HPLC and GC, structural isomers typically co-elute as a single peak. The chromatographic separation of NAs has been improved by packed column supercritical fluid chromatography (SFC); Pereira and Martin[90] demonstrated that SFC/Orbitrap-MS could partially and fully resolve isobaric chemical species, including classical NAs and unknown sulfur- and nitrogen-containing compounds.

1.4.5 Comprehensive two-dimensional gas chromatography mass spectrometry

Comprehensive two-dimensional gas chromatography coupled to mass spectrometry (GC×GC/MS) offers unparalleled chromatographic resolution and peak capacity, and has been used in recent years to significantly improve the separation of NAs. GC×GC/MS has been used

to analyze NAs within OSPW[14,15,91], composite tailings pore water[16], groundwater[92], petroleum[93], and commercial NA mixtures[91].

1.4.5.1 Fundamentals of GC×GC

The first application of comprehensive two-dimensional gas chromatography was introduced in 1991 by Phillips and Liu.[94] The GC×GC instrument (see Figure 2) is comprised of two columns in succession to separate analytes using orthogonal separation. The primary column is typically long (generally 30–120 m), while the secondary column is shorter (typically ~1 m), ensuring quick second dimension elution. The two columns are connected by a modulator which collects effluent from the first column, focuses it into a narrow plug, and re-injects it onto the second column. The detector records a one-dimensional trace of modulated peaks, which are then transformed and reconstructed into a two-dimensional chromatogram (see Figure 3). In the first dimension, the analytes are generally separated based on boiling point, and with some influence from the stationary phase of the column. The separations by the secondary column are rapid and isothermal, and are based solely on the interactions between the analyte and the stationary phase.

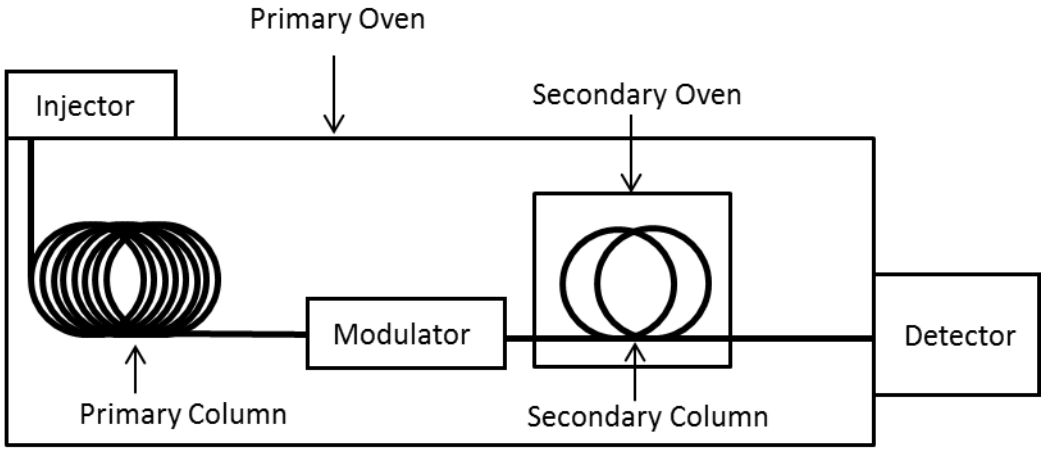

Figure 2. Diagram of GC×GC instrument.

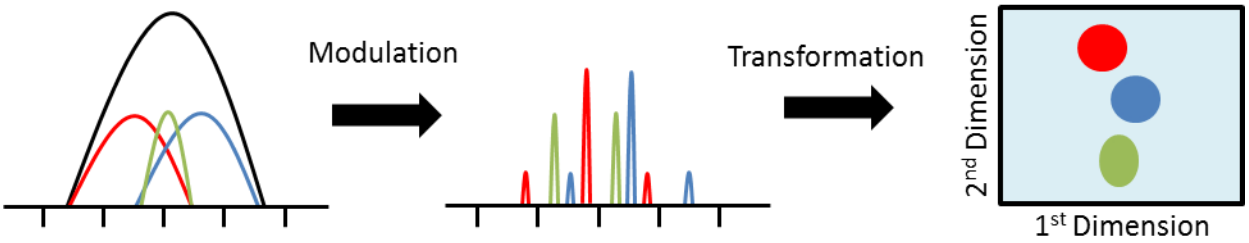

Figure 3. Schematic of the GC×GC separation of 3 co-eluting peaks and the transformation of data into a GC×GC contour plot

There are numerous modulator designs for GC×GC systems[95,96], but the most common is the dual stage quad jet thermal modulator, developed by LECO corporation. This modulator is used in the experiments described in Chapters 2-4. Briefly, the quad-jet modulator consists of two hot air jets and two cold air jets (see Figure 4a). The cold air traps and focuses the effluent from the primary column, while the hot air thermally desorbs the effluent. Another modulator design is the two stage loop-style modulator (see Figure 4b), commercialized by Zoex Corporation, which was used in Chapter 5 of this thesis. In this modulator design, the column is looped twice within a manifold that is in the pathway of a hot and cold jet. The cold jet continuously flows on a portion of the loop to trap and focus effluent, while the hot jet is pulsed at regular intervals to remobilize the effluent.

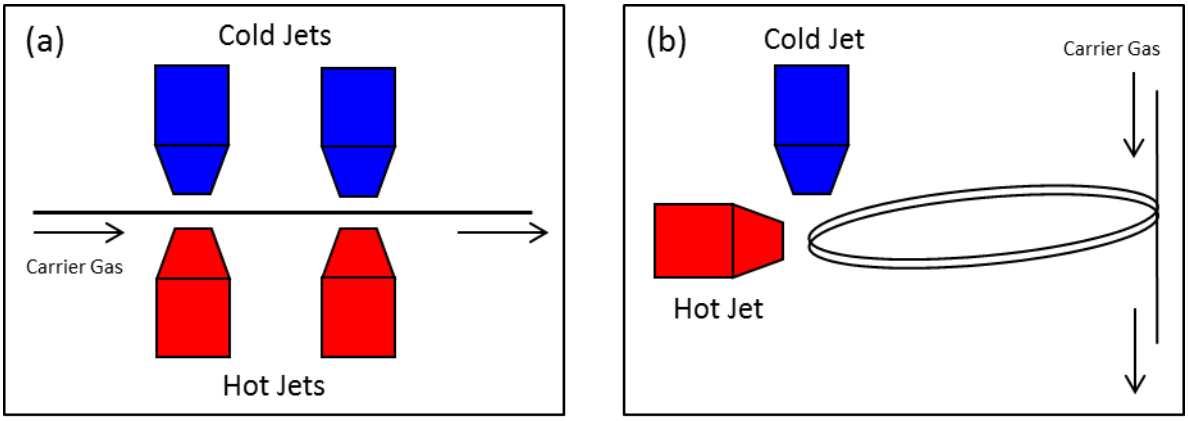

Figure 4. Schematic of (a) dual stage quad-jet thermal modulator, and (b) two-stage loop modulator

There are several advantages that GC×GC offers over one-dimensional chromatography techniques, such as the potential for higher peak capacity, and signal enhancement due to analyte focusing by modulator. GC×GC is well suited to the non-targeted analysis of complex mixtures since the technique produces structured two-dimensional chromatograms, which aid in the identification of unknowns.[97] Figure 5 shows the GC×GC contour plot of a standard mix containing alkanes, fatty acid methyl esters, and PAHs, and the second dimension separation of

the three chemical classes is clearly demonstrated. Furthermore, structured GC×GC chromatograms allow the rapid identification of structural isomers and homologues. Figure 6 displays a GC×GC contour plot which illustrates the chromatographic resolution of the methyl esters of C_8-, C_9-, and C_{10}- monocyclic carboxylic acids. It is observed that structural isomers elute in bands on the GC×GC chromatogram (with similar second dimension retention times), and an increase in alkylation leads to an increase in the second dimension retention time.

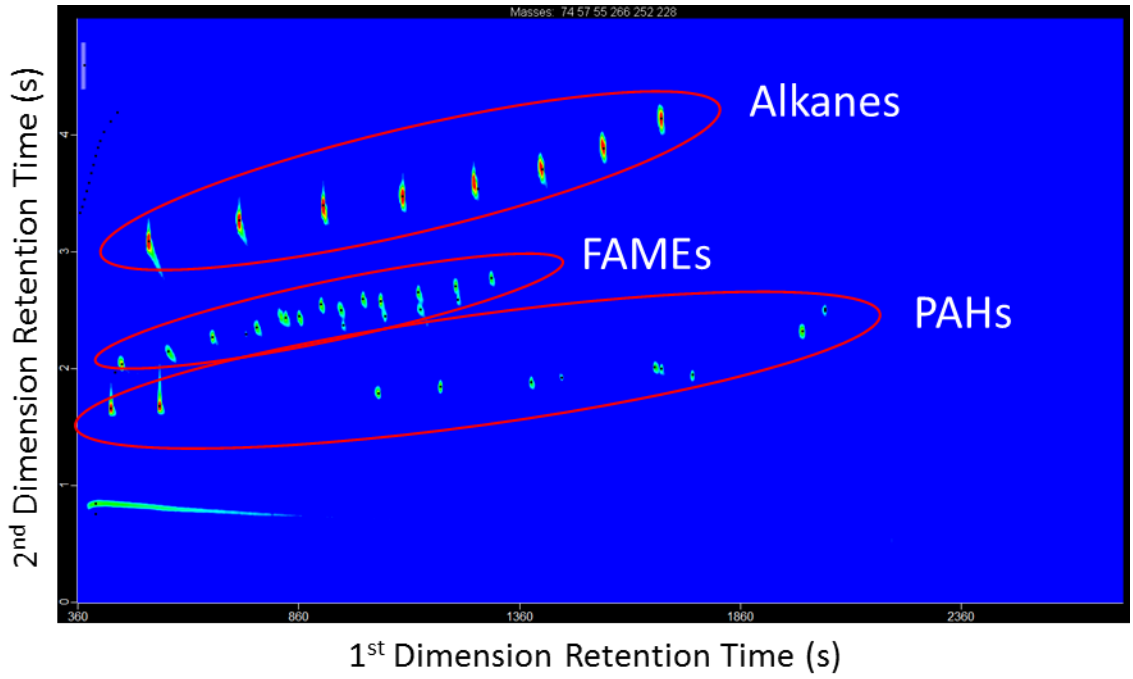

Figure 5. GC×GC contour plot demonstrating the separation of a standard mixture comprised of alkanes, fatty acid methyl esters (FAMEs) and polycyclic aromatic hydrocarbons (PAHs). Primary column stationary phase: DB-5ms, (5%-Phenyl)-methylpolysiloxane; Secondary column stationary phase: DB-17, (50%-phenyl)-methylpolysiloxane.

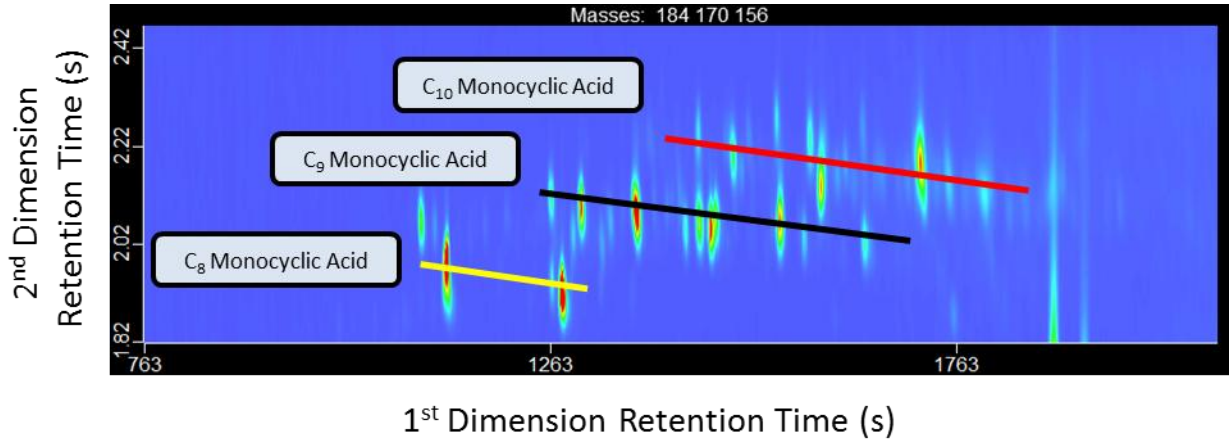

Figure 6. GC×GC contour plot demonstrating the structure nature of the 2D chromatogram. Isomers elute in bands with similar second dimension retention times, while homologues with increasing degrees of alkylation, in general, possess increased first and second dimension retention times.

1.4.5.2 Characterization of NAs by GC×GC/MS

GC×GC coupled to time-of-flight mass spectrometry (TOFMS) was first applied for the characterization of NAs (as methyl esters) in 2005 by Hao *et al*.[91], who analyzed two commercial mixtures and one extract from a Syncrude tailings pond. The authors reported the chromatographic resolution of individual acyclic and monocyclic NAs. NAs with higher degrees of cyclicity (Z-values ranging between -4 to -8) were detected in the samples, but the method did not allow the resolution of isomers. Nevertheless, the authors noted that they were able to detect differences in the patterns of the acyclic and monocyclic NAs between the three samples, demonstrating, for the first time, the use of GC×GC/MS for the fingerprinting of NAs and differentiation of sources.

To date, the most notable contribution of GC×GC/MS to the study of naphthenic acids has been the structural elucidation of individual NAs. Since very few EI mass spectra of NAs are present within mass spectral library databases or in literature, NAs have primarily been identified by (1) interpretation of the 'unknown' EI mass spectra from first principles enabling tentative structural assignments, and (2) confirmation of structural proposals by comparing the GC×GC retention times and EI mass spectra of unknowns with that of commercially available or synthesized reference standards. In lieu of reference standards, some NAs have been tentatively identified based on mass spectral similarities to literature EI mass spectra.[37,98] The analyses of NAs by GC×GC/MS have firmly identified the following structural moieties by comparison to reference standards: monocyclic-[16,99], bicyclic-[15,99], tricyclic-[14,16], tetracyclic-[100], and pentacyclic[100] alicyclic carboxylic acids; monocyclic-[101] and bicyclic[16,93] aromatic carboxylic acids; tricyclic[102] dicarboxylic acids; and 'sulfur-containing' thiophene carboxylic acids[16]. In

addition, steroidal-type carboxylic acids have been identified in OSPW extracts based on their EI mass spectra.[37] GC×GC coupled to high resolution mass spectrometry (HRMS) has been used to identify a number of diaromatic sulfur-containing carboxylic acids based on mass accuracy and mass spectral fragmentation patterns.[98] West *et al*. demonstrated that GC×GC/HRMS (5 ppm mass accuracy) was useful for distinguishing organic compounds from different heteroatom classes, and the authors reported the identification of a number of C_{16} tetracyclic carboxylic acids.[103]

In recent years, GC×GC/MS has been used as a qualitative fingerprinting tool in the field of oil sands forensics to investigate compositional differences between OSPW from different industries[18], differentiate OSPW contamination in groundwater systems from naturally occurring NAs[92], and assess the temporal and spatial variations within tailing ponds[20,104]. However, to date, only the occurrences of adamantane- and steroidal-type carboxylic acids have been investigated in such studies.

1.5 Reclamation of tailings in the Athabasca oil sands region

1.5.1 Dry landscape reclamation – Sandhill Fen reclamation site

Composite tailings (CT) is a dry reclamation technology which is formed by combining FFT with post-processed sand and gypsum ($CaSO_4 \bullet 2H_2O$; 1 kg per m^3 of FFT). Gypsum acts as a coagulant and assists in the separation of water from the solids. Composite tailings are placed into mined-out pits, where the mixture is allowed to dewater. The pore water released from the CT material is recycled back into the extraction process. Once the CT deposit solidifies, reclaimed landscapes can be established overtop.[105–107]

Syncrude Canada's Sandhill Fen Reclamation Site is the first reclaimed wetland on a CT deposit in the AOSR. Sandhill Fen has an area of 52 ha and is located in Syncrude's East-In pit, north of Fort McMurrary, AB, Canada (57°02'23.6"N 111°35'30.0"W). At the site, an open-cast mine pit was in-filled with 35 m of composite tailings material over an 8 year period [108], and then capped with 10 m of processed tailings sand. A 0.5 m layer of clay-till was placed over the sand cap as a base for wetland construction, and development of the wetland began in the summer of 2011 [107]. First, stockpiled and salvaged peat material from a nearby mine site was placed on top of the clay-till layer, then the peat was seeded with fen vegetation. The wetland was then established by flooding the fen with freshwater from the Mildred Lake Reservoir in May 2012.

During the initial phases of wetland construction in 2009, emissions of hydrogen sulphide (H_2S) gas were discovered at surface dewatering wells, suggesting the occurrence of microbial sulphate reduction within the site. It has been previously shown that sulfate reducing bacteria (SRB) occur within oil sands tailings ponds [109,110], and the addition of large quantities of gypsum to tailings can stimulate such bacterial communities. Reid and Warren[107] characterized the *in situ*

aqueous distributions of sulfur compounds at the site and detected H_2S (aq) within the surface water samples collected from the overlying fen, and the pore water samples from the sand cap, and composite tailings deposit. Bradford *et al.*[111] demonstrated that microbial communities within the sand cap and composite tailings deposit were degrading modern carbon sources at the site. However, it is unknown whether NAs or other OSPW-derived compounds were also being utilized. It is plausible that the degradation of labile, modern carbon sources may stimulate the degradation of recalcitrant compounds, such as NAs, via the priming effect[112,113], which would be beneficial from a reclamation perspective.

1.5.2 Wet landscape reclamation: End pitlakes (EPLs)

End pit lakes (EPLs) have been proposed as a wet reclamation strategy whose purpose is to provide a sustainable landscape feature and a final remediation solution for oil sands tailings and OSPW. EPLs are established by depositing FFT into an excavated mine pit, and covering the tailings with a water cover. In contrast to tailings ponds, which serve as a temporary holding basin for tailings during mine operations, end pit lakes allow the permanent storage of FFT. [114]

Syncrude's Base Mine Lake (BML) is the first demonstration end pit lake in the AOSR. BML is located at the Mildred Lake Mine site, which is approximately 35 km north of Fort McMurrary, Alberta, Canada (111.622279W,57.010263N). The FFT deposit has a maximum depth of 45 m, and a total volume of ~186 Mm^3. The FFT was deposited at the site over an 18 year period, from 1994 to 2012. The water cap comprises of a mixture of OSPW and fresh water from Beaver Creek Reservoir, and possesses an average depth of 8.5 m. The approximate volume of the water cap is 65 Mm^3. During the summer, the water cap displays thermally stratified conditions and can be divided into three distinct zones: epilimnion, metalimnion, and hypolimnion. The system experiences turnover in the fall and the spring. During the winter, the water cap is ice covered and is weakly stratified. An important consideration of BML is the management and remediation of toxic compounds present in FFT and OSPW, such as NAs and polycyclic aromatic hydrocarbons (PAHs). While the geochemistry of the water cap is expected to be similar to OSPW initially, water quality is expected to improve over time due to fresh water inputs and natural attenuation. However, since the settling and dewatering of FFT will contribute pore water to the overlying water cap, it is important that on-going assessments are performed to monitor the long-term geochemical evolution of BML.

1.6 Thesis objectives and overview

The overall objective of this thesis was to develop analytical methodologies utilizing GC×GC/MS for the improved characterization of individual NAs at oil sands reclamation sites in Fort McMurray, AB, Canada. Multidimensional chromatography is advantageous since it offers

unparalleled chromatographic resolution and peak capacity, and allows the examination of individual constituents within complex mixtures. In recent years, GC×GC/TOFMS (nominal mass resolution) has been used to significantly improve the separation of NAs and, most notably, resolve structural isomers. However, due to several factors (e.g. extreme complexity of NA mixtures and lack of available reference standards), a large number of NAs within OSPW and related samples are unknown. Moreover, the monitoring of NA isomer distributions by GC×GC has great potential as a fingerprinting tool to aid in the differentiation of sources. However, very little is known about the variabilities of isomer profiles within tailings ponds, reclamation sites, or in rivers and ground waters. Only a few studies to date[20,104] have begun to explore the spatial and short-term temporal variabilities of NAs, and such studies were limited to the monitoring of single families of NAs. In addition, since it has been reported that structural isomers of NAs display varying levels of susceptibility to degradation[64,65], the monitoring of NA isomer distributions via multidimensional chromatography may allow greater insight into the cycling of NAs.

The second chapter of this thesis presents an analytical methodology utilizing GC×GC/TOFMS (with nominal mass resolution) for the improved separation of NAs. In this study, GC×GC/TOFMS was used as a discovery tool to identify individual NAs within a pore water extract from Syncrude's Sandhill Fen reclamation site.

The third chapter of this thesis characterizes the spatial and temporal trends of individual NAs at Sandhill Fen. This study demonstrates that GC×GC/TOFMS can be used as a fingerprinting tool to differentiate sources of NAs and also monitor NA compositional changes.

Chapter four applies GC×GC/TOFMS to monitor the spatial and temporal trends of NAs at Syncrude's Base Mine Lake. This study is the first to perform semi-quantitative assessments of NAs by GC×GC/TOFMS (by external calibration). This study demonstrates that the monitoring of isomers was useful for detecting subtle temporal and spatial differences, which are not observed by comparing the total concentrations of each isomer series.

Chapter five reports the first application of GC×GC coupled to a high resolution QTOF-MS for characterization of NAs. This study demonstrates that GC×GC/QTOF-MS can not only resolve structural isomers and generate isomer profiles, but can also provide information on chemical classes, double bond equivalents, and carbon numbers based on mass accuracy. Furthermore, it is shown that Kendrick mass defect plots are useful for simplifying complex GC×GC datasets and providing a global overview of the elemental compositions within NA mixtures.

1.7 References

(1) Government of Alberta. Alberta Energy: Facts and Statistics. http://www.energy.alberta.ca/OilSands/791.asp (accessed Mar 19, 2017).

(2) Clemente, J. S.; Fedorak, P. M. A review of the occurrence, analyses, toxicity, and biodegradation of naphthenic acids. *Chemosphere* **2005**, 60 (5), 585–600.

(3) Eckert, W. F.; Masliyah, J. H.; Gray, M. R.; Fedorak, P. M. Prediction of sedimentation and consolidation of fine tails. *AIChE J.* **1996**, 42 (4), 960–972.

(4) Allen, E. W. Process water treatment in Canada's oil sands industry: I. Target pollutants and treatment objectives. *J. Environ. Eng. Sci.* **2008**, 7 (2), 123–138.

(5) MacKinnon, M. D.; Boerger, H. Description of two treatment methods for detoxifying oil sands tailings pond water. *Water Qual. Res. J. Canada* **1986**, 21 (4), 496–512.

(6) Brown, L. D.; Ulrich, A. C. Oil sands naphthenic acids: A review of properties, measurement, and treatment. *Chemosphere* **2015**, 127, 276–290.

(7) Ross, M. S.; Pereira, A. dos S.; Fennell, J.; Davies, M.; Johnson, J.; Sliva, L.; Martin, J. W. Quantitative and qualitative analysis of naphthenic acids in natural waters surrounding the Canadian oil sands industry. *Environ. Sci. Technol.* **2012**, 46 (23), 12796–12805.

(8) Ferguson, G. P.; Rudolph, D. L.; Barker, J. F. Hydrodynamics of a large oil sand tailings impoundment and related environmental implications. *Can. Geotech. J.* **2009**, 46, 1446–1460.

(9) Oiffer, A. A. L.; Barker, J. F.; Gervais, F. M.; Mayer, K. U.; Ptacek, C. J.; Rudolph, D. L. A detailed field-based evaluation of naphthenic acid mobility in groundwater. *J. Contam. Hydrol.* **2009**, 108 (3–4), 89–106.

(10) Grewer, D. M.; Young, R. F.; Whittal, R. M.; Fedorak, P. M. Naphthenic acids and other acid-extractables in water samples from Alberta: What is being measured? *Sci. Total Environ.* **2010**, 408 (23), 5997–6010.

(11) Headley, J. V.; Peru, K. M.; Armstrong, S. A.; Han, X.; Martin, J. W.; Mapolelo, M. M.; Smith, D. F.; Rogers, R. P.; Marshall, A. G. Aquatic plant-derived changes in oil sands naphthenic acid signatures determined by low-, high-, and ultrahigh-resolution mass spectrometry. *Rapid Commun. Mass Spectrom.* **2009**, 23, 515–522.

(12) Barrow, M. P.; Witt, M.; Headley, J. V.; Peru, K. M. Athabasca oil sands process water: Characterization by atmospheric pressure photoionization and electrospray ionization Fourier transform ion cyclotron resonance mass spectrometry. *Anal. Chem.* **2010**, 82 (9), 3727–3735.

(13) Bauer, A. E.; Frank, R. A.; Headley, J. V.; Peru, K. M.; Hewitt, L. M.; Dixon, D. G. Enhanced characterization of oil sands acid-extractable organics fractions using electrospray ionization-high-resolution mass spectrometry and synchronous fluorescence spectroscopy. *Environ. Toxicol. Chem.* **2015**, 34 (5), 1001–1008.

(14) Rowland, S. J.; Scarlett, A. G.; Jones, D.; West, C. E.; Frank, R. a. Diamonds in the rough: Identification of individual naphthenic acids in oil sands process water. *Environ. Sci. Technol.* **2011**, 45 (7), 3154–3159.

(15) Wilde, M. J.; West, C. E.; Scarlett, A. G.; Jones, D.; Frank, R. A.; Hewitt, L. M.; Rowland, S. J. Bicyclic naphthenic acids in oil sands process water: Identification by comprehensive multidimensional gas chromatography–mass spectrometry. *J. Chromatogr. A* **2015**, 1378, 74–87.

(16) Bowman, D. T.; Slater, G. F.; Warren, L. A.; McCarry, B. E. Identification of individual thiophene-, indane-, tetralin-, cyclohexane-, and adamantane-type carboxylic acids in composite tailings pore water from Alberta oil sands. *Rapid Commun. Mass Spectrom.* **2014**, 28 (19), 2075–2083.

(17) Pereira, A. S.; Bhattacharjee, S.; Martin, J. W. Characterization of oil sands process-affected waters by liquid chromatography orbitrap mass spectrometry. *Environ. Sci. Technol.* **2013**, 47 (10), 5504–5513.

(18) Rowland, S. J.; West, C. E.; Scarlett, A. G.; Ho, C.; Jones, D. Differentiation of two industrial oil sands process-affected waters by two-dimensional gas chromatography/mass spectrometry of diamondoid acid profiles. *Rapid Commun. Mass Spectrom.* **2012**, 26 (5), 572–576.

(19) Holowenko, F. M.; Mackinnon, M. D.; Fedorak, P. M. Characterization of naphthenic acids in oil sands wastewaters by gas chromatography-mass spectrometry. *Water Res.* **2002**, 36, 2843–2855.

(20) Frank, R. A.; Milestone, C. B.; Rowland, S. J.; Headley, J. V.; Kavanagh, R. J.; Lengger, S. K.; Scarlett, A. G.; West, C. E.; Peru, K. M.; Hewitt, L. M. Assessing spatial and temporal variability of acid-extractable organics in oil sands process-affected waters. *Chemosphere* **2016**, 160, 303–313.

(21) Peters, L. E.; MacKinnon, M.; Van Meer, T.; van den Heuvel, M. R.; Dixon, D. G. Effects of oil sands process-affected waters and naphthenic acids on yellow perch (Perca flavescens) and Japanese medaka (Orizias latipes) embryonic development. *Chemosphere* **2007**, 67 (11), 2177–2183.

(22) Nero, V.; Farwell, A.; Lee, L. E. J.; Van Meer, T.; MacKinnon, M. D.; Dixon, D. G. The effects of salinity on naphthenic acid toxicity to yellow perch: Gill and liver histopathology. *Ecotoxicol. Environ. Saf.* **2006**, 65 (2), 252–264.

(23) Kavanagh, R. J.; Frank, R. A.; Burnison, B. K.; Young, R. F.; Fedorak, P. M.; Solomon, K. R.; Van Der Kraak, G. Fathead minnow (Pimephales promelas) reproduction is impaired when exposed to a naphthenic acid extract. *Aquat. Toxicol.* **2012**, 116–117, 34–42.

(24) Fattah, Q.; Wort, D. Metabolic responses of bush bean plants to naphthenate application. *Can. J. Bot.* **1970**, 48 (5), 861–866.

(25) Rogers, V. V.; Wickstrom, M.; Liber, K.; MacKinnon, M. D. Acute and subchronic mammalian toxicity of naphthenic acids from oil sands tailings. *Toxicol. Sci.* **2002**, 66 (2), 347–355.

(26) Leung, S. S.-C.; Mackinnon, M. D.; Smith, R. E. Aquatic Reclamation in the Athabasca, Canada, Oil Sands: Naphthenate and Salt Effects on Phytoplankton Communities. *Environ. Toxicol. Chem.* **2001**, 20 (7), 1532–1543.

(27) Leung, S. S.; MacKinnon, M. D.; Smith, R. E. H. The ecological effects of naphthenic acids and salts on phytoplankton from the Athabasca oil sands region. *Aquat. Toxicol.* **2003**, 62 (1), 11–26.

(28) Melvin, S. D.; Trudeau, V. L. Toxicity of Naphthenic Acids to Wood Frog Tadpoles (Lithobates sylvaticus). *J. Toxicol. Environ. Heal. Part A* **2012**, 75 (3), 170–173.

(29) Frank, R. A.; Fischer, K.; Kavanagh, R.; Kent Burnison, B.; Arsenault, G.; Headley, J. V; Peru, K. M.; Van Glen Kraak, D. E. R.; Solomon, K. R. Effect of carboxylic acid content on the acute toxicity of oil sands naphthenic acids. *Environ. Sci. Technol.* **2009**, 43 (2), 266–271.

(30) Frank, R. A.; Sanderson, H.; Kavanagh, R.; Burnison, B. K.; Headley, J. V; Solomon, K. R. Use of a (Quantitative) Structure-Activity Relationship [(Q)Sar] Model to Predict the Toxicity of Naphthenic Acids. *J. Toxicol. Environ. Heal. Part A* **2010**, 73 (4), 319–329.

(31) Thomas, K. V; Langford, K.; Petersen, K.; Smith, A. J.; Tollefsen, K. E. Effect-directed identification of naphthenic acids as important in vitro xeno-estrogens and anti-androgens in North Sea offshore produced water discharges. *Environ. Sci. Technol.* **2009**, 43 (21), 8066–8071.

(32) Hong, S.; Giesy, J. P.; Lee, J.; Lee, J.; Khim, J. S. Effect-Directed Analysis: Current Status and Future Challenges. *Ocean Sci. J.* **2016**, 51, 413–433.

(33) Yue, S.; Ramsay, B. A.; Wang, J.; Ramsay, J. Toxicity and composition profiles of solid phase extracts of oil sands process-affected water. *Sci. Total Environ.* **2015**, 538, 573–582.

(34) Morandi, G. D.; Wiseman, S. B.; Pereira, A.; Mankidy, R.; Gault, I. G. M.; Martin, J. W.; Giesy, J. P. Effects-Directed Analysis of Dissolved Organic Compounds in Oil Sands Process-Affected Water. *Environ. Sci. Technol.* **2015**, 49 (20), 12395–12404

(35) Yue, S.; Ramsay, B. A.; Brown, R. S.; Wang, J.; Ramsay, J. A. Identification of estrogenic compounds in oil sands process waters by effect directed analysis. *Environ. Sci. Technol.* **2015**, 49 (1), 570–577.

(36) Reinardy, H. C.; Scarlett, A. G.; Henry, T. B.; West, C. E.; Hewitt, L. M.; Frank, R. A.; Rowland, S. J. Aromatic naphthenic acids in oil sands process-affected water, resolved by GCxGC-MS, only weakly induce the gene for vitellogenin production in zebrafish (danio rerio) larvae. *Environ. Sci. Technol.* **2013**, 47 (12), 6614–6620.

(37) Rowland, S. J.; West, C. E.; Jones, D.; Scarlett, A. G.; Frank, R. A.; Hewitt, L. M. Steroidal aromatic Naphthenic Acids in oil sands process-affected water: Structural comparisons

with environmental estrogens. *Environ. Sci. Technol.* **2011**, 45 (22), 9806–9815.

(38) Quagraine, E. K.; Peterson, H. G.; Headley, J. V. In Situ Bioremediation of Naphthenic Acids Contaminated Tailing Pond Waters in the Athabasca Oil Sands Region—Demonstrated Field Studies and Plausible Options: A Review. *J. Environ. Sci. Heal. Part A* **2005**, 40 (3), 685–722.

(39) Frank, R. A.; Kavanagh, R.; Kent Burnison, B.; Arsenault, G.; Headley, J. V.; Peru, K. M.; Van Der Kraak, G.; Solomon, K. R. Toxicity assessment of collected fractions from an extracted naphthenic acid mixture. *Chemosphere* **2008**, 72 (9), 1309–1314.

(40) Herman, D. C.; Fedorak, P. M.; MacKinnon, M. D.; Costerton, J. W. Biodegradation of naphthenic acids by microbial populations indigenous to oil sands tailings. *Can. J. Microbiol.* **1994**, 40 (6), 467–477.

(41) Scott, A. C.; MacKinnon, M. D.; Fedorak, P. M. Naphthenic acids in athabasca oil sands tailings waters are less biodegradable than commercial naphthenic acids. *Environ. Sci. Technol.* **2005**, 39 (21), 8388–8394.

(42) Del Rio, L. F.; Hadwin, A. K. M.; Pinto, L. J.; MacKinnon, M. D.; Moore, M. M. Degradation of naphthenic acids by sediment micro-organisms. *J. Appl. Microbiol.* **2006**, 101 (5), 1049–1061.

(43) Biryukova, O. V.; Fedorak, P. M.; Quideau, S. A. Biodegradation of naphthenic acids by rhizosphere microorganisms. *Chemosphere* **2007**, 67 (10), 2058–2064.

(44) Quesnel, D. M.; Bhaskar, I. M.; Gieg, L. M.; Chua, G. Naphthenic acid biodegradation by the unicellular alga Dunaliella tertiolecta. *Chemosphere* **2011**, 84 (4), 504–511.

(45) Clemente, J. S.; MacKinnon, M. D.; Fedorak, P. M. Aerobic biodegradation of two commercial naphthenic acids preparations. *Environ. Sci. Technol.* **2004**, 38 (4), 1009–1016.

(46) Martin, J. W.; Barri, T.; Han, X.; Fedorak, P. M.; El-Din, M. G.; Perez, L.; Scott, A. C.; Jiang, J. T. Ozonation of oil sands process-affected water accelerates microbial bioremediation. *Environ. Sci. Technol.* **2010**, 44 (21), 8350–8356.

(47) He, Y.; Wiseman, S. B.; Zhang, X.; Hecker, M.; Jones, P. D.; El-Din, M. G.; Martin, J. W.; Giesy, J. P. Ozonation attenuates the steroidogenic disruptive effects of sediment free oil sands process water in the H295R cell line. *Chemosphere* **2010**, 80 (5), 578–584.

(48) Scott, A. C.; Zubot, W.; Mackinnon, M. D.; Smith, D. W.; Fedorak, P. M. Ozonation of oil sands process water removes naphthenic acids and toxicity. *Chemosphere* **2008**, 71, 156–160.

(49) Wang, N.; Chelme-Ayala, P.; Perez-Estrada, L.; Garcia-Garcia, E.; Pun, J.; Martin, J. W.; Belosevic, M.; Gamal El-Din, M. Impact of ozonation on naphthenic acids speciation and toxicity of oil sands process-affected water to vibrio fischeri and mammalian immune system. *Environ. Sci. Technol.* **2013**, 47, 6518–6526.

(50) Sohrabi, V.; Ross, M. S.; Martin, J. W.; Barker, J. F. Potential for in situ chemical oxidation of acid extractable organics in oil sands process affected groundwater. *Chemosphere* **2013**, 93 (11), 2698–2703.

(51) McMartin, D. W.; Headley, J. V; Friesen, D. A.; Peru, K. M.; Gillies, J. A. Photolysis of Naphthenic Acids in Natural Surface Water. *J. Environ. Sci. Heal. Part A* **2004**, 39 (6), 1361–1383.

(52) Mishra, S.; Meda, V.; Dalai, A. K.; McMartin, D. W.; Headley, J. V.; Peru, K. M. Photocatalysis of Naphthenic Acids in Water. *J. Water Resour. Prot.* **2010**, 2 (7), 644–650.

(53) Armstrong, S. A.; Headley, J. V; Peru, K. M.; Germida, J. J. Phytotoxicity of oil sands naphthenic acids and dissipation from systems planted with emergent aquatic macrophytes. *J. Environ. Sci. Heal. Part a-Toxic/Hazardous Subst. Environ. Eng.* **2008**, 43 (1), 36–42.

(54) Armstrong, S. A.; Headley, J. V.; Peru, K. M.; Mikula, R. J.; Germida, J. J. Phytotoxicity and naphthenic acid dissipation from oil sands fine tailings treatments planted with the emergent macrophyte Phragmites australis. *J. Environ. Sci. Heal. Part A* **2010**, 45 (8), 1008–1016.

(55) Blakley, E. R. The microbial degradation of cyclohexanecarboxylic acid by β -oxidation pathway with simultaneous induction to the utilization of benzoate. *Can. J. Microbiol.* **1978**, 24, 847–855.

(56) Quagraine, E. K.; Headley, J. V.; Peterson, H. G. Is Biodegradation of Bitumen a Source of Recalcitrant Naphthenic Acid Mixtures in Oil Sands Tailing Pond Waters? **J. Environ. Sci. Heal. Part A** *2005*, 40 (3), 671–684.

(57) Johnson, R. J.; West, C. E.; Swaih, A. M.; Folwell, B. D.; Smith, B. E.; Rowland, S. J.; Whitby, C. Aerobic biotransformation of alkyl branched aromatic alkanoic naphthenic acids via two different pathways by a new isolate of Mycobacterium. *Environ. Microbiol.* **2012**, 14 (4), 872–882.

(58) Johnson, R. J.; Smith, B. E.; Rowland, S. J.; Whitby, C. Biodegradation of alkyl branched aromatic alkanoic naphthenic acids by Pseudomonas putida KT2440. *Int. Biodeterior. Biodegradation* **2013**, 81, 3–8.

(59) Rowland, S. J.; Jones, D.; Scarlett, A. G.; West, C. E.; Hin, L. P.; Boberek, M.; Tonkin, A.; Smith, B. E.; Whitby, C. Synthesis and toxicity of some metabolites of the microbial degradation of synthetic naphthenic acids. *Sci. Total Environ.* **2011**, 409 (15), 2936–2941.

(60) Rontani, J. F.; Bonin, P. Utilization of Normal-Alkyl-Substituted Cyclohexanes by a Marine Alcaligenes. *Chemosphere* **1992**, 24 (10), 1441–1446.

(61) Blakley, E. R. The microbial degradation of cyclohexanecarboxylic acid : a pathway involving aromatization to form p-hydroxybenzoic acid. *Can. J. Microbiol.* **1974**, 20, 1297–1306.

(62) Taylor, D. G.; Trudgill, P. W. Metabolism of Cyclohexane Carboxylic Acid by

Alcaligenes Strain W1. *J. Bacteriol.* **1978**, 134 (2), 401–411.

(63) Han, X.; Scott, A. C.; Fedorak, P. M.; Bataineh, M.; Martin, J. W. Influence of molecular structure on the biodegradability of naphthenic acids. *Environ. Sci. Technol.* **2008**, 42 (4), 1290–1295.

(64) Misiti, T. M.; Tezel, U.; Pavlostathis, S. G. Effect of alkyl side chain location and cyclicity on the aerobic biotransformation of naphthenic acids. *Environ. Sci. Technol.* **2014**, 48 (14), 7909–7917.

(65) Johnson, R. J.; Smith, B. E.; Sutton, P. A.; McGenity, T. J.; Rowland, S. J.; Whitby, C. Microbial biodegradation of aromatic alkanoic naphthenic acids is affected by the degree of alkyl side chain branching. *ISME J.* **2011**, 5 (3), 486–496.

(66) Yen, T. W.; Marsh, W. P.; MacKinnon, M. D.; Fedorak, P. M. Measuring naphthenic acids concentrations in aqueous environmental samples by liquid chromatography. *J. Chromatogr. A* **2004**, 1033 (1), 83–90.

(67) Jones, D. M.; Watson, J. S.; Meredith, W.; Chen, M.; Bennett, B. Determination of naphthenic acids in crude oils using nonaqueous ion exchange solid-phase. *Anal. Chem.* **2001**, 73 (3), 703–707.

(68) Smith, B. E.; Lewis, C. A.; Belt, S. T.; Whitby, C.; Rowland, S. J. Effects of alkyl chain branching on the biotransformation of naphthenic acids. *Environ. Sci. Technol.* **2008**, 42 (24), 9323–9328.

(69) St John, W. P.; Rughani, J.; Green, S. A.; McGinnis, G. D. Analysis and characterization of naphthenic acids by gas chromatography–electron impact mass spectrometry of tert.-butyldimethylsilyl derivatives. *J. Chromatogr. A* **1998**, 807, 241–251.

(70) Holowenko, F. M.; MacKinnon, M. D.; Fedorak, P. M. Naphthenic acids and surrogate naphthenic acids in methanogenic microcosms. *Water Res.* **2001**, 35 (11), 2595–2606.

(71) Rudzinski, W. E.; Oehlers, L.; Zhang, Y. Tandem mass spectrometric characterization of commercial naphthenic acids and a Maya crude oil. *Energy Fuels* **2002**, 16 (5), 1178–1185.

(72) Bataineh, M.; Scott, a. C.; Fedorak, P. M.; Martin, J. W. Capillary HPLC/QTOF-MS for characterizing complex naphthenic acid mixtures and their microbial transformation. *Anal. Chem.* **2006**, 78 (24), 8354–8361.

(73) Martin, J. W.; Han, X.; Peru, K. M.; Headley, J. V. Characterization of high- and low-resolution electrospray ionization mass spectrometry for the analysis of naphthenic acid mixtures in oil sands process water. *Rapid Commun. Mass Spectrom.* **2008**, 22, 1919–1924.

(74) Clemente, J. S.; Fedorak, P. M. Evaluation of the analyses of tert-butyldimethylsilyl derivatives of naphthenic acids by gas chromatography–electron impact mass spectrometry. *J. Chromatogr. A* **2004**, 1047 (1), 117–128.

(75) Headley, J. V; Mohamed, M. H.; Frank, R. A.; Martin, J. W.; Hazewinkel, R. R. O.; Humphries, D.; Gurprasad, N. P.; Hewitt, L. M.; Muir, D. C. G.; Lindeman, D.; et al. Chemical fingerprinting of naphthenic acids and oil sands process waters — A review of analytical methods for environmental samples. *J. Environ. Sci. Heal. Part A.* **2013**, 48 (10), 1145–1163.

(76) Wang, X.; Kasperski, K. L. Analysis of naphthenic acids in aqueous solution using HPLC-MS/MS. *Anal. Methods* **2010**, 2 (11), 1715.

(77) Hindle, R.; Noestheden, M.; Peru, K.; Headley, J. Quantitative analysis of naphthenic acids in water by liquid chromatography–accurate mass time-of-flight mass spectrometry. *J. Chromatogr. A* **2013**, 1286, 166–174.

(78) Shang, D.; Kim, M.; Haberl, M.; Legzdins, A. Development of a rapid liquid chromatography tandem mass spectrometry method for screening of trace naphthenic acids in aqueous environments. *J. Chromatogr. A* **2013**, 1278, 98–107.

(79) Brunswick, P.; Shang, D.; van Aggelen, G.; Hindle, R.; Hewitt, L. M.; Frank, R. A.; Haberl, M.; Kim, M. Trace analysis of total naphthenic acids in aqueous environmental matrices by liquid chromatography/mass spectrometry-quadrupole time of flight mass spectrometry direct injection. *J. Chromatogr. A* **2015**, 1405, 49–71.

(80) Woudneh, M. B.; Coreen Hamilton, M.; Benskin, J. P.; Wang, G.; McEachern, P.; Cosgrove, J. R. A novel derivatization-based liquid chromatography tandem mass spectrometry method for quantitative characterization of naphthenic acid isomer profiles in environmental waters. *J. Chromatogr. A* **2013**, 1293, 36–43.

(81) Barrow, M. P.; Headley, J. V.; Peru, K. M.; Derrick, P. J. Fourier transform ion cyclotron resonance mass spectrometry of principal components in oilsands naphthenic acids. *J. Chromatogr. A* **2004**, 1058 (1–2), 51–59.

(82) Headley, J. V.; Barrow, M. P.; Peru, K. M.; Fahlman, B.; Frank, R. A.; Bickerton, G.; McMaster, M. E.; Parrott, J.; Hewitt, L. M. Preliminary fingerprinting of Athabasca oil sands polar organics in environmental samples using electrospray ionization Fourier transform ion cyclotron resonance mass spectrometry. *Rapid Commun. Mass Spectrom.* **2011**, 25 (13), 1899–1909.

(83) Headley, J. V.; Peru, K. M.; Janfada, A.; Fahlman, B.; Gu, C.; Hassan, S. Characterization of oil sands acids in plant tissue using Orbitrap ultra-high resolution mass spectrometry with electrospray ionization. *Rapid Commun. Mass Spectrom.* **2011**, 25 (3), 459–462.

(84) Barrow, M. P.; McDonnell, L. a; Feng, X.; Walker, J.; Derrick, P. J. Determination of the nature of naphthenic acids present in crude oils using nanospray Fourier transform ion cyclotron resonance mass spectrometry: the continued battle against corrosion. *Anal. Chem.* **2003**, 75 (4), 860–866.

(85) Stanford, L. A.; Kim, S.; Klein, G. C.; Smith, D. F.; Rodgers, R. P.; Marshall, A. G. Identification of Water-Soluble Heavy Crude Oil Organic-Acids, Bases, and Neutrals by

Electrospray Ionization and Field Desorption Ionization Fourier Transform Ion Cyclotron Resonance Mass Spectrometry. *Environ. Sci. Technol.* **2007**, 41 (8), 2696–2702.

(86) Barrow, M. P.; Headley, J. V; Derrick, P. J. Data Visualization for the Characterization of Naphthenic Acids within Petroleum Samples. *Energy Fuels* **2009**, No. 12, 2592–2599.

(87) Rowland, S. M.; Robbins, W. K.; Corilo, Y. E.; Marshall, A. G.; Rodgers, R. P. Solid-Phase Extraction Fractionation To Extend the Characterization of Naphthenic Acids in Crude Oil by Electrospray Ionization Fourier Transform Ion Cyclotron Resonance Mass Spectrometry. *Energy Fuels* **2014**, 28, 5043–5048.

(88) Ortiz, X.; Jobst, K. J.; Reiner, E. J.; Backus, S.; Peru, K. M.; McMartin, D. W.; O'Sullivan, G.; Taguchi, V. Y.; Headley, J. V. Characterization of naphthenic acids by gas chromatography-fourier transform ion cyclotron resonance mass spectrometry. *Anal. Chem.* **2014**, 86 (15), 7666–7673.

(89) Barrow, M. P.; Peru, K. M.; Headley, J. V. An added dimension: GC atmospheric pressure chemical ionization FTICR MS and the Athabasca oil sands. *Anal. Chem.* **2014**, 86 (16), 8281–8288.

(90) Pereira, A. S.; Martin, J. W. Exploring the complexity of oil sands process-affected water by high efficiency supercritical fluid chromatography/orbitrap mass spectrometry. *Rapid Commun. Mass Spectrom.* **2015**, 29 (8), 735–744.

(91) Hao, C.; Headley, J. V.; Peru, K. M.; Frank, R.; Yang, P.; Solomon, K. R. Characterization and pattern recognition of oil–sand naphthenic acids using comprehensive two-dimensional gas chromatography/time-of-flight mass spectrometry. *J. Chromatogr. A* **2005**, 1067 (1–2), 277–284.

(92) Frank, R. A.; Roy, J. W.; Bickerton, G.; Rowland, S. J.; Headley, J. V.; Scarlett, A. G.; West, C. E.; Peru, K. M.; Parrott, J. L.; Conly, F. M.; et al. Profiling oil sands mixtures from industrial developments and natural groundwaters for source identification. *Environ. Sci. Technol.* **2014**, 48 (5), 2660–2670.

(93) West, C. E.; Pureveen, J.; Scarlett, A. G.; Lengger, S. K.; Wilde, M. J.; Korndorffer, F.; Tegelaar, E. W.; Rowland, S. J. Can two-dimensional gas chromatography/mass spectrometric identification of bicyclic aromatic acids in petroleum fractions help to reveal further details of aromatic hydrocarbon biotransformation pathways? *Rapid Commun. Mass Spectrom.* **2014**, 28 (9), 1023–1032.

(94) Liu, Z.; Phillips, J. B. Comprehensive Two-Dimensional Gas Chromatography using an On-Column Thermal Modulator Interface. *J. Chromatogr. Sci.* **1991**, 29 (6), 227–231.

(95) Edwards, M.; Mostafa, A.; Górecki, T. Modulation in comprehensive two-dimensional gas chromatography: 20 years of innovation. *Anal. Bioanal. Chem.* **2011**, 401 (8), 2335–2349.

(96) Tranchida, P. Q.; Purcaro, G.; Dugo, P.; Mondello, L.; Tranchida, P. Q.; Purcaro, G.; Dugo, P.; Mondello, L. Modulators for comprehensive two-dimensional gas chromatography.

Trends Anal. Chem. **2011**, 30 (9), 1437–1461.

(97) Murray, J. a. Qualitative and quantitative approaches in comprehensive two-dimensional gas chromatography. *J. Chromatogr. A* **2012**, 1261, 58–68.

(98) West, C. E.; Scarlett, A. G.; Tonkin, A.; O'Carroll-Fitzpatrick, D.; Pureveen, J.; Tegelaar, E.; Gieleciak, R.; Hager, D.; Petersen, K.; Tollefsen, K.-E.; et al. Diaromatic sulphur-containing "naphthenic" acids in process waters. *Water Res.* **2014**, 51, 206–215.

(99) Rowland, S. J.; West, C. E.; Scarlett, A. G.; Jones, D. Identification of individual acids in a commercial sample of naphthenic acids from petroleum by two-dimensional comprehensive gas chromatography/mass spectrometry. *Rapid Commun. Mass Spectrom.* **2011**, 25 (12), 1741–1751.

(100) Rowland, S. J.; West, C. E.; Scarlett, A. G.; Jones, D.; Frank, R. a. Identification of individual tetra- and pentacyclic naphthenic acids in oil sands process water by comprehensive two-dimensional gas chromatography/mass spectrometry. *Rapid Commun. Mass Spectrom.* **2011**, 25 (9), 1198–1204.

(101) Rowland, S. J.; West, C. E.; Scarlett, a. G.; Jones, D.; Boberek, M.; Pan, L.; Ng, M.; Kwong, L.; Tonkin, a. Monocyclic and monoaromatic naphthenic acids: Synthesis and characterisation. *Environ. Chem. Lett.* **2011**, 9 (4), 525–533.

(102) Lengger, S. K.; Scarlett, A. G.; West, C. E.; Rowland, S. J. Diamondoid diacids ('O4' species) in oil sands process-affected water. *Rapid Commun. Mass Spectrom.* **2013**, 27 (23), 2648–2654.

(103) West, C. E.; Scarlett, A. G.; Pureveen, J.; Tegelaar, E. W.; Rowland, S. J. Abundant naphthenic acids in oil sands process-affected water: studies by synthesis, derivatisation and two-dimensional gas chromatography/high-resolution mass spectrometry. *Rapid Commun. Mass Spectrom.* **2013**, 27 (2), 357–365.

(104) Lengger, S. K.; Scarlett, A. G.; West, C. E.; Frank, R. A.; Hewitt, L. M.; Milestone, C. B.; Rowland, S. J. Use of the distributions of adamantane acids to profile short-term temporal and pond-scale spatial variations in the composition of oil sands process-affected waters. *Environ. Sci. Process. Impacts* **2015**, 17 (8), 1415–1423.

(105) Matthews, J. G.; Shaw, W. H.; Mackinnon, M. D.; Cuddy, R. G. Development of Composite Tailings Technology at Syncrude. *Int. J. Surf. Min.* **2010**, No. September 2011, 37–41.

(106) Han, X.; MacKinnon, M. D.; Martin, J. W. Estimating the in situ biodegradation of naphthenic acids in oil sands process waters by HPLC/HRMS. *Chemosphere* **2009**, 76 (1), 63–70.

(107) Reid, M. L.; Warren, L. A. S reactivity of an oil sands composite tailings deposit undergoing reclamation wetland construction. *J. Environ. Manag.* **2016**, 166, 321–329.

(108) Vitt, D. H.; House, M.; Hartsock, J. A. Sandhill Fen, An Initial Trial for Wetland Species Assembly on In-pit Substrates: Lessons after Three Years. *Botany* **2016**, 94, 1015–1025.

(109) Ramos-Padron, E.; Bordenave, S.; Lin, S.; Bhaskar, I. M.; Dong, X.; Sensen, C. W.; Fournier, J.; Voordouw, G.; Gieg, L. M. Carbon and Sulfur Cycling by Microbial Communities in a Gypsum-Treated Oil Sands Tailings Pond. *Environ. Sci. Technol.* **2011**, 45, 439–446.

(110) Penner, T. J.; Foght, J. M. Mature fine tailings from oil sands processing harbour diverse methanogenic communities. *Can. J. Microbiol.* **2010**, 56 (6), 459–470.

(111) Bradford, L. M.; Ziolkowski, L. A.; Goad, C.; Warren, L. A.; Slater, G. F. Elucidating carbon sources driving microbial metabolism during oil sands reclamation. *J. Environ. Manag.* **2017**, 188, 246–254.

(112) Kuzyakov, Y.; Friedel, J. K.; Stahr, K. Review of mechanisms and quantification of priming effects. *Soil Biol. Biochem.* **2000**, 32 (11–12), 1485–1498.

(113) Fontaine, S.; Mariotti, A.; Abbadie, L. The priming effect of organic matter: A question of microbial competition? *Soil Biol. Biochem.* **2003**, 35 (6), 837–843.

(114) Dompierre, K. A.; Lindsay, M. B. J.; Cruz-Hernández, P.; Halferdahl, G. M. Initial geochemical characteristics of fluid fine tailings in an oil sands end pit lake. *Sci. Total Environ.* **2016**, 556, 196–206.

Chapter Two: Identification of individual thiophene-, indane-, tetralin-, cyclohexane-, and adamantane-type carboxylic acids in composite tailings pore water from Alberta oil sands

David T. Bowman[1], Gregory F. Slater[2], Lesley A. Warren[2], Brian E. McCarry[1]

The work in this chapter has been published in: "D.T. Bowman, G.F. Slater, L.A. Warren, B.E. McCarry, Rapid Commun. Mass Spectrom. 28 (2014) 2075–2083. doi:10.1002/rcm.6996."

Author Affiliations:

[1]Department of Chemistry and Chemical Biology, McMaster University, 1280 Main Street West, Hamilton, ON, Canada, L8S 4M1
[2]School of Geography and Earth Sciences, McMaster University, 1280 Main Street West, Hamilton, ON, Canada, L8S 4K1

Author Contributions:

BEM, GFS, and LAW conceived and designed the study. DTB performed the sample extraction, GC×GC/TOFMS instrumental analysis, data analysis and interpretation, and wrote the manuscript. GFS and LAW edited the manuscript.

Abstract

Rationale: Naphthenic acids (NAs) accumulate in oil sands process-affected water (OSPW) as a result of the water-based extraction processes, and represent one of the toxic fractions in OSPW. They exist as a complex mixture and so the development of an analytical method to characterize and quantify individual acids has been an on-going challenge. The multidimensional separation technique of two dimensional gas chromatography (GC×GC) has the potential to provide a fingerprint of the sources of NAs and can potentially resolve individual analytes for target analysis. However, the identity and toxicity of a large proportion of the acids present in tailing waters are still unknown.

Methods: Comprehensive two-dimensional gas chromatography time-of-flight mass spectrometry (GC×GC/TOFMS) was used to characterize naphthenic acids in a pore water sample from a Syncrude composite tailings (CT) deposit in Fort McMurray, Alberta, Canada. The extractable organic acid fraction was derivatized with diazomethane and the structures of selected resolved esters were elucidated through interpretation of their electron ionization (EI) mass spectra and, if available, confirmed by comparison with the spectra of reference standards.

Results: The high resolving power of the GC×GC/TOFMS technique allowed for the structure elucidation of numerous as yet unidentified acids in the CT pore water sample such as carboxylic acids containing a thiophene, indane, tetralin or cyclohexane moiety. Seventeen members of the previously reported class of adamantane-type carboxylic acids in oil sands process water could also be identified in the sample.

Conclusions: This study underlines the complexity of naphthenic acid isomer distributions in composite tailings and provides a useful inventory of individual acids.

1. Introduction:

The Alberta oil sands represent the third largest oil reserve in the world, containing in excess of 170 billion barrels of oil.[1] Most oil from Alberta is produced using a warm water caustic extraction process, which uses large volumes of water to isolate bitumen from sand and clay.[2] Tailings are produced as a by-product and comprise of oil sands process-affected water (OSPW), sand, silt, clay, and unrecovered bitumen.[3] Oil sands tailings exist as an aqueous slurry and are required to be stored on-site in tailing ponds as a result of a zero-discharge policy.[4] OSPW is known to be acutely toxic to aquatic biota, primarily due to the accumulation of naphthenic acids (NA), polycyclic aromatic hydrocarbons (PAH), and salts.[2,5] While coarse solids are able to settle quickly in tailing ponds, the fine particulates consolidate slowly to form fluid fine tailings (FFT). Clarified OSPW is released slowly from the FFT into the overlying water and is eventually recycled back into the extraction process.[6]

In order to accelerate the release of water from FFT for more rapid reclamation, technologies such as the Composite Tailings process have been developed. Composite tailings (CT) is a dry reclamation technology which combines fluid fine tailings with gypsum to form a non-segregating deposit.[6] Gypsum acts as a coagulant and allows for the accelerated consolidation of tailings. Pore water is also released from the CT, and is recycled back into the extraction process.[7] The CT deposits can be capped by sand and reclaimed landscapes (i.e. wetlands) can be developed over the deposit.[6]

Naphthenic acids are traditionally defined as a complex mixture of aliphatic and alicylic carboxylic acids ($C_nH_{2n+z}O_2$ where n = number of carbons, Z = degree of unsaturation). However, studies using high-resolution mass spectrometry have shown that oil sands tailing waters also contain acids with aromatic rings, sulphur and/or nitrogen heteroatoms, as well as acids with additional oxygen containing substituents ($C_nH_{2n+z}O_x$, where x is an integer $2 \geq x \leq 5$)[6,8–10]. The structure of the majority of the individual acids that make up the NA profile is unknown, primarily due to the complexity of the mixtures and lack of readily accessible standards.[5] There are thousands of acids present in oil sands tailings waters, so that the development of an analytical method for their identification and quantification has been an on-going challenge. Such analytical methods would enable further characterization of toxic and/or biodegradable components of naphthenic acid mixtures. It is expected that the profiling of individual organic compounds, such as sulfur containing species, may allow for distinguishing sources of naphthenic acids released to the environment.[5]

Comprehensive two-dimensional gas chromatography coupled to time-of-flight mass spectrometry has been shown to be a promising tool to resolve individual naphthenic acids in tailings waters and identify their structures.[11] Previous analyses of OSPW have confirmed the structures of individual naphthenic acids such as diamondoid[12,13], tetra and pentacyclic acids[14] on

the basis of a comparison with reference standards. In addition, steroidal[15] and diaromatic-thiophene acids[16] have been tentatively identified on the basis of their EI mass spectra. Nevertheless, the identity of the large majority of the acids in tailings remains unknown.

In this study, comprehensive two-dimensional gas chromatography time-of-flight mass spectrometry (GC×GC/TOFMS) was used to analyze the methyl ester derivatives of the acid extractable organics (AEO) in pore water from a composite tailings reclamation site in Fort McMurray, Alberta. The extract contains several thiophene-, cyclohexane- indane- and tetralin-type acids, whose structures were elucidated. Many isomers belonging to the previously identified class of adamantane acids were also present in this sample. This study describes these new classes of naphthenic acids, increases the inventory of known acids, and exemplifies the complexity of isobaric analytes within CT pore water.

2. Experimental

2.1 Site location and sampling methods

Approximately 500 mL of pore water was collected from a monitoring well installed at 9 m depth in the overlying sandcap of a composite tailings (CT) deposit at Syncrude's Mildred Lake site in Fort McMurray, AB on July 27th, 2011. Pore water samples were collected from the site by an inertial lift pump system. The pore water samples were stored in pre-cleaned Nalgene plastic bottles at -20°C and thawed prior to extraction.

2.2 Chemicals and reagents

Dichloromethane (distilled in glass) was purchased from Caledon Laboratories (Georgetown, Ontario, Canada). To aid in the identification of the unknowns, the following compounds were purchased: adamantane-1-carboxylic acid (99 %, Sigma-Aldrich, St. Louis, MO, USA), adamantane-1-acetic acid (98 %, Sigma-Aldrich), 3,5-dimethyladamantane-1-carboxylic acid (97 %, Sigma-Aldrich), 3-ethyladamantane-1-carboxylic acid (Aldrich^{CPR}, Milwaukee, MO, USA), cyclohexane carboxylic acid (98 %, Sigma-Aldrich), 1-methylcyclohexane-1-carboxylic acid (99 %, Sigma-Aldrich), 2-methylcyclohexane-1-carboxylic acid (mixture of cis and trans, 99 %, Sigma-Aldrich), trans-4-ethylcyclohexane-1-carboxylic acid (Aldrich^{CPR}), 1,2,3,4-tetrahydro-2-naphthoic acid (98 %, Sigma), 2-indanylacetic acid (Aldrich^{CPR}), 5-methylthiophene-2-carboxylic acid (98 %, Sigma-Aldrich), 2-methylthiophene-3-carboxylic acid (Aldrich^{CPR}), 5-ethylthiophene-2-carboxylic acid (Aldrich^{CPR}), 2,5-dimethyl-thiophene-3-carboxylic acid (Aldrich^{CPR}), 4-ethyl-5-methylthiophene-3-carboxylic acid (Aldrich^{CPR}).

2.3 Extraction procedure

The protocol for the extraction of naphthenic acids from pore water was modified from the method developed by Hao *et al.*[11] Briefly, water samples (20 mL) were passed through a sterile Acrodisc 0.45 µm syringe filter (Gelman Sciences, Ann Arbor, MI, USA), acidified to pH 2 and extracted with dichloromethane (4 x 15 mL). The extract was concentrated to 1 mL by rotary evaporation and quantitatively transferred to a glass vial, in which it was further concentrated to 30 µL by blowing gently with nitrogen. 2-Hexyldecanoic acid in dichloromethane was added as an internal standard (final concentration: 1 ppm). Diazomethane in CH_2Cl_2 was added dropwise to the sample until the yellow colour persisted. The resulting methyl ester derivatives were analyzed by GC×GC/TOFMS.

2.4 Analysis by GC×GC/TOFMS

Samples were analyzed using a Pegasus 4D system (LECO corp, St. Joseph, MI, USA). The instrument utilized Rtx-17sil ms (30 m x 0.25 mm x 0.15 µm) as the primary column and DB-5ms (1 m x 0.1 mm x 0.1 µm) as the secondary column. The primary oven was programmed to hold for 1 minute at 40°C, ramp to 310°C at 2.5°C/min, and hold at 310°C for 20 minutes. The secondary oven offset was set to +5°C relative to the primary oven. A modulation period of 4 seconds was used. The modulator offset was +15°C relative to the secondary oven. The ion source and transfer line temperature were set to 200°C and 280°C, respectively. Helium was used as the carrier gas at a flow rate of 1 mL/min. The time-of-flight mass spectrometer (TOF-MS) scanned over a mass range of 30 to 500 *m/z* at a sample acquisition rate of 200scans per second. Data processing was performed by ChromaTOF v.4.50.8.0 (LECO). Library searches were conducted with the NIST/EPA/NIH Mass Spectral Library 2008 (NIST 08, Gaithersburg, MD, USA) and a user library containing the purchased reference standards.

3. Results and discussion

3.1 Thiophene-type carboxylic acids

A series of alkyl substituted thiophenecarboxylic acids has been identified in the pore water extract. The extracted ion chromatogram (EIC) displayed in Fig. 1 shows the chromatographic resolution of numerous C_1-(methyl substituted), C_2-(dimethyl or ethyl substituted), and C_3-thiophenecarboxylic acids. An increase in the degree of alkylation of an acid appears to lead to an increase of its first and second dimension retention times. Isobaric compounds show a tendency to cluster together in the two dimensional chromatogram, allowing for a rapid detection of analogues.

The methyl ester of 5-methyl-thiophene-2-carboxylic acid was identified in the sample by comparison with the GC×GC RTs and the EI mass spectrum of an authentic standard (see Figs. 2A and 2B). The spectrum displays a prominent molecular ion at *m/z* 156 with the expected

[M+2] ^{34}S isotope peak. The base peak at *m/z* 125 results from direct bond cleavage of the ester methoxy group, while the peak at *m/z* 97 represents the loss of the entire ester moiety $CH_3OCO^{\bullet}$.

In the same vein, the presence of the methyl ester of 2-methyl-thiophene-3-carboxylic acid in the sample was established. The mass spectrum (see Figs. 2C and 2D) closely resembles that of its isomer shown in Figs. 2A and 2B, but it features prominent fragment ions at *m/z* 141 (loss of $CH_3^{\bullet}$) and *m/z* 124 (loss of CH_3OH). The methanol loss is readily ascribed to a 1,5-H shift from the CH_3 substituent to the neighboring ester CH_3O moiety. This rearrangement represents an example of the so-called *ortho*-effect[17]: when the methyl substituent is in the *ortho* position relative to the ester, an energetically favourable six-membered-ring transition state is realized.

As a previous mass spectrometric study of some substituted thiophene-2-carboxylic acids[18] has shown that loss of H_2O is clearly associated with the *ortho*-effect, it seems reasonable to assume that a significant peak for loss of CH_3OH in the spectra of the methyl esters of unknown alkyl substituted thiophenecarboxylic acids is also due to this effect.

Two additional sample components that elute in the 'cluster' of the two dimensional chromatogram of the above reference standards, yield the mass spectra presented in Figs. 2E and 2F. Comparison of these spectra with those of Figs. 2A-D leaves little doubt that we are dealing with positional isomers of the methyl esters identified above. Using the ortho-effect leading to loss of CH_3OH as a criterion, we propose that the structure of the analyte of Fig. 2E contains a methyl substituent positioned ortho to the ester, whereas the analyte of Fig. 2F does not.

A cluster of six isomers with apparent molecular ions at *m/z* 170 and similar fragmentation patterns was also identified in the sample. We propose that these are methyl esters of C_2-thiophene carboxylic acids. Their mass spectra are presented in Figures 3C-H. Those of the methyl esters of the reference standards, the 2,5-dimethyl-3-thiophene and 5-ethyl-2-thiophene carboxylic acids, are presented in Fig. 3A and 3B. Neither standard could be traced in the water sample but both do elute in the "isomer cluster" of the six unknowns when spiked into the sample. As expected, the spectra of the six isomers all yield a high similarity match in a mass spectral library search with a user library containing the two standards.

Three C_3-thiophene carboxylic acids were identified in the sample by comparing their mass spectrum, shown in Figs. 4A-C, with that of the methyl ester of 4-ethyl-5-methylthiophene-3-carboxylic acid (Fig. 4D). The four spectra are similar in appearance and share a sulphur containing molecular ion at *m/z* 184 and prominent primary fragment ions at *m/z* 169 (loss of $CH_3^{\bullet}$) and *m/z* 153 (loss of $CH_3O^{\bullet}$). The spectrum of the reference standard displays two more prominent peaks in the high mass region, *viz. m/z* 152, whose generation is readily ascribed to loss of CH_3OH following a 1,5-H shift, and *m/z* 139, whose mechanism of formation and structure assignment is less obvious. A detailed gas-phase ion chemistry study involving labelled

analogues would shed more light on this question. It could also lead to the assignment of specific structures to the three identified C_3-thiophenecarboxylic acids.

In this context we note that tentative structures of sulphur containing naphthenic acids have been proposed in a recent study[16]. However, this is the first study in which structures of thiophene acids have been established by comparison with reference standards. The presence of thiophene-type hydrocarbons in petroleum and crude oils is well known and we propose that the thiophene carboxylic acids identified in our pore water sample are oxidative biotransformation products of alkylated thiophenes. The bacterial oxidation of 4-methyl-benzo-thiophene has been studied previously[19] and it appears that the $-CH_3$ substituent can be oxidized to $-CH_2OH$ and further to $-COOH$. A similar biotransformation may well have occurred with alkylated thiophenes in crude oil.

3.2 Indane- and tetralin-type carboxylic acids

Indane- and tetralin-derived carboxylic acids also appear to be constituents of the pore water extract. The EIC chromatogram (*m/z* 130+116*)* of Fig. 5A shows the chromatographic resolution of the methyl esters of this class of analytes.

The presence of the methyl ester of 2-indanylacetic acid (Analyte (1) in Fig. 5A) is shown by the closely similar GC×GC RTs and EI mass spectra of the analyte and its reference standard: compare the spectra of Fig. 5B and 5C, which display a molecular ion at *m/z* 190 and fragment ions at *m/z* 116 (base peak) and *m/z* 74 originating from a McLafferty type rearrangement[17].

The same approach made it possible to unambiguously identify tetralin-2-carboxylic acid (Analyte (4) in Fig. 5A) as a constituent of the pore water sample. The closely similar mass spectra of Figs. 5D and 5E are characterized by a molecular ion at *m/z* 190 and fragment ions in the high mass region at *m/z* 158 (loss of CH_3OH via a 1,4-H shift) and *m/z* 130 (base peak). The latter ion possibly results from a facile decarbonylation of the *m/z* 158 ions into an energetically favourable product ion.

The mass spectra of Analytes (2) and (3) of Fig. 5A, whose first dimension RTs are considerably different from that of tetralin-2-carboxylic acid, are presented in Supplementary Fig. S1A and S1B (Supporting Information). The two mass spectra are remarkably close to that of tetralin-2-carboxylic acid but we feel that in the absence of additional information a structure assignment is not warranted.

To our knowledge, this is the first time that the above carboxylic acids have been confirmed as constituents of CT pore water. Naphthalene-, tetralin-, and indane-type acids were recently identified in partially degraded petroleum fractions, and it was suggested that these acids

may be indicative of bacterial processes occurring in reservoirs.[20] The degradation of naphthalene has been studied previously, and it was shown that naphthalene- and tetralin-type acids are produced as metabolites of the biotransformation.[21,22] It is proposed that tetralin-type acids may be produced following the reduction of naphthalene-type acids, or alternatively, following the carboxylation of tetralin hydrocarbons.[22] Reference standards for 1- and 2-naphthoic acid were obtained, but neither acid was detected in our sample. The absence of naphthalene-type acids in the pore water may suggest an advanced stage of biotransformation within the CT.

3.3 Cyclohexane-type carboxylic acids

Detailed studies by Rowland *et al.*[23,24] have identified several cyclohexane-type carboxylic acids in a commercial naphthenic acid mixture derived from petroleum. It has not been established whether OSPW also contains this class of acids but our study indicates that numerous cyclohexane-type carboxylic acids are present in the CT pore water extract which is derived from OSPW.

The parent cyclohexane carboxylic acid was identified by comparison of the GC×GC RTs and the mass spectrum of its methyl ester with those of the authentic standard (see Figs. 6A and 6B). The mass spectrum displays a molecular ion at *m/z* 142 and a pattern of fragment ions resulting from H-shifts and concomitant ring cleavage such as *m/z* 110 (loss of CH_3OH), *m/z* 87 (loss of $C_4H_7^{\bullet}$), and *m/z* 55 ($C_4H_7^{+}$). The same approach (see the mass spectra of Figs. 6C-F) led to the positive identification of the methyl esters of the homologous 1- and 2-methyl-cyclohexane carboxylic acids in the sample. Three additional analytes, whose mass spectra are shown in Supplementary Figs. S2A-C (Supporting Information), may well be other C_1-cyclohexane (or C_2-cyclopentane) carboxylic acid isomers, judging from their high mass spectral similarity to the authentic standards and their similar RTs. The spectrum of Figure S2C may well be that of the methyl ester of 3-methyl-cyclohexane carboxylic acid, as it is very close to that of the authentic standard reported in the study by Rowland *et al*.[24]

Finally, we note that the mass spectra of the set of nine *m/z* 170 analytes presented in Supplementary Fig. S3A-I (Supporting Information) may well be assigned to methyl esters of C_2-cyclohexane and/or C_3-cyclopentane carboxylic acids. The spectra are similar to those of the methyl esters of 4-ethyl-cyclohexane carboxylic acid (Supplementary Fig. S3J (Supporting Information), reference standard) and 1-ethyl-cyclohexane carboxylic acid (NIST 08 database). Their GC×GC RTs are also in agreement with this proposal, as the analytes form a cluster with a slightly increased 1st and 2nd dimensional retention time relative to the group of alicyclic acids with M=156 discussed above.

3.4 Adamantane-type carboxylic acids

A previous study[12] has shown that this class of acids is an important constituent of OSPW and numerous members thereof are also present in our CT pore water extract.

The presence of the methyl ester of adamantane-1-carboxylic acid in the sample was established by comparison of its EI mass spectrum and RTs with those of an authentic standard (Figs. 7A and 7B). The methyl ester of adamantane-2-carboxylic acid was also identified. This isomer elutes at a slightly longer retention time in the first dimension and yields the mass spectrum shown in Supplementary Fig. S4A (Supporting Information). This spectrum is entirely compatible with that reported in Rowland *et al*[12]. The closely similar RTs and EI mass spectra of analyte and authentic standard (see Supplentary Fig. S4B and S4C, Supporting Information) indicate that the methyl ester of adamantane-1-acetic acid is also a component of the sample. The dissociation characteristics of these analytes have been discussed previously by Rowland *et al*.[12]

Using the EI mass spectra and structure assignments of Rowland *et al*.[12] as a guide, we tentatively propose that the spectra of the three analytes shown in Figs. 7C and Supplementary S4D and S4E (Supporting Information) refer to methyl esters of methyl substituted adamantane-1-carboxylic acids. The spectra are characterized by a molecular ion at *m/z* 208, a base peak at *m/z* 149 (loss of $CH_3OCO^{\bullet}$), and prominent secondary fragment ions at *m/z* 107 and *m/z* 93. The spectra of the four analytes presented in Figures 7D and Supplementary S4F-S4H (Supporting Information) also display these peaks, but they are dominated by odd electron fragment ions at *m/z* 176 (loss of CH_3OH) and *m/z* 148 (probably resulting from the subsequent decarbonylation of the *m/z* 176 ion). The methyl ester of adamantane-2-carboxylic acid[12] shows basically the same dissociation behaviour, indicating that these four analytes are methyl substituted homologues thereof.

The presence of the methyl ester of 3,5-dimethyladamantane-1-carboxylic acid in the sample was established by comparison of its mass spectrum and GC×GC RTs with those of an authentic standard (see Figs. 7E and 7F). The spectrum displays a molecular ion at *m/z* 222 and a prominent fragment ion at *m/z* 163 (loss of $CH_3OCO^{\bullet}$). The five mass spectra presented in Supplementary Figs. S5A-S5E (Supporting Information) are most probably methyl esters of isomeric dimethyladamantanecarboxylic acids. The spectra possess common fragments to that of the reference isomer (Fig. 7F), but also display a peak at *m/z* 190 (loss of CH_3OH) of varying relative intensity. This variation is undoubtedly related to the position of the $–COOCH_3$ group of the isomers and its proximity to the methyl substituents.

A reference standard of 3-ethyladamantane-1-carboxylic acid was also available. Its mass spectrum (see Supplementary Fig. S5F, Supporting Information) shows a prominent peak at *m/z* 193 for loss of $C_2H_5^{\bullet}$ which clearly is of structure diagnostic value. This compound could not be

detected in our water sample but the sample component with the mass spectrum shown in Supplementary Fig. S5G (Supporting Information) is likely that of a closely related isomer.

4. Conclusions

In this study, an oil sands composite tailings pore water sample has been examined by GC×GC/TOFMS and compelling evidence is provided for the presence of numerous naphthenic acids that belong to five different classes of compounds. These include carboxylic acids having (alkyl substituted) thiophene, indane, tetralin, cyclohexane or adamantane as a structure motif. The structure of a number of the individual components of each class could be firmly established by comparing the EI mass spectrum and GC×GC RTs of the analytes with those of an authentic reference standard. The compounds identified in this study enlarge the inventory of individual naphthenic acids that may be used for fingerprinting samples of natural waters and differentiation of input sources.

Acknowledgements:

This work is dedicated to the memory of Dr. Brian E. McCarry (1946-2013), who initiated and guided the work described in this manuscript. Funding for this work was provided by NSERC Canada and Syncrude Canada (Grant no. CRDPJ 403361-10). The authors would like to thank Syncrude Canada personnel for assistance in field sampling on site in Fort McMurray, AB (Tara Penner, Carla Wytrykush, Jessica Clarke, Lori Cyprien), the Dr. Warren Field Group led by Tara Colenbrander Nelson for field sampling, Dr. Johan K. Terlouw for enlightening discussions, and the Centre for Microbial Chemical Biology (CMCB) at McMaster University for access to the GC×GC/TOF-MS instrument.

References

(1) Headley, J. V.; Peru, K. M.; Fahlman, B.; Colodey, A.; McMartin, D. W. Selective solvent extraction and characterization of the acid extractable fraction of Athabasca oils sands process waters by Orbitrap mass spectrometry. *Int. J. Mass Spectrom.* **2013**, *345–347*, 104–108.

(2) Toor, N. S.; Franz, E. D.; Fedorak, P. M.; MacKinnon, M. D.; Liber, K. Degradation and aquatic toxicity of naphthenic acids in oil sands process-affected waters using simulated wetlands. *Chemosphere* **2013**, *90* (2), 449–458.

(3) Ahad, J. M. E.; Pakdel, H. Direct evaluation of in situ biodegradation in athabasca oil sands tailings ponds using natural abundance radiocarbon. *Environ. Sci. Technol.* **2013**, *47* (18), 10214–10222.

(4) Rogers, V. V; Liber, K.; MacKinnon, M. D. Isolation and characterization of naphthenic acids from Athabasca oil sands tailings pond water. *Chemosphere* **2002**, *48* (5), 519–527.

(5) Taylor, P.; Headley, J. V; Mohamed, M. H.; Frank, R. A.; Martin, J. W. Chemical fingerprinting of naphthenic acids and oil sands process waters — A review of analytical methods for environmental samples. *J. Environ. Sci. Heal. Part A Toxicol. Hazard. Subst. Environ. Eng.* **2013**, *48* (10), 1146–1163.

(6) Han, X.; MacKinnon, M. D.; Martin, J. W. Estimating the in situ biodegradation of naphthenic acids in oil sands process waters by HPLC/HRMS. *Chemosphere* **2009**, *76* (1), 63–70.

(7) Matthews, J. G.; Shaw, W. H.; Mackinnon, M. D.; Cuddy, R. G. Development of Composite Tailings Technology at Syncrude. *Int. J. Surf. Min.* **2002**, *16*, 24–39.

(8) Barrow, M. P.; Headley, J. V; Derrick, P. J. Data Visualization for the Characterization of Naphthenic Acids within Petroleum Samples. *Energy & Fuels* **2009**, *23*, 2592–2599.

(9) Grewer, D. M.; Young, R. F.; Whittal, R. M.; Fedorak, P. M. Naphthenic acids and other acid-extractables in water samples from Alberta: What is being measured? *Sci. Total Environ.* **2010**, *408* (23), 5997–6010.

(10) Headley, J. V.; Peru, K. M.; Janfada, A.; Fahlman, B.; Gu, C.; Hassan, S. Characterization of oil sands acids in plant tissue using Orbitrap ultra-high resolution mass spectrometry with electrospray ionization. *Rapid Commun. Mass Spectrom.* **2011**, *25* (3), 459–462.

(11) Hao, C.; Headley, J.; Peru, K.; Frank, R.; Yang, P.; Solomon, K. Characterization and pattern recognition of oil–sand naphthenic acids using comprehensive two-dimensional gas chromatography/time-of-flight mass spectrometry. *J. Chromatogr. A* **2005**, *1067* (1–2), 277–284.

(12) Rowland, S. J.; Scarlett, A. G.; Jones, D.; West, C. E.; Frank, R. a. Diamonds in the rough: Identification of individual naphthenic acids in oil sands process water. *Environ. Sci. Technol.* **2011**, *45* (7), 3154–3159.

(13) Lengger, S. K.; Scarlett, A. G.; West, C. E.; Rowland, S. J. Diamondoid diacids ('O4' species) in oil sands process-affected water. *Rapid Commun. Mass Spectrom.* **2013**, *27* (23), 2648–2654.

(14) Rowland, S. J.; West, C. E.; Scarlett, A. G.; Jones, D.; Frank, R. a. Identification of individual tetra- and pentacyclic naphthenic acids in oil sands process water by comprehensive two-dimensional gas chromatography/mass spectrometry. *Rapid Commun. Mass Spectrom.* **2011**, *25* (9), 1198–1204.

(15) Rowland, S. J.; West, C. E.; Jones, D.; Scarlett, A. G.; Frank, R. A.; Hewitt, L. M. Steroidal aromatic Naphthenic Acids in oil sands process-affected water: Structural comparisons with environmental estrogens. *Environ. Sci. Technol.* **2011**, *45* (22), 9806–9815.

(16) West, C. E.; Scarlett, A. G.; Tonkin, A.; O'Carroll-Fitzpatrick, D.; Pureveen, J.; Tegelaar, E.; Gieleciak, R.; Hager, D.; Petersen, K.; Tollefsen, K.-E.; et al. Diaromatic sulphur-containing "naphthenic" acids in process waters. *Water Res.* **2013**, 1–10.

(17) McLafferty, F.; Turecek, F. *Interpretation of Mass Spectra*, 4th ed.; University Science Books: Mill Valley, CA, 1993.

(18) Fisichella, S.; Occhipinti, S.; Consiglio, O.; Spinelli, D.; Noto, R. The mass spectra of some substituted thiophene-2-carboxylic acids. *Phosphorus Sulfur Relat. Elem.* **1982**, *13* (March 2014), 59–68.

(19) Kropp, K.; Fedorak, P. A review of the occurrence, toxicity, and biodegradation of condensed thiophenes found in petroleum. *Can. J. Microbio.* **1998**, *44*, 605–622.

(20) West, C. E.; Pureveen, J.; Scarlett, A. G.; Lengger, S. K.; Wilde, M. J.; Korndorffer, F.; Tegelaar, E. W.; Rowland, S. J. Can two-dimensional gas chromatography/mass spectrometric identification of bicyclic aromatic acids in petroleum fractions help to reveal further details of aromatic hydrocarbon biotransformation pathways? *Rapid Commun. Mass Spectrom.* **2014**, *28* (9), 1023–1032.

(21) Meckenstock, R. U.; Annweiler, E.; Michaelis, W.; Richnow, H. H.; Schink, B.; Annweiler, E. V. A. Anaerobic Naphthalene Degradation by a Sulfate-Reducing Enrichment Culture. *Appl. Environ. Microbiol.* **2000**, *66* (7), 2743–2747.

(22) Annweiler, E.; Michaelis, W.; Meckenstock, R. U. Identical Ring Cleavage Products during Anaerobic Degradation of Naphthalene, 2-Methylnaphthalene, and Tetralin Indicate a New Metabolic Pathway. *Appl. Environ. Microbiol.* **2002**, *68* (2), 852–858.

(23) Rowland, S. J.; West, C. E.; Scarlett, a. G.; Jones, D.; Boberek, M.; Pan, L.; Ng, M.; Kwong, L.; Tonkin, a. Monocyclic and monoaromatic naphthenic acids: Synthesis and characterisation. *Environ. Chem. Lett.* **2011**, *9* (4), 525–533.

(24) Rowland, S. J.; West, C. E.; Scarlett, A. G.; Jones, D. Identification of individual acids in a commercial sample of naphthenic acids from petroleum by two-dimensional comprehensive gas chromatography/mass spectrometry. *Rapid Commun. Mass Spectrom.* **2011**, *25* (12), 1741–1751.

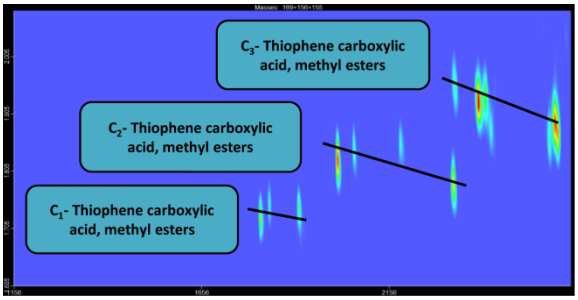

Figure 1. Two-dimensional contour plot illustrating the extensive series of thiophene-type carboxylic acids found in composite tailings water samples. (EIC m/z 169+155+156).

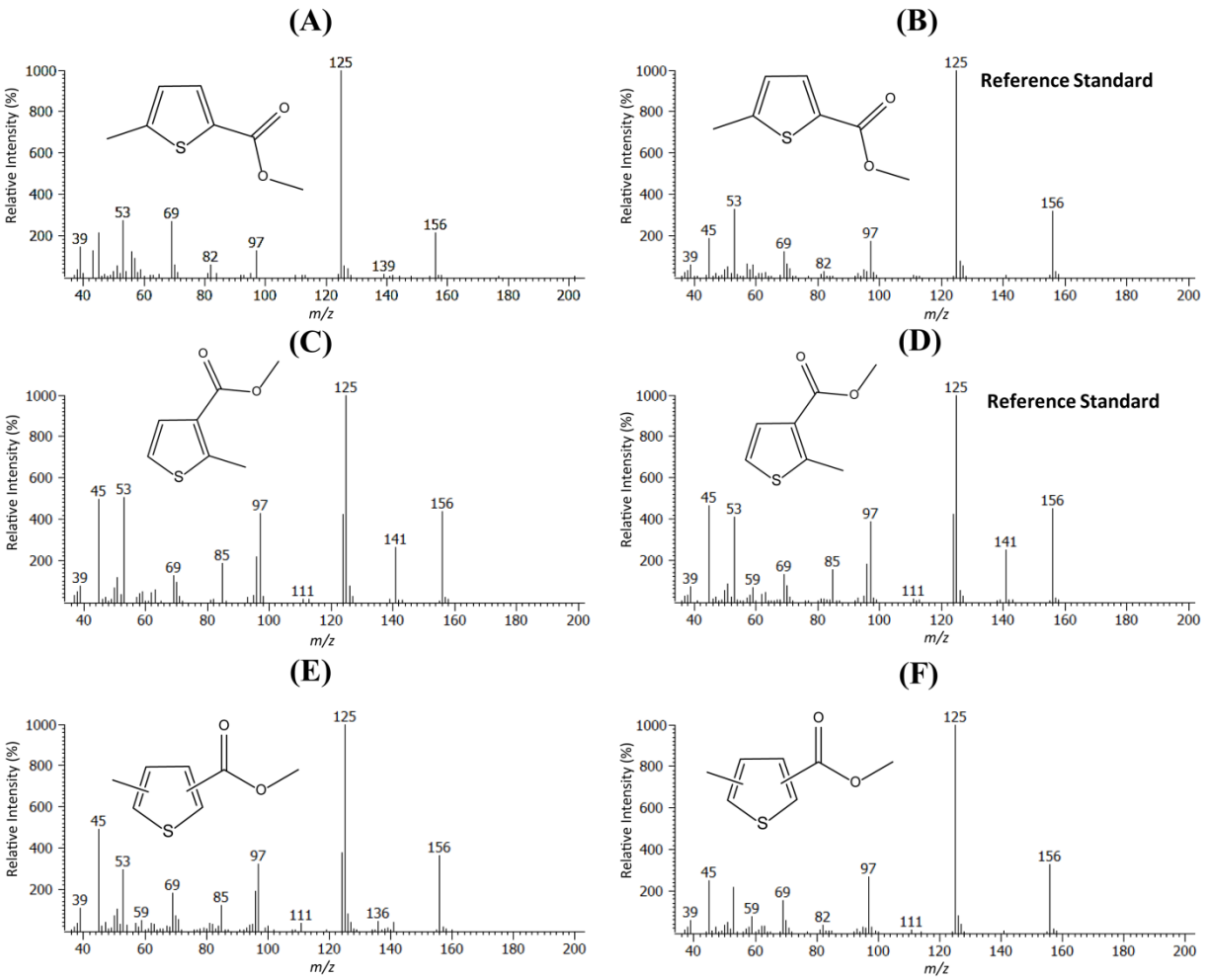

Figure 2. EI mass spectra of the methyl esters of: (A) 5-methylthiophene-2-carboxylic acid; (B) authentic standard of (A); (C) 2-methylthiophene-3-carboxylic acid; (D) authentic standard of (C); (E) and (F) unknown C_1-thiophenecarboxylic acids.

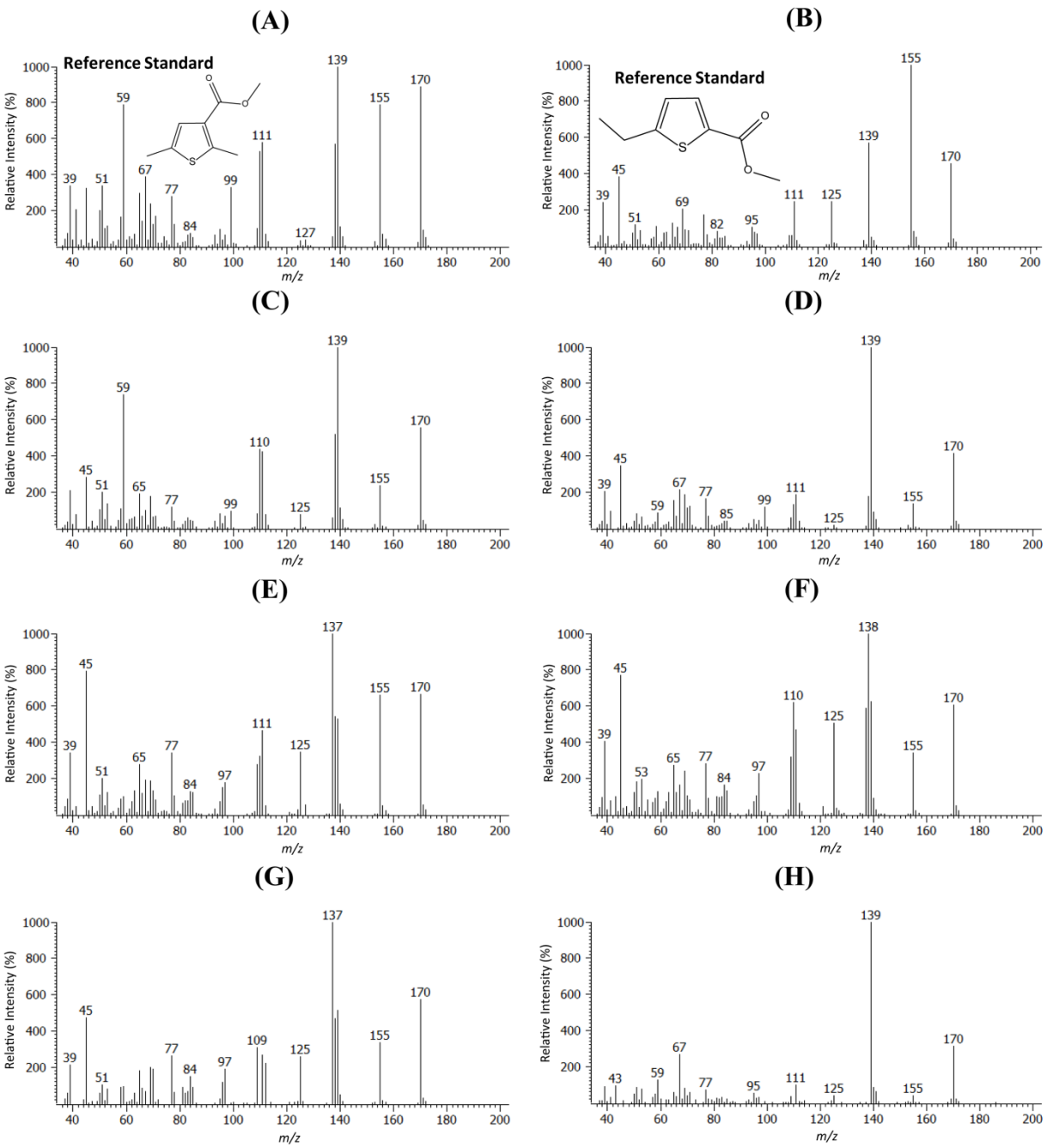

Figure 3. EI mass spectra of: (A) 2,5-dimethylthiophene-3-carboxylic acid, methyl ester (authentic standard); (B) 5-ethylthiophene-2-carboxylic acid, methyl ester (authentic standard); (C-H) unknown compounds tentatively identified as methyl esters of C_2-thiophenecarboxylic acids.

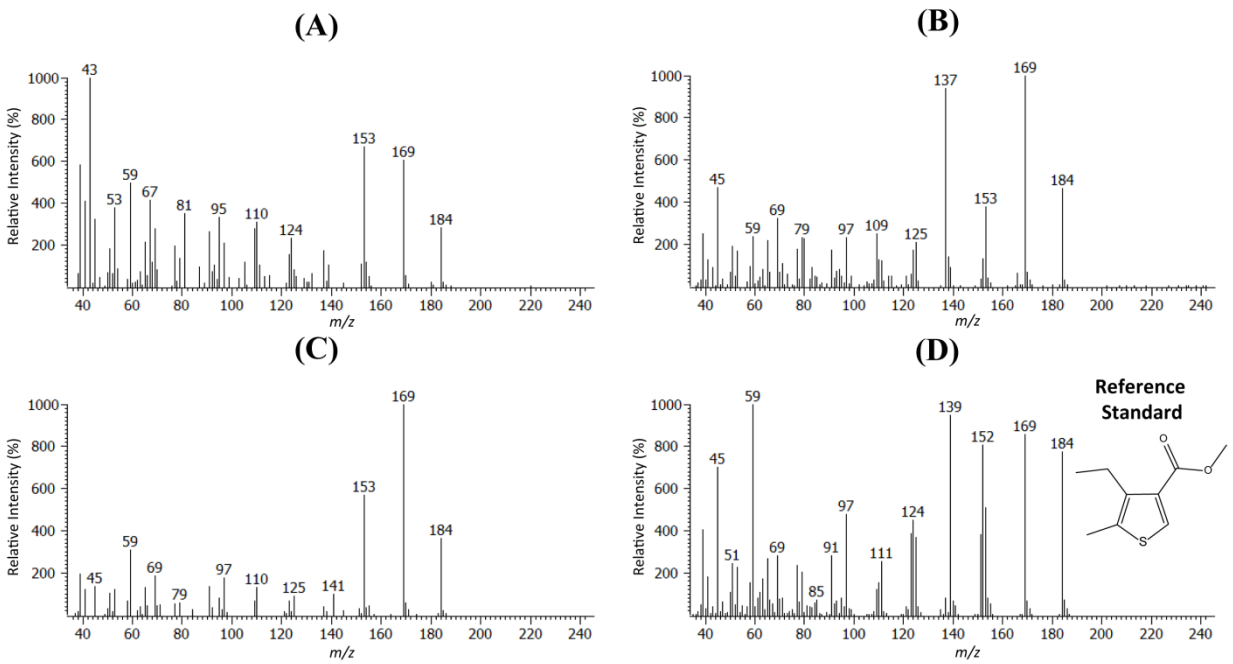

Figure 4. EI mass spectra of: (A–C) unknown compounds tentatively identified as methyl esters of C_3-thiophenecarboxylic acids and (D) authentic standard of the methyl ester of 4-ethyl- 5-methylthiophene-3-carboxylic acid.

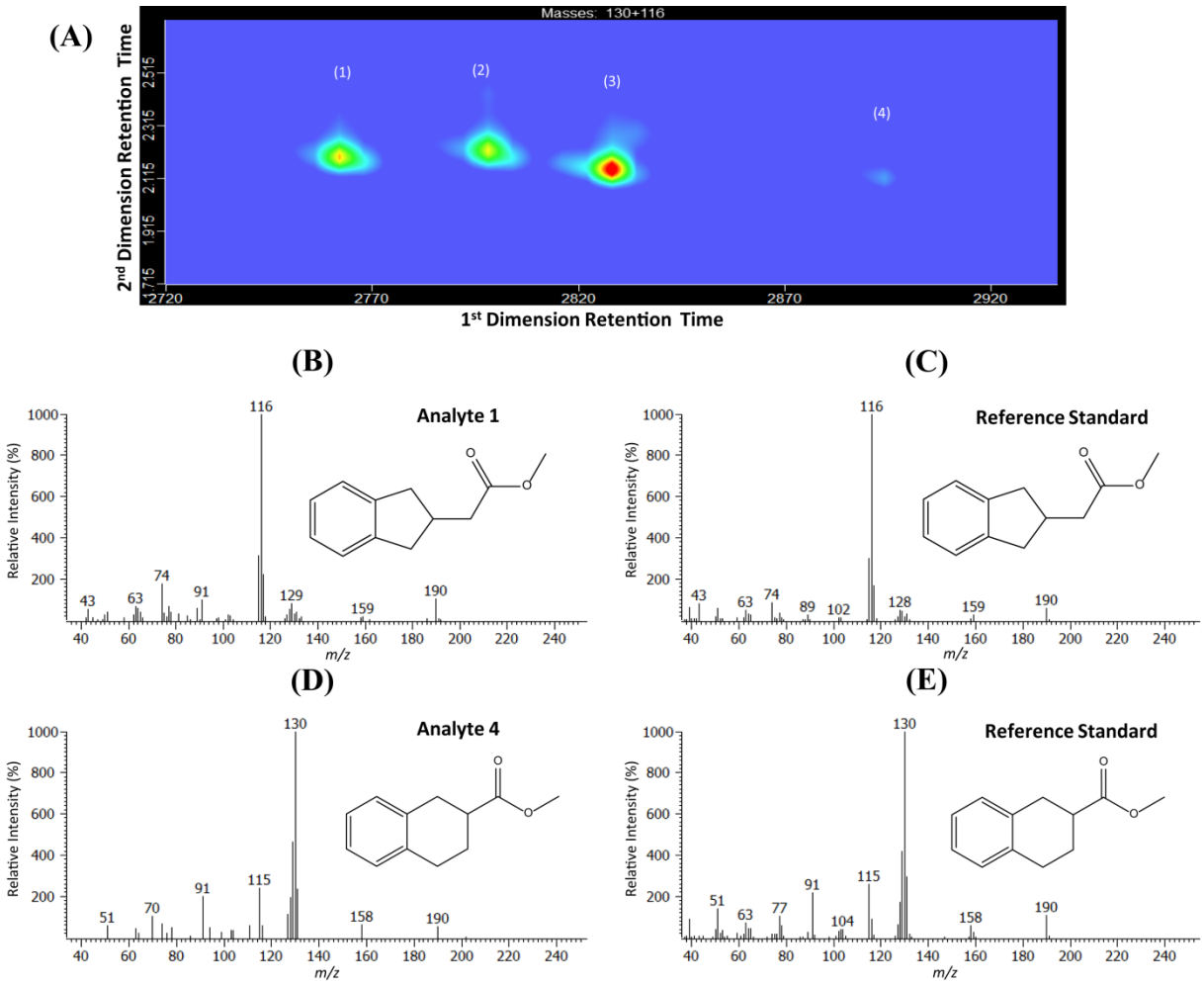

Figure 5. (A) GC×GCTOFMS EIC contour plot (m/z 130+116) showing the chromatographic resolution of the methyl esters of the indane- and tetralin-type acids identified in pore water. (B–E) EI mass spectra of the methyl esters of: (B) 2-indanylacetic acid; (C) authentic standard of (B); (D) tetralin-2-carboxylic acid; and (E) authentic standard of (D).

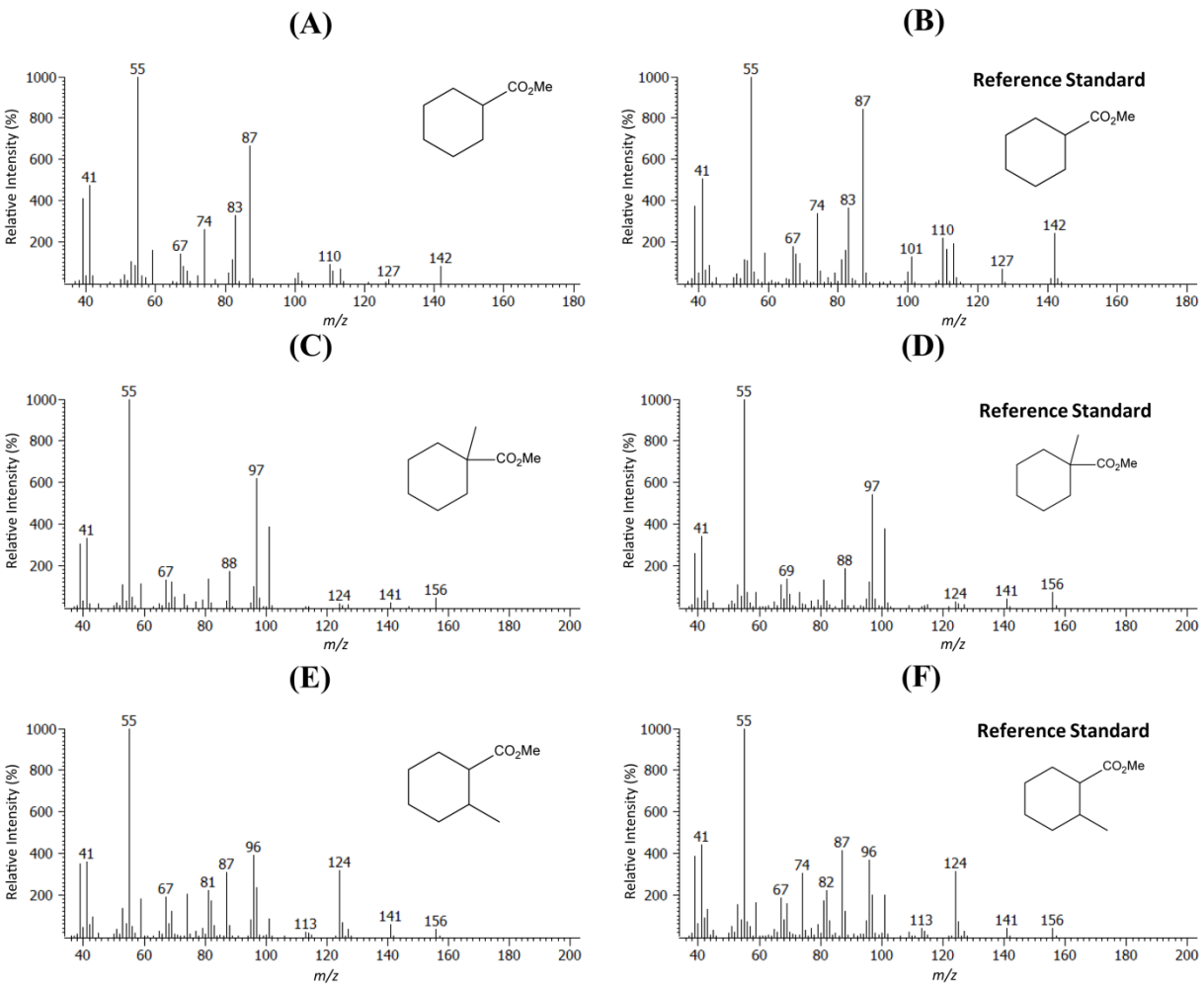

Figure 6. EI mass spectra of the methyl esters of: (A) cyclohexane carboxylic acid; (B) authentic standard of (A); (C) 1-methylcyclohexane-1-carboxylic acid; (D) authentic standard of (C); (E) 2-methylcyclohexane-1-carboxylic acid; and (F) authentic standard of (E).

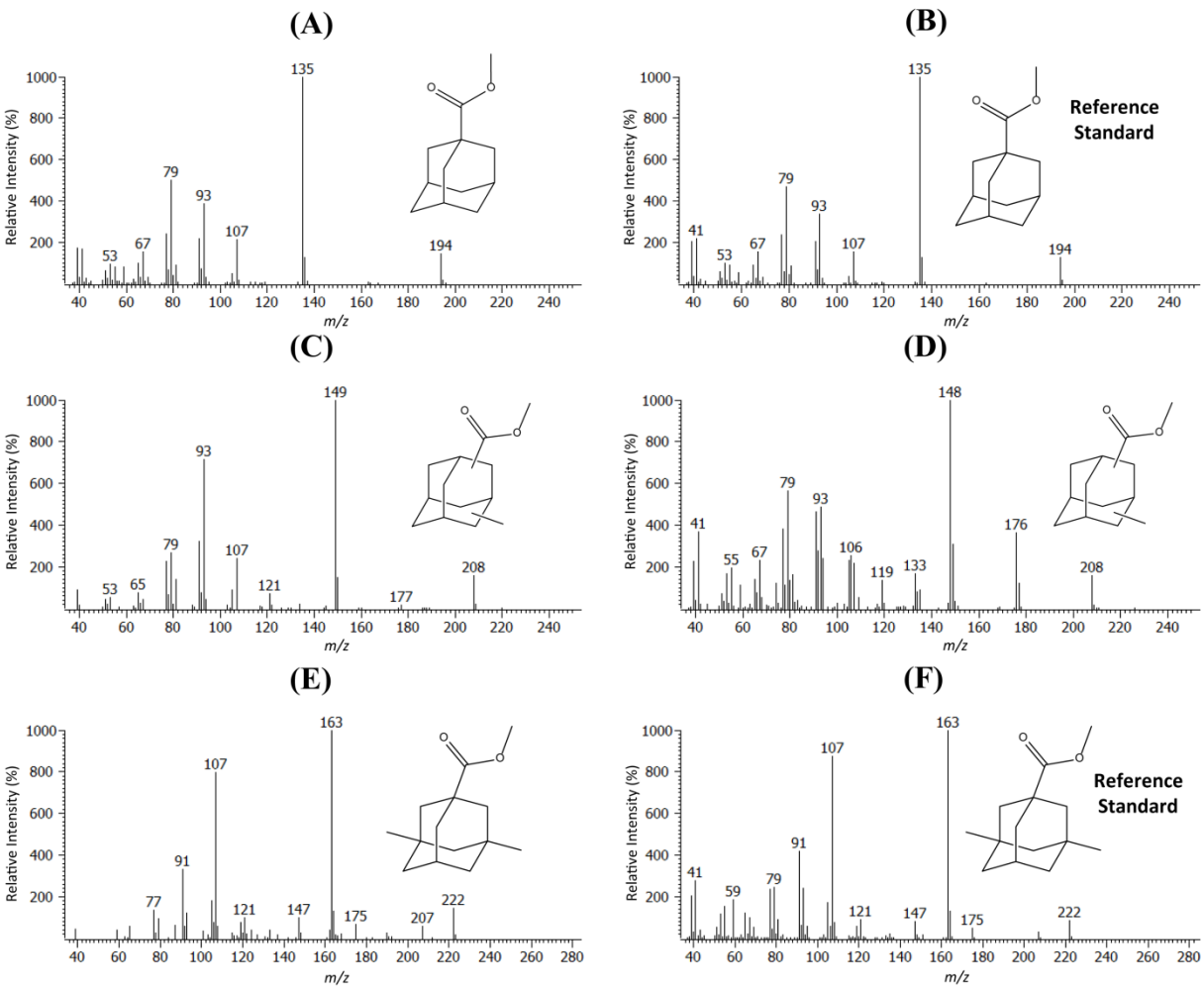

Figure 7. EI mass spectra of the methyl esters of: (A) adamantane-1-carboxylic acid, (B) authentic standard of (A); (C, D) unknown compounds tentatively identified as methyladamantane carboxylic acids; (E) 3,5-dimethyladamantane-1-carboxylic acid; (F) authentic standard of (E)

Supporting Information

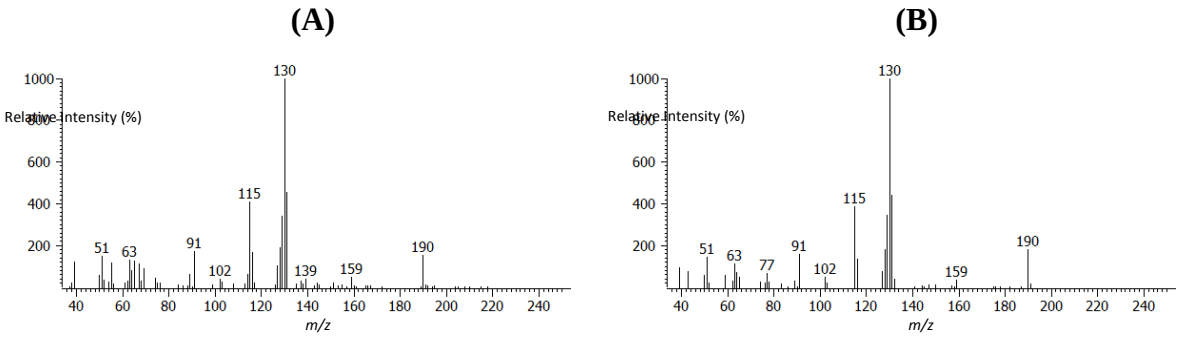

Figure S1. EI mass spectra of two unknowns whose spectra are very close to that of the methyl ester of tetralin-2-carboxylic acid.

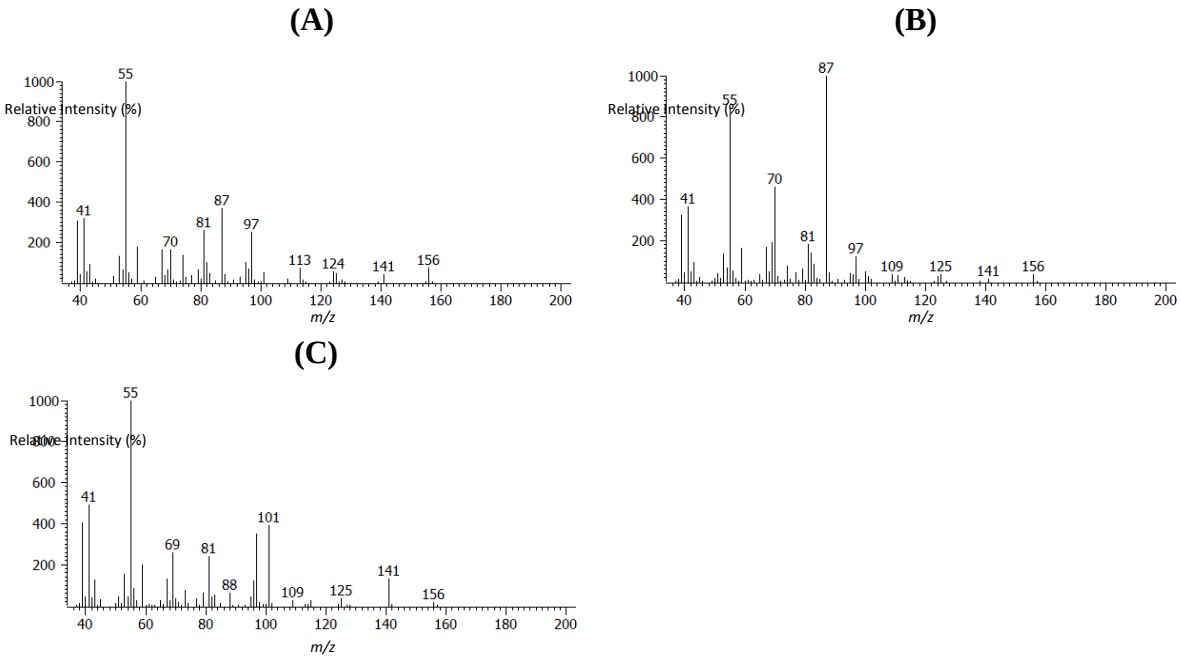

Figure S2. EI mass spectra of three additional unknown compounds tentatively identified as methyl esters of C_1-cyclohexane- and/or C_2-cyclopentane-carboxylic acids.

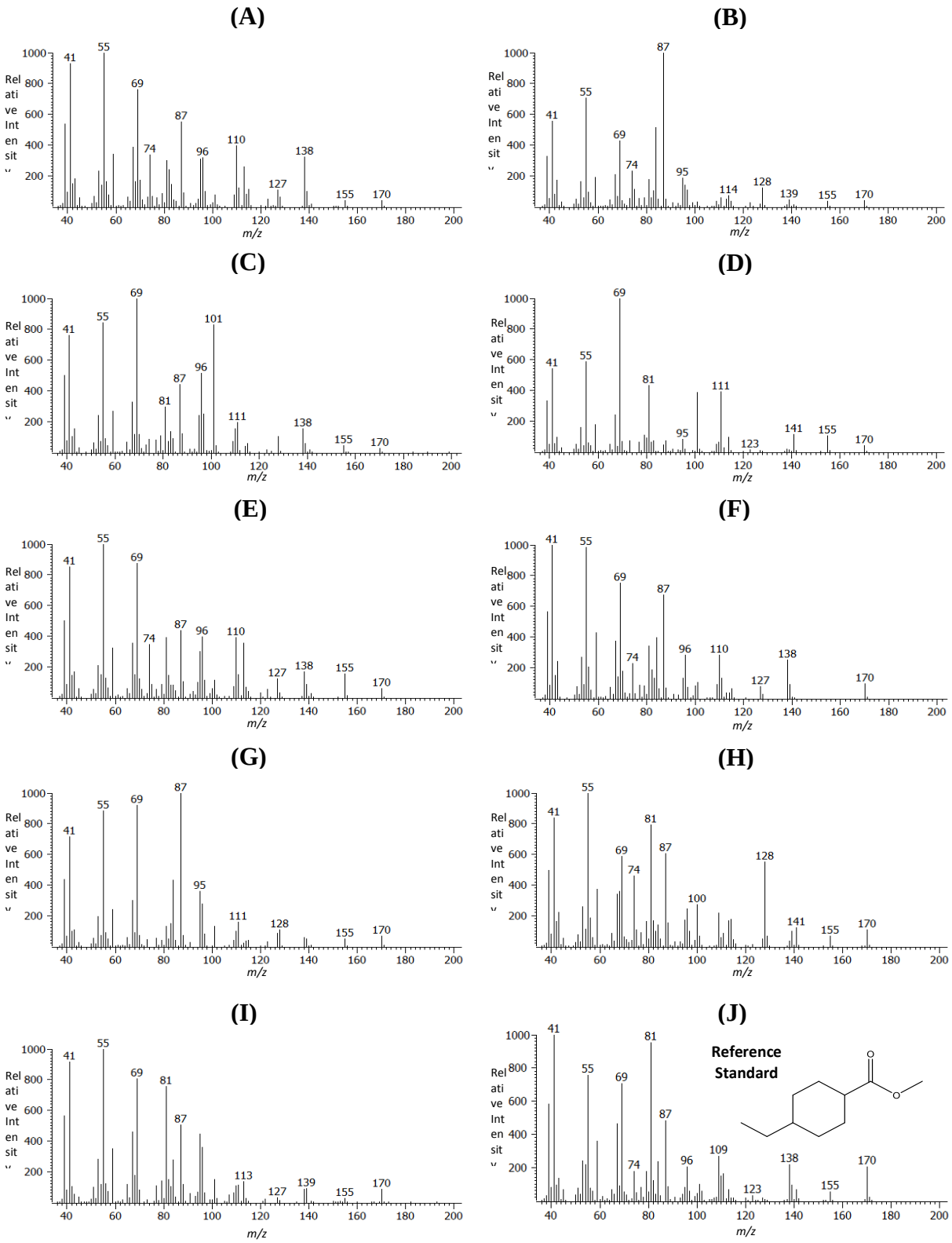

Figure S3. EI mass spectra of: (A-I) unknown compounds tentatively identified as the methyl esters of C_2-cyclohexane- and/or C_3-cyclopentane-carboxylic acids; (J) authentic standard of the methyl ester of 4-ethylcyclohexane-1-carboxylic acid.

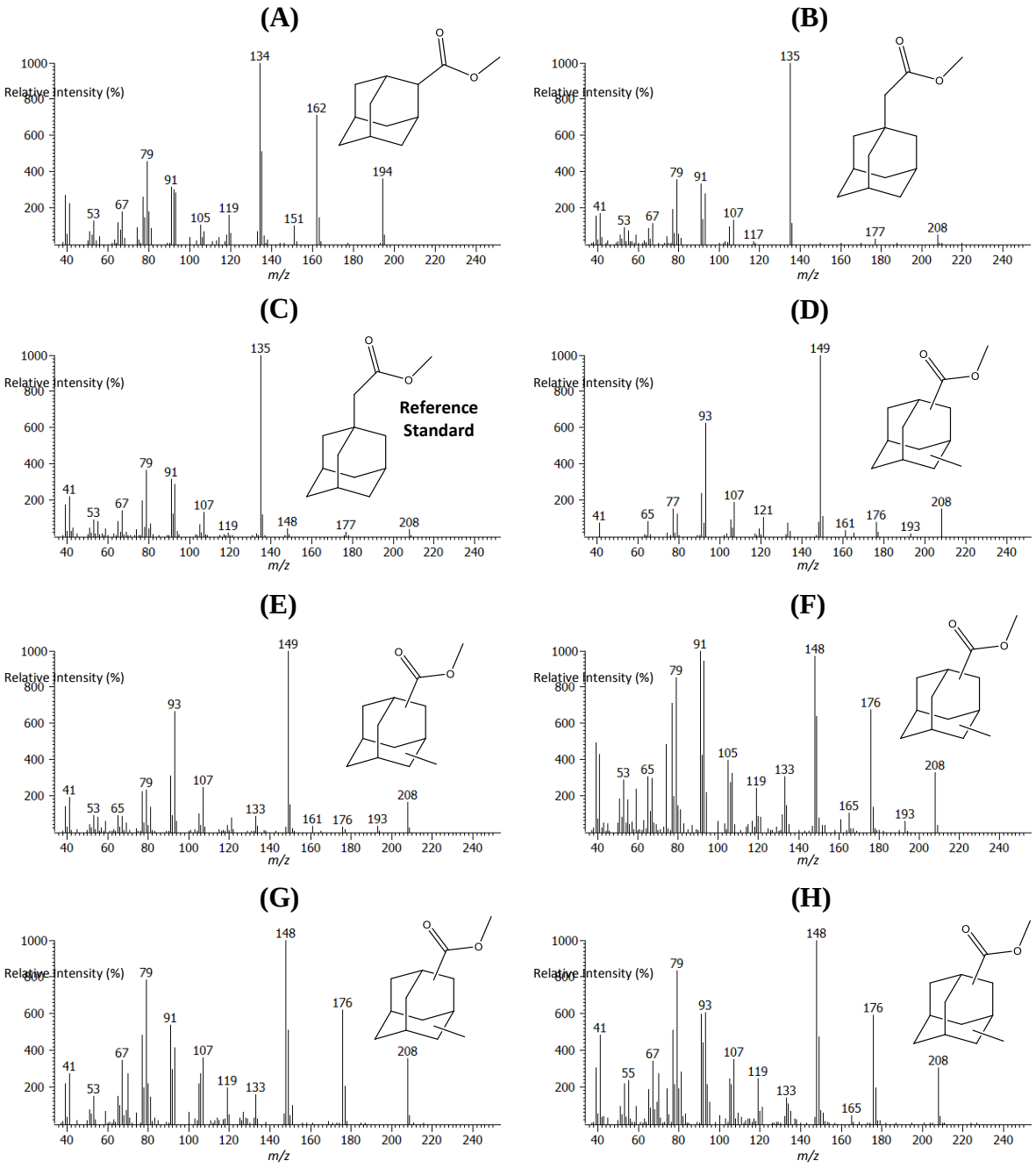

Figure S4. EI mass spectra of the methyl esters of: (A) adamantane-2-carboxylic acid; (B) adamantane-1-acetic acid; (C) authentic standard of (B); (D-H) unknown compounds tentatively identified as methyl esters of methyladamantanecarboxylic acids.

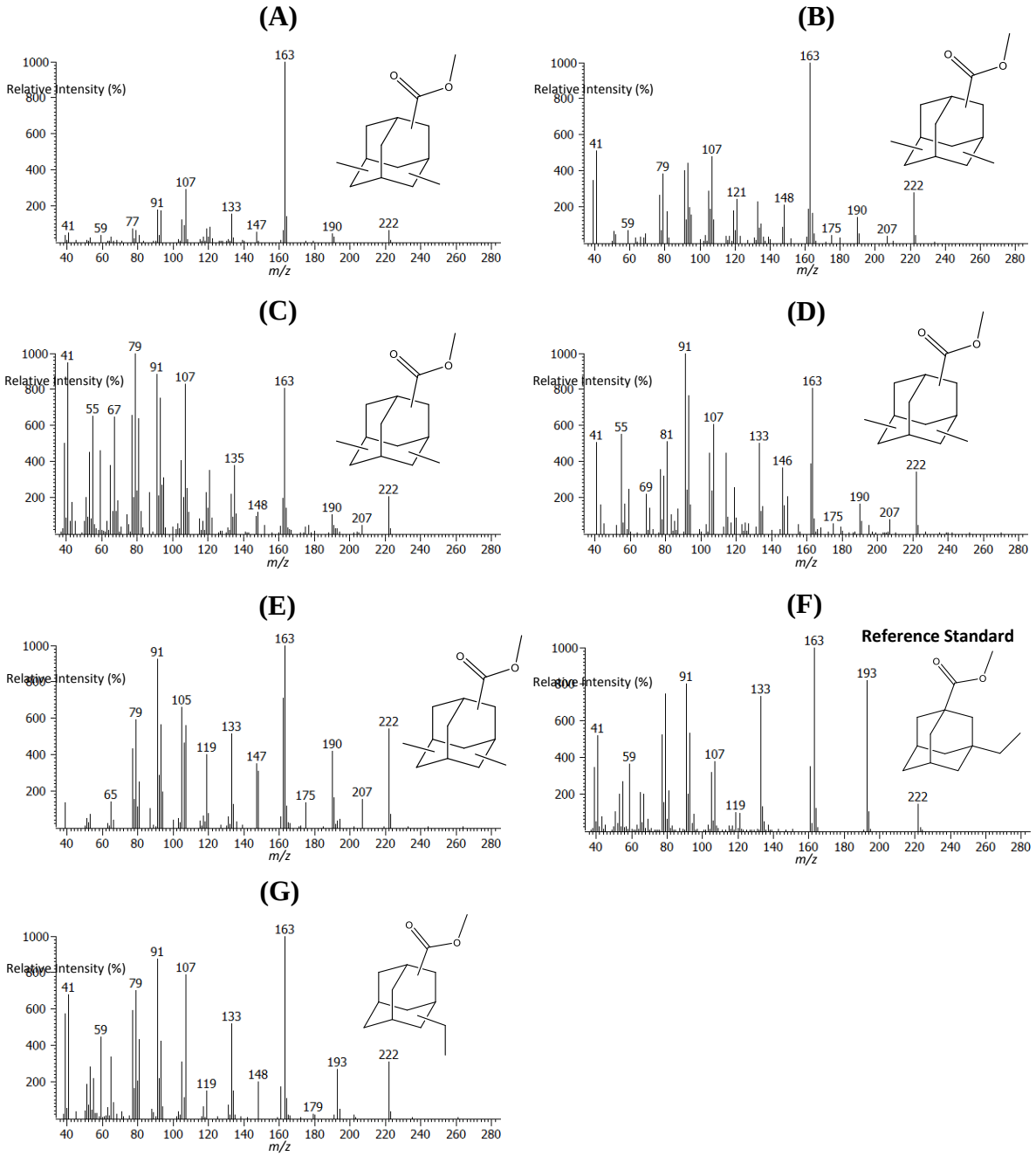

Figure S5. EI mass spectra of the methyl esters of: (A-E) unknown compounds proposed to be isomers of 3,5-dimethyladamantane-1-carboxylic acid; (F) 3-ethyladamantane-1-carboxylic acid (authentic standard); (G) unknown compound proposed to be an isomer of (F).

Chapter Three: Profiling of individual naphthenic acids at a composite tailings reclamation fen by comprehensive two-dimensional gas chromatography-mass spectrometry

David T. Bowman[1], Brian E. McCarry[1], Lesley A. Warren[2,3], Gregory F. Slater[1,2]

The work in this chapter has been submitted to a peer-reviewed journal.

Author Affiliations:

[1]Department of Chemistry and Chemical Biology, McMaster University, 1280 Main Street West, Hamilton, ON, Canada, L8S 4M1
[2]School of Geography and Earth Sciences, McMaster University, 1280 Main Street West, Hamilton, ON, Canada, L8S 4K1
[3]Department of Civil Engineering, University of Toronto, 35 St. George Street, Toronto, ON, Canada, M5S 1A4

Author Contributions:

BEM, GFS, and LAW conceived and designed the study. DTB performed the sample extraction, GC×GC/TOFMS instrumental analysis, data analysis and interpretation, and wrote the manuscript. GFS and LAW edited the manuscript.

Abstract

Naphthenic acids (NAs) are naturally occurring in the Athabasca oil sands region (AOSR) and accumulate in tailings as a result of water-based extraction processes. NAs exist as a complex mixture, so the development of an analytical technique to characterize them has been an on-going challenge. The monitoring of individual NAs and their associated isomers by multidimensional chromatography has the potential to provide greater insight into the behavior of NAs in the environment. The aim of this study was to use comprehensive two-dimensional gas chromatography time-of-flight mass spectrometry to monitor individual naphthenic acids within a wetland reclamation site in the AOSR. Samples were collected from four monitoring wells at the site and the extracts were found to contain numerous isomers of monocyclic-, bicyclic-, tricyclic-, indane-, and tetralin-type carboxylic acids from the O_2 chemical class, and monocyclic- and thiophene-type carboxylic acids from the SO_2 chemical class. NA profiles (comprised of resolved NAs possessing the aforementioned structural moieties) were normalized to the C_{11} tricyclic carboxylic acids (adamantane-1- and -2-carboxylic acid), and distinct distributions were observed at each site. Few significant changes were observed over the sampling period, with the exception of one well (Well 6A). At Well 6A, many isomers of monocyclic (O_2 class) and sulfur-containing NAs underwent significant decreases over the sampling period of the study, which we propose may be caused in part by the downward movement of freshwater from the fen. In addition, percentage compositions were calculated for each set of structural isomers, and multivariate statistical analyses (principal component analysis and hierarchical cluster analysis) revealed high spatial variation at the site. However, consistent distributions were observed for some sets of NA isomers (such as: C_{11}- and C_{12}-tricyclic carboxylic acids, and the C_{10}- and C_{11}-bicyclic carboxylic acids). Hierarchical cluster analysis was able to differentiate NA isomer distributions associated with the sand cap from the composite tailings deposit. The methods and results presented in this study shed light on the occurrence of NA isomer distributions at a wetland reclamation site and are not only of relevance to the Alberta Oil Sands, but also to other petroleum deposits.

1. Introduction:

The Alberta oil sands is the third largest oil reserve in the world and is estimated to contain over 170 billion barrels of oil.[1,2] The warm water caustic extraction of bitumen generates tailings as a by-product, which are comprised of oil sands process-affected water (OSPW), solids (eg. sand, silt and clay), unrecovered bitumen, and dissolved metals and organic compounds.[3] Naphthenic acids (NAs) are naturally occurring in oil sands deposits and accumulate in OSPW and tailings porewater.[4] NAs are traditionally defined as a complex mixture of alkyl-substituted aliphatic and alicyclic monocarboxylic acids ($C_nH_{2n+Z}O_2$, where n = carbon number, Z = degree of unsaturation), but the definition has been expanded in recent years to include chemical species with aromatic ring functional groups, sulfur and/or nitrogen heteroatoms, and mono- and polyoxygenated substituents[5–8]. NAs are of environmental interest because they have been linked with the acute and chronic toxicity of OSPW[9–11], and have the potential to migrate from tailings impoundments into natural systems via surface and/or groundwater exchange.[12–14] The monitoring of NAs derived from oil sands processing in natural waters is complicated due to: (a) the extreme complexity of NA compositions, (b) the lack of knowledge of compositional differences within source OSPW samples (e.g.: between industries and spatial variations within tailing ponds), and (c) natural inputs of NAs into river and groundwater systems via the erosion of exposed oil sands deposits. The combination of these factors creates significant challenges in differentiating sources and/or demonstrating biodegradation of these compounds in environmental systems which need to be addressed in order to demonstrate the effectiveness of reclamation activities.

Mass spectrometry (MS) has emerged in recent years as the most effective analytical tool for the characterization of NA mixtures. Notable applications of MS-based techniques (often coupled with offline and/or online fractionation) for the analysis of NAs have been summarized in recent review articles.[15,16] Comprehensive two-dimensional gas chromatography mass spectrometry (GC×GC/MS) is a promising tool in the field of environmental forensics[17–22] and has been applied in recent studies related to the Alberta oil sands[23–25]. GC×GC coupled with nominal[26–30] and high resolution[31–33] MS has been used to significantly improve the chromatographic separation of NAs, allowing the resolution of structural isomers and other isobaric interferences, and facilitating the structural elucidation of many individual NAs[27,34–36,30,37–40]. The profiling of structural isomers via multidimensional chromatography has the potential to shed light on the occurrence and fate of NAs in tailing ponds and the greater environment. It has been shown that the biodegradation of NAs is structure specific, and the position/degree of alkyl branching can impact the extent of their transformation.[41–45] Therefore, resolved isomer profiles generated by GC×GC/MS may be able to detect subtle differences in NA compositions which, when analyzed by direct infusion MS or separation techniques with lower peak capacity, are masked by the co-elution of structural isomers and/or other isobaric interferences.

In recent years, a few studies have begun to explore the application of GC×GC/MS in oil sands forensics. The proof-of-concept study by Rowland *et al.*[46] demonstrated that distributions of methyl esters of adamantane carboxylic acids resolved by GC×GC/MS could be used to differentiate two OSPW samples from different industries. The authors suggested that variations between the two samples may reflect differences in the extent of biotransformation of OSPW. Frank *et al*[25] used GC×GC/MS and Orbitrap MS (with negative electrospray ionization) to distinguish OSPW contamination in groundwater systems from waters exposed to natural bitumen deposits. The authors reported that OSPW sources were characterized by the presence of two families of steroidal-type monoaromatic NAs (detected by GC×GC/MS) and measurements of high O_2:O_4 ion class ratios (detected by Orbitrap MS). In a recent study[24], a suite of advanced analytical techniques (e.g.: GC×GC/MS, synchronous fluorescence spectroscopy, liquid chromatography-quadrupole time-of-flight mass spectrometry, gas chromatography-quadrupole time-of-flight mass spectrometry) were used to characterize the short-term temporal and pond-scale spatial variations of two OSPW sample sets. The GC×GC/MS method was applied to the sample sets in two companion studies: Frank *et al.*[24] monitored the suspected monoaromatic carboxylic acids, and Lengger *et al.*[47] monitored distributions of adamantane mono- and dicarboxylic acids[47]. The authors reported that the greatest differences were observed for the pond-scale spatial sample set, and the differences were most likely caused by differences in tailing inputs and surface run-off. However, despite the recent studies, there still remains a lack of knowledge in the occurrences of many of the other NAs identified in OSPW and related samples, such as cyclohexane-[29,30,40], bicyclic-[29,39], tetracyclic-[35], pentacyclic-[35], indane-[34,30], tetralin-[34,30], and thiophene-type[30] carboxylic acids. The aforementioned NAs have been reported to contain diverse isomers distributions, which may be useful from a monitoring perspective.

In this study, we report the use of comprehensive two-dimensional gas chromatography time-of-flight mass spectrometry (GC×GC/TOFMS) to profile resolved components within the NA mixture at Syncrude Canada's Sandhill Fen reclamation site. Numerous isomers of monocyclic-, bicyclic-, tricyclic, monoaromatic bicyclic-type carboxylic acids from the "O_2" chemical class, and monocyclic- and thiophene-type carboxylic acids from the "SO_2" chemical class were detected in the extracts. NA profiles, consisting of isomeric carboxylic acids possessing the aforementioned structural moieties, were normalized to the C_{11} tricyclic NAs (adamantane-1-carboxylic acid and adamantane-2-carboxylic acid), and the relative abundances were used to evaluate the temporal and spatial variation at the site. Furthermore, percent compositions were calculated for each set of structural isomers to further assess the variability of isomer distributions for each elemental composition identified at the site.

2. Materials and Methods:

2.1 Site Description:

The field investigation was carried out at Syncrude's pilot wetland reclamation project, Sandhill Fen Reclamation Site. This site is located in Syncrude's East-In pit, north of Fort McMurrary, AB, Canada (57°02'23.6"N 111°35'30.0"W). At this site, an open-cast mine pit was in-filled with 35 m of composite tailings material over an 8 year period.[3F9] Composite tailings is formed by combining fluid fine tailings (FFT) with post-processed sand and gypsum ($CaSO_4 \bullet 2H_2O$; 1 kg per m3 of FFT). Gypsum acts as a coagulant and accelerates the dewatering of FFT. In 2009, the CT deposit was capped with 10 m of processed tailings sand. A 0.5 m layer of clay-till was placed over the sand cap as a base for wetland construction, and development of the wetland began in the summer of 2011.[49] First, stockpiled and salvaged peat materials from a nearby mine site were placed on top of the clay-till layer, and then the peat was seeded with fen vegetation. The wetland was then established by flooding the fen with freshwater from the Mildred Lake Reservoir in May 2012.

2.2 - Pore Water Sampling:

Water samples (grab samples, volumes: 500 mL) were collected from four monitoring wells at the site. There were two monitoring wells installed which sampled the intermediary sand cap (Well 6A: 9.7 m depth; and Sump Vault: 10 m depth), and two wells which sampled the CT deposit (Well 8C: 25 m depth; and Well 5D: 17 m depth). A map of the study site and well locations is shown in Figure S1. Each monitoring well was sampled at least three times and monitored for over a one year period. Well 6A was sampled on July 27 2011, May 30 2012, and Nov 6 2012; Sump Vault was sampled on July 27 2011, May 30 2012, August 7 2012, and November 6 2012; Well 8C was sampled on July 27 2011, May 30 2012, and August 8 2012; Well 5D was sampled on July 27 2011, May 30 2012, and July 13, 2013. Pore water samples were collected from the site by an inertial lift pump system and were stored in pre-cleaned Nalgene plastic bottles. All samples were kept on ice until they could be stored in a freezer at -20°C.

2.3 - Chemicals and Reagents:

Dichloromethane (distilled in glass) was purchased from Caledon Laboratories (Georgetown, Ontario, Canada). The following compounds were purchased and used as recovery/internal standards in this study: 2-Hexyldecanoic acid (96%, Sigma-Aldrich), 4-tertbutylcyclohexane-1-carboxylic acid (99%, Sigma-Aldrich), and phenyl-1-cyclohexane carboxylic acid (98%, Sigma-Aldrich).

2.4 - Extraction Procedure:

The pore water samples were extracted using a methodology described in a previous study.[30] Briefly, water samples (20 mL) were filtered with an Acrodisc 0.45 µm syringe filter (Gelman Sciences, Ann Arbor, MI, USA) to remove suspended particles, and the pH was lowered to < 2 using concentrated HCl. The water samples were then extracted with dichloromethane (4 x 15 mL). The extracts were combined was then concentrated to 30 µL by use of a rotary evaporator, followed by blowing gently with nitrogen. The carboxylic acids were converted to methyl esters by adding diazomethane (dissolved in dichloromethane) dropwise to the sample until the yellow colour persisted. Methyl 2-hexyl-decanoate dissolved in dichloromethane was added to the samples as an internal standard following derivatization (final concentration: 1 ng/µL). 4-tertbutylcyclohexane-1-carboxylic acid and phenyl-1-cyclohexane carboxylic acid were added as recovery standards to assess extraction efficiency.

2.5 - Instrumental Analysis:

The methylated extracts were analyzed using a Pegasus 4D system (LECO Corp., St Joseph, MI, USA). The instrument utilized Rtx-17sil ms (30 m x 0.25 mm x 0.15 µm) as the primary column and DB-5 ms (1.5 m x 0.10 mm x 0.10 µm) as the secondary column. The primary oven was programmed to hold at 40 °C for one minute, ramp to 310 °C at a rate of 2.5 °C/min, and hold at 310 °C for 20 min. The secondary oven offset was set to +5 °C relative to the primary oven. A modulation period of 5.5 s was used. The modulator temperature offset was +15 °C relative to the secondary oven. The ion source and transfer line temperatures were set to 200 °C and 280 °C, respectively. Helium was used as the carrier gas at a flow rate of 1 mL/min. The time-of-flight mass spectrometer was scanned over a mass range of m/z 30 to 500 at a sample acquisition rate of 200 scans/s. Data processing of GC×GC/TOFMS data was performed by ChromaTOF version 4.50.8.0 (LECO Corp), which included automatic peak finding with mass spectral deconvolution. Library searches were conducted with the NIST/EPA/NIH Mass Spectral Library 2008 (NIST 08, Gaithersburg, MC, USA) and a user library containing NA reference standards.

2.6 –Identification of Naphthenic Acids

The identification of NAs in this study was reliant on the comparison of the relative retention times and mass spectra of unknowns with: (a) the retention times and mass spectra of authentic standards, (b) mass spectra from the NIST08 database, and (c) mass spectra found in literature[27,40,39,50–52]. When the aforementioned materials were not available, NAs were tentatively identified by manual mass spectral interpretation. The EI mass spectra for all of the NAs monitored in this study are presented in a mass spectral library report in the SI. The identifications of the monocyclic, tricyclic, monoaromatic bicyclic (indane and tetralin-type) carboxylic acids from the O_2 chemical class and thiophene carboxylic acids from the SO_2 chemical class have been discussed in a previous study[30]. Discussion of the identifications of the

bicyclic carboxylic acids from the O_2 class and the sulfur-containing monocyclic carboxylic acids (speculated to possess a tetrahydrothiophene and/or thiacyclohexane ring structure) are found in the SI. The plots of the retention times for the sulfur-containing monocyclic carboxylic acids and bicyclic carboxylic acids are shown in Figure S2.

2.7 – Statistical Analysis

Univariate statistical analysis was carried out using SPSS statistical software package (Version 17.0.0, SPSS Inc., Chicago, Il, USA). Data was tested for normality and homogeneity of variance using Shapiro-Wilk ($\alpha = 0.05$) and Levene's test ($\alpha = 0.05$), respectively. Data which did not meet the parametric assumptions of normality and homoscedasticity was log transformed. One-way analysis of variance (ANOVA) with $p < 0.01$ was used to test for differences between three or more means. Student's t-test was used to test for differences between two means, with $p < 0.01$. Volcano plots were used to visualize changes within wells between sampling dates. Differences were determined to be significant when fold change (FC) > ±1.5 and $p < 0.01$. Principal component analysis (PCA) and combined heat map and hierarchal cluster analysis (HCA) were performed using MetaboAnalyst 3.0.[53] HCA was based on Pearson distances and Ward clustering algorithm. PCA and HCA were performed on log-transformed and autoscaled data. NAs which were not detected in more than 60% of the samples were removed from the dataset prior to PCA and HCA.

3. Results and Discussion:

3.1 Detection of Relative Changes in NA Profile via the Monitoring of Individual NAs

Figure 1 displays a typical two-dimensional total ion current chromatogram (TIC) of a methylated pore water extract, and the complex nature of NA mixtures is clearly demonstrated. A total of 110 resolved NAs belonging to 15 elemental compositions were identified within the pore water extracts. Table 1 summarizes the number of isomers from each compound class which were detected at the four monitoring wells. Consistent with previous studies employing multidimensional chromatographic separation for the analysis of NAs[26,27,29,40], numerous structural isomers were detected for each elemental composition.

An objective of this study was to assess whether the monitoring of individual NAs via GC×GC could shed light on temporal and spatial variations of the NA profile at Sandhill reclamation fen. In order to differentiate the effects of differing levels of dilution from compositional changes in the NA profile, the suite of identified NAs were normalized within each sample to the C_{11} tricyclic carboxylic acids (adamantane-1-carboxylic acid and adamantane-2-carboxylic acid). The C_{11} tricyclic carboxylic acids were selected to normalize each sample because the two isomers were observed to be prominent, stable components of the

NA mixture. The ratio of the two C_{11} tricyclic carboxylic acids did not significantly differ between the extracts from the four monitoring wells (one-way ANOVA: p = 0.448). Furthermore, the ratio of the total C_{12} tricyclic carboxylic acids over the total C_{11} tricyclic carboxylic acids was found to be statistically similar at each of the monitoring wells following one-way ANOVA (p = 0.376).The extracted ion chromatograms displayed in Figure 2 show that the full suite of C_{11} and C_{12} tricyclic carboxylic acids could be detected at each well, with the same relative abundance.

Principal component analysis (PCA) was performed on the normalized dataset, and high spatial variation was observed at the site. The PCA scores plot presented in Figure 3 shows that the pore water extracts from Sump Vault, Well 8C, and Well 5D clustered based on their sampling location. The pore water extracts from Well 6A were distinguished from the other wells, but were also separated from each other along PC1. This suggests that components within the NA mixture at Well 6A were undergoing a compositional change over the sampling period. The heat map presented in Figure S3, which illustrates the relative abundance of each profiled NA, is consistent with the PCA scores plot and clearly shows that unique patterns are observed at each well.

Volcano plots (see Figure S4) were used to visualize the number of NAs which were significantly changed within each monitoring well (compared to the first sampling time point, July 27 2011). Tables S1- S6 lists the significantly altered NAs from each sampling date, along with their calculated fold changes and *p*-values. Well 6A displayed the greatest number of significantly altered NAs. The samples collected on May 2012 and November 2012 from Well 6A possessed 12 and 46 significantly altered NAs, respectively. Worthy of note, the significantly altered NAs from Well 6A were predominantly monocyclic NAs from the O_2 class and sulfur-containing NAs. The sample collected from Well 6A on November 2012 possessed 10 monocyclic NAs and 29 sulfur-containing NAs which underwent a significant decrease relative the first sampling period.

In contrast to Well 6A, very few changes were observed at the other wells from the site. At Well 8C, there were two altered NAs detected in the samples from May 2012 and August 2012, both of which were sulfur-containing NAs. At Well 5D, ten and eight NAs were significantly altered on May 2012, and July 2013, respectively. There were no significant changes observed in the normalized NA profile at the sump vault. Worthy of note, the magnitudes of the fold changes at Well 6A were much greater than the other wells (see Figure S4).

3.2 Evaluation of NA Isomer Distributions at Sandhill Fen

While it has been established that numerous structural isomers exist for many chemical moieties within OSPW and petroleum samples, the spatial variability of such isomer

distributions are not well understood. Percentage compositions were calculated for each set of structural isomers to evaluate the variability of isomer distributions at the site. Briefly, the peak areas of each isomer was divided by the sum of the peak areas of all structural isomers detected in more than 60 percent of the samples from the dataset. Non-detects that remained were replaced with half of the lowest value in the dataset, with the assumption that the missing values were due to compounds being present below the detection limit.

Multivariate statistical analyses of the percentage composition dataset revealed that unique NA isomer distributions were detected at each monitoring well. The combined heat map and HCA dendrogram plot (shown in Figure S5) visualizes the relative abundances of each NA's percent composition within its congener group, and the differences between the monitoring wells are clearly observed. The HCA dendrogram plot shows that the pore water extracts are segregated into two major clusters: extracts that originate from (1) the CT deposit and (2) the sand cap. Each cluster is further differentiated into subclusters based on the monitoring well. Principal component analysis (PCA) was also performed on the dataset and the two-dimensional scores plot is presented in Figure 4. It is revealed that the two components explained over 76% of the variance in the dataset. The sand cap and CT deposit samples could be distinguished along PC1. Similar to the HCA results, the pore water extracts were observed to tightly cluster in the PCA scores plot based on their sampling location, indicating the presence of relatively stable fingerprints at each monitoring well.

As mentioned in the previous section, the profiles of tricyclic NAs from the O_2 chemical class were consistent between the four monitoring wells. The percentage composition graphs for the C_{11} and C_{12} tricyclic NAs are presented in Figure 5. In contrast to the stable fingerprints of C_{11} and C_{12} tricyclic acids at Sandhill Fen, the occurrence of individual tricyclic carboxylic acids have been previously shown to be variable in tailing ponds from two un-named industries[47]. The authors reported that specific C_{11} and C_{12} tricyclic carboxylic acids (e.g.: adamantane-1-carboxylic acid, adamantane-2-carboxylic acid, 3-methyl-adamantane-1-carboxylic acid, and adamantane-1-acetic acid) could not be reliably detected in fresh OSPW samples from both industries. The FFT deposited at the site is expected to be more aged than the fresh OSPW samples from the study by Lengger *et al*.[47], so perhaps the reliable detection of adamantane acids at Sandhill fen is the result of the enrichment of adamantane carboxylic acids. Consistent with our observations, Fowler *et al*.[54] performed anaerobic degradation studies of model PAHs and NA surrogates and reported that adamantane-1-carboxylic acid was not degraded after 260 days by oil sands microbes under sulphate-reducing and methanogenic conditions.

Figure 6 displays the percentage graphs of the C_8 and C_9 bicyclic carboxylic acids from each sample in this study. The C_8 and C_9 bicyclic carboxylic acids displayed distinct isomer profiles at each monitoring well. The fingerprints of the C_8 bicyclic carboxylic acids were the most variable of the bicyclic acids. Figure 6a shows that Isomer 1 of the C_8 bicyclic carboxylic

acids was the most abundant isomer in Well 6A, representing an average of 82% (± 2) of the relative percentage composition for the set of isomers. At other sites at Sandhill Fen, Isomer 1 was less dominant, representing an average percentage of 45% ± 5, 17% ± 1, and 8% ± 3 at Sump Vault, Well 8C, and Well 5D, respectively. In contrast to the C_8, and C_9 bicyclic carboxylic acids, the relative abundances of the C_{10} and C_{11} bicyclic carboxylic acids were also consistent between the sampling wells (see Figure S6). The percentage compositions of the monocyclic (O_2), monocyclic (SO_2), and thiophene carboxylic acids were also calculated and are presented in the Figures S7, S8-9, and S10, respectively. Generally, the percentage compositions of the aforementioned naphthenic acids displayed unique fingerprints at each monitoring well.

As evident in Figures 4 and S5, the comparison of NA isomer distributions did not reveal the compositional changes that were observed by normalizing each analyte to the C_{11}-tricyclic carboxylic acids. The NA profile changes detected at Well 6A on November 2012 were predominantly driven by the simultaneous decrease of nearly all of the monocyclic carboxylic acids (O_2 class) and sulfur-containing carboxylic acids (see Table S2). Since the related isomers experienced similar fold changes, their relative proportions to one another did not significantly change relative to the first sampling event.

3.3 Implications for the monitoring of naphthenic acids

This study illustrates the use of GC×GC/TOFMS for the qualitative analysis of individual naphthenic acids at Sandhill Fen. It was demonstrated that by normalizing the NA profile to the C_{11} tricyclic carboxylic acids, it was possible to assess the spatial and temporal variability of individual NAs at the site. Well 6A showed the greatest fold changes (when compared to first sampling date), and it was observed that altered species were predominantly sulfur-containing carboxylic acids and monocyclic carboxylic acids (O_2 class). Worthy of note, the significant changes at Well 6A coincide with the flooding of the fen in May 2012. While some of the changes may be the result of the microbial degradation of NAs, the alterations may also be caused by the movement of water within the site and the mixing of sources. In a concurrent study at Sandhill fen[55], conservative salt tracers suggested the downward movement of water from the overlying fen into Well 6A. Dissolved sodium and chloride concentrations within pore water samples at Well 6A (samples collected on July and September 2013) were consistent with values from the overlying wetland, and were distinct from values measured at other wells within the sand cap and CT deposit. The downward migration of water from the fen to the sand cap of Sandhill fen was also supported by Bradford *et al*[56]. The authors demonstrated that microbial communities within the sand cap and composite tailings deposit were utilizing carbon sources whose $\Delta^{14}C$ signatures were consistent with measured $\Delta^{14}C$ values from the fen. In order to better elucidate the cause of the NA profile changes at Well 6A, it may be necessary perform laboratory degradation studies where the source water is well characterized and water movement is constrained. Understanding the biodegradation potential of individual NAs would help focus reclamation strategies for oil sands producers.

The NA isomer distributions were also evaluated for each elemental composition, and the percentage composition calculations revealed that distinct distributions were present at each monitoring well. It was shown that the relative proportions of structural isomers could be used to provide a fingerprint to distinguish samples from the composite tailings deposit and the sand cap. There are a few possible reasons why distinct isomer profiles were detected at each site. The composite tailings material was deposited at the site over an 8 year period, and since the locations of each well is spatially distinct (see Figure S1), it is likely that the tailings material across the site originates from different oil sands ore which contains a unique distribution of NAs. Furthermore, each of the wells monitored a different depth at the site and differences within each monitoring well may result from the weathering of NAs. The deeper CT material at the site is presumed to be more aged, relative to the more shallow CT material, and has likely been subjected to longer periods of natural attenuation processes which would be expected to alter NA isomer profiles. Table 1 reveals that Well 8C, the deepest well in this study (25 m depth), contains the lowest number of detected isomers.

A limitation of this study is the small number of monitoring wells sampled from Sandhill fen. Two wells were sampled within the sand cap and CT deposit, and each well monitored a different depth and spatial location at the site (see Figure S1). While the results clearly show that distinct NA profiles can be observed at each of the monitoring wells, a more in depth analysis of the spatial variability of the site would be useful to improve our understanding of NA mixtures. It would be valuable to understand the variability of isomer profiles with changes in depth or variations in small distances around a single location. Furthermore, the addition of ultrahigh resolution mass spectrometry would be complementary to the data obtained from GC×GC/MS experiments, since the accurate mass information obtained from such techniques can provide additional information for chemical species which were not monitored by GC×GC/MS in this study, and also analytes which are not amenable to GC analysis (see Barrow *et al.* [57] and Headley *et al.*[16] and references therein). The complementary nature of multidimensional chromatography-based techniques and ultrahigh resolution mass spectrometry has been demonstrated in recent environmental studies.[24,25,58–62]

Acknowledgements:

This manuscript is dedicated to the memory of Dr. Brian E. McCarry. Funding was provided by the Natural Sciences and Engineering Research Council of Canada and Syncrude Canada (CRDPJ 403361–10). The authors would like to thank Syncrude Canada Limited Reclamation and Closure Research Group for field sampling support, T. Colenbrander-Nelson, K. Kendra, and M. Reid for sample collection, Dr. Fan Fei for insightful discussions regarding chemometrics, and the Centre for Microbial Chemical Biology (CMCB) at McMaster University for access to the GC×GC/TOF-MS instrument.

Supporting Information:

Supporting information (SI) document contains: ten figures, six tables, and descriptions of identifications of bicyclic carboxylic acids and monocyclic sulfur-containing carboxylic acids.
An additional SI document contains a mass spectral library report for the profiled naphthenic acids.

References:

(1) Headley, J. V.; Peru, K. M.; Fahlman, B.; Colodey, A.; McMartin, D. W. Selective solvent extraction and characterization of the acid extractable fraction of Athabasca oils sands process waters by Orbitrap mass spectrometry. *Int. J. Mass Spectrom.* **2013**, *345–347*, 104–108.

(2) Ahad, J. M. E.; Pakdel, H. Direct evaluation of in situ biodegradation in athabasca oil sands tailings ponds using natural abundance radiocarbon. *Environ. Sci. Technol.* **2013**, *47* (18), 10214–10222.

(3) Allen, E. W. Process water treatment in Canada's oil sands industry: I. Target pollutants and treatment objectives. *J. Environ. Eng. Sci.* **2008**, *7* (2), 123–138.

(4) Giesy, J. P.; Anderson, J. C.; Wiseman, S. B. Alberta oil sands development. *Proc. Natl. Acad. Sci.* **2010**, *107* (3), 951–952.

(5) Grewer, D. M.; Young, R. F.; Whittal, R. M.; Fedorak, P. M. Naphthenic acids and other acid-extractables in water samples from Alberta: What is being measured? *Sci. Total Environ.* **2010**, *408* (23), 5997–6010.

(6) Headley, J. V.; Barrow, M. P.; Peru, K. M.; Derrick, P. J. Salting-out effects on the characterization of naphthenic acids from Athabasca oil sands using electrospray ionization. *J. Environ. Sci. Heal. Part A* **2011**, *46* (8), 844–854.

(7) Kavanagh, R. J.; Burnison, B. K.; Frank, R. A.; Solomon, K. R.; Van Der Kraak, G. Detecting oil sands process-affected waters in the Alberta oil sands region using synchronous fluorescence spectroscopy. *Chemosphere* **2009**, *76* (1), 120–126.

(8) Barrow, M. P.; Witt, M.; Headley, J. V.; Peru, K. M. Athabasca oil sands process water: Characterization by atmospheric pressure photoionization and electrospray ionization Fourier transform ion cyclotron resonance mass spectrometry. *Anal. Chem.* **2010**, *82* (9), 3727–3735.

(9) MacKinnon, M. D.; Boerger, H. Description of two treatment methods for detoxifying oil sands tailings pond water. *Water Qual. Res. J. Canada* **1986**, *21* (4), 496–512.

(10) Clemente, J. S.; Fedorak, P. M. A review of the occurrence, analyses, toxicity, and biodegradation of naphthenic acids. *Chemosphere* **2005**, *60* (5), 585–600.

(11) Brown, L. D.; Ulrich, A. C. Oil sands naphthenic acids: A review of properties, measurement, and treatment. *Chemosphere* **2015**, *127*, 276–290.

(12) Ross, M. S.; Pereira, A. dos S.; Fennell, J.; Davies, M.; Johnson, J.; Sliva, L.; Martin, J. W. Quantitative and qualitative analysis of naphthenic acids in natural waters surrounding the Canadian oil sands industry. *Environ. Sci. Technol.* **2012**, *46* (23), 12796–12805.

(13) Ferguson, G. P.; Rudolph, D. L.; Barker, J. F. Hydrodynamics of a large oil sand tailings impoundment and related environmental implications. **2009**, *1460*, 1446–1460.

(14) Oiffer, A. A. L.; Barker, J. F.; Gervais, F. M.; Mayer, K. U.; Ptacek, C. J.; Rudolph, D. L. A detailed field-based evaluation of naphthenic acid mobility in groundwater. *J. Contam. Hydrol.* **2009**, *108* (3–4), 89–106.

(15) Headley, J. V.; Peru, K. M.; Barrow, M. P. Advances in Mass Spectrometric Characterization of Naphthenic Acids Fraction Compounds in Oil Sands Environmental Samples and Crude Oil - A Review. *Mass Spectrom. Rev.* **2015**, *35* (2), 311–328.

(16) Headley, J. V; Mohamed, M. H.; Frank, R. A.; Martin, J. W.; Hazewinkel, R. R. O.; Humphries, D.; Gurprasad, N. P.; Hewitt, L. M.; Muir, D. C. G.; Lindeman, D.; et al. Chemical fingerprinting of naphthenic acids and oil sands process waters — A review of analytical methods for environmental samples. *J. Environ. Sci. Heal. Part A.* **2013**, *48* (10), 1145–1163.

(17) Llewellyn, G. T.; Dorman, F.; Westland, J. L.; Yoxtheimer, D.; Grieve, P.; Sowers, T.; Humston-Fulmer, E.; Brantley, S. L. Evaluating a groundwater supply contamination incident attributed to Marcellus Shale gas development. *Proc. Natl. Acad. Sci.* **2015**, *112* (20), 6325–6330.

(18) Megson, D.; Reiner, E. J.; Jobst, K. J.; Dorman, F. L.; Robson, M.; Focant, J.-F. A review of the determination of persistent organic pollutants for environmental forensics investigations. *Anal. Chim. Acta* **2016**, *941*, 10–25.

(19) Sampat, A.; Lopatka, M.; Sjerps, M.; Vivo-Truyols, G.; Schoenmakers, P.; van Asten, A. Forensic potential of comprehensive two-dimensional gas chromatography. *Trends Anal. Chem.* **2016**, *80*, 345–363.

(20) Frysinger, G. GC×GC—A New Analytical Tool For Environmental Forensics. *Environ. Forensics* **2002**, *3* (1), 27–34.

(21) Seeley, J. V.; Seeley, S. K. Multidimensional Gas Chromatography: Fundamental

Advances and New Applications. *Anal. Chem.* **2013**, *85* (2), 557–578.

(22) Hoh, E.; Dodder, N. G.; Lehotay, S. J.; Pangallo, K. C.; Reddy, C. M.; Maruya, K. A. Nontargeted comprehensive two-dimensional gas chromatography/time-of-flight mass spectrometry method and software for inventorying persistent and bioaccumulative contaminants in marine environments. *Environ. Sci. Technol.* **2012**, *46* (15), 8001–8008.

(23) Manzano, C. A.; Muir, D.; Marvin, C. Separation of thia-arenes and aza-arenes from polycyclic aromatics in snowpack samples from the Athabasca oil sands region by GC×GC/ToF-MS. *Int. J. Environ. Anal. Chem.* **2016**, *96* (10), 905–920.

(24) Frank, R. A.; Milestone, C. B.; Rowland, S. J.; Headley, J. V.; Kavanagh, R. J.; Lengger, S. K.; Scarlett, A. G.; West, C. E.; Peru, K. M.; Hewitt, L. M. Assessing spatial and temporal variability of acid-extractable organics in oil sands process-affected waters. *Chemosphere* **2016**, *160*, 303–313.

(25) Frank, R. A.; Roy, J. W.; Bickerton, G.; Rowland, S. J.; Headley, J. V.; Scarlett, A. G.; West, C. E.; Peru, K. M.; Parrott, J. L.; Conly, F. M.; et al. Profiling oil sands mixtures from industrial developments and natural groundwaters for source identification. *Environ. Sci. Technol.* **2014**, *48* (5), 2660–2670.

(26) Hao, C.; Headley, J. V.; Peru, K. M.; Frank, R.; Yang, P.; Solomon, K. R. Characterization and pattern recognition of oil–sand naphthenic acids using comprehensive two-dimensional gas chromatography/time-of-flight mass spectrometry. *J. Chromatogr. A* **2005**, *1067* (1–2), 277–284.

(27) Rowland, S. J.; Scarlett, A. G.; Jones, D.; West, C. E.; Frank, R. a. Diamonds in the rough: Identification of individual naphthenic acids in oil sands process water. *Environ. Sci. Technol.* **2011**, *45* (7), 3154–3159.

(28) Shepherd, A. G.; van Mispelaar, V.; Nowlin, J.; Genuit, W.; Grutters, M. Analysis of Naphthenic Acids and Derivatization Agents Using Two-Dimensional Gas Chromatography and Mass Spectrometry: Impact on Flow Assurance Predictions †. *Energy Fuels* **2010**, *24* (4), 2300–2311.

(29) Damasceno, F. C.; Gruber, L. D. A.; Geller, A. M.; de Campos, M. C. V.; Gomes, A. O.; Guimaraes, R. C. L.; Peres, V. F.; Jacques, R. A.; Caramao, E. B. Characterization of naphthenic acids using mass spectroscopy and chromatographic techniques: study of technical mixtures. *Anal. Methods* **2014**, *6*, 807–816.

(30) Bowman, D. T.; Slater, G. F.; Warren, L. A.; McCarry, B. E. Identification of individual thiophene-, indane-, tetralin-, cyclohexane-, and adamantane-type carboxylic acids in composite tailings pore water from Alberta oil sands. *Rapid Commun. Mass Spectrom.* **2014**, *28* (19), 2075–2083.

(31) West, C. E.; Scarlett, A. G.; Pureveen, J.; Tegelaar, E. W.; Rowland, S. J. Abundant naphthenic acids in oil sands process-affected water: studies by synthesis, derivatisation and two-dimensional gas chromatography/high-resolution mass spectrometry. *Rapid Commun. Mass Spectrom.* **2013**, *27* (2), 357–365.

(32) West, C. E.; Scarlett, A. G.; Tonkin, A.; O'Carroll-Fitzpatrick, D.; Pureveen, J.; Tegelaar, E.; Gieleciak, R.; Hager, D.; Petersen, K.; Tollefsen, K.-E.; et al. Diaromatic sulphur-containing "naphthenic" acids in process waters. *Water Res.* **2014**, *51*, 206–215.

(33) Bowman, D. T.; Jobst, K. J.; Ortiz, X.; Reiner, E. J.; Warren, L. A.; Mccarry, B. E.; Slater, G. F. Improved coverage of naphthenic acid fraction compounds by comprehensive two-dimensional gas chromatography coupled with high resolution mass spectrometry. *J. Chromatogr. A* **2017**. https://doi.org/10.1016/j.chroma.2017.07.017

(34) West, C. E.; Pureveen, J.; Scarlett, A. G.; Lengger, S. K.; Wilde, M. J.; Korndorffer, F.; Tegelaar, E. W.; Rowland, S. J. Can two-dimensional gas chromatography/mass spectrometric identification of bicyclic aromatic acids in petroleum fractions help to reveal further details of aromatic hydrocarbon biotransformation pathways? *Rapid Commun. Mass Spectrom.* **2014**, *28* (9), 1023–1032.

(35) Rowland, S. J.; West, C. E.; Scarlett, A. G.; Jones, D.; Frank, R. A. Identification of individual tetra- and pentacyclic naphthenic acids in oil sands process water by comprehensive two-dimensional gas chromatography/mass spectrometry. *Rapid Commun. Mass Spectrom.* **2011**, *25* (9), 1198–1204.

(36) Lengger, S. K.; Scarlett, A. G.; West, C. E.; Rowland, S. J. Diamondoid diacids ('O4' species) in oil sands process-affected water. *Rapid Commun. Mass Spectrom.* **2013**, *27* (23), 2648–2654.

(37) Rowland, S. J.; West, C. E.; Jones, D.; Scarlett, A. G.; Frank, R. A.; Hewitt, L. M. Steroidal aromatic Naphthenic Acids in oil sands process-affected water: Structural comparisons with environmental estrogens. *Environ. Sci. Technol.* **2011**, *45* (22), 9806–9815.

(38) Rowland, S. J.; West, C. E.; Scarlett, a. G.; Jones, D.; Boberek, M.; Pan, L.; Ng, M.;

Kwong, L.; Tonkin, a. Monocyclic and monoaromatic naphthenic acids: Synthesis and characterisation. *Environ. Chem. Lett.* **2011**, *9* (4), 525–533.

(39) Wilde, M. J.; West, C. E.; Scarlett, A. G.; Jones, D.; Frank, R. A.; Hewitt, L. M.; Rowland, S. J. Bicyclic naphthenic acids in oil sands process water: Identification by comprehensive multidimensional gas chromatography–mass spectrometry. *J. Chromatogr. A* **2015**, *1378*, 74–87.

(40) Rowland, S. J.; West, C. E.; Scarlett, A. G.; Jones, D. Identification of individual acids in a commercial sample of naphthenic acids from petroleum by two-dimensional comprehensive gas chromatography/mass spectrometry. *Rapid Commun. Mass Spectrom.* **2011**, *25* (12), 1741–1751.

(41) Misiti, T. M.; Tezel, U.; Pavlostathis, S. G. Effect of alkyl side chain location and cyclicity on the aerobic biotransformation of naphthenic acids. *Environ. Sci. Technol.* **2014**, *48* (14), 7909–7917.

(42) Clothier, L. N.; Gieg, L. M. Anaerobic biodegradation of surrogate naphthenic acids. *Water Res.* **2016**, *90*, 156–166.

(43) Vaiopoulou, E.; Misiti, T. M.; Pavlostathis, S. G. Removal and toxicity reduction of naphthenic acids by ozonation and combined ozonation-aerobic biodegradation. *Bioresour. Technol.* **2015**, *179*, 339–347.

(44) Johnson, R. J.; Smith, B. E.; Sutton, P. A.; McGenity, T. J.; Rowland, S. J.; Whitby, C. Microbial biodegradation of aromatic alkanoic naphthenic acids is affected by the degree of alkyl side chain branching. *ISME J.* **2011**, *5* (3), 486–496.

(45) Smith, B. E.; Lewis, C. A.; Belt, S. T.; Whitby, C.; Rowland, S. J. Effects of alkyl chain branching on the biotransformation of naphthenic acids. *Environ. Sci. Technol.* **2008**, *42* (24), 9323–9328.

(46) Rowland, S. J.; West, C. E.; Scarlett, A. G.; Ho, C.; Jones, D. Differentiation of two industrial oil sands process-affected waters by two-dimensional gas chromatography/mass spectrometry of diamondoid acid profiles. *Rapid Commun. Mass Spectrom.* **2012**, *26* (5), 572–576.

(47) Lengger, S. K.; Scarlett, A. G.; West, C. E.; Frank, R. A.; Hewitt, L. M.; Milestone, C. B.; Rowland, S. J. Use of the distributions of adamantane acids to profile short-term temporal and pond-scale spatial variations in the composition of oil sands process-affected waters.

Environ. Sci. Process. Impacts **2015**, *17* (8), 1415–1423.

(48) Vitt, D. H.; House, M.; Hartsock, J. A. Sandhill Fen, An Initial Trial for Wetland Species Assembly on In-pit Substrates: Lessons after Three Years. *Botany* **2016**, *94*, 1015–1025.

(49) Reid, M. L.; Warren, L. A. S reactivity of an oil sands composite tailings deposit undergoing reclamation wetland construction. *J. Environ. Manage.* **2016**, *166*, 321–329.

(50) Fedorak, P. M.; Payzant, J. D.; Montgomery, D. S.; Westlake, D. W. S. Microbial degradation of n-alkyl tetrahydrothiophenes found in petroleum. *Appl. Environ. Microbiol.* **1988**, *54* (5), 1234–1248.

(51) Tanaka, H.; Maeda, H.; Suzuki, H.; Kamibayashi, A.; Tonomura, K. Metabolism of Thiophene-2-carboxylate by a Photosynthetic Bacterium. *Agric. Biol. Chem.* **1982**, *46* (6), 1429–1438.

(52) Ranade, V. S.; Consiglio, G.; Prins, R. Functional-Group-Directed Diastereoselective Hydrogenation of Aromatic Compounds. 1. *J. Org. Chem.* **1999**, *64* (24), 8862–8867.

(53) Xia, J.; Sinelnikov, I. V.; Han, B.; Wishart, D. S. MetaboAnalyst 3.0-making metabolomics more meaningful. *Nucleic Acids Res.* **2015**, *43* (W1), W251–W257.

(54) Folwell, B. D.; McGenity, T. J.; Price, A.; Johnson, R. J.; Whitby, C. Exploring the capacity for anaerobic biodegradation of polycyclic aromatic hydrocarbons and naphthenic acids by microbes from oil-sands-process-affected waters. *Int. Biodeterior. Biodegradation* **2015**, 1–8.

(55) Reid, M. L. Biogeochemical Zonation in an Athabasca Oil Sands Composite Tailings Deposit Undergoing Reclamation Wetland Construction, McMaster University, 2014.

(56) Bradford, L. M.; Ziolkowski, L. A.; Goad, C.; Warren, L. A.; Slater, G. F. Elucidating carbon sources driving microbial metabolism during oil sands reclamation. *J. Environ. Manag.* **2017**, *188*, 246–254.

(57) Barrow, M. P.; Headley, J. V.; Peru, K. M.; Derrick, P. J. Fourier transform ion cyclotron resonance mass spectrometry of principal components in oilsands naphthenic acids. *J. Chromatogr. A* **2004**, *1058* (1–2), 51–59.

(58) Fernando, S.; Jobst, K. J.; Taguchi, V. Y.; Helm, P. A.; Reiner, E. J.; McCarry, B. E. Identification of the Halogenated Compounds Resulting from the 1997 Plastimet Inc. Fire

in Hamilton, Ontario, using Comprehensive Two-Dimensional Gas Chromatography and (Ultra)High Resolution Mass Spectrometry. *Environ. Sci. Technol.* **2014**, *48* (18), 10656–10663.

(59) Myers, A. L.; Watson-Leung, T.; Jobst, K. J.; Shen, L.; Besevic, S.; Organtini, K.; Dorman, F. L.; Mabury, S. a; Reiner, E. J. Complementary nontargeted and targeted mass spectrometry techniques to determine bioaccumulation of halogenated contaminants in freshwater species. *Environ. Sci. Technol.* **2014**, *48* (23), 13844–13854.

(60) Tessarolo, N. S.; Silva, R. C.; Vanini, G.; Pinho, A.; Romão, W.; de Castro, E. V. R.; Azevedo, D. A. Assessing the chemical composition of bio-oils using FT-ICR mass spectrometry and comprehensive two-dimensional gas chromatography with time-of-flight mass spectrometry. *Microchem. J.* **2014**, *117*, 68–76.

(61) Megson, D.; Ortiz, X.; Jobst, K. J.; Reiner, E. J.; Mulder, M. F. A.; Balouet, J.-C. A comparison of fresh and used aircraft oil for the identification of toxic substances linked to aerotoxic syndrome. *Chemosphere* **2016**, *158*, 116–123.

(62) Sühring, R.; Ortiz, X.; Pena-Abaurrea, M.; Jobst, K. J.; Freese, M.; Pohlmann, J.-D.; Marohn, L.; Ebinghaus, R.; Backus, S.; Hanel, R.; et al. Evidence for High Concentrations and Maternal Transfer of Substituted Diphenylamines in European Eels Analyzed by Two-Dimensional Gas Chromatography− Time-of-Flight Mass Spectrometry and Gas Chromatography-Fourier Transform Ion Cyclotron Resonance Mass Sp. *Environ. Sci. Technol.* **2016**, *50*, 12678–12685.

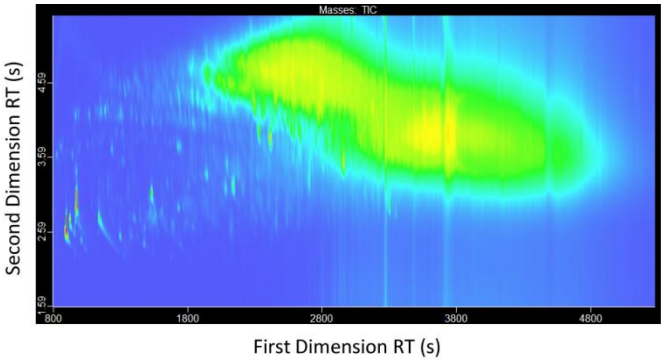

Figure 1. Total ion current (TIC) chromatogram of a methylated pore water extract from July 27 2011 at Sump Vault.

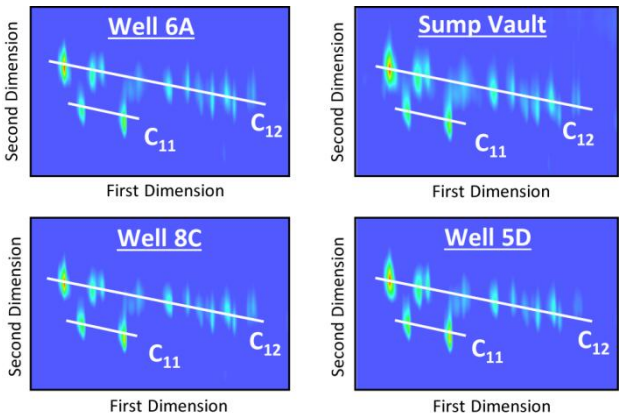

Figure 2. GC×GC contour plots (*m/z* 208 + 194) showing the chromatographic separation of C_{11} and C_{12} tricyclic carboxylic acids from pore extracts sampled on July 2011.

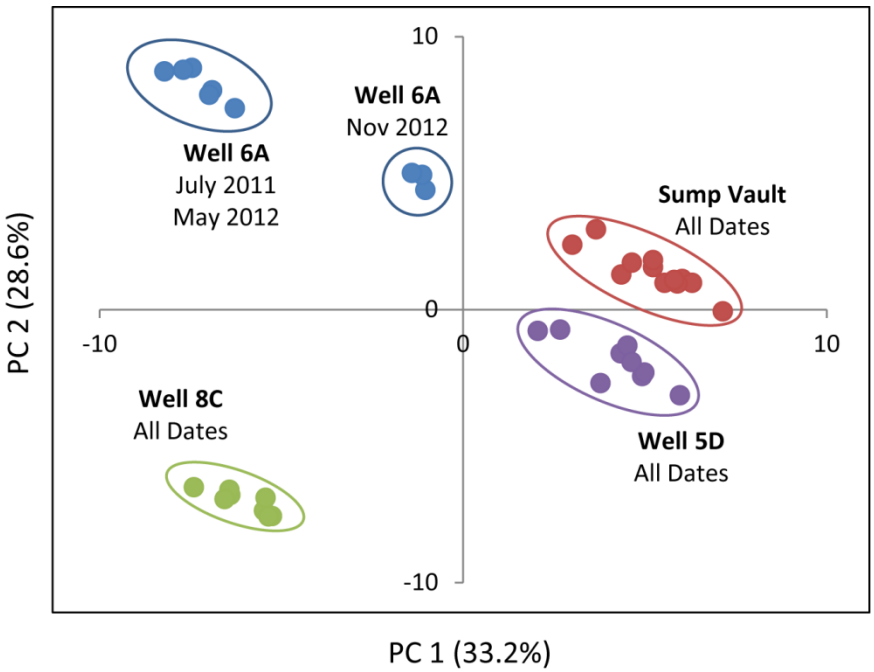

Figure 3. Principal component analysis (PCA) was used to differentiate the NA profiles following normalization to the C_{11} tricyclic carboxylic acids.

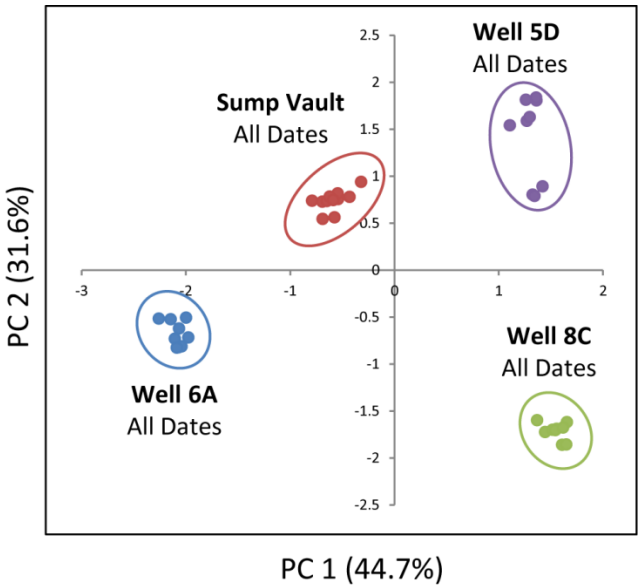

Figure 4. Principal component analysis (PCA) of naphthenic acid isomer percentage composition profiles compared between the four monitoring wells at Sandhill Fen.

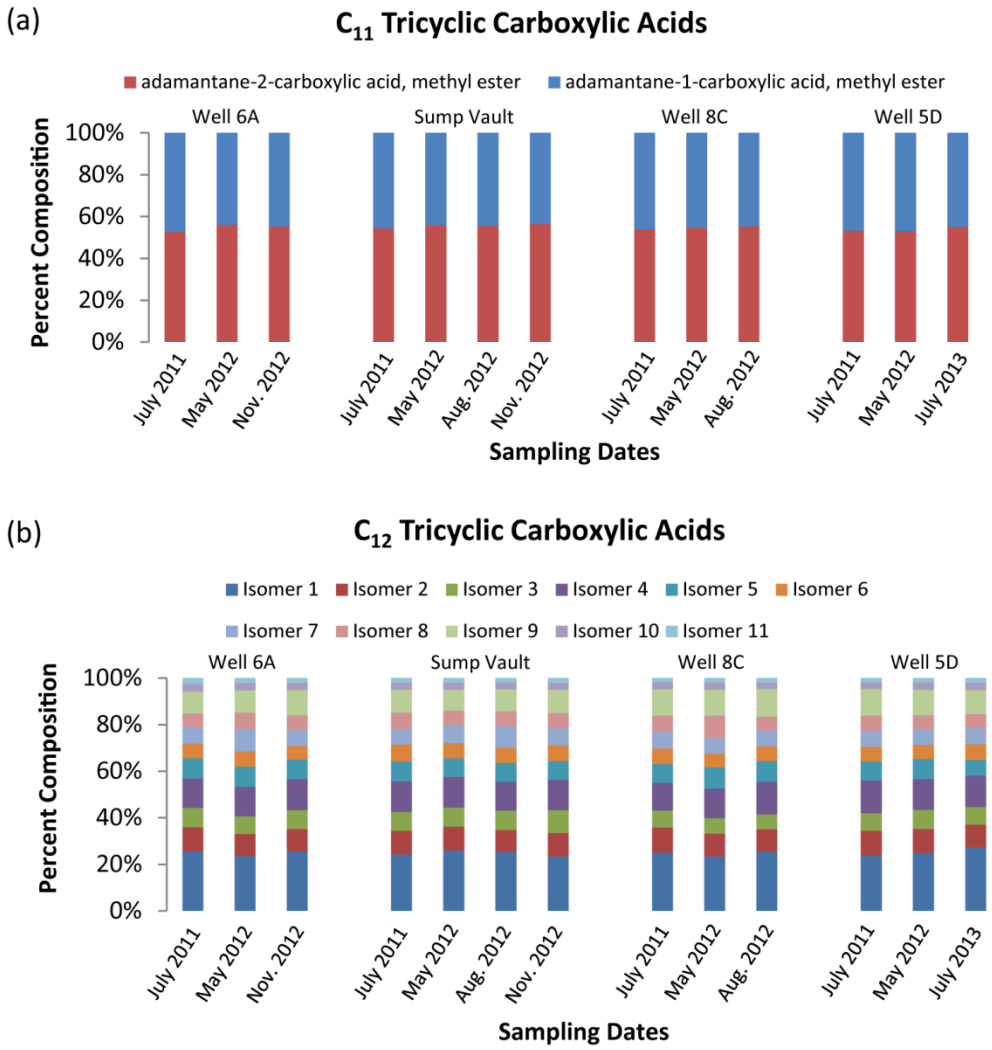

Figure 5. Percentage composition graphs of the (a) C_{11} and (b) C_{12} tricyclic carboxylic acids.

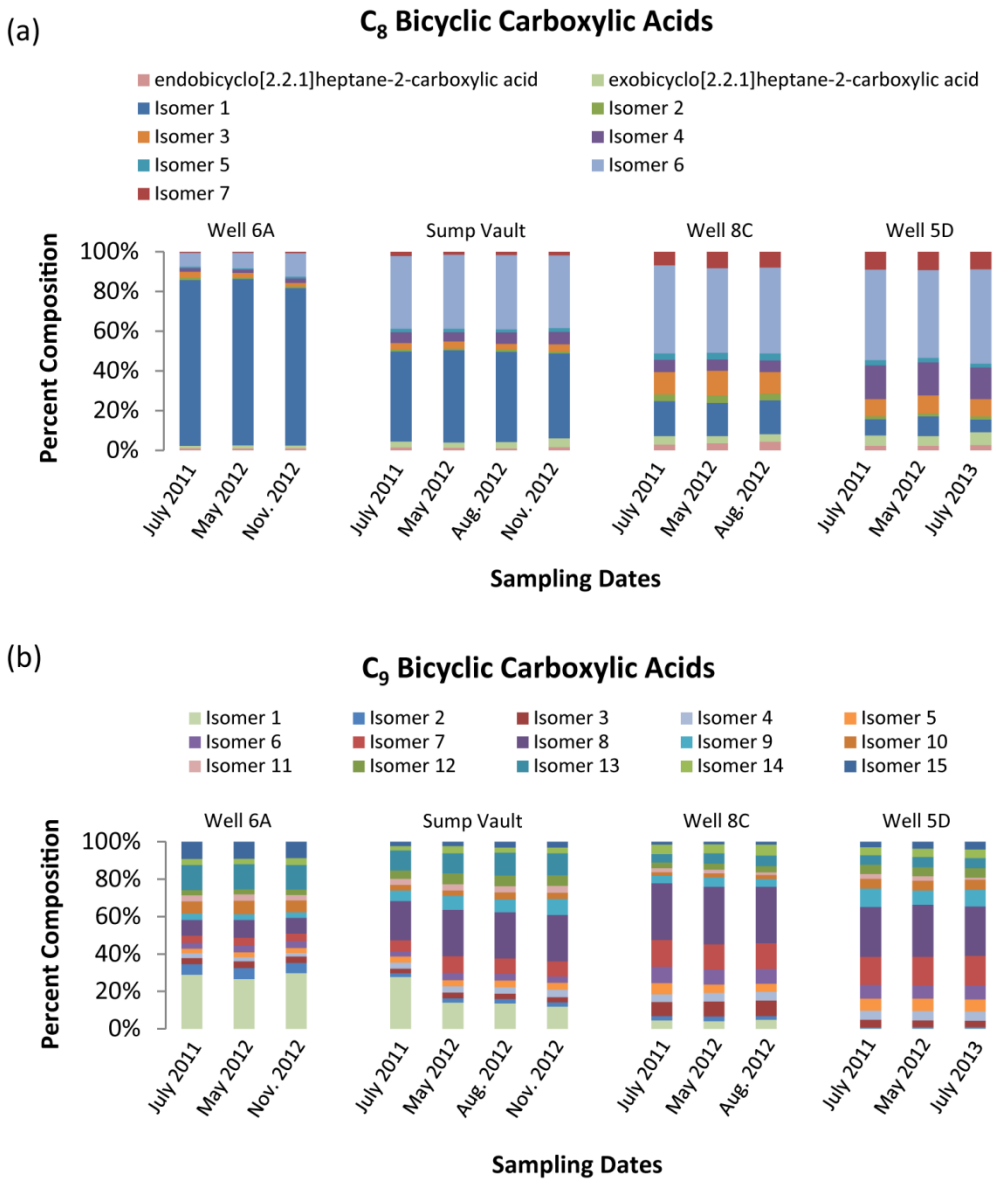

Figure 6. Percentage composition graphs of the (a) C_8 and (b) C_9 bicyclic carboxylic acids.

Table 1. Number of detected naphthenic acids from each monitoring well.

Chemical Class	Naphthenic Acid Core Structure	Carbon Number	Well 6A	Sump Vault	Well 8C	Well 5D
O_2	Monocyclic	C_8	7	7	2	3
		C_9	14	14	3	12
	Bicyclic	C_8	9	9	9	9
		C_9	15	15	15	15
		C_{10}	11	11	11	11
		C_{11}	10	10	10	10
	Tricyclic	C_{11}	2	2	2	2
		C_{12}	11	11	11	11
	Monoaromatic Bicyclic	C_{11}	3	3	0	0
SO_2	Sulfur-Containing Monocyclic	C_6	2	2	2	1
		C_7	7	7	5	6
		C_8	7	7	5	7
		C_9	2	3	3	3
	Thiophene	C_6	4	4	0	0
		C_7	6	6	1	2

Supporting Information

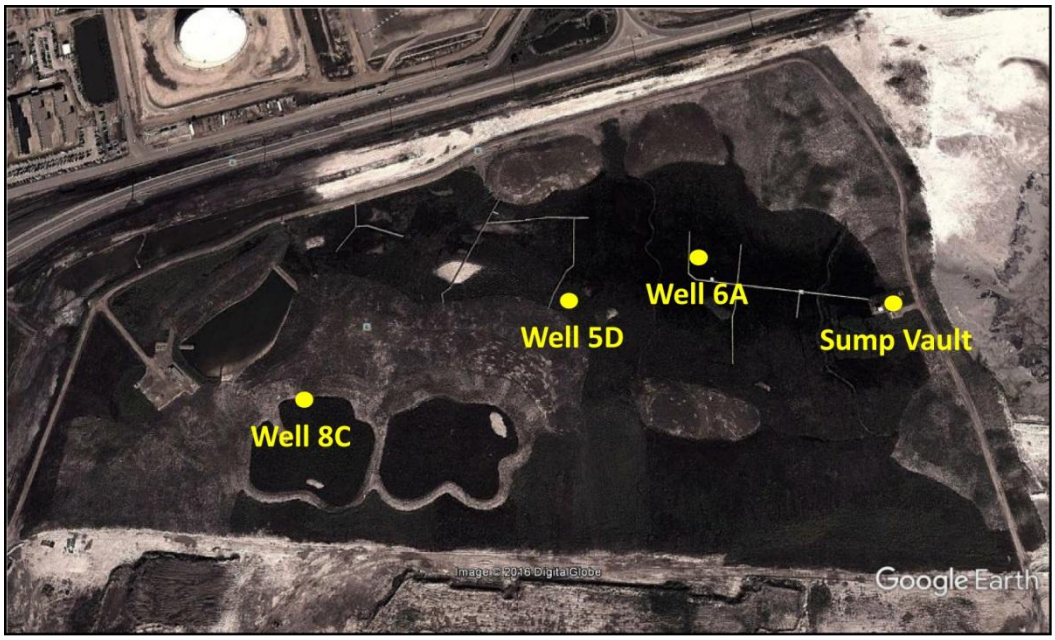

Figure S1. A map of the study site, illustrating the locations of the sampling wells.

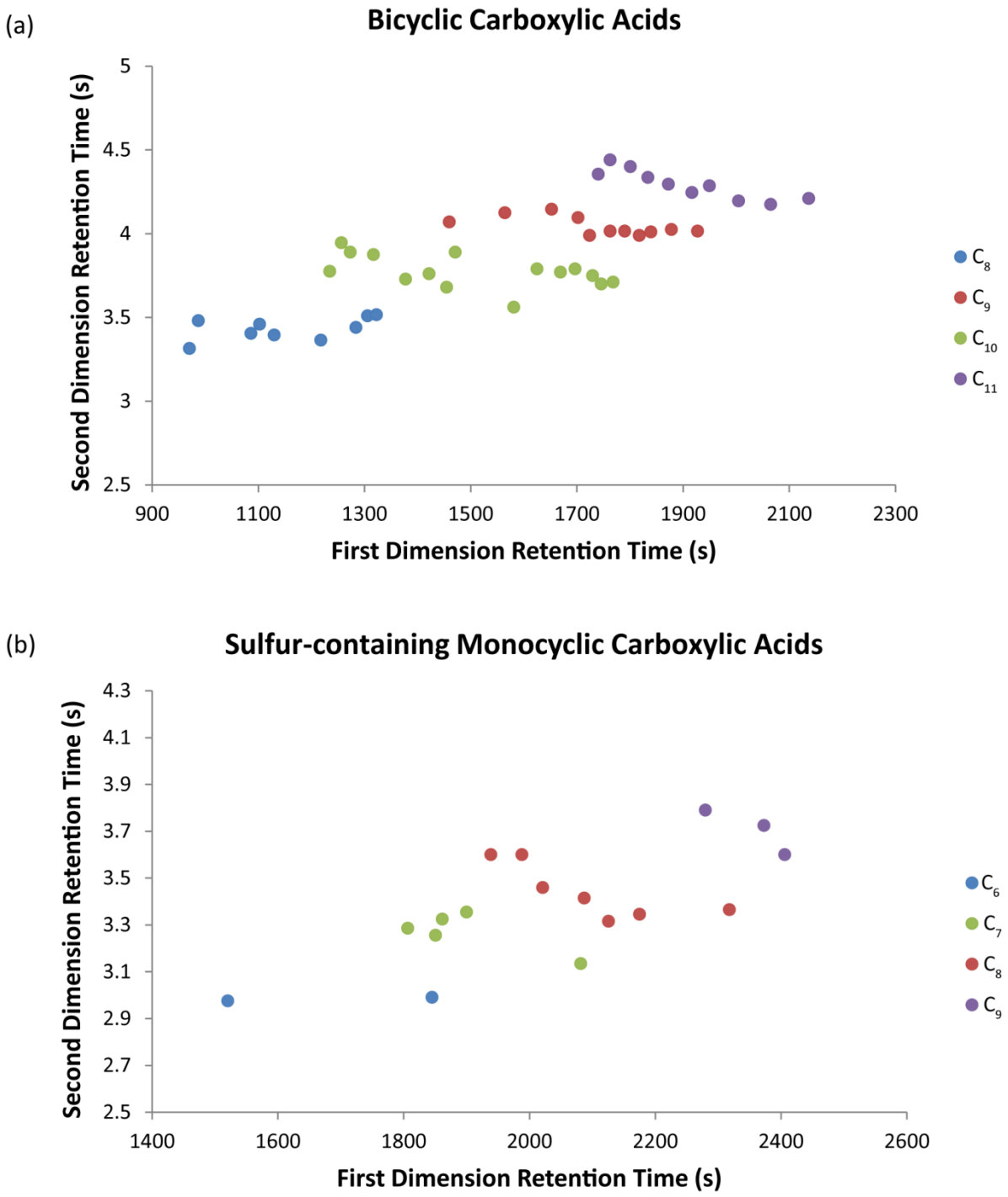

Figure S2. The first and second dimension retention times for the analytes identified as (a) bicyclic carboxylic acids and (b) sulfur-containing monocyclic carboxylic acids.

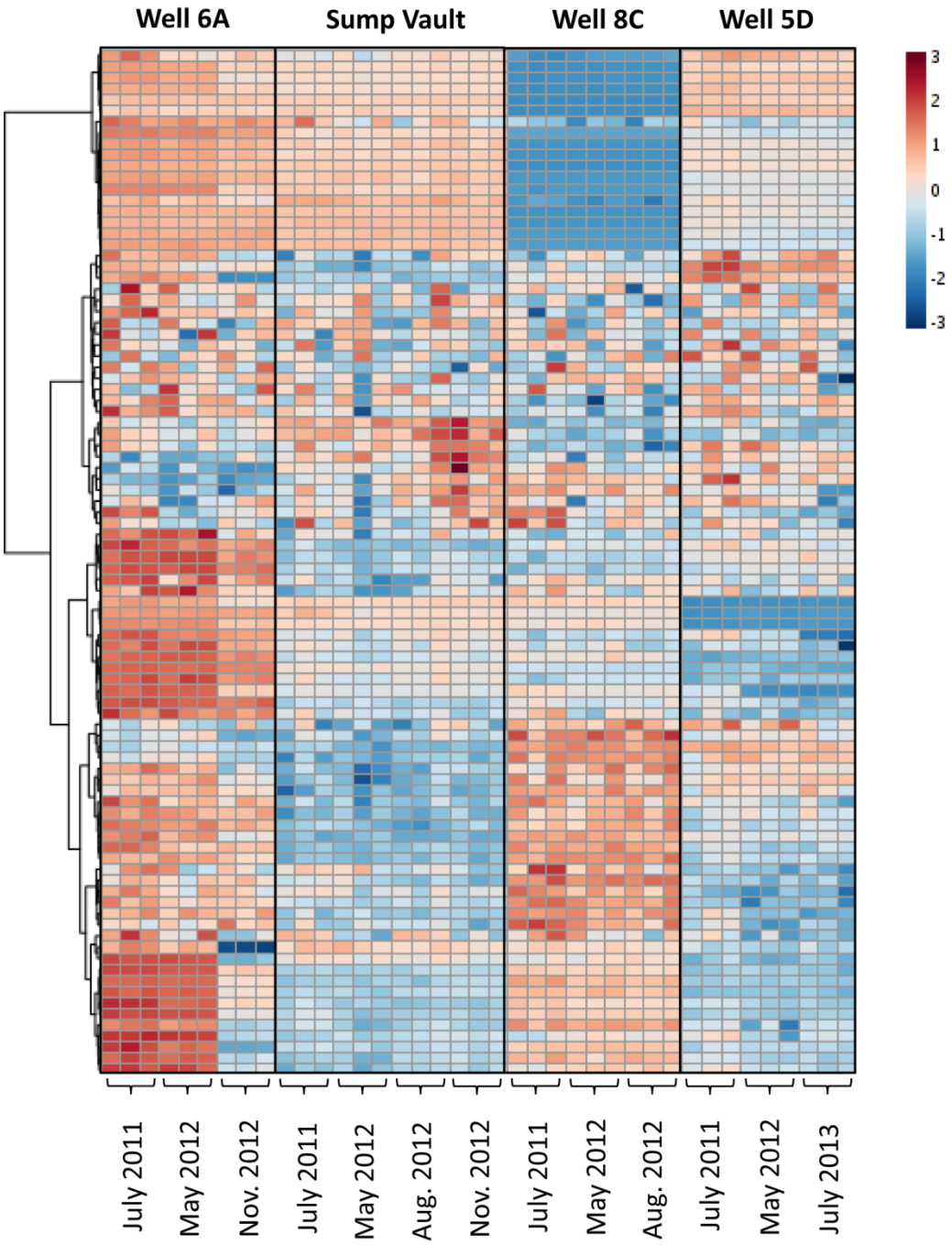

Figure S3. Heat map diagram showing the abundances of individual naphthenic acids, relative to the C_{11} tricyclic carboxylic acids. Triplicate values are plotted for each sampling date. Data was log transformed prior to heat map analysis.

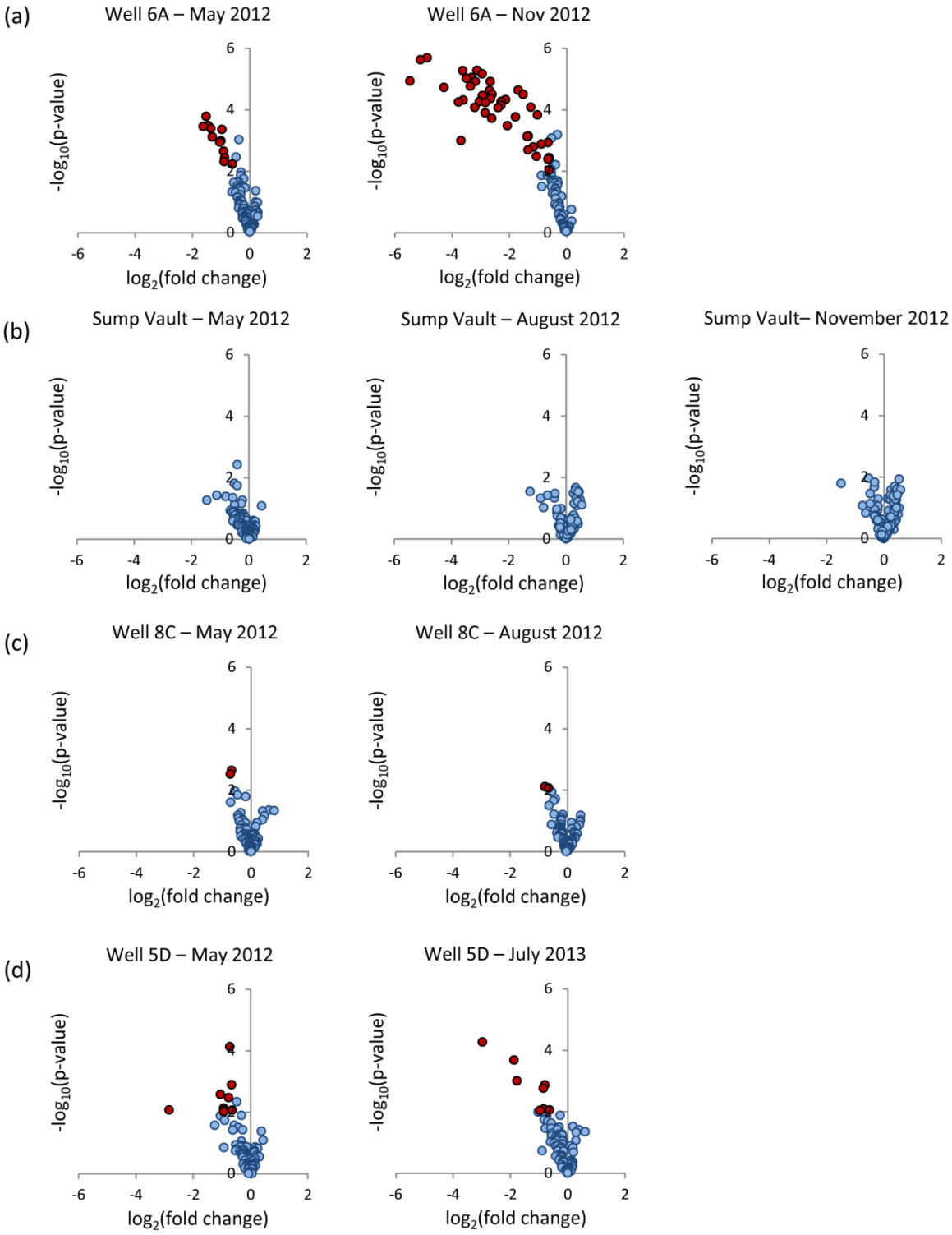

Figure S4. Volcano plots indicating the number of NAs that were significantly altered at each sampling time point, when compared to first sampling date on July 2011. The peak areas of each naphthenic acid were normalized to the sum of the C_{11} tricyclic carboxylic acids. Red dots indicate NAs with $p < 0.01$ and fold change $> \pm 1.5$. Blue dots indicate NAs with $p > 0.01$ and/or fold change $< \pm 1.5$.

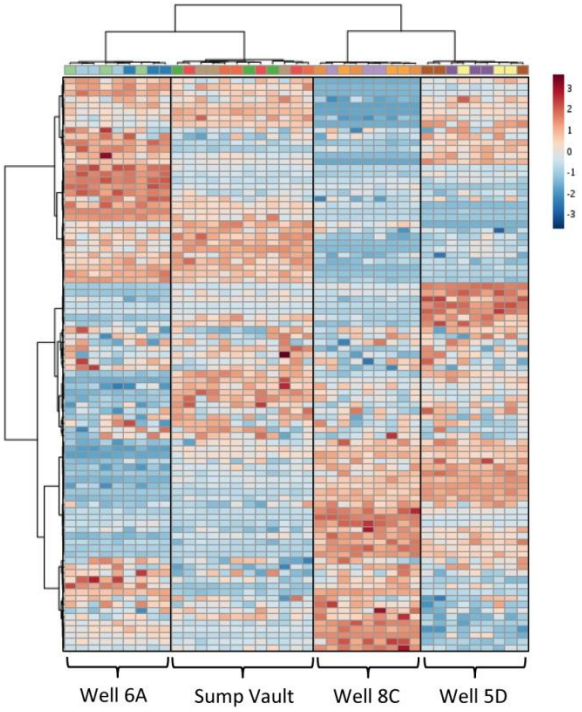

Figure S5. Hierarchal cluster analysis (HCA) and heat map visualization of the isomer percentage composition profiles with Pearson distance and Ward clustering.

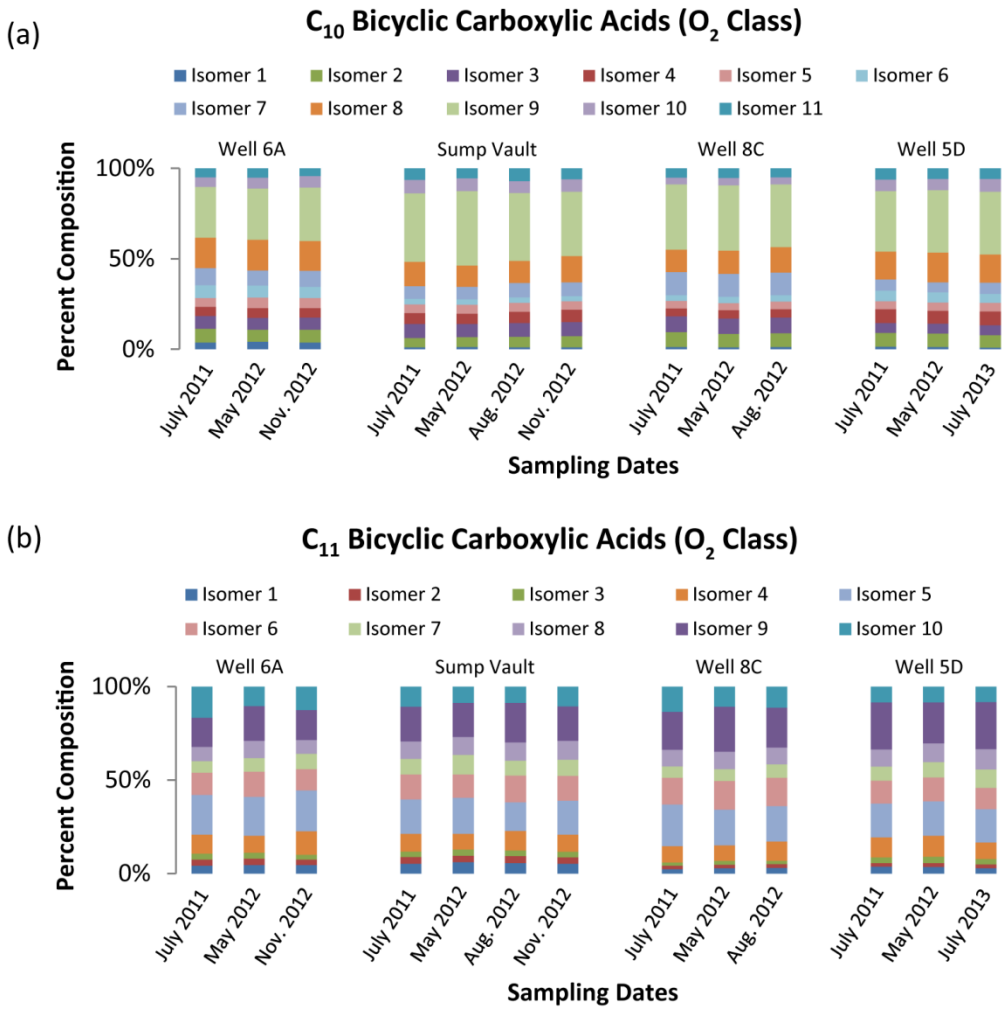

Figure S6. Percentage composition graphs of the (a) C_{10} and (b) C_{11} bicyclic carboxylic acids.

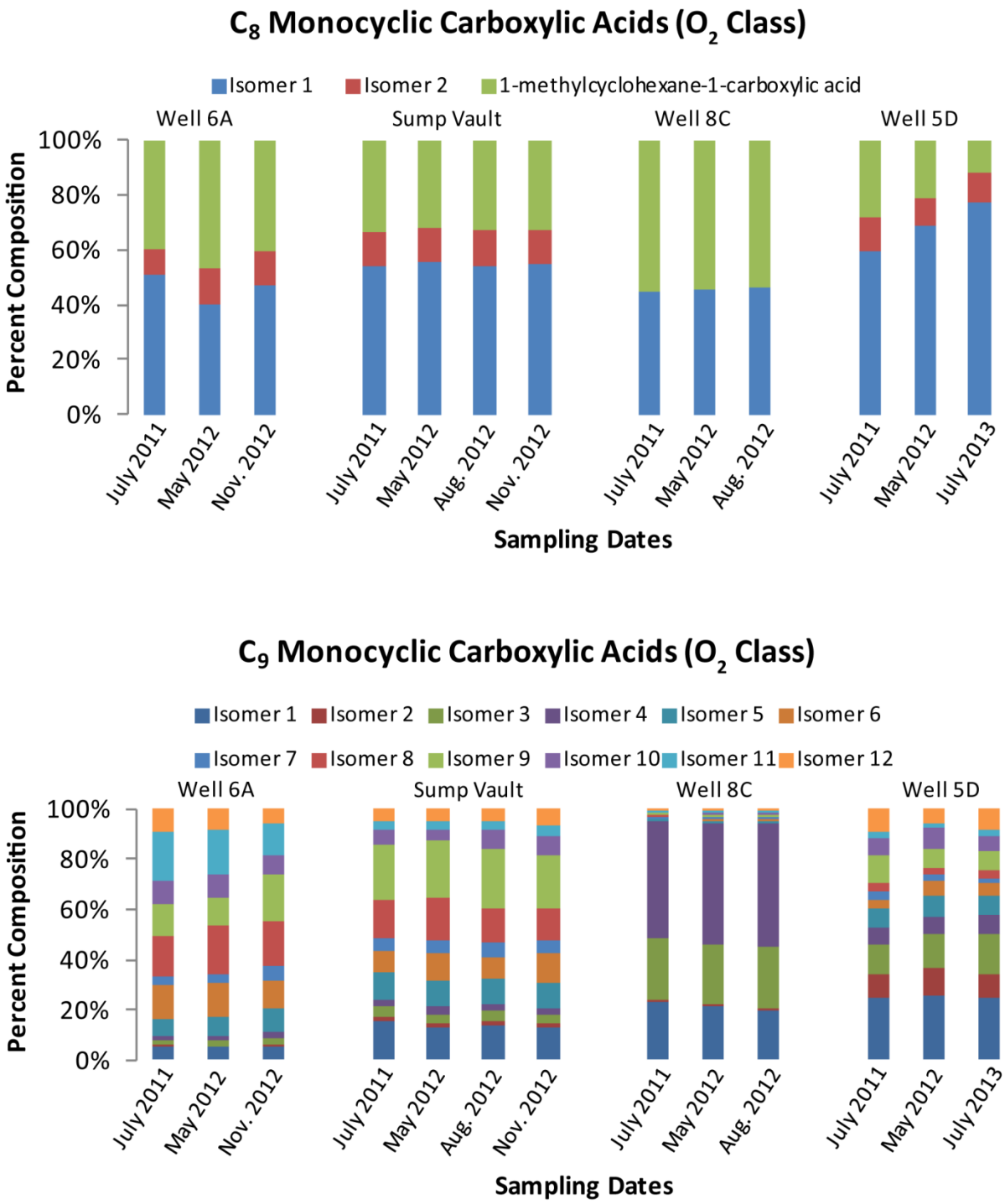

Figure S7. Percentage composition graphs of the C_8 and C_9 monocyclic carboxylic acids from the O_2 chemical class.

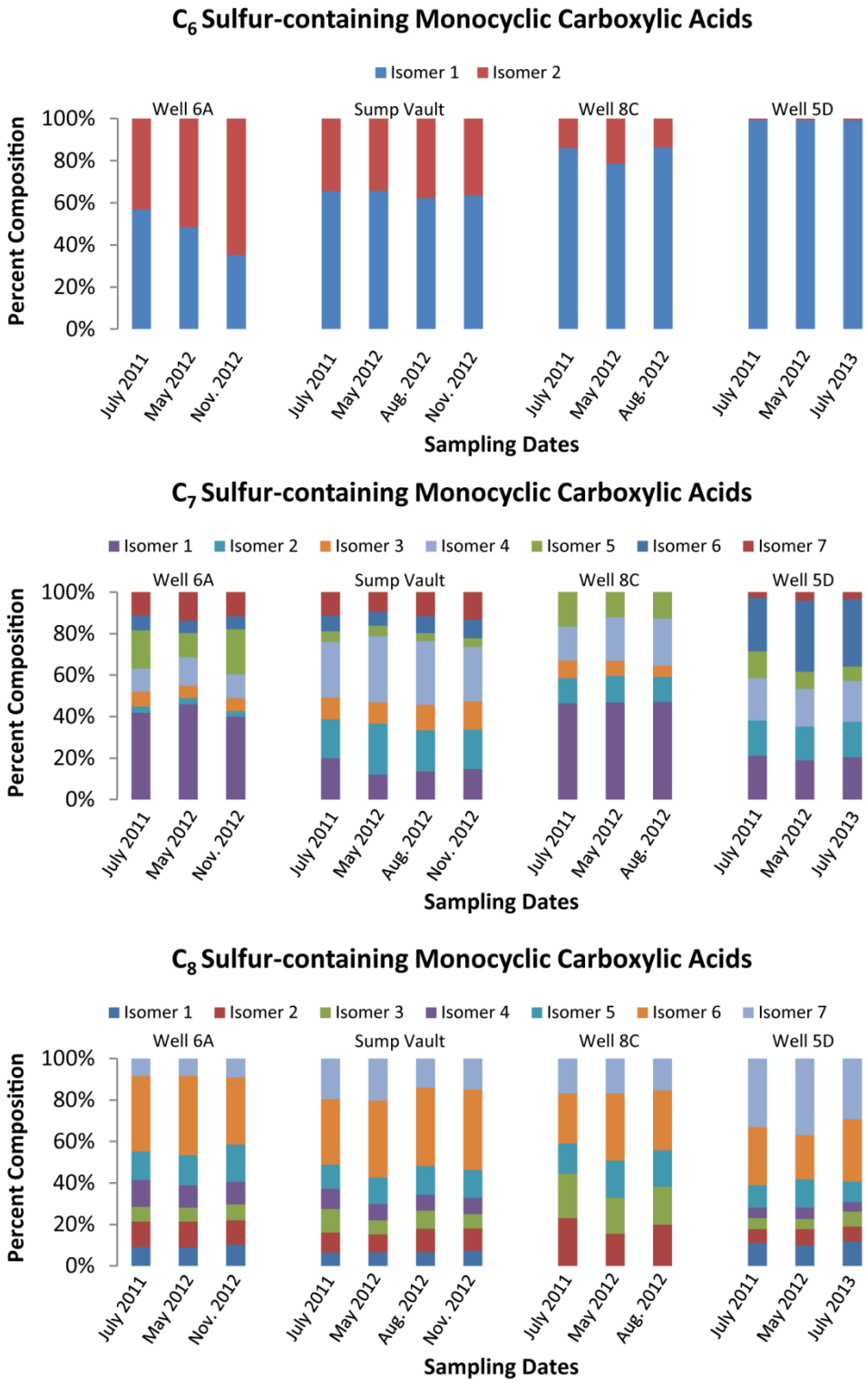

Figure S8. Percentage composition graphs of the C_6, C_7, and C_8 sulfur-containing monocyclic carboxylic acids.

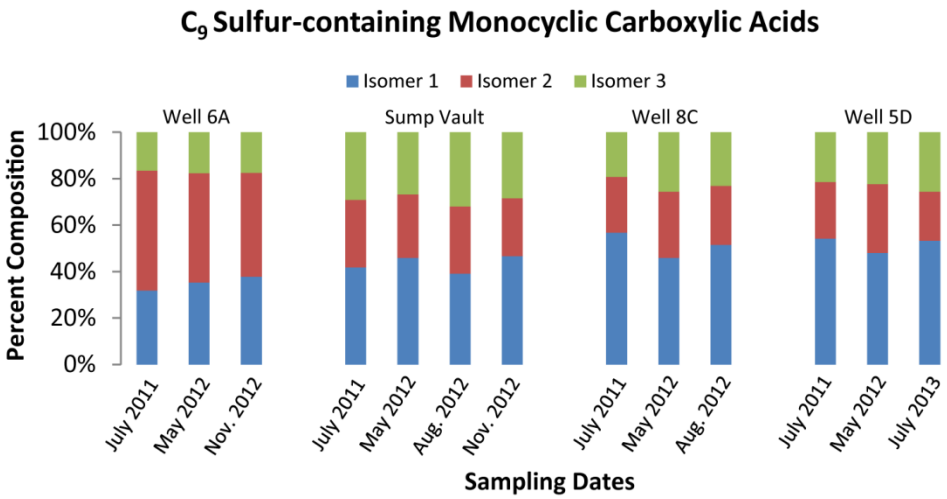

Figure S9. Percentage composition graphs of the C_9 sulfur-containing monocyclic carboxylic acids

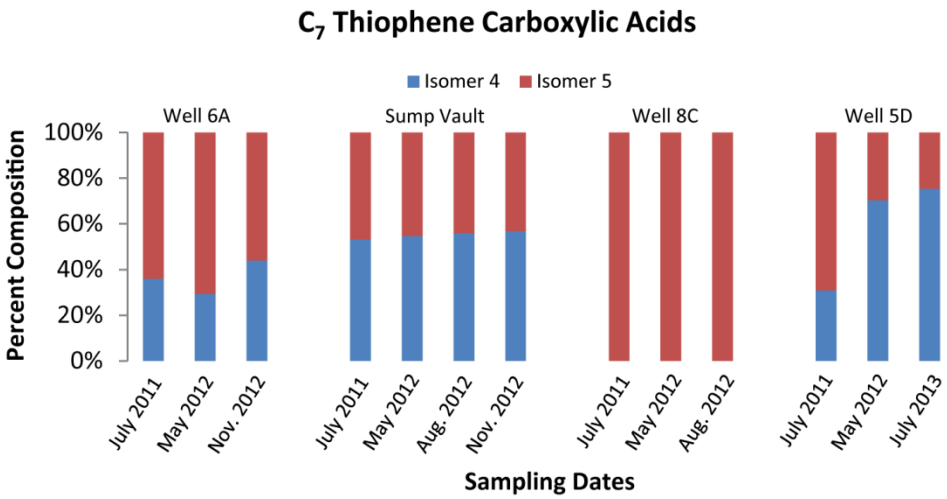

Figure S10. Percentage composition graphs of the C_7 thiophene carboxylic acids.

Table S1. $\log_2$(Fold Changes) and $-\log_{10}$(*p*-values) values for significantly altered naphthenic acids detected on May 2012 at Well 6A (Compared to July 2011).

Naphthenic Acid	$\log_2$(Fold Change)	$-\log_{10}$(*p*-value)
C_8 monocyclic carboxylic acid, methyl ester: Isomer 1	-0.886	2.315
C_9 monocyclic carboxylic acid, methyl ester: Isomer 14	-1.521	3.780
C_8 bicyclic carboxylic acid, methyl ester: Isomer 2	-1.044	2.950
C_{11} bicyclic carboxylic acid, methyl ester: Isomer 10	-1.003	2.985
C_7 sulfur-containing monocyclic acid, methyl ester: Isomer 5	-0.968	3.356
2-methylthiophene-3-carboxylic acid, methyl ester	-1.618	3.454
methylthiophene carboxylic acid, methyl ester: Isomer 1	-1.306	3.116
5-methylthiophene-2-carboxylic acid, methyl ester	-1.353	3.389
dimethyl/ethylthiophene carboxylic acid, methyl ester: Isomer 1	-1.436	3.475
dimethyl/ethylthiophene carboxylic acid, methyl ester: Isomer 2	-0.903	2.652
dimethyl/ethylthiophene carboxylic acid, methyl ester: Isomer 3	-0.875	2.435
dimethyl/ethylthiophene carboxylic acid, methyl ester: Isomer 6	-0.609	2.231

Table S2. $\log_2$(Fold Changes) and $-\log_{10}$(*p*-values) value for significantly altered naphthenic acids detected on November 2012 at Well 6A (Compared to July 2011).

Naphthenic Acid	$\log_2$(Fold Change)	$-\log_{10}$(*p*-value)
C_8 monocyclic carboxylic acid, methyl ester: Isomer 3	-0.649	2.391
C_8 monocyclic carboxylic acid, methyl ester: Isomer 4	-1.520	4.499
2-methylcyclohexane carboxylic acid, methyl ester	-1.166	2.785
C_8 monocyclic carboxylic acid, methyl ester: Isomer 5	-4.280	4.721
C_9 monocyclic carboxylic acid, methyl ester: Isomer 1	-0.609	2.041
C_9 monocyclic carboxylic acid, methyl ester: Isomer 6	-1.018	3.833
C_9 monocyclic carboxylic acid, methyl ester: Isomer 10	-1.053	2.484
C_9 monocyclic carboxylic acid, methyl ester: Isomer 11	-1.249	4.084
C_9 monocyclic carboxylic acid, methyl ester: Isomer 12	-1.344	2.686
C_9 monocyclic carboxylic acid, methyl ester: Isomer 14	-3.189	4.919
C_8 bicyclic carboxylic acid, methyl ester: Isomer 1	-0.650	2.929
C_8 bicyclic carboxylic acid, methyl ester: Isomer 2	-0.878	2.884
C_8 bicyclic carboxylic acid, methyl ester: Isomer 3	-1.339	3.142
C_{11} bicyclic carboxylic acid, methyl ester: Isomer 10	-0.614	2.445
C_6 sulfur-containing monocyclic acid, methyl ester: Isomer 1	-3.360	4.760
C_6 sulfur-containing monocyclic acid, methyl ester: Isomer 2	-2.067	3.474
C_7 sulfur-containing monocyclic acid, methyl ester: Isomer 6	-3.774	4.246
C_7 sulfur-containing monocyclic acid, methyl ester: Isomer 7	-3.494	5.020
C_7 sulfur-containing monocyclic acid, methyl ester: Isomer 5	-3.319	5.042
C_7 sulfur-containing monocyclic acid, methyl ester: Isomer 1	-3.626	5.267
C_7 sulfur-containing monocyclic acid, methyl ester: Isomer 2	-3.689	2.995
C_7 sulfur-containing monocyclic acid, methyl ester: Isomer 3	-3.774	4.246
C_7 sulfur-containing monocyclic acid, methyl ester: Isomer 4	-3.494	5.020
C_8 sulfur-containing monocyclic acid, methyl ester: Isomer 1	-2.603	4.500
C_8 sulfur-containing monocyclic acid, methyl ester: Isomer 2	-2.846	3.893
C_8 sulfur-containing monocyclic acid, methyl ester: Isomer 3	-2.651	4.363
C_8 sulfur-containing monocyclic acid, methyl ester: Isomer 4	-3.039	4.263
C_8 sulfur-containing monocyclic acid, methyl ester: Isomer 5	-2.386	4.061
C_8 sulfur-containing monocyclic acid, methyl ester: Isomer 6	-2.950	5.167
C_8 sulfur-containing monocyclic acid, methyl ester: Isomer 7	-2.685	4.624
C_9 sulfur-containing monocyclic acid, methyl ester: Isomer 1	-2.666	4.916
C_9 sulfur-containing monocyclic acid, methyl ester: Isomer 2	-3.129	5.274
C_9 sulfur-containing monocyclic acid, methyl ester: Isomer 3	-2.834	4.235
2-methylthiophene-3-carboxylic acid, methyl ester	-3.609	4.313
methylthiophene carboxylic acid, methyl ester: Isomer 1	-2.940	4.455
methylthiophene carboxylic acid, methyl ester: Isomer 2	-2.609	3.721
5-methylthiophene-2-carboxylic acid, methyl ester	-4.866	5.687
dimethyl/ethylthiophene carboxylic acid, methyl ester: Isomer 1	-5.098	5.623
dimethyl/ethylthiophene carboxylic acid, methyl ester: Isomer 2	-5.465	4.932
dimethyl/ethylthiophene carboxylic acid, methyl ester: Isomer 3	-3.205	4.069
dimethyl/ethylthiophene carboxylic acid, methyl ester: Isomer 4	-1.788	3.769
dimethyl/ethylthiophene carboxylic acid, methyl ester: Isomer 5	-2.290	4.147
dimethyl/ethylthiophene carboxylic acid, methyl ester: Isomer 6	-2.284	4.263
2-indanylacetic acid, methyl ester	-1.381	3.134
tetralin carboxylic acid, methyl ester: Isomer 1	-2.128	4.330

Table S3. $\log_2$(Fold Changes) and $-\log_{10}$(*p*-values) for significantly altered naphthenic acids detected on May 2012 at Well 8C (Compared to July 2011).

Naphthenic Acid	$\log_2$(Fold Change)	$-\log_{10}$(*p*-value)
C_7 sulfur-containing monocyclic acid, methyl ester: Isomer 5	-0.673	2.643
dimethyl/ethylthiophene carboxylic acid, methyl ester: Isomer 5	-0.713	2.518

Table S4. $\log_2$(Fold Changes) and $-\log_{10}$(*p*-values) for significantly altered naphthenic acids detected on August 2012 at Well 8C (Compared to July 2011).

Naphthenic Acid	$\log_2$(Fold Change)	$-\log_{10}$(*p*-value)
C_7 sulfur-containing monocyclic acid, methyl ester: Isomer 3	-0.784	2.108
dimethyl/ethylthiophene carboxylic acid, methyl ester: Isomer 5	-0.653	2.069

Table S5: Log_2(Fold Changes) and $-log_{10}$(p-values) for significantly altered naphthenic acids detected on May 2012 at Well 5D (Compared to July 2011).

Naphthenic Acid	log_2(Fold Change)	$-log_{10}$(*p*-value)
C_8 monocyclic carboxylic acid, methyl ester: Isomer 2	-0.477	2.333
1-methylcyclohexane carboxylic acid, methyl ester	-0.653	2.075
C_9 monocyclic carboxylic acid, methyl ester: Isomer 7	-0.913	2.893
C_9 monocyclic carboxylic acid, methyl ester: Isomer 12	-0.934	2.477
C_7 sulfur-containing monocyclic acid, methyl ester: Isomer 5	-0.936	2.011
C_8 sulfur-containing monocyclic acid, methyl ester: Isomer 1	-1.043	2.066
C_8 sulfur-containing monocyclic acid, methyl ester: Isomer 2	-0.637	2.577
C_8 sulfur-containing monocyclic acid, methyl ester: Isomer 4	-0.763	2.062
C_8 sulfur-containing monocyclic acid, methyl ester: Isomer 7	-0.715	2.124
dimethyl/ethylthiophene carboxylic acid, methyl ester: Isomer 5	-2.832	4.127

Table S6: Log_2(Fold Changes) and $-log_{10}$(p-values) for significantly altered naphthenic acids detected on July 2013 at Well 5D (Compared to July 2011).

Naphthenic Acid	log_2(Fold Change)	$-log_{10}$(*p*-value)
C_8 monocyclic carboxylic acid, methyl ester: Isomer 2	-0.791	2.868
1-methylcyclohexane carboxylic acid, methyl ester	-1.871	3.675
C_9 monocyclic carboxylic acid, methyl ester: Isomer 7	-1.764	3.006
C_9 monocyclic carboxylic acid, methyl ester: Isomer 9	-0.964	2.035
C_9 monocyclic carboxylic acid, methyl ester: Isomer 12	-0.628	2.053
C_8 sulfur-containing monocyclic acid, methyl ester: Isomer 4	-0.837	2.087
C_8 sulfur-containing monocyclic acid, methyl ester: Isomer 7	-0.846	2.762
dimethyl/ethylthiophene carboxylic acid, methyl ester: Isomer 5	-2.972	4.262

1. Identification of Bicyclic Naphthenic Acids

Bicyclic naphthenic acids (Z=-4) with carbon numbers ranging from C_8 to C_{11} were detected in the pore water extracts from Sandhill fen. Figure S2a shows the two-dimensional retention positions of the methyl esters of the C_{8-11} bicyclic naphthenic acids. Due to the structured nature of the GC×GC chromatogram, isomers with the same carbon number generally elute in clusters on the two dimensional chromatogram. It was observed that an increase in carbon number, or degree of alkylation, leads to an increase in both the first and second dimension retention times of the cluster of isomers.

1.1 C_8 Bicyclic Naphthenic Acids

The C_8 bicyclic acids were observed as methyl esters and displayed molecular ions at *m/z* 154. The methyl ester of endo-bicyclo[2.2.1]heptane-2-carboxylic acid was identified in the sample by comparison to the retention times and electron ionization (EI) mass spectrum of the reference standard (see Figs. A3a and A3b in the mass spectral library report). The methyl ester of exo-bicyclo[2.2.1]heptane-2-carboxylic acid was identified by comparison with a NIST library spectrum (see Figs. A3c and A3d in the mass spectral library report). The endo/exo isomers of bicyclo[2.2.1]heptane-2-carboxylic acid have been previously detected in an OSPW sample.[1]

Five unknowns were tentatively identified as C_8 bicyclic acids by mass spectral interpretation and comparison to the literature EI mass spectra published by Wilde *et al*[1]. The five unknowns eluted in the same cluster on the GC×GC chromatogram as the methyl esters of endo- and exo-bicyclo[2.2.1]heptane-2-carboxylic acid (see Fig. S2a). The EI mass spectra for the five unknowns are presented in Figures A3e-i in the mass spectral library report. In general, the EI mass spectra display a molecular ion at *m/z* 154 and a prominent base peak at *m/z* 95, which was generated by the loss of the entire methyl ester chemical moiety. A small fragment ion at *m/z* 122 (M-32, loss of methanol following hydrogen transfer) was detected in three of the aforementioned unknowns (see Figs. A3g-i in the mass spectral library report).

An additional unknown (EI mass spectrum presented in Figure A3j in the mass spectral library report) possessed a spectrum which was similar to the methyl ester of bicyclo[2.2.1]heptane-1-carboxylic acid, previously published by Wilde *et al*.[1], and is speculated to be an isomer.

Lastly, an unknown, whose mass spectrum is shown in Figure A3k in the mass spectral library report, was detected in the sample, and we tentatively propose that the analyte is the methyl ester of bicyclo[2.1.1]hexane- or bicyclo[2.2.0]hexane ethanoic acid. The unknown displayed a molecular ion at *m/z* 154 and an intense base peak at *m/z* 80 (M-74, loss of methyl ethanoate following hydrogen transfer). The presence of a base peak at *m/z* 80, rather than *m/z* 95, suggests that the unknown may contain a C_6 bicyclic ring skeleton, such as bicyclo[2.1.1]hexane or bicyclo[2.2.0]hexane. In a previous study, the EI mass spectrum of the methyl ester of bicyclo[2.2.1]heptane-2-ethanoic acid was reported[1], and, similarly, it displayed an intense base peak for the loss of the ethanoate side chain (M-73, 100% relative intensity).

1.2 C_9 Bicyclic Naphthenic Acids

A set of 15 unknowns were tentatively identified as the methyl esters of C_9 bicyclic carboxylic acid. Consistent with our assignments, Figure S2a shows that the C_9 bicyclic acids form a cluster with increased first and second dimension retention times, relative to the cluster of C_8 bicyclic acids. The EI mass spectra for the unknowns are presented in Figure A4 in the mass spectral library report. Reference standards of C_9 bicyclic acids could not be obtained for this study, but tentative identifications were made following comparisons to literature EI mass spectra[1,2] of methyl esters with bicyclo[2.2.2]octane, bicyclo[3.2.1]octane, and bicycle[3.3.0]octane ring skeletons.

The EI mass spectra of five unknowns (shown in Figs. A4a-e in the mass spectral library report) displayed a molecular ion at *m/z* 168, an intense base peak at *m/z* 109 (100% relative intensity), generated by the loss of the methylated carboxy radical ($CH_3OCO^{\bullet}$), and fragment ions at *m/z* 93, 79, 67, and 55. The EI mass spectrum of the methyl ester of bicyclo[2.2.2]octane-2-carboxylic acid, which was reported by Wilde *et al.*[1], displayed the same molecular ion (*m/z* 168), prominent base peak (*m/z* 109), and common fragment ions (*m/z* 93, 79, and 67). However, the literature EI-MS contained a large fragment ion at *m/z* 139 (~90% relative intensity), which was not present in the unknowns. Nevertheless, the abundant base peak at m/z 109 indicates the four unknowns may contain a C_8 bicyclic ring structure. However, the identities of the ring structures (e.g., bicyclo[2.2.2]octane, bicyclo[3.2.1]octane, and/or bicycle[3.3.0]octane) are not obvious without standards.

The EI mass spectra of the unknowns in Figures A4f-h also displayed the *m/z* 109 fragment ion, but with lower intensity (approximately 50% relative intensity). All of the unknowns presented in Figures A4a-h displayed the similar fragment ions at *m/z* 67, 79, and 93. The *m/z* 139 fragment ion (M-29, loss of ethyl) was observed with in some of the detected compounds (see Figs. A4e-g in the mass spectral library report), but it possessed a lower relative intensity (~30-50% relative intensity).

The EI mass spectra of three unknowns shown in Figures A4i-k are characterized by a small molecular ion at *m/z* 168, a base peak at *m/z* 95/94 (80-100%, relative intensity), and other fragment ions at *m/z* 79, 77, and 67. The abundant base peaks at *m/z* 95 (M-73) and 94 (M-74) indicate the presence of an enthanoate side chain. The mass spectra of Figures A4j-k also display a small fragment ion at *m/z* 136 (loss of methanol) and *m/z* 137 (loss of $CH_3O^{\bullet}$), respectively, which is typical of methyl esters. The mass spectra of the three analytes share similarities to the mass spectrum of the methyl ester of bicyclo[2.2.1]heptane-2-ethanoic acid[1], which also contained the same molecular ion (*m/z* 168) and intense base peak (*m/z* 95, 100% relative intensity).

The mass spectra of four additional unknowns are shown in Figures A4l-o; the compounds displayed a molecular ion at m/z 168, an intense peak at *m/z* 136 (loss of methanol), and additional fragment ions at *m/z* 109, 79, and 67. The mass spectra of the methyl esters of bicyclo[3.3.0]octane-2-carboxylic acid, bicyclo[2.2.2]octane-2-carboxylic acid, and

bicyclo[3.2.1]octane-6-carboxylic acid displayed similar dissociation patterns and fragment ions.[1]

1.3 C_{10} Bicyclic Naphthenic Acids

A total of 11 unknowns were tentatively identified as C_{10} bicyclic acids by comparison to literature EI mass spectra[1,3], manual mass spectral interpretations, and relative GC×GC retention positions (see Fig. S2a). The EI mass spectra of the C_{10} bicyclic acids are presented in Figure A5 in the mass spectral library report.

In general, the mass spectra of the C_{10} bicyclic acids were characterized by a molecular ion at *m/z* 182 and abundant lower mass fragment ions at *m/z* 81, 79, 67, 59, 55. Two analytes, whose EI mass spectra are shown in Figures A5a and A5b, displayed a prominent fragment ion at *m/z* 123 (M–59, loss of $CH_3OCO^{\bullet}$), which was similar to the literature mass spectrum of the methyl ester of bicyclo[3.3.1]nonane-3-carboxylic acid[1]. However, the two analytes did not contain the M-32 fragment ion (loss of methanol), which was present in the literature EI mass spectrum.

The mass spectra of the remaining C_{10} bicyclic acids (See Figs A5c-k in the mass spectral library report) possessed fragment ions at *m/z* 123, 81, 79, 67, 59, and 55. The identities of bicyclic structures are not obvious but the presence of fragment ions at *m/z* 167 (loss of CH_3) and 153 (loss of C_2H_5), indicate that some of the unknowns may be alkylated homologues of C_9 (e.g., bicyclo[2.2.2]octane, bicyclo[3.2.1]octane, bicyclo[3.3.0]octane, etc.) or C_8 (e.g., bicyclo[2.2.1]heptane, bicyclo[3.2.0]heptane) bicyclic naphthenic acids.

1.4 C_{11} Bicyclic Naphthenic Acids

A collection of 10 unknowns were tentatively identified as C_{11} bicyclic acids by comparison to literature EI mass spectra[1], manual mass spectral interpretations, and relative GC×GC retention times (see Fig. S2a). The mass spectra of the C_{11} bicyclic acids are shown in Figure A6 in the mass spectra library report. In general, the mass spectra were characterized by a molecular ion at *m/z* 196, and a fragment ion at *m/z* 137, representing the loss of the entire ester moiety ($CH_3OCO^{\bullet}$). In addition, predominant fragment ions were present at *m/z* 122, 107, 95, 79, 81, 67, and 55. Similar fragment ions were prevalent in the mass spectra of reference standards (methyl esters of 5-methylbicyclo[3.3.1]nonane-1-carboxylic acid, bicyclo[4.4.0]decane-3-carboxylic acid, and bicyclo[4.4.0]decane-1-carboxylic acid)[1].

2. Identification of Sulfur-Containing Monocyclic Naphthenic Acids

A series of unknowns were detected in the Sandhill fen pore water samples and were tentatively identified as monocyclic naphthenic acids (NAs) from the SO_2 chemical class. It is speculated that the unknowns contain tetrahydrothiophene and/or thiacyclohexane ring structures and a carboxylic acid functional group (see below). The plot displayed in Figure S2b shows the retention times of the C_6, C_7, C_8, and C_9 monocyclic SO_2 NAs.

2.1 C_6 Sulfur-Containing Monocyclic Naphthenic Acids

Two analytes in the pore water extracts were tentatively identified as C_6 monocyclic NAs from the SO_2 chemical class. The EI mass spectra of the two analytes are presented in Figures A10a and A10c in the mass spectral library report. The EI mass spectra were characterized by molecular ions at *m/z* 160, which possess the characteristic [M + 2] ^{34}S isotope peak, and an intense base peak at *m/z* 101 (loss of $CH_3OCO^{\bullet}$). The unknowns were confirmed as carboxylic acids following the derivatization of a pore water sample (Well 6A – sampled on July 27, 2011) by BF_3/methanol-d_3. The mass spectra of the deuterated methyl esters (see Figs. A10b and A10d in the mass spectral library report) displayed a molecular ion which was 3 Da higher than the non-deuterated methyl esters, thus confirming the presence of a carboxylic acid chemical moiety. The base peak ion at *m/z* 101 is speculated to be $C_5H_9S^+$, which we propose may be a methyl-substituted-tetrahydrothiophene and/or thiacyclohexane ring. In agreement with our structural assignments, lower mass fragment ions at *m/z* 85 ($C_4H_5S^+$), 59 ($C_2H_3S^+$), and 45 (CHS^+) have been noted to be characteristic of tetrahydrothiophene ring structures in a previous mass spectrometric study of methyl 3-hydroxytetrahydrothiophene-2-carboxylate[4]. The fragment ion at *m/z* 59 was identified as $C_2H_3S^+$ and not CH_3OCO^+ since the deuterated methyl esters also possess the *m/z* 59 fragment.

The EI mass spectra (from NIST database) of thiacyclohexane- and methyl-tetrahydrothiophene-type hydrocarbons were compared (see Figs. A10e-h in the mass spectral library report) and both ring structures displayed similar dissociation patterns to the unknown acids and shared common fragment ions (i.e.: *m/z* 101, 67, 59, and 55). However, the EI mass spectra did not display any obvious diagnostic ions which allowed the differentiation of the ring structures. The fragment ion at *m/z* 87 appears to be more prominent in the thiacyclohexane ring structures (Fig. A10f,h), but it was also detected in the EI mass spectrum of 2-propyl-3-methyltetrahydrothiophene (Fig. A10g).

2.2 C_7 Sulfur-Containing Monocyclic Naphthenic Acids

A set of seven isomers with apparent molecular ions at *m/z* 174 were tentatively identified as C_7 sulfur-containing monocyclic acids. All of the isomers contained the [M + 2] ^{34}S isotope peaks and were confirmed as carboxylic acids following derivatization by BF_3/methanol-d_3. As shown in Figure S2b, the C_7 monocyclic SO_2 NAs showed a slightly increased first and second dimension retention times, relative to the C_6 monocyclic SO_2 NAs. The EI mass spectra for the C_7 sulfur-containing monocyclic acids are presented in Figure A11 in the mass spectral library report.

Four analytes within the series (EI mass spectra shown in Figs. A11a-d in mass spectral library report) showed similar dissociation behavior to the C_6 monocyclic SO_2 NAs discussed above. The four isomers displayed molecular ions at *m/z* 174, and intense base peaks at *m/z* 115 (loss of methyl ester moiety). We suggest that the unknowns may be methyl-substituted analogues of the two C_6 monocyclic SO_2 NAs in the sample (i.e. the methyl esters of ethyl/dimethyl-tetrahydrothiophene carboxylic acid, and/or methyl-thiacyclohexane carboxylic acid).

The EI mass spectrum of an additional isomer is shown in Figure A11e and is characterized by a molecular ion at *m/z* 174 and a base peak at *m/z* 101 (M-73). Fedorak *et al.*[5] previously reported that the EI mass spectrum of the methyl ester of tetrahydrothiophene-1-acetic acid possessed a molecular ion at *m/z* 160 and a base peak at *m/z* 87 (M-73). Given the similar dissociation patterns, we suggest the isomer may be the methyl ester of methyl-tetrahydrothiophene acetic acid, or thiacyclohexane acetic acid.

Lastly, there were two isomers within the series tentatively identified as structural isomers of tetrahydrothiophene propanoic acid. The mass spectra for the isomers (see Figures A11f-g in mass spectral library report). are consistent with the spectrum of the methyl ester of tetrahydrothiophene-1-propanoic acid, previously reported by Fedorak *et al.*[5] The molecular ion was observed at *m/z* 174, and a base peak ion was present at *m/z* 87 (M-87), resulting from the loss of the methyl ester of propanoic acid. A fragment ion at *m/z* 143 was also observed, corresponding to the loss of $CH_3O^{\bullet}$.

2.3 C_8 Sulfur-Containing Monocyclic Naphthenic Acids

A collection of seven unknowns were tentatively identified as C_8 sulfur-containing monocyclic carboxylic acids. The mass spectra for the seven isomers were very similar (See Fig. A12a-g in mass spectral library report); each EI mass spectrum displayed a molecular ion at *m/z* 188 and a large base peak at *m/z* 101 (M–87, loss of methylated propanoic acid). In addition, the seven compounds also possessed characteristic fragment ions at *m/z* 85 ($C_4H_5S^+$), 59 ($C_2H_3S^+$), and 45 (CHS^+). Using the EI mass spectrum of the methyl ester of tetrahydrothiophene-1-propanoic acid[5] as a guide, the unknowns were tentatively identified as isomers of methyltetrahydrothiophene propanoic acid and/or thiacyclohexane propanoic acid.

2.4 C_9 Sulfur-Containing Monocyclic Naphthenic Acids

Lastly, there were three unknowns which have been tentatively identified as C_9 sulfur-containing monocyclic carboxylic acids. The EI mass spectra of the unknowns are presented in Figures A13a-c in the mass spectral library report. The EI mass spectrum of the three unknowns displayed a molecular ion at *m/z* 202 with the [M + 2] ^{34}S isotope peak. The base peak at *m/z* 115 is speculated to be a methyl-subtituted thiacyclohexane ring or a dimethyl/ethyl-substituted tetrahydrothiophene ring. The loss of 87 suggests the loss of propanoic acid from the ring structure.

References:

(1) Wilde, M. J.; West, C. E.; Scarlett, A. G.; Jones, D.; Frank, R. A.; Hewitt, L. M.; Rowland, S. J. Bicyclic naphthenic acids in oil sands process water: Identification by comprehensive multidimensional gas chromatography–mass spectrometry. *J. Chromatogr. A* **2015**, *1378*, 74–87.

(2) Rowland, S. J.; West, C. E.; Scarlett, A. G.; Jones, D. Identification of individual acids in a commercial sample of naphthenic acids from petroleum by two-dimensional comprehensive gas chromatography/mass spectrometry. *Rapid Commun. Mass Spectrom.* **2011**, *25* (12), 1741–

1751.
(3) Ranade, V. S.; Consiglio, G.; Prins, R. Functional-Group-Directed Diastereoselective Hydrogenation of Aromatic Compounds. 1. *J. Org. Chem.* **2000**, *65*, 1132–1138.
(4) Tanaka, H.; Maeda, H.; Suzuki, H.; Kamibayashi, A.; Tonomura, K. Metabolism of Thiophene-2-carboxylate by a Photosynthetic Bacterium. *Agric. Biol. Chem.* **1982**, *46* (6), 1429–1438.
(5) Fedorak, P. M.; Payzant, J. D.; Montgomery, D. S.; Westlake, D. W. S. Microbial degradation of n-alkyl tetrahydrothiophenes found in petroleum. *Appl. Environ. Microbiol.* **1988**, *54* (5), 1234–1248.

Appendix: Mass Spectral Library Report

Summary:

Contains EI-MS of the profiled naphthenic acids included in this study.

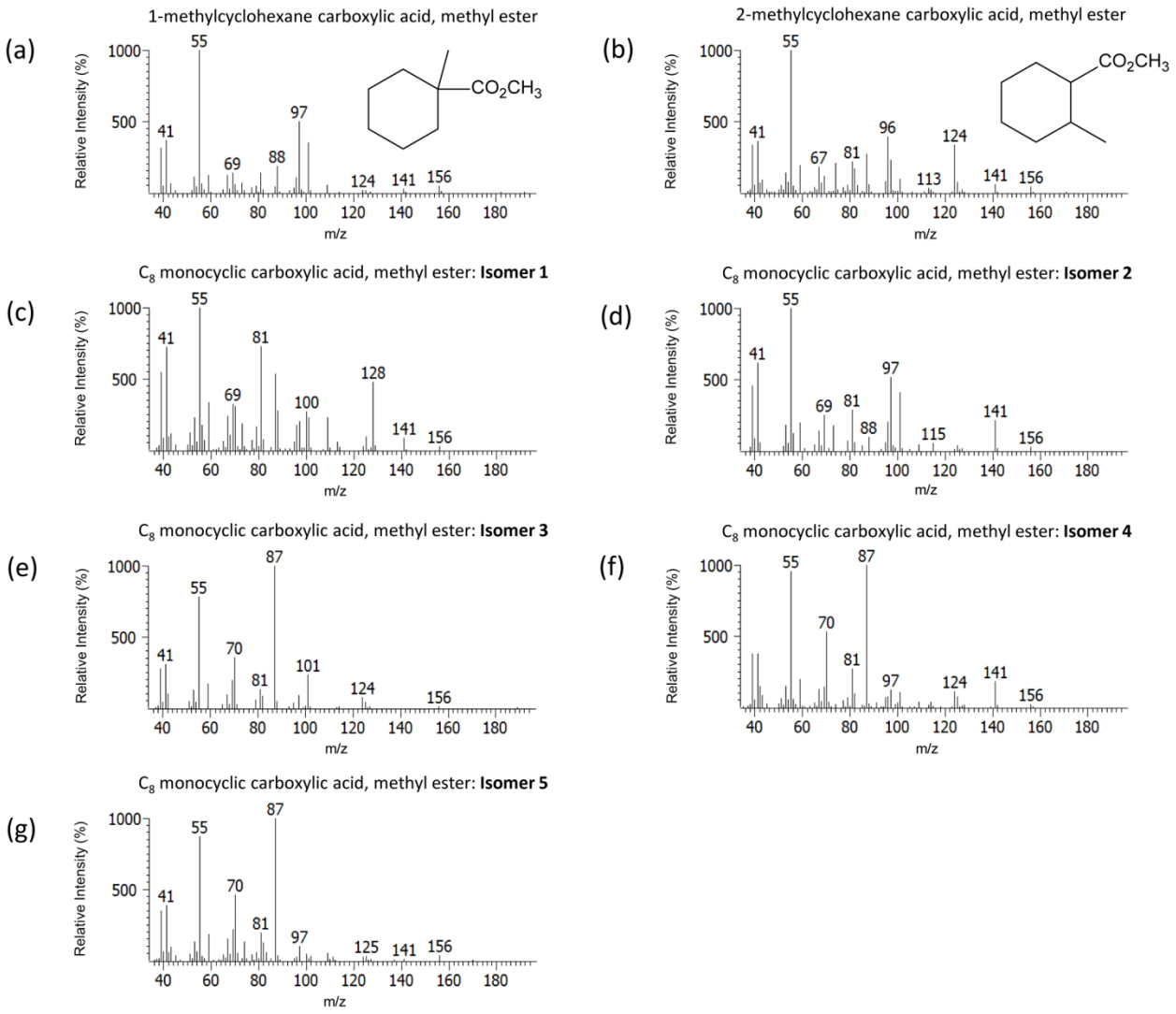

Figure A1. EI mass spectra of the methyl esters of (a) 1-methylcyclohexane carboxylic acid, (b) 2-methylcyclohexane carboxylic acid, and (c-g) unknowns tentatively identified as the methyl esters of C_8 monocyclic carboxylic acid.

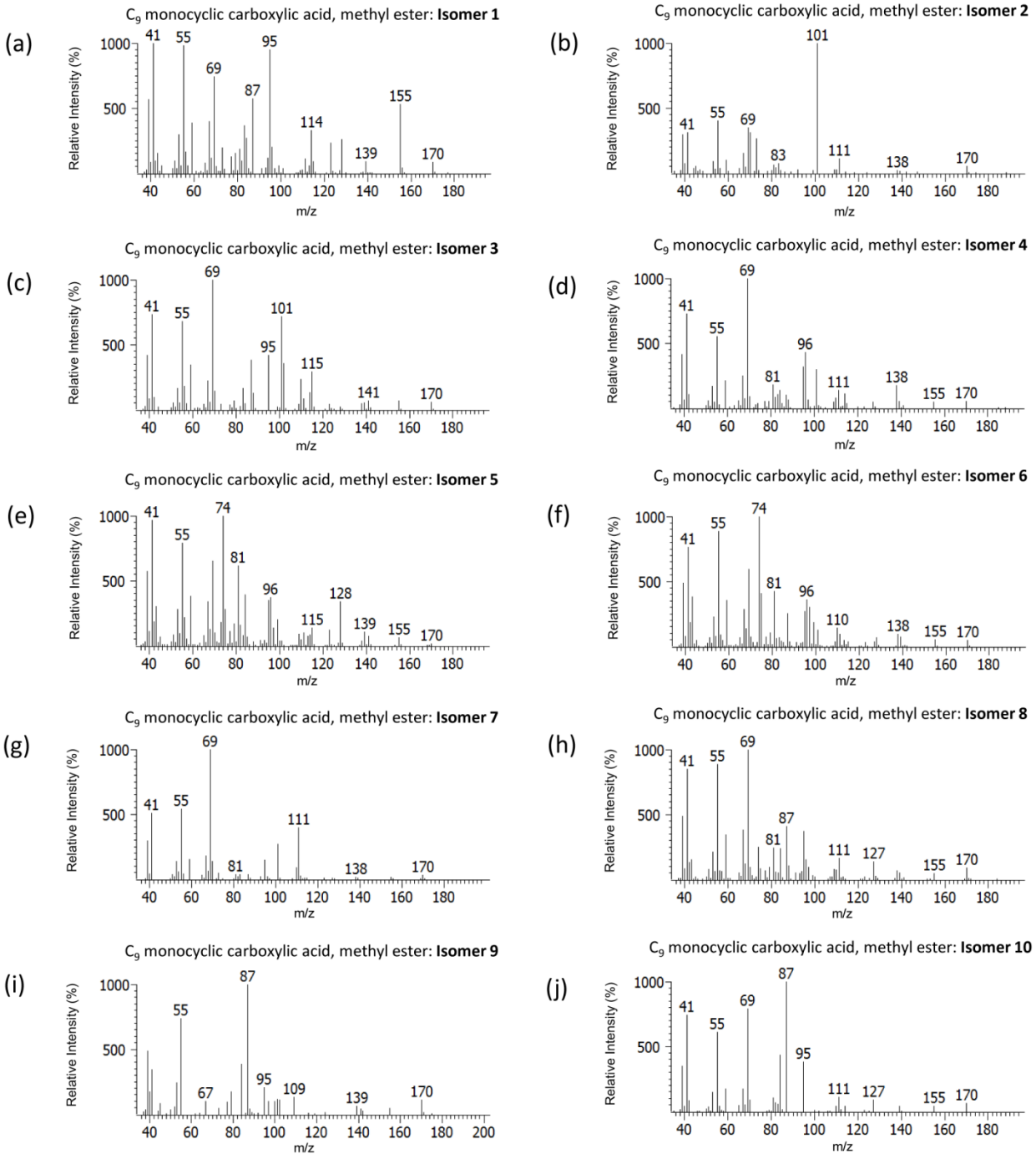

(Figure Continued on Next Page)

(Figure Continued from Last Page)

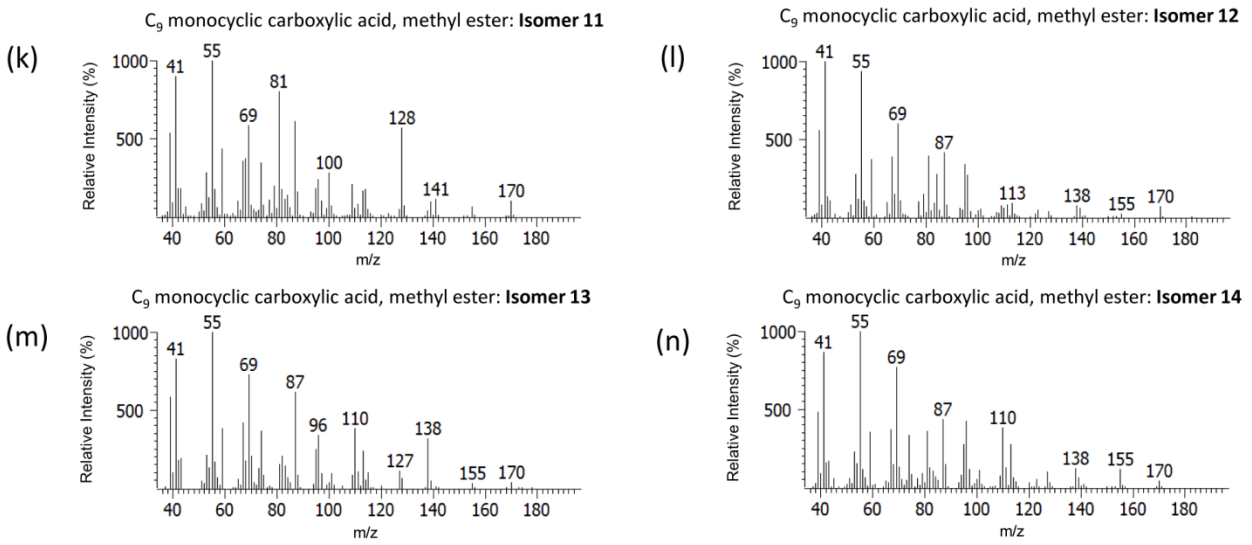

Figure A2. EI mass spectra of unknown compounds tentatively identified as the methyl esters of C_9 monocyclic carboxylic acid.

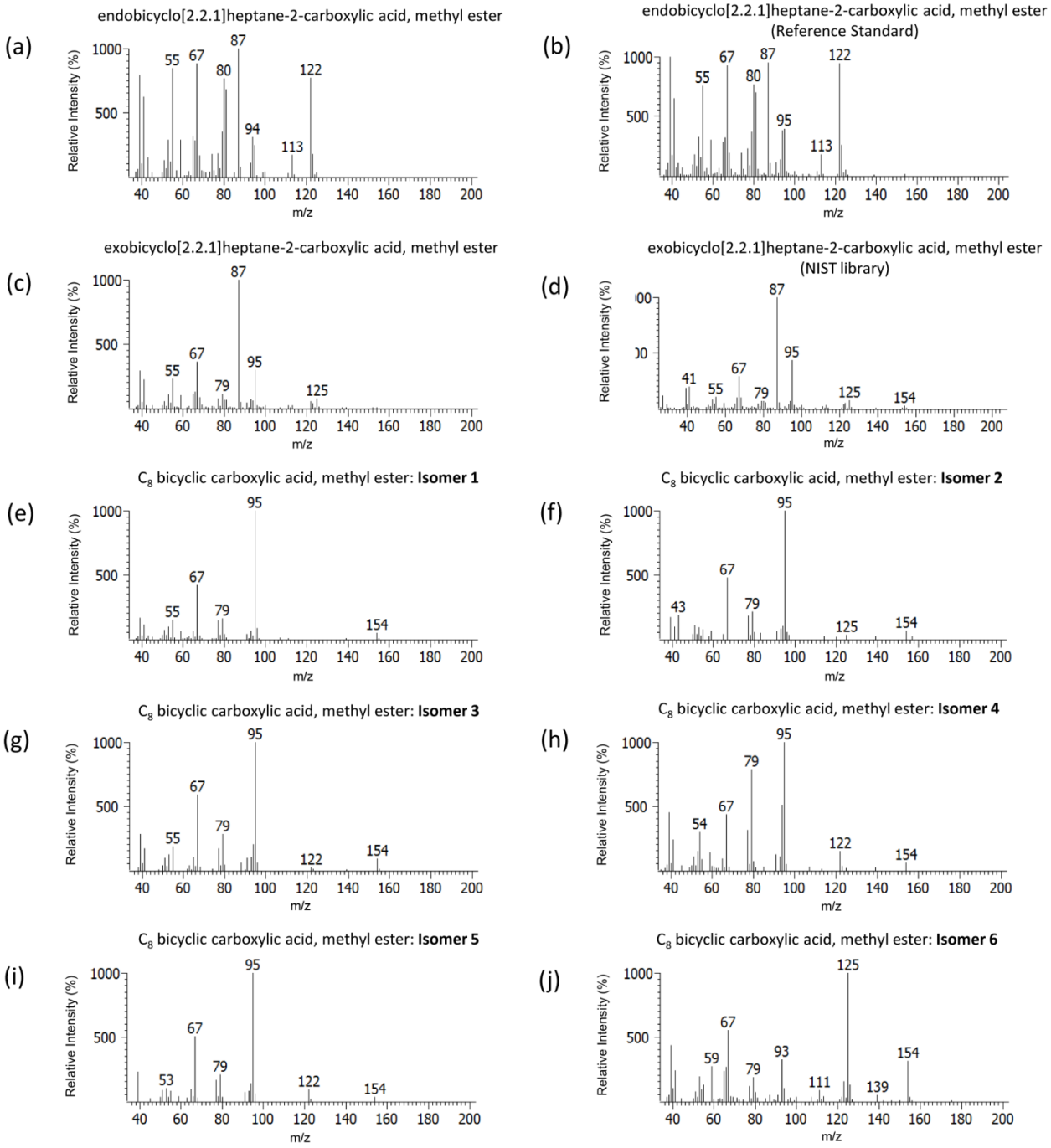

(Figure Continued on Next Page)

(Figure Continued from Last Page)

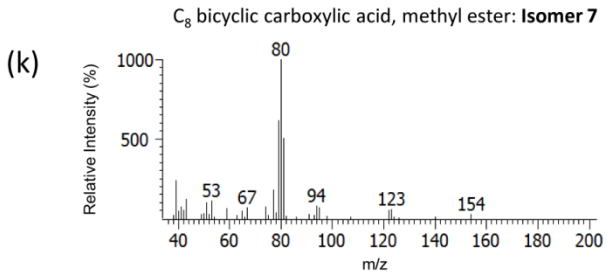

Figure A3. EI mass spectra of the methyl esters of (a) endobicyclo[2.2.1]heptane-2-carboxylic acid, (b) authentic standard of (a), (c) exobicyclo[2.2.1]heptane-2-carboxylic acid, (d) a NIST library spectrum of (c), (e-k) unknown compounds tentatively identified as the methyl esters of C_8 bicyclic carboxylic acid.

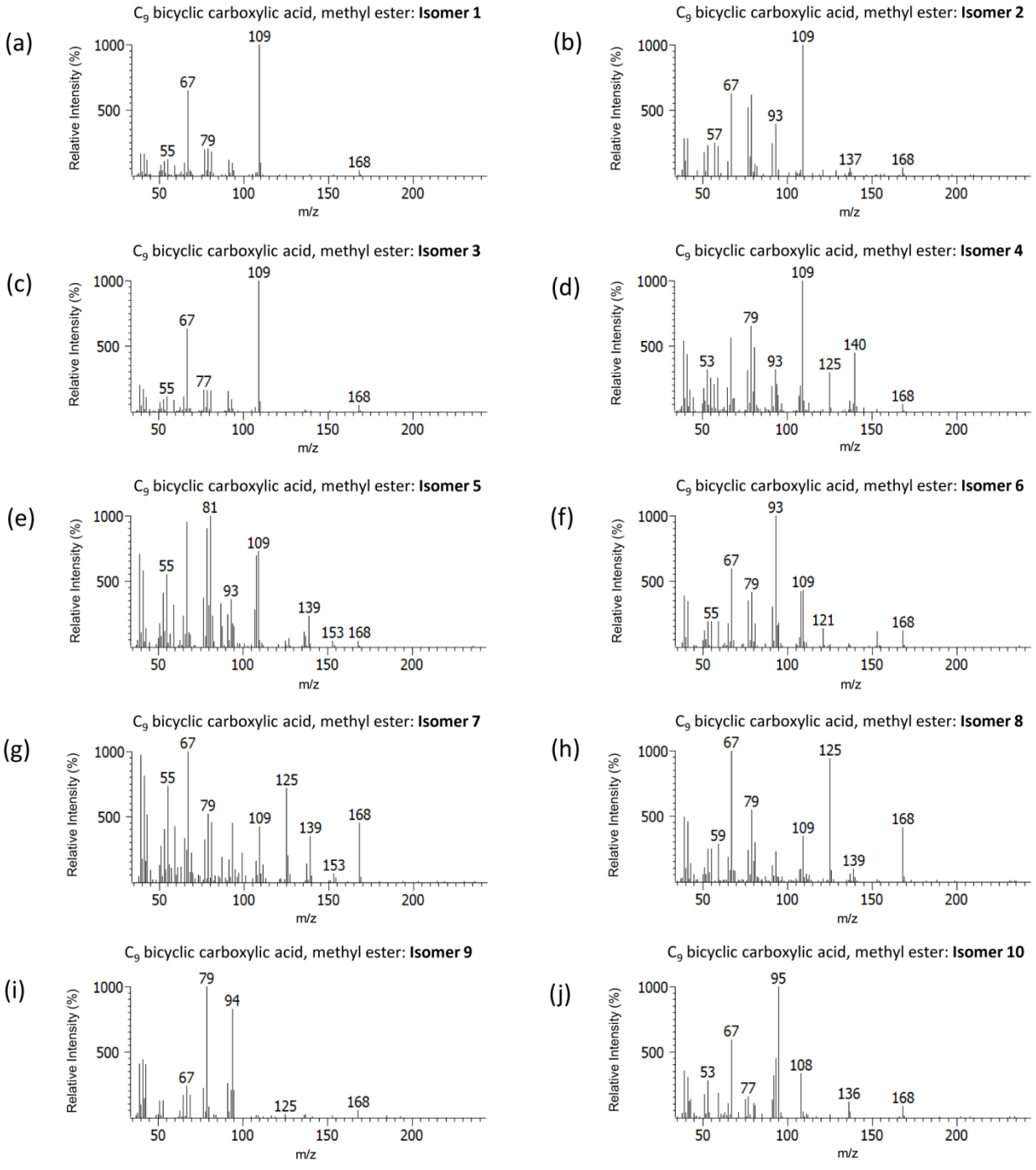

(Figure Continued on Next Page)

(Figure Continued from Last Page)

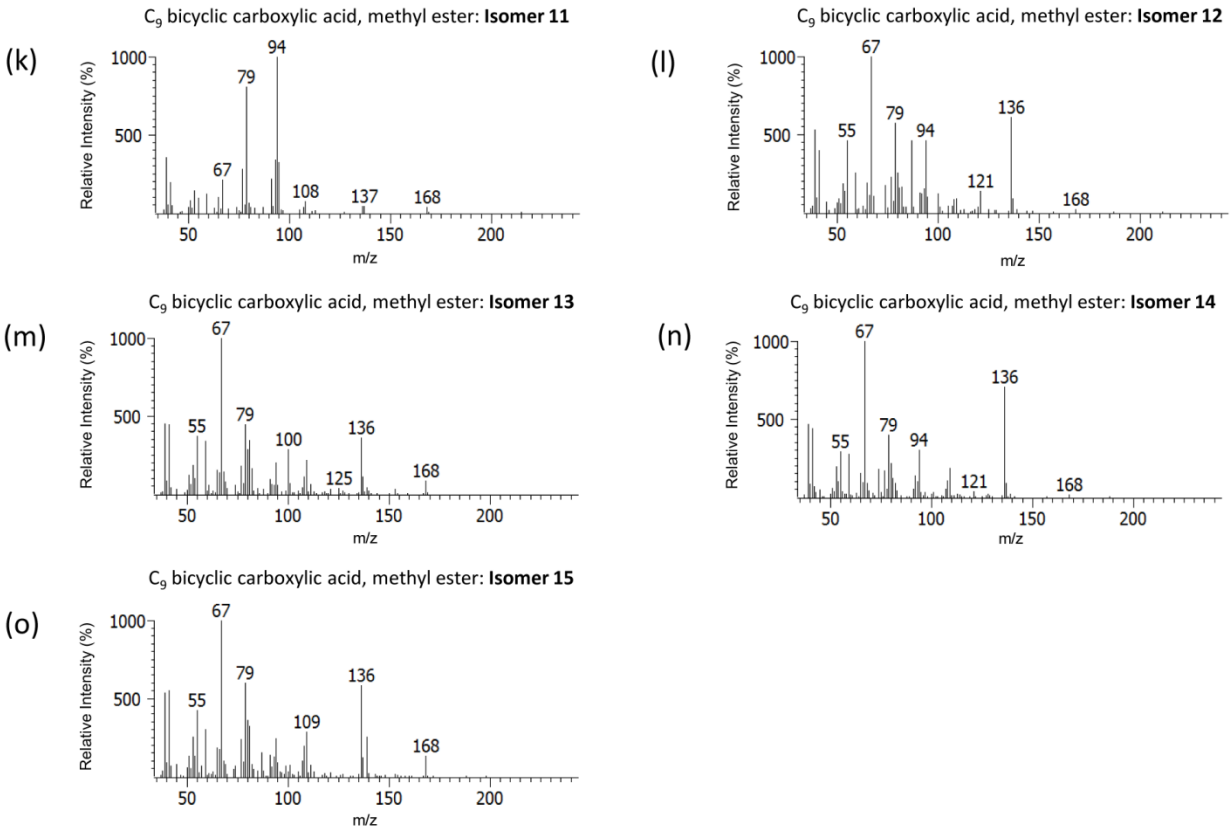

Figure A4. EI mass spectra of unknown compounds tentatively identified as the methyl esters of C_9 bicyclic carboxylic acid.

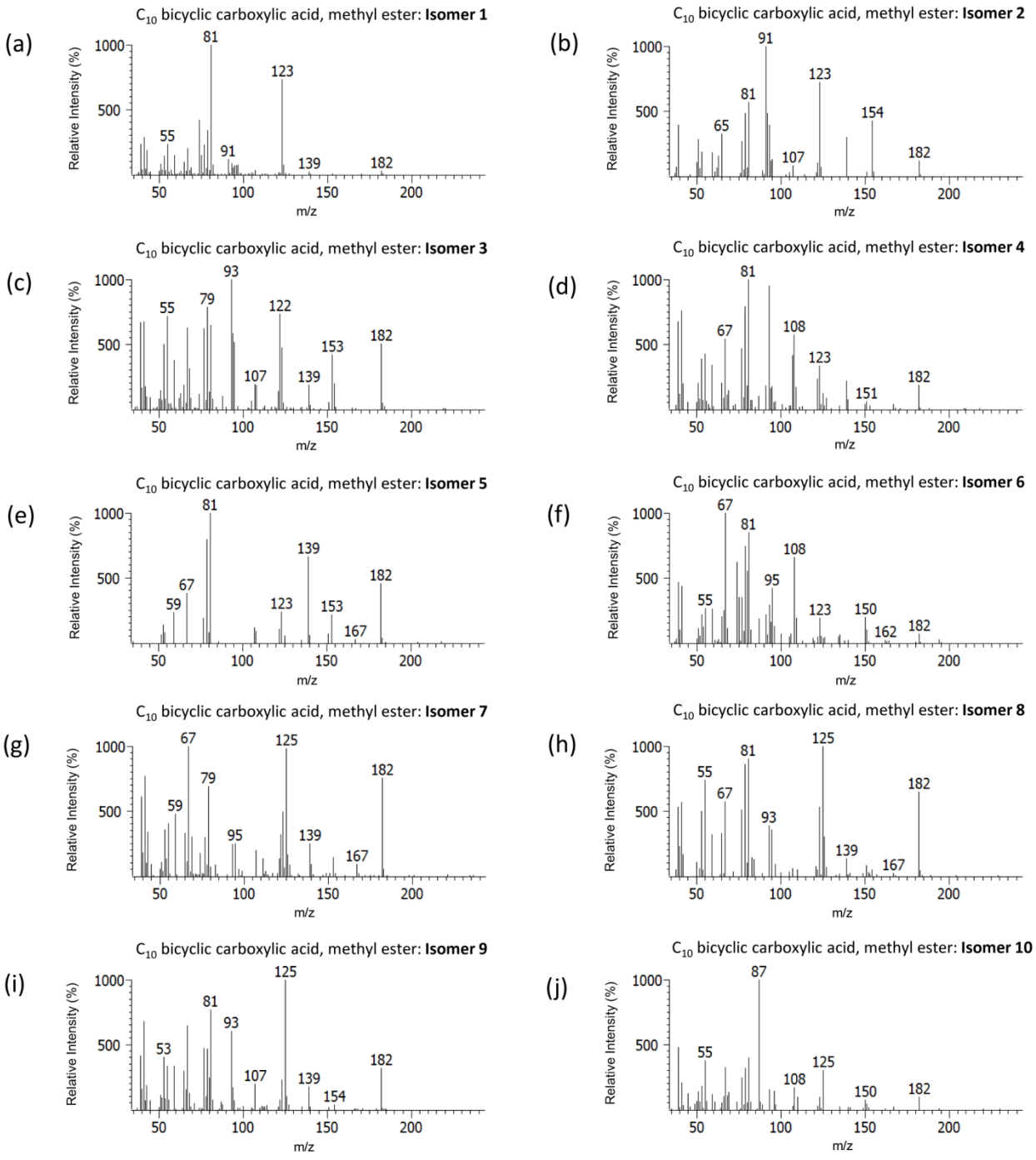

(Figure Continued on Next Page)

(Figure Continued from Last Page)

(k)

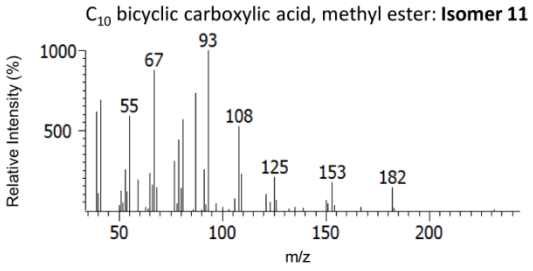

Figure A5. EI mass spectra of unknown compounds tentatively identified as the methyl esters of C_{10} bicyclic carboxylic acid.

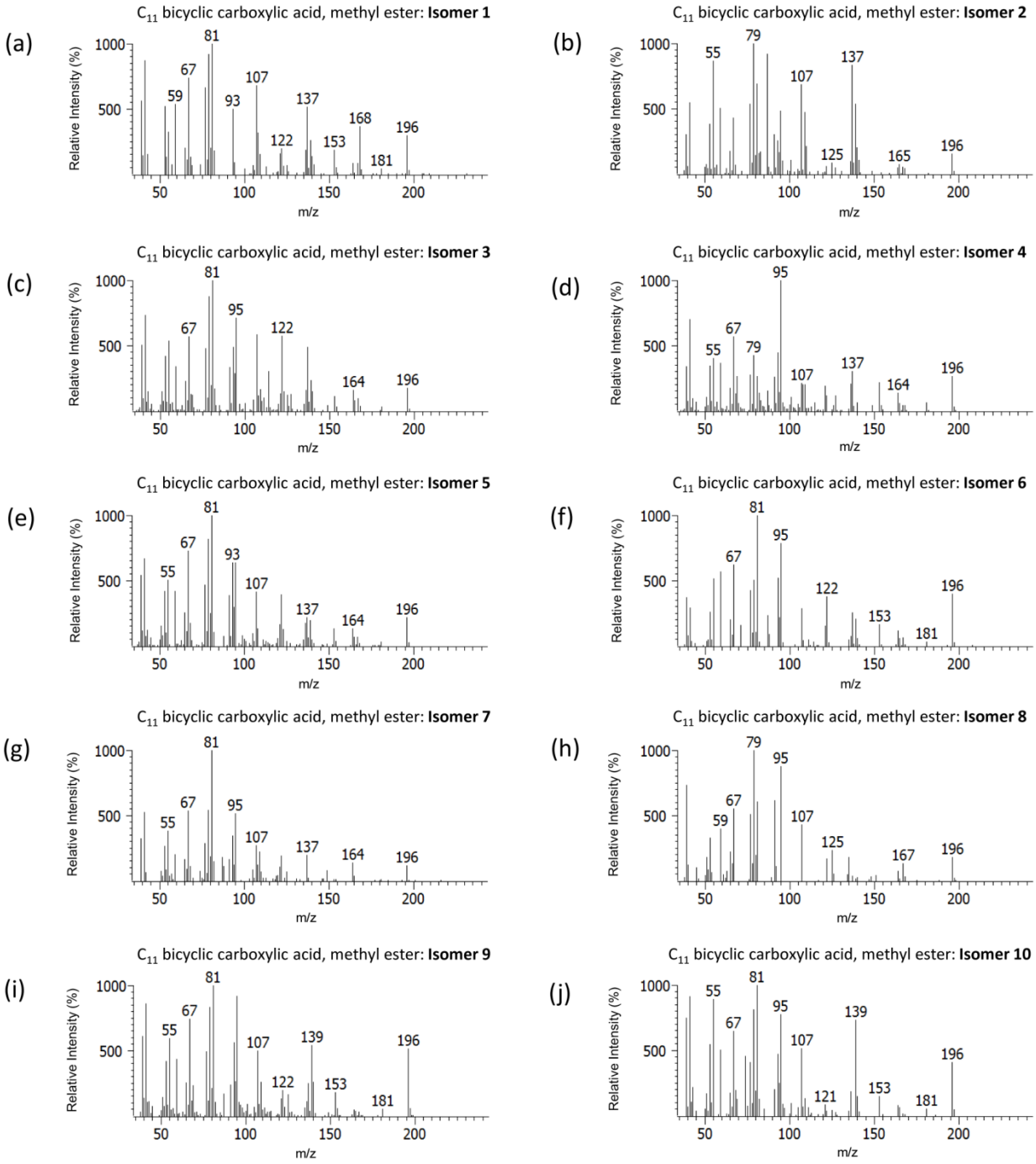

Figure A6. EI mass spectra of unknown compounds tentatively identified as the methyl esters of C_{11} bicyclic carboxylic acid.

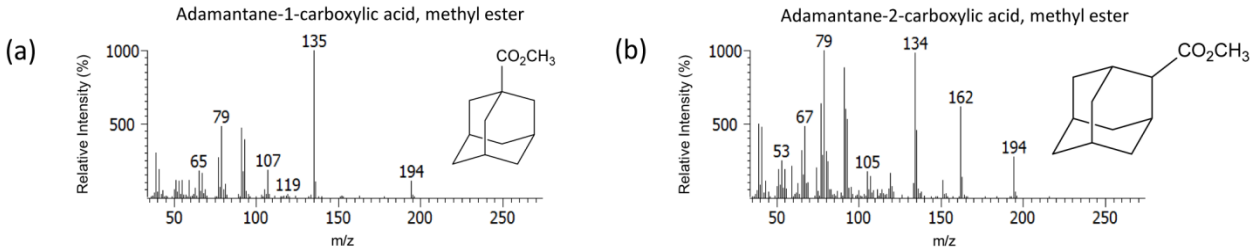

Figure A7. EI mass spectra of the methyl esters of (a) adamantane-1-carboxylic acid, and (b) adamantane-2-carboxylic acid.

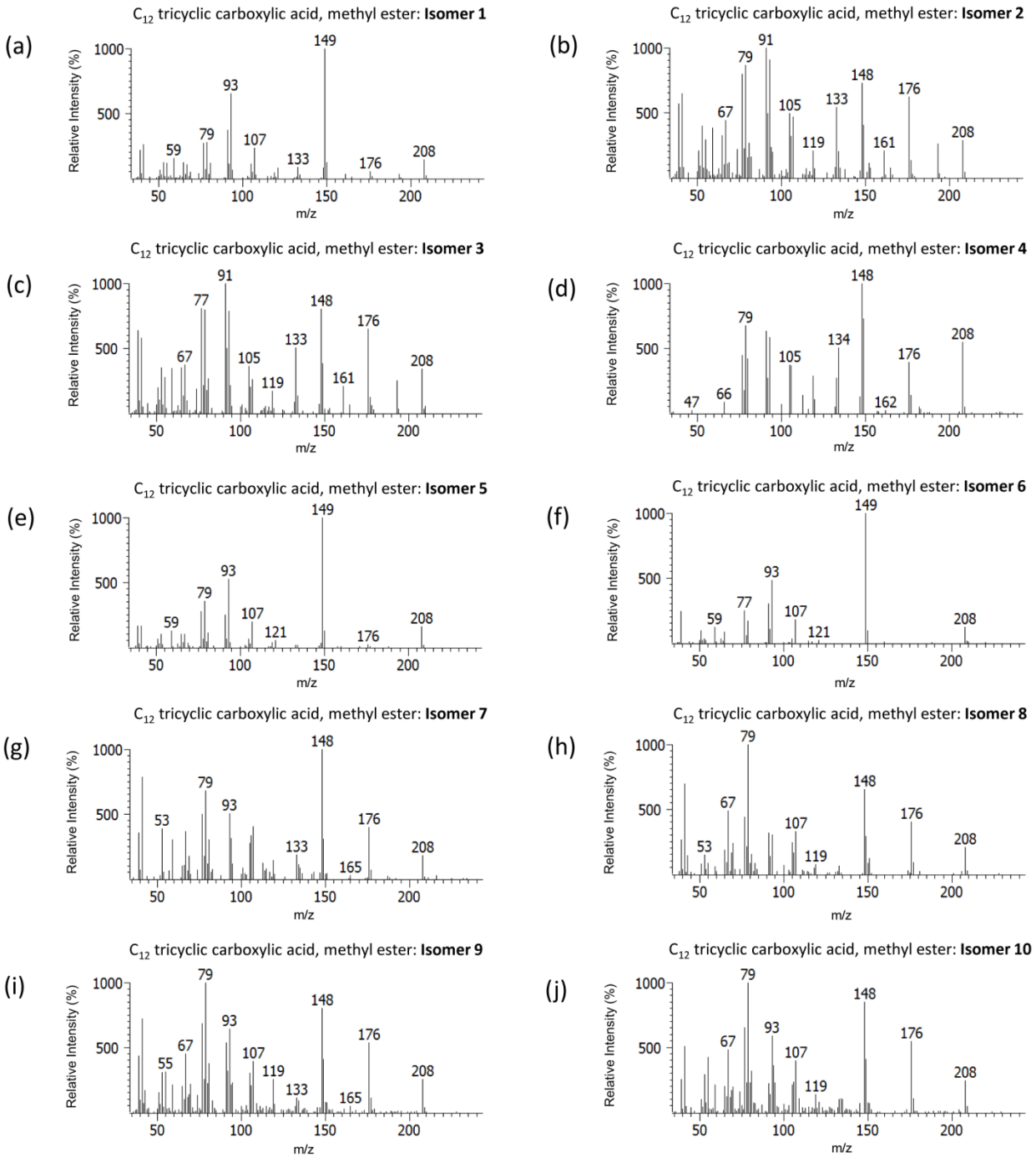

(Figure Continued on Next Page)

(Figure Continued from Last Page)

(k)

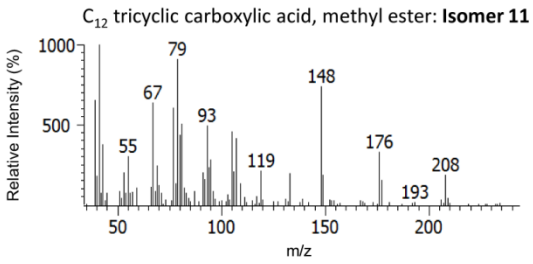

Figure A8. EI mass spectra of unknown compounds tentatively identified as the methyl esters of C_{12} tricyclic carboxylic acid. The mass spectra showed similarities to those of methyladamantane carboxylic acid.

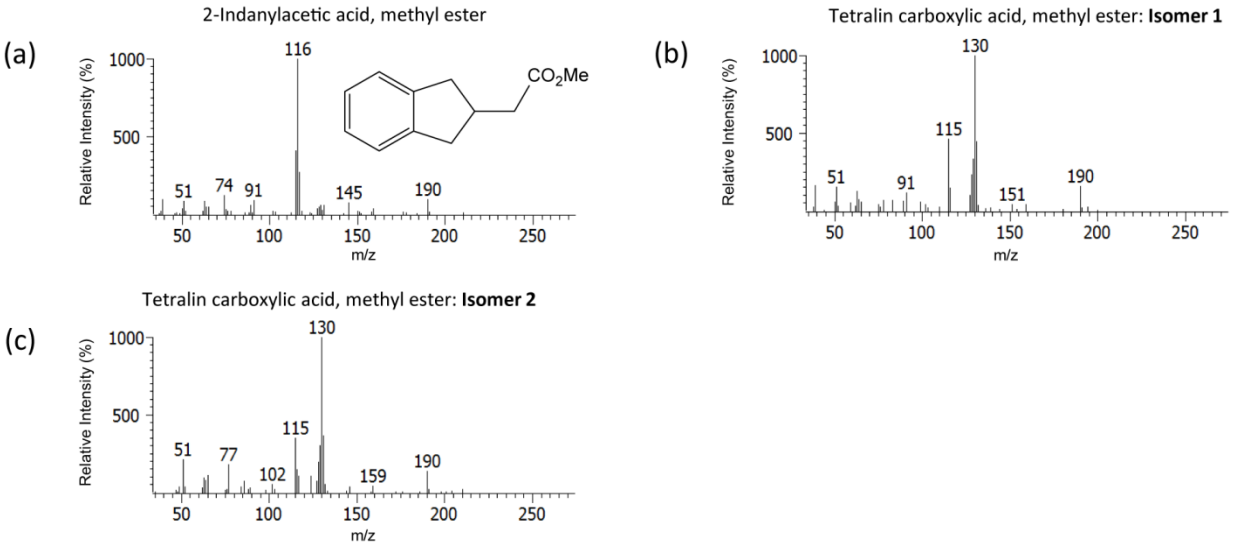

Figure A9. EI mass spectra of the methyl esters of (a) 2-indanylacetic acid and (b-c) unknown compounds tentatively identified isomers of tetralin-2-carboxylic acid.

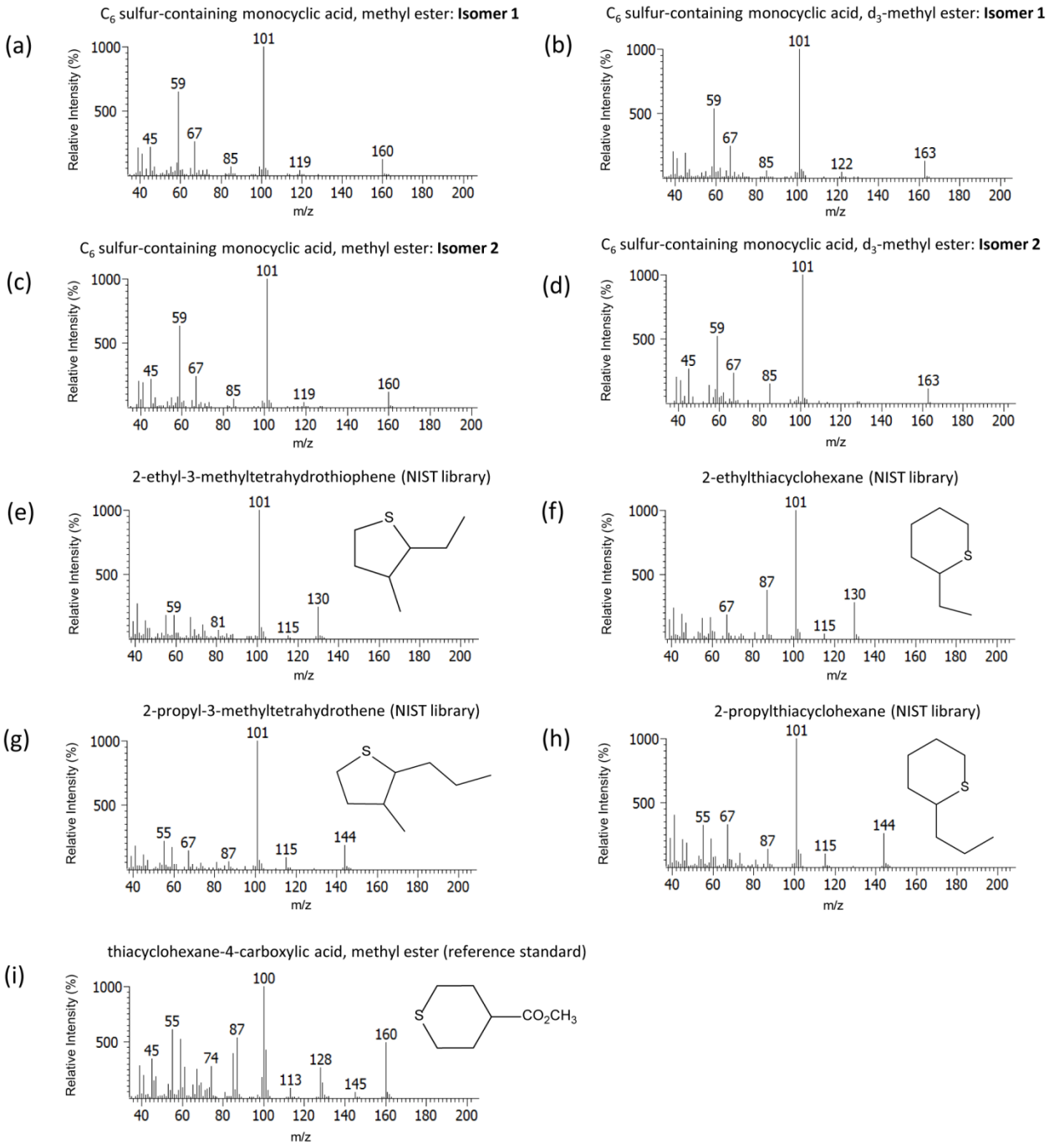

Figure A10. EI mass spectra of (a and c) unknowns tentatively identified as methyl esters of C_6 sulfur-containing monocyclic acid, (b) d_3-methyl ester of (a), (d) d_3-methyl ester of (a). EI mass spectra of compounds from NIST library: (e) 2-ethyl-3-methyltetrahydrothiophene, (f) 2-ethylthiacyclohexane, (g) 2-propyl-3-methyltetrahydrothene, and (h) 2-propylthiacyclohexane. EI mass spectrum of reference standard: (i) thiacyclohexane-4-carboxylic acid, methyl ester.

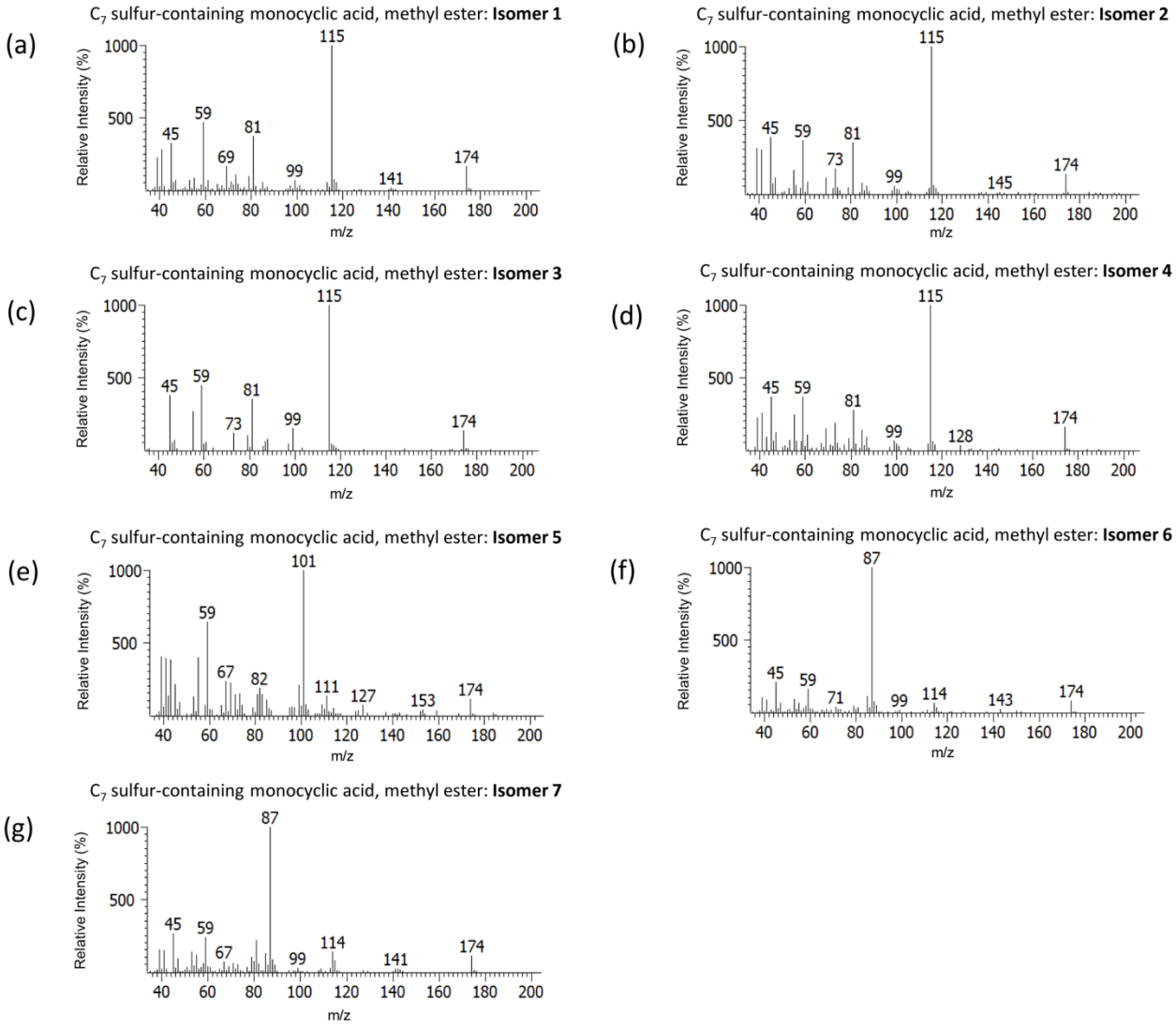

Figure A11. EI mass spectra of unknown compounds tentatively identified as the methyl esters of C_7 sulfur-containing monocyclic carboxylic acid.

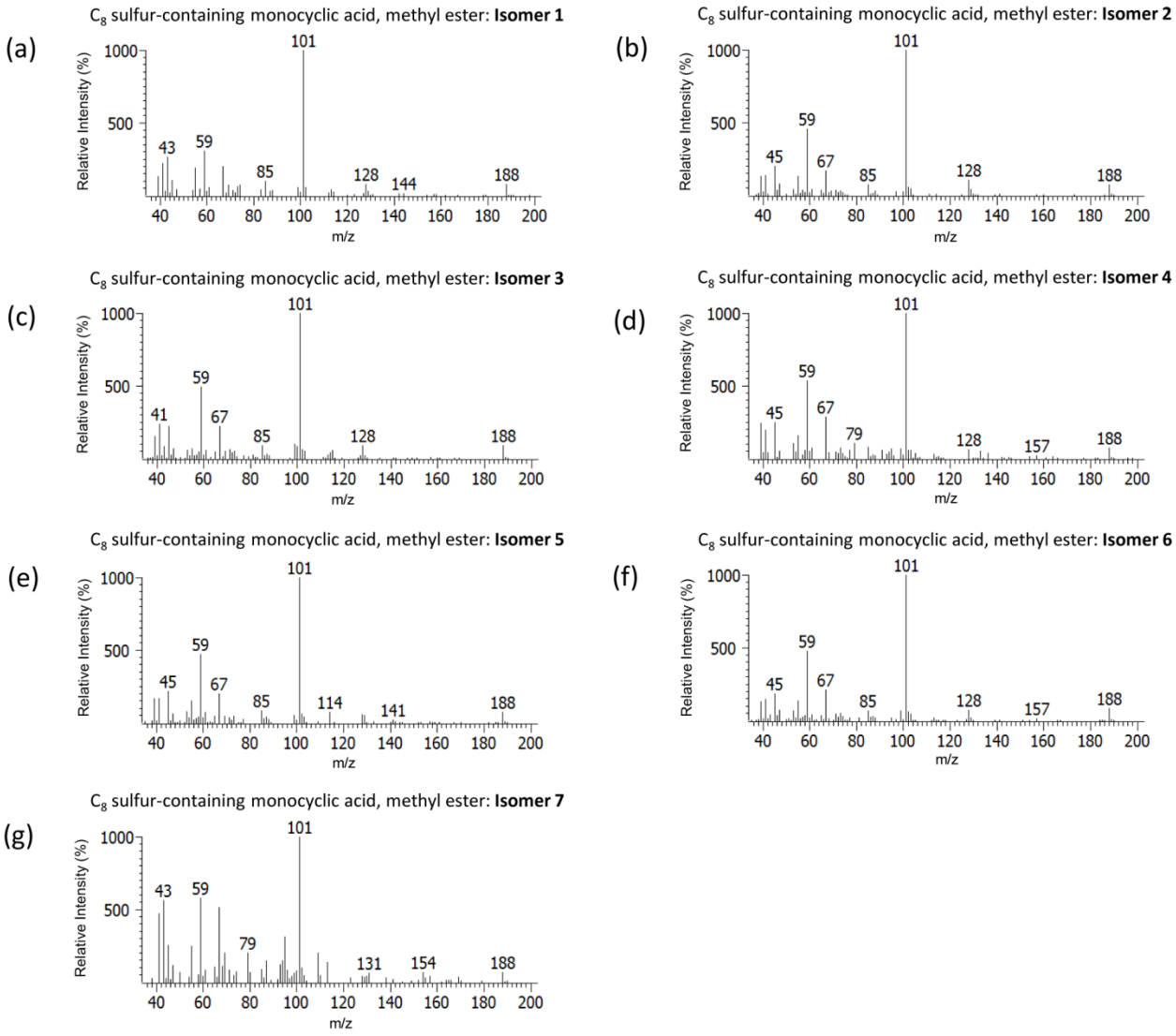

Figure A12. EI mass spectra of unknown compounds tentatively identified as the methyl esters of C_8 sulfur-containing monocyclic carboxylic acid.

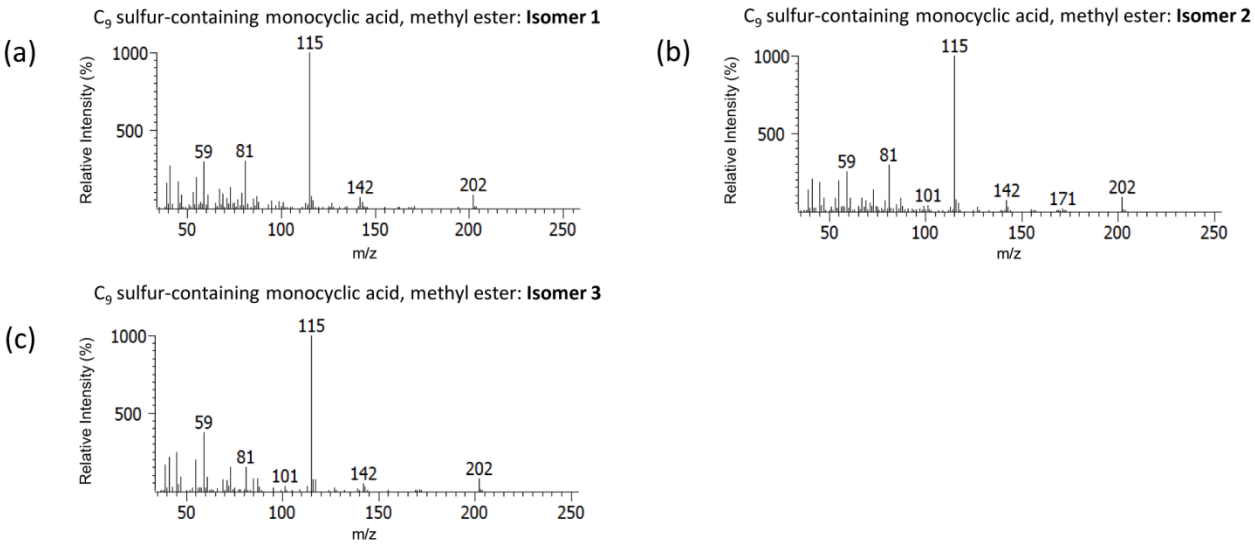

Figure A13. EI mass spectra of unknown compounds tentatively identified as the methyl esters of C_9 sulfur-containing monocyclic carboxylic acid.

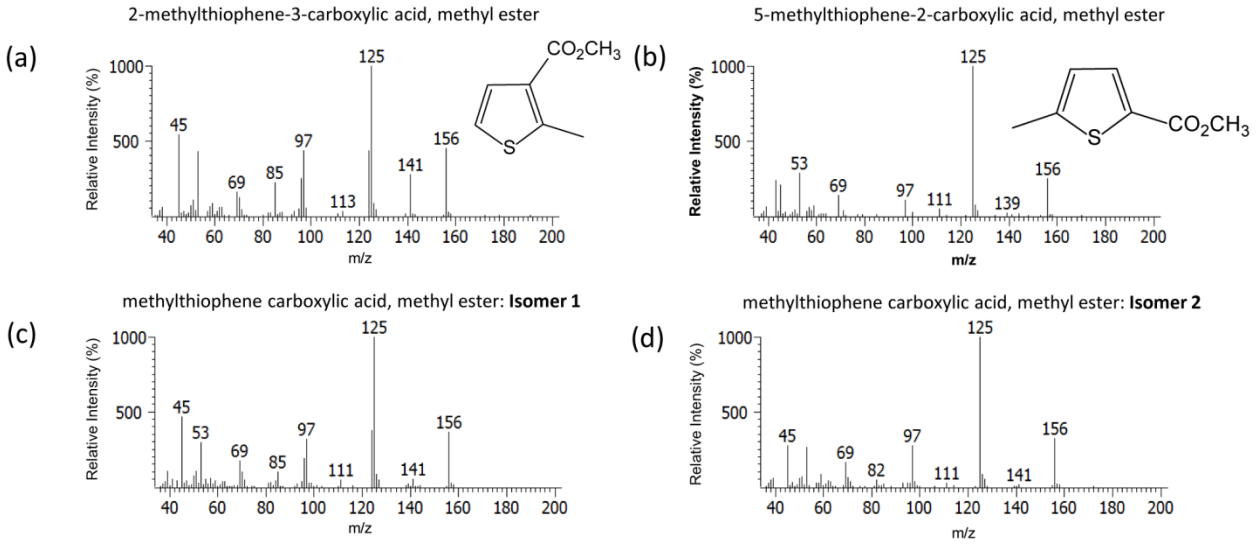

Figure A14. EI mass spectra of: compounds identified as the methyl esters of (a) 2-methylthiophene-3-carboxylic acid, and (b) 5-methylthiophene-2-carboxylic acid; (c-d) unknowns tentatively identified as isomers of methylthiophene carboxylic acid.

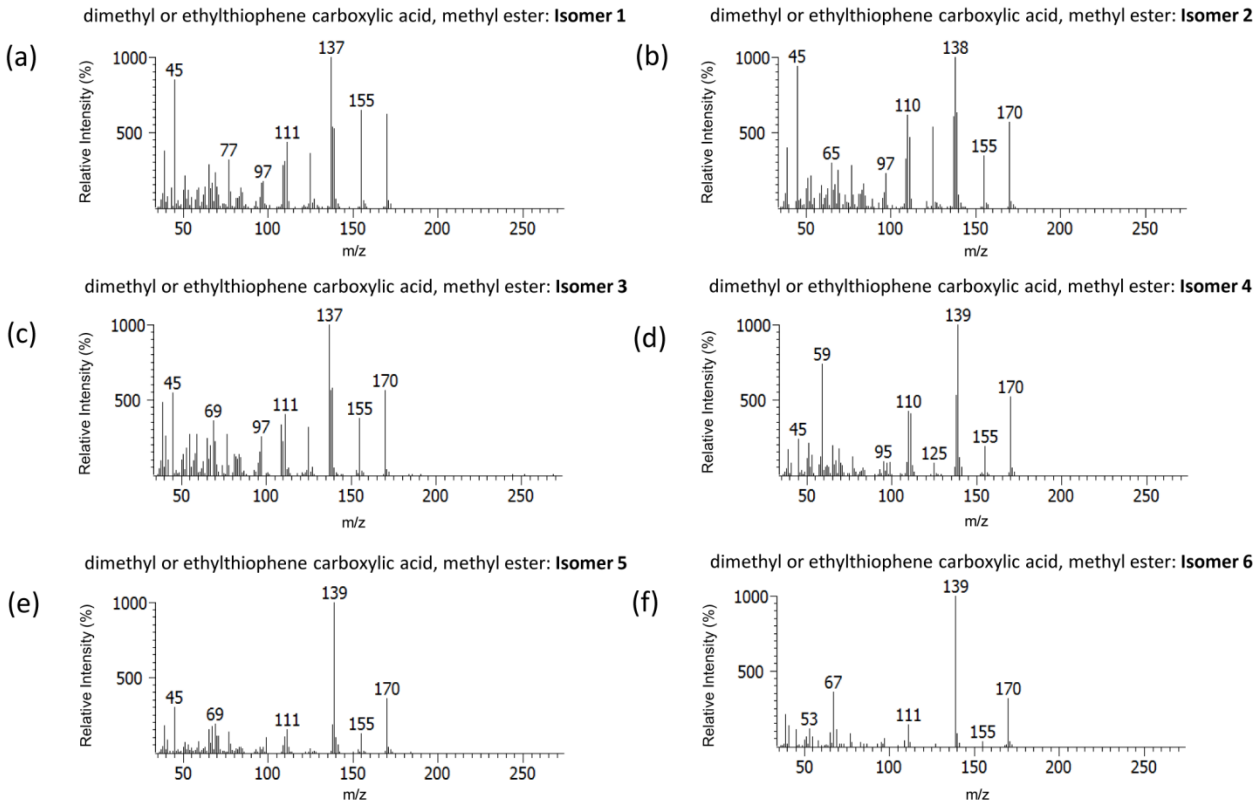

Figure A15. EI mass spectra of unknown compounds tentatively identified as the methyl esters of dimethyl and/or ethyl thiophene carboxylic acid.

Chapter Four: Evaluation of the spatial and short-term temporal variability of individual naphthenic acids at an oil sands end pit lake

David T. Bowman[1], Lesley A. Warren[2,3], Gregory F. Slater[1,2*]

Author Affiliations:

[1]Department of Chemistry and Chemical Biology, McMaster University, 1280 Main Street West, Hamilton, ON, Canada, L8S 4M1
[2]School of Geography and Earth Sciences, McMaster University, 1280 Main Street West, Hamilton, ON, Canada, L8S 4K1
[3]Department of Civil Engineering, University of Toronto, 35 St. George Street, Toronto, ON, Canada, M5S 1A4

Author Contributions:

GFS and LAW conceived the study. DTB, GFS, and LAW designed the study. DTB performed the sample extraction, GC×GC/TOFMS instrumental analysis, data analysis and interpretation, and wrote the manuscript. GFS and LAW edited the manuscript.

Abstract:

Naphthenic acids (NAs) are persistent, toxic contaminants that are found to accumulate in oil sands process-affected water (OSPW) and tailings after bitumen extraction. A number of strategies for the reclamation of oil sands tailings are currently being tested, including the development of the first demonstration end pit lake by Syncrude Canada, Base Mine Lake (BML). An important component of reclamation activities is understanding the source and cycling of naphthenic acids within such reclamation systems. However, naphthenic acids exist as a highly complex mixture of thousands of compounds which makes their analysis an ongoing challenge. In this study, comprehensive two-dimensional gas chromatography coupled to time of flight mass spectrometry (GC×GC/TOFMS) was used to analyze the methylated extracts of water samples from the water cap and fluid fine tailings (FFT) deposit of BML. A collection of monocyclic-, bicyclic-, tricyclic-, and thiophene-type carboxylic acids were identified within the samples; each of the structural moieties contained diverse isomer distributions. Total concentrations of each NA class (by summation of all detected isomers) and individual isomer concentrations were compared across the site, and the greatest differences were detected between fluid fine tailings samples and the water cap. The two samples from the FFT were highly distinct from each other and the overlying water cap. In general, minimal temporal and spatial variability was detected within the stratified water cap. GC×GC/TOFMS was advantageous in this study since the profiling of individual isomer concentrations allowed for the detection of additional compositional differences between water cap samples which were not apparent when total NA concentrations were utilized.

1. Introduction:

The extraction of bitumen from the Alberta oil sands produces significant volumes of oil sands process-affected water (OSPW).[1] OSPW has demonstrated acute and chronic toxicity towards aquatic biota, and this has been primarily attributed to the presence of naphthenic acids.[2–8] Alberta oil sands operators have adopted a zero-discharge strategy, and as a result large volumes of oil sands tailings are stored on-site in tailing ponds and settling basins[1]. While coarse solid particulate matter settles quickly within tailing ponds, the fines fraction (<44μm particle size) consolidates slowly to form an aqueous slurry (25 – 35 wt% solids) known as fluid fine tailings (FFT). The reclamation of FFT is challenging due to its slow sedimentation and consolidation rates[9]. End pit lakes (EPL) have been proposed as a wet reclamation strategy for FFT and OSPW. EPLs are constructed by filling decommissioned mined-out pits with FFT and covering the tailings with a water cap. EPLs are advantageous since they allow oil operators to incorporate tailings waste into oil sands mine closure landscapes and reduce the inventories of FFT within tailings ponds.[10] While the water cap of an EPL will initially consist of OSPW, the water quality is expected to improve over time, as a result of *in situ* biogeochemical processes and fresh water inputs, and evolve into a natural lake system capable of supporting aquatic life. However, since the strategy is still in its demonstration stage, there is a need to chemically characterize and monitor the biogeochemistry of the system, and in particular, to understand the behaviour of toxic components, such as naphthenic acids.

Naphthenic acids (NAs) are naturally occurring in the Athabasca oil sands region (AOSR). NAs are traditionally defined as acyclic and alicyclic monocarboxylic acids (general formula $C_nH_{2n+Z}O_2$, where n = carbon number, Z = degree of unsaturation)[11], but, in light of recent studies using ultrahigh resolution mass spectrometry[12–17], the definition has been broadened to include heteroatomic chemical species, such as oxygen-, nitrogen-, and sulfur-containing compounds. NAs are of environmental concern since they have been linked with the acute and chronic toxicity of OSPW[18–23] and are known to persist within tailing ponds and other reclamation sites[24,25]. NAs exist as highly complex mixture within OSPW and FFT pore water and the identities of many of the individual components within NA mixtures are unknown. As a result, the development of a suitable analytical technique to monitor the environmental fate of NAs and discriminate sources has been an on-going challenge.

In recent years, a plethora of analytical methods utilizing mass spectrometry have been developed for the characterization of NAs within oil sands related samples.[26,27] Advances in ultrahigh resolution mass spectrometry have significantly improved our understanding of NA mixtures. The high mass resolving power and high mass accuracy of such techniques have enabled the unambiguous assignment of elemental compositions within OSPW and have been useful in studies related to oil sands forensics.[28,29,16] Comprehensive two-dimensional gas chromatography (GC×GC) coupled to nominal[30–34] and high resolution[35–37] mass spectrometry

has significantly improved the characterization of NAs and has facilitated the identification of many individual naphthenic acids with a variety of structural motifs.[31,34,36,38–45] The high resolving power of GC×GC/TOFMS allows the generation of diverse isomer profiles which may be useful for NA monitoring programs and discriminating NA sources. It has been shown that resolved adamantane-type carboxylic acids can be used as biomarkers to not only differentiate OSPW sources[46], but also assess the short-term temporal and spatial variability of tailing ponds[47]. In addition, the GC×GC profiling of tentatively identified aromatic acids has been used in two separate studies to distinguish OSPW contamination in groundwater systems from waters exposed to natural bitumen deposits (in conjunction with Orbitrap MS)[48] and to evaluate temporal and spatial trends within tailing ponds.[49] However, despite these recent studies, the occurrences of most identified naphthenic acids, such as cyclohexane-[31,33], bicyclic-[33,38], indane-[31,39], tetralin-[31,39], and thiophene[31]-type carboxylic acids, are unknown within tailing ponds and the greater environment.

In this study, GC×GC/TOFMS was used to assess the spatial and short-term temporal variability of naphthenic acids at Syncrude's Base Mine Lake (BML). Analyses by GC×GC/TOFMS allowed the detection of monocyclic-, bicyclic-, tricyclic-, and thiophene-type carboxylic acids within samples collected from the overlying water cap and FFT. Diverse isomer distributions were obtained for each structural moiety, and individual naphthenic acids were semi-quantified using the closest available standards. Total concentrations for each NA class (by summation of all isomers within isomer series) and individual isomer concentrations were compared across the site, and distinct differences were detected between FFT samples and the water cap. In general, minimal temporal and spatial variability was detected within the stratified water cap. However, the comparison of individual isomer concentrations allowed for the detection of additional subtle differences between samples which were not apparent when total NA concentrations were utilized.

2. Materials and Methods:

2.1. Chemicals and Reagents:

Dichloromethane (distilled in glass) was purchased from Caledon Laboratories (Georgetown, Ontario, Canada). The following standards were purchased: adamantane-1-carboxylic acid (99%, Sigma-Aldrich, St. Louis, MO, USA), 1-methylcyclohexane-1-carboxylic acid (99% Sigma-Aldrich), *trans*-4-ethylcyclohexane-1-carboxylic acid (Aldrich^{CPR}, Milwaukee, WI, USA), octahydro-3-methylpentalene-1-carboxylic acid, and 5-ethylthiophene-2-carboxylic acid (99%, Sigma-Aldrich).

2.2. Site Description

Samples were collected from Base Mine Lake (BML), located at Sycrude's Mildred Lake mine site, north of Fort McMurrary, Alberta, Canada. The end pit lake was established within a depleted open mine pit (West-in Pit), which was in-filled with approximately 186 Mm^3 of FFT beginning in 1994. When filling was complete in October 2012, the FFT deposit possessed a maximum thickness of 48 m and was overlaid with a water cover (depth of 6 m). Water was pumped into BML from the adjacent Beaver Creek Reservoir (BCR) to reach a water surface elevation of 308.7 meters above sea level. The water cap has an average depth of 8.5 m and covers a surface area of approximately 8 km^2. The volume of the water cap is approximately 65 Mm^3. Depth-dependent temperature and dissolved oxygen profiles were measured at BML during the summer of 2015, and thermally stratified conditions were observed within the lake. Three distinct zones were detected within the water cap: Epilimnion (depth from surface: 0 m to 4 m), Metalimnion (depth from surface: 4 m to 6 m), Hypolimnion (depth from surface: 6 m to 9 m). The water cap of BML is ice covered through the winter and experiences turnover in the fall and spring.

Each year, inputs of fresh water (5 to 10 Mm^3) from BCR are pumped into BML to simulate future water inflow from adjacent reclaimed landscapes. Therefore, in order to maintain the lake surface elevation, water is removed from BML and is recycled for use in the bitumen extraction process. To date, dilution has resulted in the displacement of approximately 20% of the total lake volume. The annual inputs of fresh water from precipitation and snowfall events are 3 Mm^3, but have been reported to be similar to evaporation outputs.[10] According to a model developed by Carrier *et al*. (2007)[50], the settling of FFT is expected to initially contribute 1 m/year of released pore water to the water cap. The FFT dewatering rate is predicted to exponentially decrease over time, reaching a plateau of approximately 0.1 m/year after 30 years.

2.3. Sampling Methods

Figure 1 presents a map of BML and the locations of the two sampling platforms (Platform 2, or P2; Platform 3, or P3), and a diagram illustrating the stratification of the water cap. Water samples were collected using a 1-L van dorn bottle on two dates from three depths during summer stratification (June 2/3, July 20/21; epilimnetic, metalimnetic and hypolimnetic; Figure 1b) and one date post stratification at the same proximate depths (September 22/23) in 2015 (Table 1). The depth-dependent oxygen and temperature profiles for the three sampling events are plotted in Figure 2 and 3. Although the lake was not stratified on September 22, samples are still categorized into stratified zones (epilimnion, metalimnion, and hypolimnion) based on their depths to allow comparisons to samples from the summer. Two FFT samples were collected on August 3, 2015 from the FFT at Platform 2 and 3, with measured depths of 18 m and 16 m from the water surface, respectively (which approximates ~ 8 and 6 meters down from the FFT-water interface respectively). FFT samples were collected by a non-commercial pneumatic piston sampling device, as described in a previous study[10]. Following collection, the water cap and FFT

samples were stored within pre-cleaned Nalgene plastic bottle at -20°C and were thawed prior to sample extraction.

2.4. Extraction of Naphthenic Acids

All water samples from the water cap of BML were filtered using a 0.45 µm syringe filter (Gelman Sciences, Ann Arbor, MI, USA), acidified to pH 2, and extracted with dichloromethane (4 x 15 mL). The extracts were combined and concentrated to 1 mL by rotary evaporation. The extract was quantitatively transferred to a glass vial and concentrated to 30 µL by blowing gently with nitrogen. The naphthenic acids were converted to methyl ester derivatives by treatment with diazomethane in dichloromethane. Diazomethane was added until the yellow colour persisted. An internal standard, pyrene-d_{10} dissolved in toluene (10 µL), was added to the extract prior to analysis (final concentration of 1 ppm). The fluid fine tailings samples were centrifuged at 2041 *g* for 60 minutes and the supernatant was removed. The supernatant was then extracted and derivatized using the method described above. The extraction procedure was performed in triplicate for each sample. Procedural blanks (HPLC grade water) were performed alongside each triplicate extraction to monitor contamination during the extraction process. The extraction efficiency of the sample preparation procedure was evaluated by calculating the percent recovery of two recovery surrogate standards: 4-tertbutylcyclohexane-1-carboxylic acid (88% ± 13) and 2-hexyldecanoic acid (90% ± 14).

2.5. Semi-quantitative Analysis of NAs by GC×GC/TOFMS

GC×GC/TOFMS analyses were performed using a Pegasus 4D system (LECO Corp., St Joseph, MI, USA). The GC×GC was equipped with Rtx-17sil ms (30 m x 0.25 mm x 0.15 µm) as the primary column and DB-5 ms (1.0 m x 0.10 mm x 0.10 µm) as the secondary column. Splitless injection of the samples was performed with a volume of 2 µL and an inlet temperature of 250°C. The primary oven temperature program was set to hold at 40 °C for one minute, ramped to 310 °C at a rate of 2.5 °C/min, and held at 310 °C for 20 min. The secondary oven was programmed to operate at a +5 °C offset, relative to the primary oven. A modulation period of 3 s was used. The modulator temperature offset was +15 °C relative to the secondary oven. Helium was used as the carrier gas at a flow rate of 1mL/min. The time-of-flight mass spectrometer operated in positive ion electron ionization mode at 70 eV and was scanned over a mass range of m/z 30 to 500 at a sample acquisition rate of 200 scans/s. The ion source and transfer line temperatures were set to 200 °C and 280 °C, respectively. Data processing of GC×GC/TOFMS data was performed by ChromaTOF version 4.50.8.0 (LECO Corp). Library searches were conducted with the NIST/EPA/NIH Mass Spectral Library 2008 (NIST 08, Gaithersburg, MC, USA) and a user library containing NA reference standards.

Semi-quantitation of NAs was based on an external 6-point calibration curve (dynamic range of 0.1 - 25 ng/µL; $r^2 > 0.990$) using NA reference standards with similar structural moieties to the target NAs. The calibrations standards used in this study and their calculated detection limits are found in Table 2. The instrumental detection limits (IDL) were estimated by multiplying the standard deviation obtained from six analyses of the lowest concentration calibration standard with the T-value (99% percentile for n-1 degrees of freedom). IDL values ranged between 24 to 43 pg/µL. Method detection limits (MDL) were calculated from the IDL, considering the analyte concentration steps within the extraction procedure.

Statistical Analysis:

Univariate statistical analysis was performed using SPSS statistical software package (Version 17.0.0, SPSS Inc., Chicago, Il, USA). Non-detects were replaced with concentration values which were one half of the MDL. Data was tested for normality and homogeneity of variance using Shapiro-Wilk ($\alpha = 0.05$) and Levene's test ($\alpha = 0.05$), respectively. Data which did not meet the parametric assumptions of normality and homoscedasticity was log transformed. Student's t-test ($\alpha = 0.01$) was used to compare two means. One-way analysis of variance (ANOVA) ($\alpha = 0.01$) was used to test for differences between three or more means. Welch's test ($\alpha = 0.01$) was used to compare means with unequal sample sizes. Principal component analysis (PCA) was performed using Metaboanalyst 3.0[51], following log transformation and pareto scaling of the dataset. Naphthenic acids which were not present in more than 60% of the samples were removed from the dataset prior to the PCA.

3. Results/Discussion

The GC×GC analyses of the water cap and FFT pore water extracts resulted in the detection of over 2500 unique compounds within each sample following data processing by ChromaTOF. In order to assess the temporal and spatial variations at BML, a subset of well-resolved naphthenic acids, which have been identified in previous studies[31,38], were compared between the samples. Table 3 lists the target NAs in this study, and the number of structural isomers detected within the surface water and FFT pore water extracts. The first and second dimension retention times of the targeted NAs are plotted in Figures 4-7.

3.1. ∑ Concentrations for NA Isomer Classes at BML

Each isomer was semi-quantified using the closest available reference standard (see Table 4), and total concentrations were calculated for each NA class by summation of all isomers (see Figure 8 and Table 5; NB: water cap concentrations are presented as an average of all sampling events). In general, the ∑ NA concentration values for the monitored classes were elevated within the FFT, relative to the water cap. The largest concentrations were observed within the

FFT pore water sample from Platform 2, where the difference of total concentration values between the FFT and water cap were as high as 30-fold. Within the water cap and the Platform 3 FFT sample, the $\sum C_{11}$ bicyclic NAs displayed the greatest concentrations, followed by the $\sum C_{12}$ tricyclic NAs. Within the FFT sample from Platform 2, the concentration of $\sum C_7$ thiophene NA was highly elevated, in addition to the $\sum C_{11}$ bicyclic NAs and $\sum C_{12}$ tricyclic NAs. For each structural moiety, the $\sum$ concentrations within the water cap generally increased with carbon number. Similar trends were observed in the FFT, with the exception of the monocyclic NAs at Platform 2, which possessed the following order of increasing concentrations: $\sum C_9$ monocyclic NA $>\sum C_{10}$ monocyclic NA $> \sum C_8$ monocyclic NA.

3.1.1. Temporal Variations of ∑ NA Concentrations within Water Cap

In order to assess the short-term temporal variations of the $\sum$ concentrations of the monitored NAs within the water cap, the $\sum$ concentration values were compared between the sampling time points within the epilimnion, metalimnion, and hypolimnion at Platforms 2 and 3. The *p*-values from the univariate statistical analyses are compiled in Table 6. The $\sum$ concentrations of the monitored NAs did not significantly differ between sampling events within the epilimnion or metalimnion at both platforms. The $\sum$ concentrations of a small number of NAs showed significant differences between the samples collected within the hypolimnion. The $\sum C_8$-bicyclic NA ($p = 0.0027$) and $\sum C_9$-bicyclic NA ($p = 0.0056$) concentration values differed within the hypolimnion at Platform 2 and the $\sum C_{10}$-monocyclic NAs concentration values ($p = 0.0012$) varied between sampling dates within the hypolimnion at Platform 3. Figure 9 presents a bar graph which plots the $\sum$ concentrations of the three aforementioned NAs measured at each of the sampling events of the hypolimnion. However, it was apparent that the temporal variations within the hypolimnion were relatively minor. The $\sum C_8$-bicyclic NA (Platform 2), $\sum C_{10}$-bicyclic NA (Platform 2), and $\sum C_{10}$-monocyclic NA (Platform 3) experienced 1.1-, 1.2-, and 1.1-fold decreases between the first and last sampling period, respectively, thus demonstrating that, even after the fall turnover, the $\sum$ NA concentrations were relatively stable within the water cap.

3.1.2. Spatial Variations of ∑ NA Concentrations between Platforms 2 and 3

Spatial variations of $\sum$ NA concentrations were assessed within the water cap by comparing differences between platforms (see Table 7 for tabulated *p*-values). Within the epiliminion and metalimnion, no significant differences were observed between Platforms 2 and 3. Within the hypolimnion, only the $\sum C_8$ monocyclic NA ($p = 0.0033$), $\sum C_{11}$ tricyclic NA ($p = 0.0062$), and $\sum C_7$ thiophene NA ($p = 0.00037$) concentration values were significantly different between Platforms 2 and 3. The $\sum$ concentrations of the three aforementioned NAs from each hypolimnion sample are plotted in Figure 10, and it is apparent that differences between the two platforms are, indeed, minor. The differences in the average $\sum$ concentration values at Platforms 2 and 3 were approximately 1.1-fold.

Within the FFT, significant spatial differences were observed between Platform 2 and 3 for most of the monitored classes of NAs (see Table 7 for *p*-values). The fold-differences between the two platforms were much larger within the FFT than within the water cap. The $\sum C_7$-thiophene NA, $\sum C_8$- monocyclic NA, and $\sum C_9$-monocyclic NA concentrations in the FFT were ~17-, 15- and 5-fold greater in Platform 2 than Platform 3, respectively. The $\sum$ concentrations of the remaining NAs displayed fold-differences which ranged between ~2.2 and 1.

3.1.3. Spatial Variations of ∑ NA Concentrations between Zones of the Water Cap

In addition, spatial variations were assessed by comparing ∑NA concentrations between the three zones of the water cap (epilimnion vs metalimnion vs hypolimnion) at Platforms 2 and 3 (see Table 8 for *p*-values). In general, very few variations were detected between the three zones of the water cap. At Platform 2, only the $\sum C_7$ thiophene NA ($p = 0.0010$) concentrations were different between the three zones, and at Platform 3, only the $\sum C_{11}$ bicyclic NA ($p = 0.004$) concentrations varied.

3.2. Profiling of Individual Naphthenic Acids at BML

The concentrations of the individual isomers were examined, and it was apparent that the differences in ∑ NA concentrations between the FFT and the water cap were driven by only a few of the isomers within each isomer series. Figure 11 presents a stacked bar graph which illustrates each individual isomer's contribution to the $\sum C_{11}$ tricyclic NA (Figure 11a) and $\sum C_8$ bicyclic NA (Figure 11b) concentration values. Figure 11a reveals that the concentrations of adamantane-1-carboxylic acid and adamantane-2-carboxylic acid were significantly higher in both of the FFT samples than the water cap samples, while the concentrations of the other isomers were similar. Figure 11b shows that the elevated $\sum C_8$ bicyclic NA concentration within the FFT pore water sample from platform 2 was driven by one isomer (Isomer 2), which was ~6-fold greater than the measured concentrations in the water cap and the FFT pore water sample from platform 3. Therefore, the monitoring of isomers by GC×GC/TOFMS is expected to allow a more in-depth assessment of NA variations at the site.

3.2.1. – Identification of Differentiating Features in the NA Profile at BML by Principal Component Analysis

Major compositional differences between the two FFT samples and the water cap were identified by principal component analysis (PCA) via the profiling of individual naphthenic acids. It was revealed that two components, PC1 and PC2, explained 72% of the total variance. The profiles of the targeted individual NAs exhibited strong similarities within the water cap and clustered tightly on the PCA scores plot (see Figure 12a). The FFT pore water samples from

Platforms 2 and 3 could be easily distinguished from the water cap and from each other, suggesting that heterogeneous NA profiles were present within the FFT. The PCA loadings plot (Figure 12b) identified a number of NAs which were driving the differentiation between the three clusters of samples from BML. Three isomers (labelled on the PCA loadings plot with red triangles) displayed elevated concentrations within the Platforms 2 and 3 FFT pore water samples, relative to the water cap samples, and were contributing to the distinction of the two FFT samples from the water cap. The concentrations of the three NAs from each of the collected samples are plotted as a bar graph in Figure 13. The five isomers labelled with red diamonds on the PCA loadings plot were also useful for differentiating the FFT from the water cap, and possessed concentrations which were approximately 1.5- to 8.5-fold lower in both of the FFT pore water samples, when compared to the water cap samples (see Figure 14 for concentrations of aforementioned NAs, plotted as a bar graph).

The FFT pore water extracts were primarily differentiated from each other by a number of NAs (labelled with a red X on the PCA loadings plot) which were only significantly elevated within the FFT sample from Platform 2. Two compounds within the C_7-thiophene NA isomer series (see Figure 15) possessed the greatest fold-differences between the FFT sample from Platform 2 and the water cap (Isomer 2 and 3:~ 43-fold greater) and Platform 3 FFT sample (Isomer 2: ~14-fold greater, Isomer 3: ~43-fold greater) samples. Lastly, there were three NAs (labelled with red squares on the PCA loadings plot) which were below detection limits in the Platform 3 FFT pore water sample, which also contributed to the differentiation of that sample from the water cap and the Platform 2 FFT pore water sample. The concentrations of the NAs labelled with a red square are plotted in Figure 16.

3.2.2 – Temporal Variations of Individual NAs within Water Cap

Beyond identifying major differences between the water cap and FFT, the profiling of individual naphthenic acids was able to capture subtle differences within the water cap which were not detected by the comparison of $\sum$ NA concentrations. Table 9 reports the number of isomers which showed significant temporal variations within each zone of the water cap at Platforms 2 and 3. Within the epilimnion, the concentrations of two isomers at Platform 2 and three isomers at Platform 3 displayed significant temporal differences. In the metalimnion, the concentrations of one isomer at Platform 2 and two isomers at Platform 3 displayed temporal variations over the sampling campaign. Worthy of note, the comparison of $\sum$ NA concentrations within the epilimnion and metalimnion did not detect any significant temporal variations, demonstrating the advantage of profiling individual NAs by GC×GC/TOFMS.

The concentrations of the NA isomers within the hypolimnion displayed the greatest temporal variations (see Table 9); the concentrations of 20 NAs showed significant temporal differences at Platform 2, and 14 NAs displayed significant temporal differences at Platform 3.

However, it should be noted that the temporal variations within all zones of the water cap were relatively minor; the fold changes between significantly different concentrations did not exceed ~1.4-fold.

3.2.3 – Spatial Variations of Individual NAs between Platforms 2 and 3

In a similar vein to the data analysis of the ∑ NA concentrations, spatial variations of individual naphthenic acids at BML were assessed by comparing differences between the two platforms. Table 10 presents the number of isomers which displayed significant differences ($p < 0.01$) between platforms within the epilimnion, metalimnion, hypolimnion, and FFT. The FFT displayed the most spatial variability between the two platforms, followed by the hypolimnion, and the epilimnion. The metalimnion displayed the least significant differences between Platforms 2 and 3; the concentrations of three isomers differed between the platforms.

The magnitudes of the fold-differences between the NA concentrations at Platforms 2 and 3 were considerably different between the three zones of the water cap and the FFT (see Figure 17). Within the three zones of the water cap, the magnitudes of the fold differences between Platforms 2 and 3 were similar to one another, and did not exceed ± 1.25. In contrast, the maximum fold difference between the FFT samples from Platform 2 and 3 was 9-fold, and the concentrations of 20 individual NAs possessed differences which exceeded 3-fold. Therefore, it is clear that significantly higher spatial variations between Platforms 2 and 3 are observed within the FFT than the three zones of the water cap.

3.2.4 – Spatial Variations of Individual NAs between Zones of Stratified Water Cap

The depth-dependent spatial variability of the water cap was assessed at the site by comparing the concentrations within each zone of the stratified water cap. In general, very few significant differences between the zones of the water cap were observed at Platforms 2 and 3. Table 11 lists the number of isomers which were significantly different between the epilimnion, metalimnion, and hypolimnion. A total of 6 and 3 individual NAs at Platform 2 and 3, respectively, were significantly different between the three zones of the water cap.

4. Conclusions

In this study, GC×GC/TOFMS was applied to semi-quantify individual naphthenic acids within three zones (epilimnion, metalimnion, and hypolimnion) of the stratified water cap at BML. Total concentrations were calculated for each of the monitored NA classes by summation of the concentrations of all detected isomers, and minimal temporal and spatial variability was observed within the water cap. In addition, two samples were collected from the FFT, and the total concentrations of the monitored chemical species were either higher or similar to those of

the water cap. The FFT pore water sample from Platform 2 contained the highest concentrations at the site. Due to the high-resolving power of GC×GC/TOFMS, individual isomers were resolved within each isomer series, and it was revealed that the differences in total NA concentrations between the water cap and FFT were driven by only a few isomers. The monitoring of individual NAs allowed the detection of subtle spatial and temporal differences within the water cap, which were masked by the total concentration values. However, despite the detection of some spatial and temporal variation within the water cap, the concentration differences were generally minimal and did not drastically change following the fall turnover event.

The fingerprinting capabilities of GC×GC/TOFMS are clearly shown in this study, as the profiling of individual naphthenic acids allowed the distinction of water cap samples from those of the FFT. In addition, significant spatial differences were observed between the two FFT samples. Since the consolidation and dewatering of FFT is expected to contribute pore water containing dissolved naphthenic acids into the water column, future studies are planned to explore the complexity of NAs compositions within the FFT, and to obtain a better understanding the water cap-FFT interface. Furthermore, since significant compositional differences were observed between the FFT pore water and the water cap, it would be useful to investigate any differences in toxicity which may exist between the samples.

Acknowledgements

Funding for this work was provided by NSERC Canada and Syncrude Canada (Grant: CRDPJ 488301-15). The authors would like to thank Syncrude Canada Limited Reclamation and Closure Research Group for field sampling support, Dr. Matthew Lindsay, Tara Colenbrander Nelson, Daniel Arriaga, Patrick Morris, and Florent Risacher for collecting the samples from Base Mine Lake and providing temperature and dissolved oxygen profiles for the water cap, and the Centre for Microbial Chemical Biology (CMCB) at McMaster University for access to the Pegasus 4D instrument.

References:

(1) Giesy, J. P.; Anderson, J. C.; Wiseman, S. B. Alberta oil sands development. *Proc. Natl. Acad. Sci.* **2010**, *107* (3), 951–952.

(2) Frank, R. A.; Kavanagh, R.; Kent Burnison, B.; Arsenault, G.; Headley, J. V.; Peru, K. M.; Van Der Kraak, G.; Solomon, K. R. Toxicity assessment of collected fractions from an extracted naphthenic acid mixture. *Chemosphere* **2008**, *72* (9), 1309–1314.

(3) Anderson, J.; Wiseman, S. B.; Moustafa, A.; Gamal El-Din, M.; Liber, K.; Giesy, J. P. Effects of exposure to oil sands process-affected water from experimental reclamation ponds on Chironomus dilutus. *Water Res.* **2012**, *46* (6), 1662–1672.

(4) Kavanagh, R. J.; Frank, R. A.; Burnison, B. K.; Young, R. F.; Fedorak, P. M.; Solomon, K. R.; Van Der Kraak, G. Fathead minnow (Pimephales promelas) reproduction is impaired when exposed to a naphthenic acid extract. *Aquat. Toxicol.* **2012**, *116–117*, 34–42.

(5) Peters, L. E.; MacKinnon, M.; Van Meer, T.; van den Heuvel, M. R.; Dixon, D. G. Effects of oil sands process-affected waters and naphthenic acids on yellow perch (Perca flavescens) and Japanese medaka (Orizias latipes) embryonic development. *Chemosphere* **2007**, *67* (11), 2177–2183.

(6) Nero, V.; Farwell, A.; Lee, L. E. J.; Van Meer, T.; MacKinnon, M. D.; Dixon, D. G. The effects of salinity on naphthenic acid toxicity to yellow perch: Gill and liver histopathology. *Ecotoxicol. Environ. Saf.* **2006**, *65* (2), 252–264.

(7) Marentette, J. R.; Frank, R. A.; Bartlett, A. J.; Gillis, P. L.; Hewitt, L. M.; Peru, K. M.; Headley, J. V.; Brunswick, P.; Shang, D.; Parrott, J. L. Sensitivity of walleye (Sander vitreus) and fathead minnow (Pimephales promelas) early-life stages to naphthenic acid fraction components extracted from fresh oil sands process-affected waters. *Environ. Pollut.* **2015**, *207*, 59–67.

(8) Reinardy, H. C.; Scarlett, A. G.; Henry, T. B.; West, C. E.; Hewitt, L. M.; Frank, R. A.; Rowland, S. J. Aromatic naphthenic acids in oil sands process-affected water, resolved by GCxGC-MS, only weakly induce the gene for vitellogenin production in zebrafish (danio rerio) larvae. *Environ. Sci. Technol.* **2013**, *47* (12), 6614–6620.

(9) Canada's Oil Sands Innovation Alliance (COSIA). *Guidelines for Performance Management of Oil Sands Fluid Fine Tailings Deposits to Meet Closure Commitments*; 2014.

(10) Dompierre, K. A.; Lindsay, M. B. J.; Cruz-Hernández, P.; Halferdahl, G. M. Initial

geochemical characteristics of fluid fine tailings in an oil sands end pit lake. *Sci. Total Environ.* **2016**, *556*, 196–206.

(11) Headley, J. V.; McMartin, D. W. A Review of the Occurrence and Fate of Naphthenic Acids in Aquatic Environments. *J. Environ. Sci. Heal. Part A* **2004**, *39* (8), 1989–2010.

(12) Grewer, D. M.; Young, R. F.; Whittal, R. M.; Fedorak, P. M. Naphthenic acids and other acid-extractables in water samples from Alberta: What is being measured? *Sci. Total Environ.* **2010**, *408* (23), 5997–6010.

(13) Headley, J. V.; Peru, K. M.; Armstrong, S. A.; Han, X.; Martin, J. W.; Mapolelo, M. M.; Smith, D. F.; Rogers, R. P.; Marshall, A. G. Aquatic plant-derived changes in oil sands naphthenic acid signatures determined by low-, high-, and ultrahigh-resolution mass spectrometry. *Rapid Commun. Mass Spectrom.* **2009**, *23*, 515–522.

(14) Barrow, M. P.; Witt, M.; Headley, J. V.; Peru, K. M. Athabasca oil sands process water: Characterization by atmospheric pressure photoionization and electrospray ionization Fourier transform ion cyclotron resonance mass spectrometry. *Anal. Chem.* **2010**, *82* (9), 3727–3735.

(15) Pereira, A. S.; Martin, J. W. Exploring the complexity of oil sands process-affected water by high efficiency supercritical fluid chromatography/orbitrap mass spectrometry. *Rapid Commun. Mass Spectrom.* **2015**, *29* (8), 735–744.

(16) Ortiz, X.; Jobst, K. J.; Reiner, E. J.; Backus, S.; Peru, K. M.; McMartin, D. W.; O'Sullivan, G.; Taguchi, V. Y.; Headley, J. V. Characterization of naphthenic acids by gas chromatography-fourier transform ion cyclotron resonance mass spectrometry. *Anal. Chem.* **2014**, *86* (15), 7666–7673.

(17) Pereira, A. S.; Bhattacharjee, S.; Martin, J. W. Characterization of oil sands process-affected waters by liquid chromatography orbitrap mass spectrometry. *Environ. Sci. Technol.* **2013**, *47* (10), 5504–5513.

(18) Yue, S.; Ramsay, B. A.; Brown, R. S.; Wang, J.; Ramsay, J. A. Identification of estrogenic compounds in oil sands process waters by effect directed analysis. *Environ. Sci. Technol.* **2015**, *49* (1), 570–577.

(19) Thomas, K. V; Langford, K.; Petersen, K.; Smith, A. J.; Tollefsen, K. E. Effect-directed identification of naphthenic acids as important in vitro xeno-estrogens and anti-androgens in North Sea offshore produced water discharges. *Environ. Sci. Technol.* **2009**, *43* (21), 8066–8071.

(20) Hughes, S. A.; Mahaffey, A.; Shore, B.; Baker, J.; Kilgour, B.; Brown, C.; Peru, K. M.;

Headley, J. V.; Bailey, H. C. Using ultrahigh-resolution mass spectrometry and toxicity identification techniques to characterize the toxicity of oil sands process-affected water: The case for classical naphthenic acids. *Environ. Toxicol. Chem.* **2017**.

(21) Bauer, A. E.; Frank, R. A.; Headley, J. V.; Peru, K. M.; Farwell, A. J.; Dixon, D. G. Toxicity of oil sands acid-extractable organic fractions to freshwater fish: Pimephales promelas (fathead minnow) and Oryzias latipes (Japanese medaka). *Chemosphere* **2017**, *171*, 168–176.

(22) Zetouni, N. C.; Siraki, A. G.; Weinfeld, M.; Pereira, A. dos S.; Martin, J. W. Screening of genotoxicity and mutagenicity in extractable organics from oil sands process–affected water. *Environ. Toxicol. Chem.* **2017**, *36* (5), 1397–1404.

(23) Peterson, K.; Hultman, M. T.; Rowland, S. J.; Tollefsen, K. E. Toxicity of organic compounds from unresolved complex mixtures (UCMs) to primary fish hepatocytes. *Aquat. Toxicol.* **2017**, *190*, 150–161.

(24) Brown, L. D.; Ulrich, A. C. Oil sands naphthenic acids: A review of properties, measurement, and treatment. *Chemosphere* **2015**, *127*, 276–290.

(25) Scott, A. C.; MacKinnon, M. D.; Fedorak, P. M. Naphthenic acids in athabasca oil sands tailings waters are less biodegradable than commercial naphthenic acids. *Environ. Sci. Technol.* **2005**, *39* (21), 8388–8394.

(26) Headley, J. V.; Peru, K. M.; Barrow, M. P. Advances in Mass Spectrometric Characterization of Naphthenic Acids Fraction Compounds in Oil Sands Environmental Samples and Crude Oil - A Review. *Mass Spectrom. Rev.* **2015**, *35* (2), 311–328.

(27) Headley, J. V; Mohamed, M. H.; Frank, R. A.; Martin, J. W.; Hazewinkel, R. R. O.; Humphries, D.; Gurprasad, N. P.; Hewitt, L. M.; Muir, D. C. G.; Lindeman, D.; et al. Chemical fingerprinting of naphthenic acids and oil sands process waters — A review of analytical methods for environmental samples. *J. Environ. Sci. Heal. Part A.* **2013**, *48* (10), 1145–1163.

(28) Headley, J. V.; Barrow, M. P.; Peru, K. M.; Fahlman, B.; Frank, R. A.; Bickerton, G.; McMaster, M. E.; Parrott, J.; Hewitt, L. M. Preliminary fingerprinting of Athabasca oil sands polar organics in environmental samples using electrospray ionization Fourier transform ion cyclotron resonance mass spectrometry. *Rapid Commun. Mass Spectrom.* **2011**, *25* (13), 1899–1909.

(29) Barrow, M. P.; Peru, K. M.; Fahlman, B.; Hewitt, L. M.; Frank, R. a.; Headley, J. V. Beyond Naphthenic Acids: Environmental Screening of Water from Natural Sources and the Athabasca Oil Sands Industry Using Atmospheric Pressure Photoionization Fourier

Transform Ion Cyclotron Resonance Mass Spectrometry. *J. Am. Soc. Mass Spectrom.* **2015**, *26*, 1508–1521.

(30) Hao, C.; Headley, J. V.; Peru, K. M.; Frank, R.; Yang, P.; Solomon, K. R. Characterization and pattern recognition of oil–sand naphthenic acids using comprehensive two-dimensional gas chromatography/time-of-flight mass spectrometry. *J. Chromatogr. A* **2005**, *1067* (1–2), 277–284.

(31) Bowman, D. T.; Slater, G. F.; Warren, L. A.; McCarry, B. E. Identification of individual thiophene-, indane-, tetralin-, cyclohexane-, and adamantane-type carboxylic acids in composite tailings pore water from Alberta oil sands. *Rapid Commun. Mass Spectrom.* **2014**, *28* (19), 2075–2083.

(32) Shepherd, A. G.; van Mispelaar, V.; Nowlin, J.; Genuit, W.; Grutters, M. Analysis of Naphthenic Acids and Derivatization Agents Using Two-Dimensional Gas Chromatography and Mass Spectrometry: Impact on Flow Assurance Predictions †. *Energy Fuels* **2010**, *24* (4), 2300–2311.

(33) Damasceno, F. C.; Gruber, L. D. A.; Geller, A. M.; de Campos, M. C. V.; Gomes, A. O.; Guimaraes, R. C. L.; Peres, V. F.; Jacques, R. A.; Caramao, E. B. Characterization of naphthenic acids using mass spectroscopy and chromatographic techniques: study of technical mixtures. *Anal. Methods* **2014**, *6*, 807–816.

(34) Rowland, S. J.; Scarlett, A. G.; Jones, D.; West, C. E.; Frank, R. a. Diamonds in the rough: Identification of individual naphthenic acids in oil sands process water. *Environ. Sci. Technol.* **2011**, *45* (7), 3154–3159.

(35) West, C. E.; Scarlett, A. G.; Pureveen, J.; Tegelaar, E. W.; Rowland, S. J. Abundant naphthenic acids in oil sands process-affected water: studies by synthesis, derivatisation and two-dimensional gas chromatography/high-resolution mass spectrometry. *Rapid Commun. Mass Spectrom.* **2013**, *27* (2), 357–365.

(36) West, C. E.; Scarlett, A. G.; Tonkin, A.; O'Carroll-Fitzpatrick, D.; Pureveen, J.; Tegelaar, E.; Gieleciak, R.; Hager, D.; Petersen, K.; Tollefsen, K.-E.; et al. Diaromatic sulphur-containing "naphthenic" acids in process waters. *Water Res.* **2014**, *51*, 206–215.

(37) Bowman, D. T.; Jobst, K. J.; Ortiz, X.; Reiner, E. J.; Warren, L. A.; Mccarry, B. E.; Slater, G. F. Improved coverage of naphthenic acid fraction compounds by comprehensive two-dimensional gas chromatography coupled with high resolution mass spectrometry. *J. Chromatogr. A* **2017**.

(38) Wilde, M. J.; West, C. E.; Scarlett, A. G.; Jones, D.; Frank, R. A.; Hewitt, L. M.; Rowland, S. J. Bicyclic naphthenic acids in oil sands process water: Identification by

comprehensive multidimensional gas chromatography–mass spectrometry. *J. Chromatogr. A* **2015**, *1378*, 74–87.

(39) West, C. E.; Pureveen, J.; Scarlett, A. G.; Lengger, S. K.; Wilde, M. J.; Korndorffer, F.; Tegelaar, E. W.; Rowland, S. J. Can two-dimensional gas chromatography/mass spectrometric identification of bicyclic aromatic acids in petroleum fractions help to reveal further details of aromatic hydrocarbon biotransformation pathways? *Rapid Commun. Mass Spectrom.* **2014**, *28* (9), 1023–1032.

(40) Rowland, S. J.; West, C. E.; Scarlett, A. G.; Jones, D.; Frank, R. a. Identification of individual tetra- and pentacyclic naphthenic acids in oil sands process water by comprehensive two-dimensional gas chromatography/mass spectrometry. *Rapid Commun. Mass Spectrom.* **2011**, *25* (9), 1198–1204.

(41) Rowland, S. J.; West, C. E.; Jones, D.; Scarlett, A. G.; Frank, R. A.; Hewitt, L. M. Steroidal aromatic Naphthenic Acids in oil sands process-affected water: Structural comparisons with environmental estrogens. *Environ. Sci. Technol.* **2011**, *45* (22), 9806–9815.

(42) Rowland, S. J.; West, C. E.; Scarlett, A. G.; Jones, D. Identification of individual acids in a commercial sample of naphthenic acids from petroleum by two-dimensional comprehensive gas chromatography/mass spectrometry. *Rapid Commun. Mass Spectrom.* **2011**, *25* (12), 1741–1751.

(43) Rowland, S. J.; West, C. E.; Scarlett, a. G.; Jones, D.; Boberek, M.; Pan, L.; Ng, M.; Kwong, L.; Tonkin, a. Monocyclic and monoaromatic naphthenic acids: Synthesis and characterisation. *Environ. Chem. Lett.* **2011**, *9* (4), 525–533.

(44) Lengger, S. K.; Scarlett, A. G.; West, C. E.; Rowland, S. J. Diamondoid diacids ('O4' species) in oil sands process-affected water. *Rapid Commun. Mass Spectrom.* **2013**, *27* (23), 2648–2654.

(45) Wilde, M. J.; Rowland, S. J. Structural Identification of Petroleum Acids by Conversion to Hydrocarbons and Multidimensional Gas Chromatography-Mass Spectrometry. *Anal. Chem.* **2015**, *87* (16), 8457–8465.

(46) Rowland, S. J.; West, C. E.; Scarlett, A. G.; Ho, C.; Jones, D. Differentiation of two industrial oil sands process-affected waters by two-dimensional gas chromatography/mass spectrometry of diamondoid acid profiles. *Rapid Commun. Mass Spectrom.* **2012**, *26* (5), 572–576.

(47) Lengger, S. K.; Scarlett, A. G.; West, C. E.; Frank, R. A.; Hewitt, L. M.; Milestone, C. B.; Rowland, S. J. Use of the distributions of adamantane acids to profile short-term temporal

and pond-scale spatial variations in the composition of oil sands process-affected waters. *Environ. Sci. Process. Impacts* **2015**, *17* (8), 1415–1423.

(48) Frank, R. A.; Roy, J. W.; Bickerton, G.; Rowland, S. J.; Headley, J. V.; Scarlett, A. G.; West, C. E.; Peru, K. M.; Parrott, J. L.; Conly, F. M.; et al. Profiling oil sands mixtures from industrial developments and natural groundwaters for source identification. *Environ. Sci. Technol.* **2014**, *48* (5), 2660–2670.

(49) Frank, R. A.; Milestone, C. B.; Rowland, S. J.; Headley, J. V.; Kavanagh, R. J.; Lengger, S. K.; Scarlett, A. G.; West, C. E.; Peru, K. M.; Hewitt, L. M. Assessing spatial and temporal variability of acid-extractable organics in oil sands process-affected waters. *Chemosphere* **2016**, *160*, 303–313.

(50) Carrier, D.; Shaw, B.; Lee, J. Syncrude West in Pit (WIP) 1995 to 2006: Consolidation modelling summary. *Syncrude Canada Ltd., Intern. Report.* **2007**.

(51) Xia, J.; Sinelnikov, I. V.; Han, B.; Wishart, D. S. MetaboAnalyst 3.0-making metabolomics more meaningful. *Nucleic Acids Res.* **2015**, *43* (W1), W251–W257.

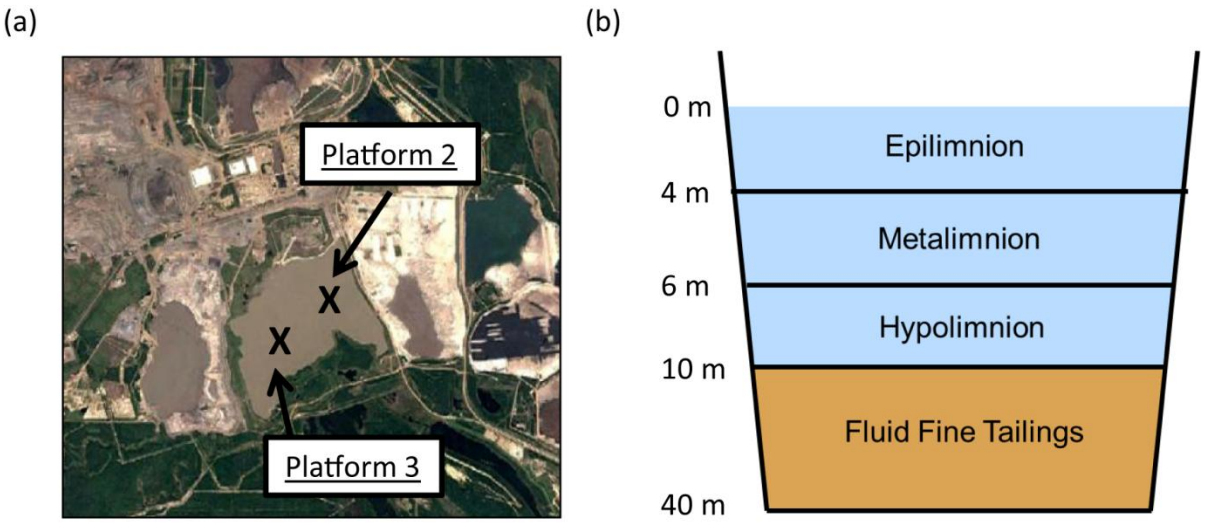

Figure 1. (a) Map of the study site with sampling platforms and (b) illustration of the zones of the stratified lake during summer (Note: depths for each zone are approximate, the range of depths change with season).

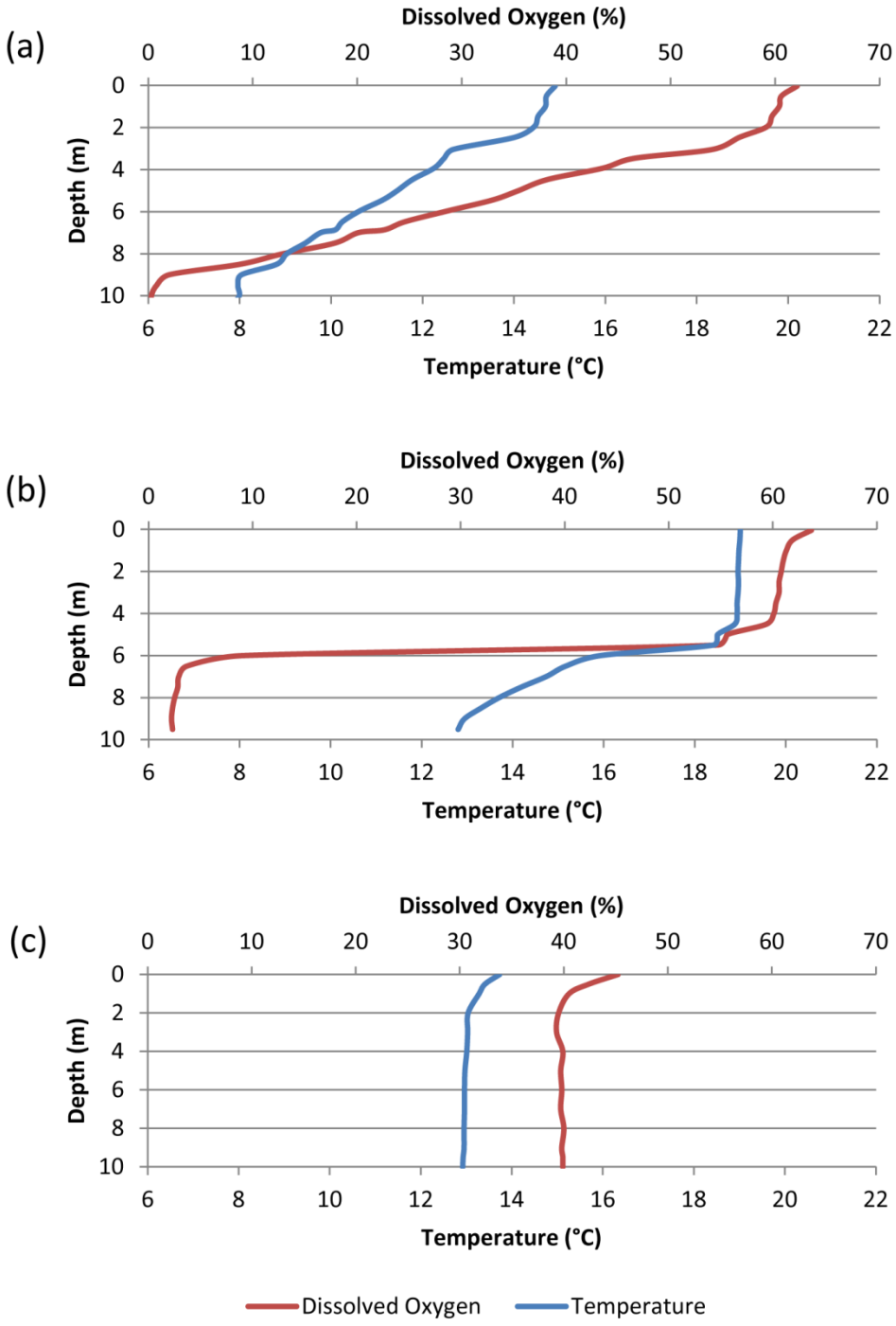

Figure 2. The dissolved oxygen and temperature profiles in the water cap at Platform 2 for the following sampling dates: (a) June 3 2015, (b) July 21 2015, (c) September 22, 2015.

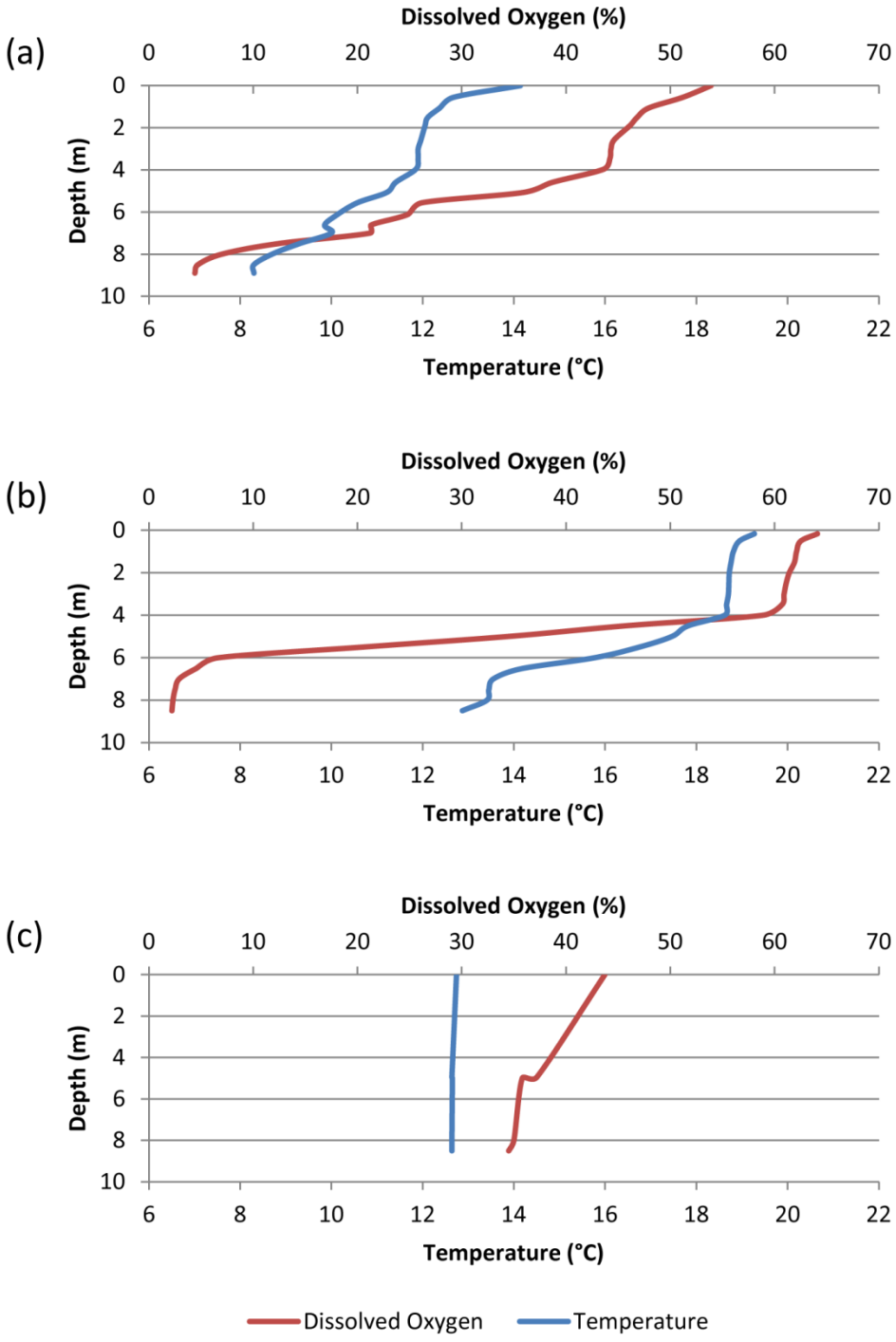

Figure 3. The dissolved oxygen and temperature profiles in the water cap at Platform 3 for the following sampling dates (a) June 2 2015, (b) July 20 2015, (c) September 23, 2015.

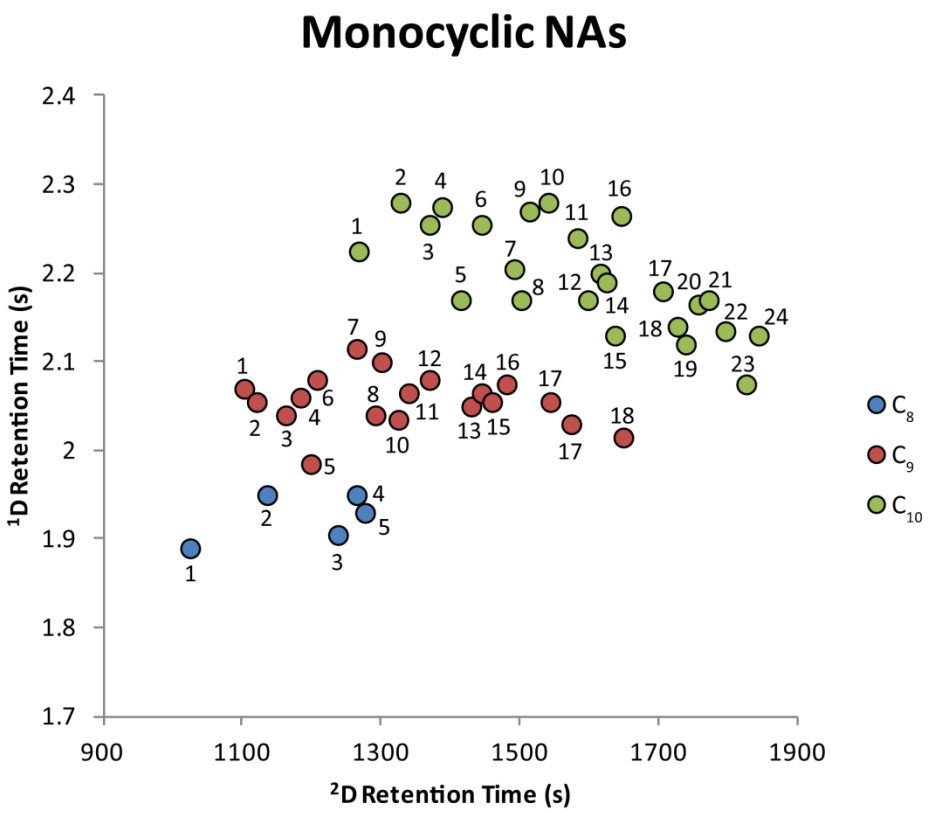

Figure 4. The first and second dimension retention times of the monocyclic NAs.

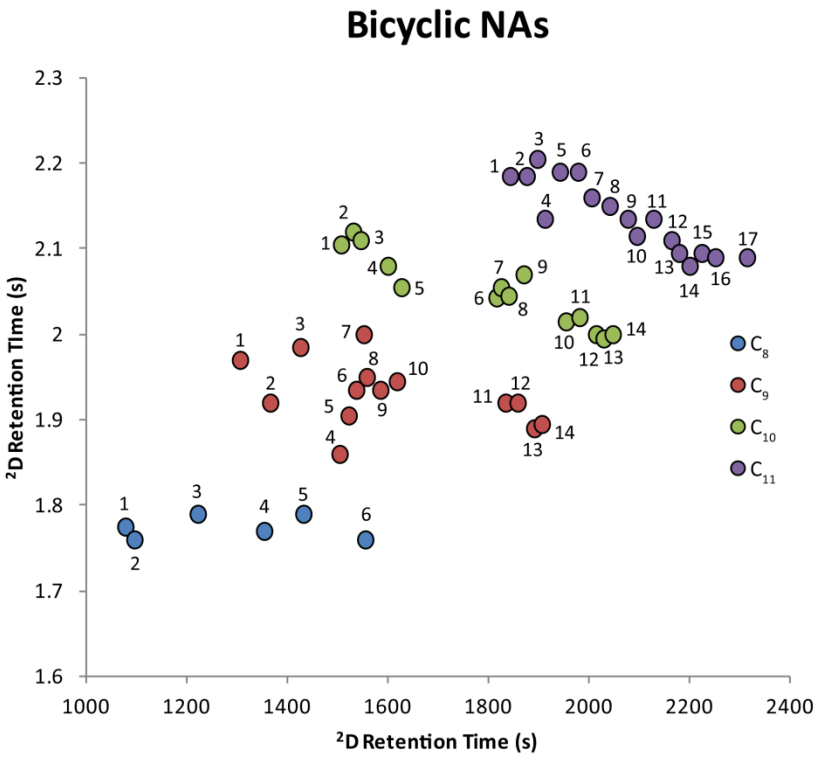

Figure 5. The first and second dimension retention times of the bicyclic NAs.

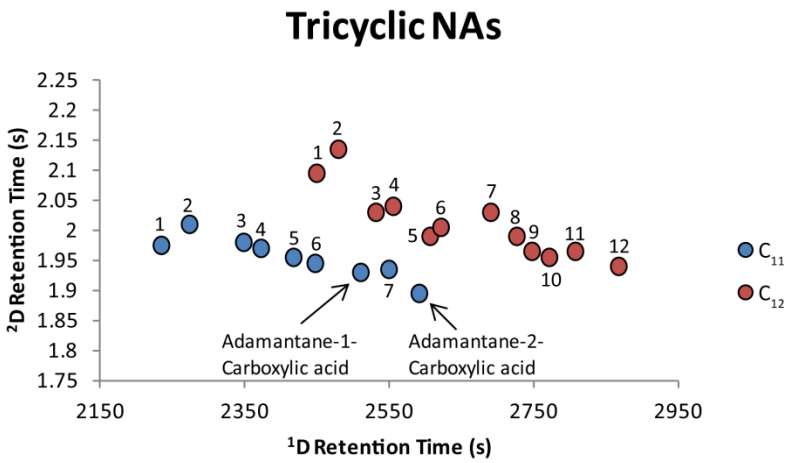

Figure 6. The first and second dimension retention times of the tricyclic NAs.

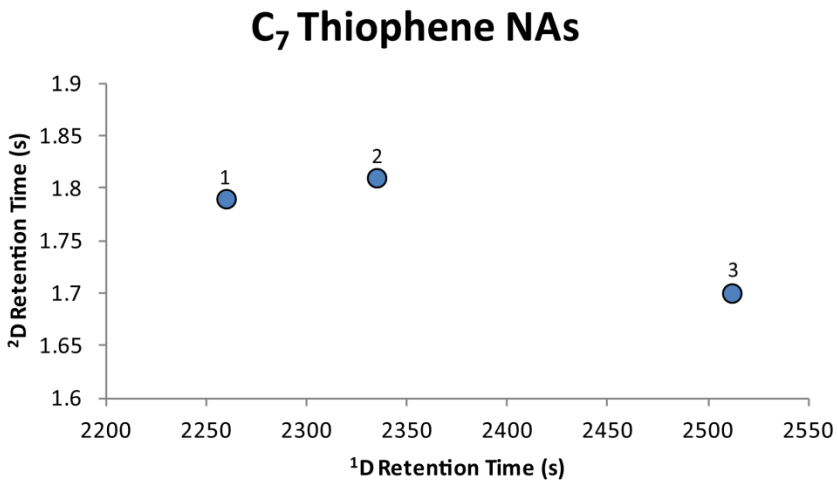

Figure 7. The first and second dimension retention times of the C_7 thiophene NAs.

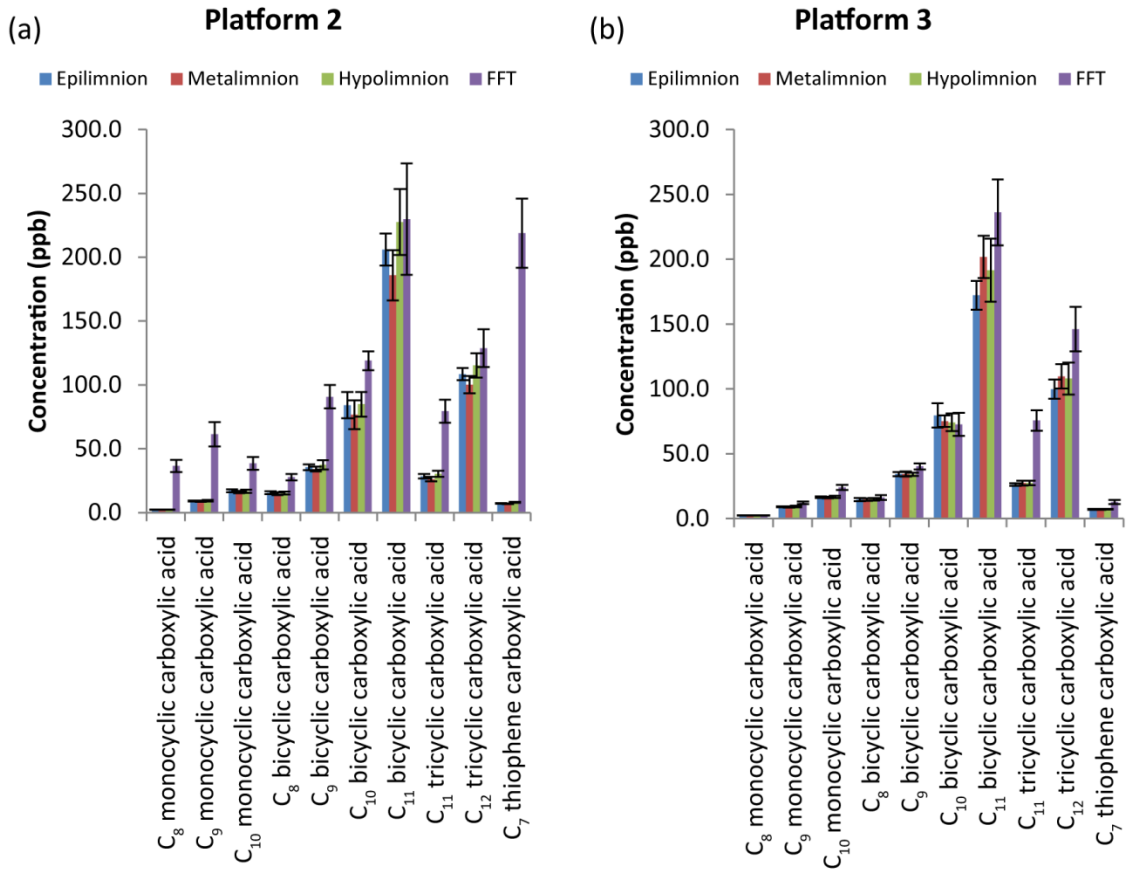

Figure 8. The total concentration values for the monitored NA classes within the epilimnion, metalimnion, hypolimnion, and FFT at (a) Platform 2 and (b) Platform 3. Concentraton values within the water cap are presented as an average of all sampling events of each zone. Errors bars represent ± one standard deviation .

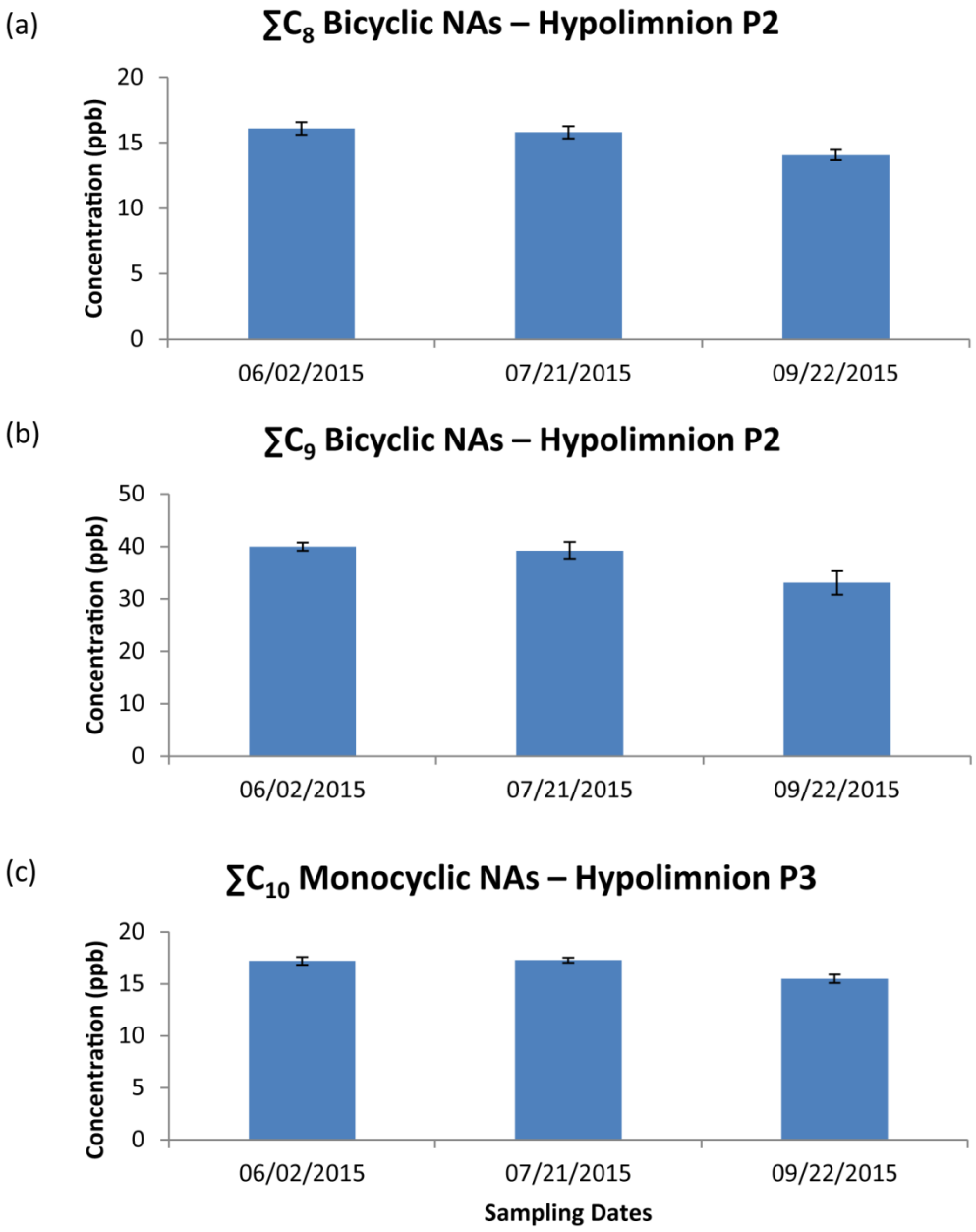

Figure 9. The semi-quantitative concentrations of (a) $\sum C_8$ bicyclic NAs (Platform 2), $\sum C_9$ bicyclic NAs (Platform 2), and (c) $\sum C_{10}$ monocyclic NAs (Platform 3) within the hypolimnion. Error bars represent ± one standard deviation.

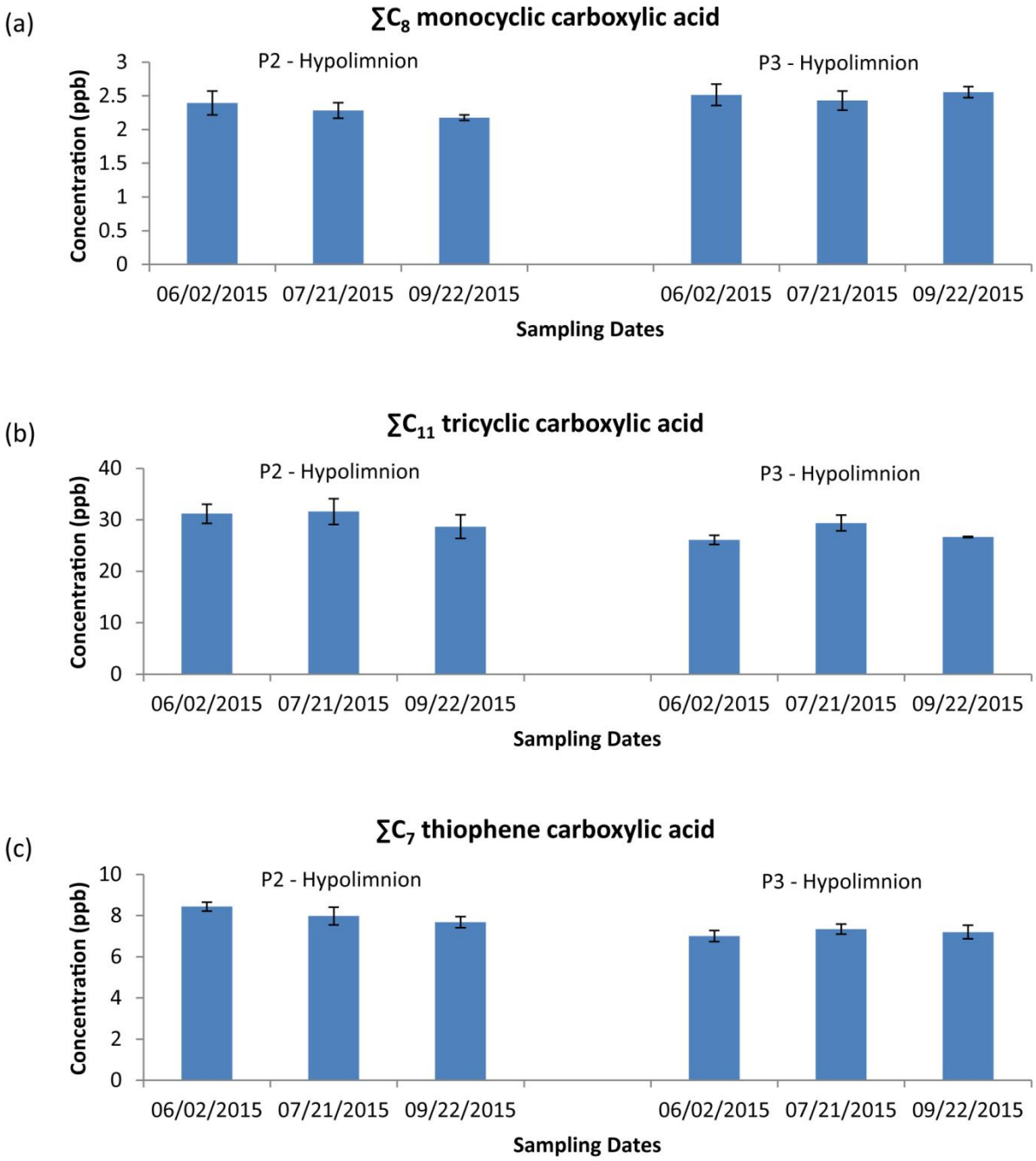

Figure 10. The semi-quantitative concentrations of (a) $\sum C_8$ bicyclic NAs, $\sum C_{11}$ tricyclic NAs, and (c) $\sum C_7$ thiophene NAs within the hypolimnion. Error bars represent ± one standard deviation.

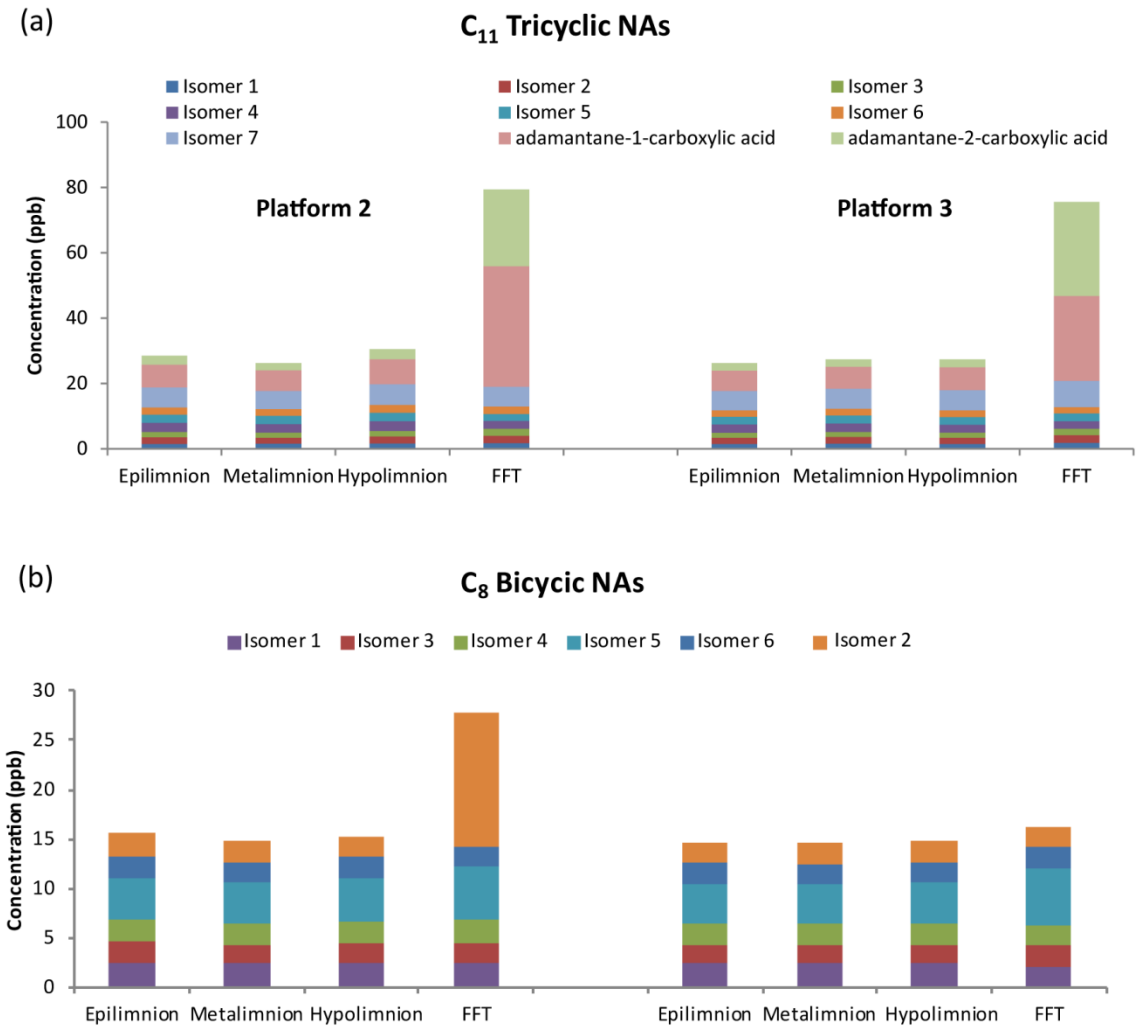

Figure 11. Stacked bar plots illustrating each isomer's contribution to the total concentration of (a) $\sum C_{11}$ tricyclic NA and (b) $\sum C_8$ bicyclic NA. NB: Error bars are not presented; the RSD% of the concentrations of all isomers was lower than 25%.

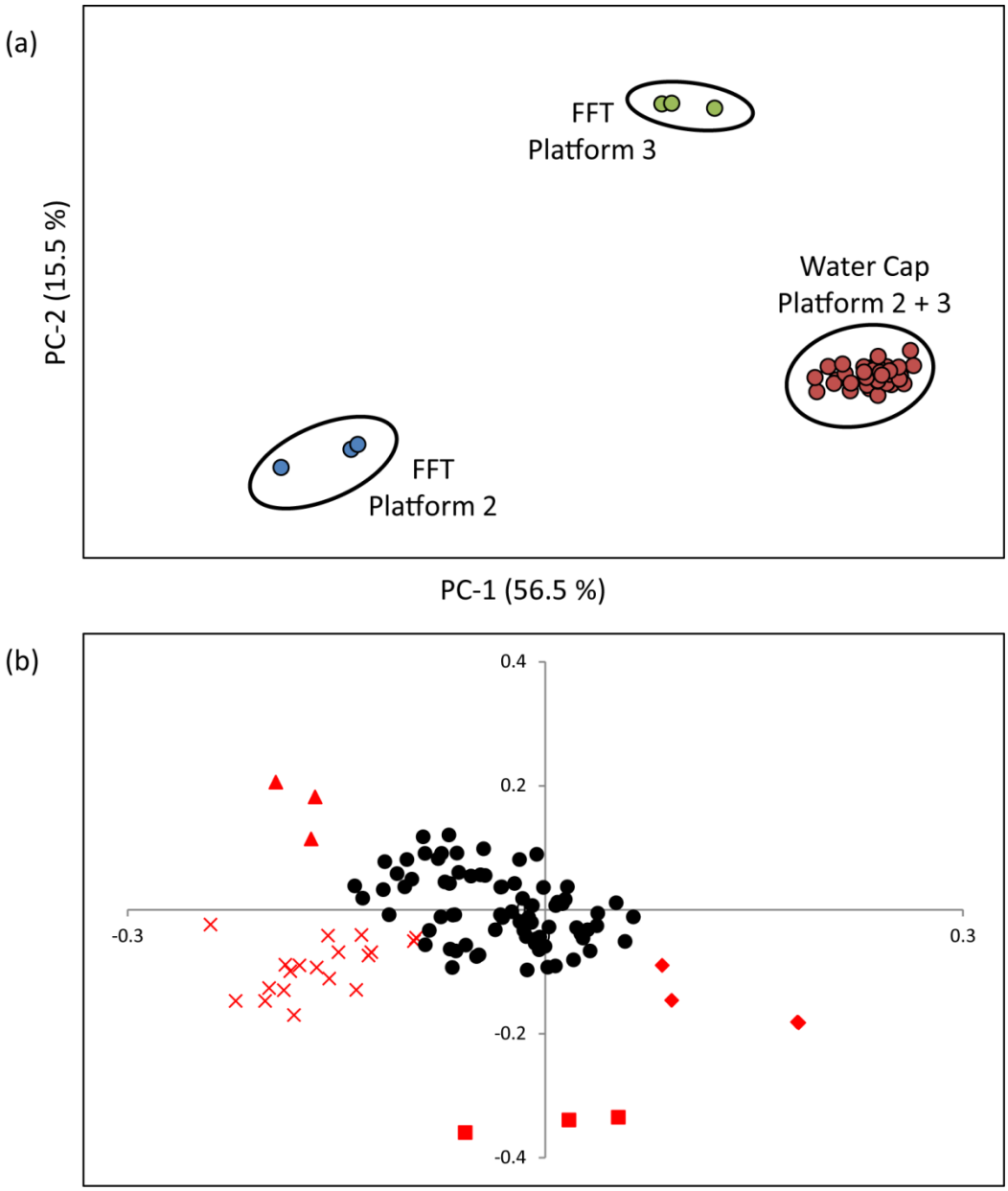

Figure 12. (a) PCA scores plot and (b) PCA loadings plot of the dataset containing the semi-quantified concentrations of the individual naphthenic acids. The red labels on the PCA loadings plot (triangle, X, square, and diamonds) represent NAs which were driving the separation of samples observed on the scores plot.

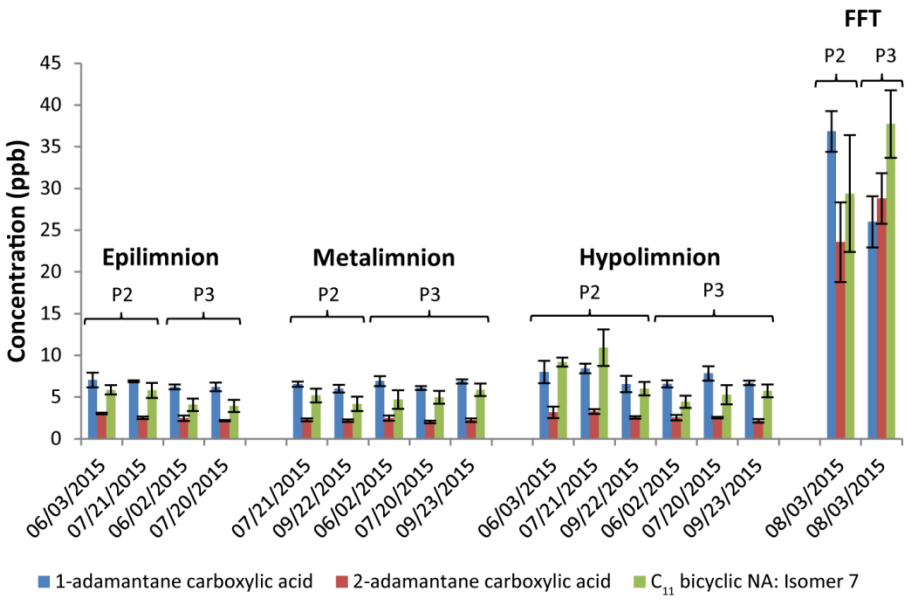

Figure 13. The semi-quantitative concentrations of naphthenic acids (adamantane-1-carboxylic acid, adamantane-2-carboxylic acid, and C_{11}-bicyclic acid isomer 7) which were elevated in both of the FFT pore water extracts, relative to the water cap. These naphthenic acids are labelled on the PCA scores plot of Fig. 12 with a red triangle.

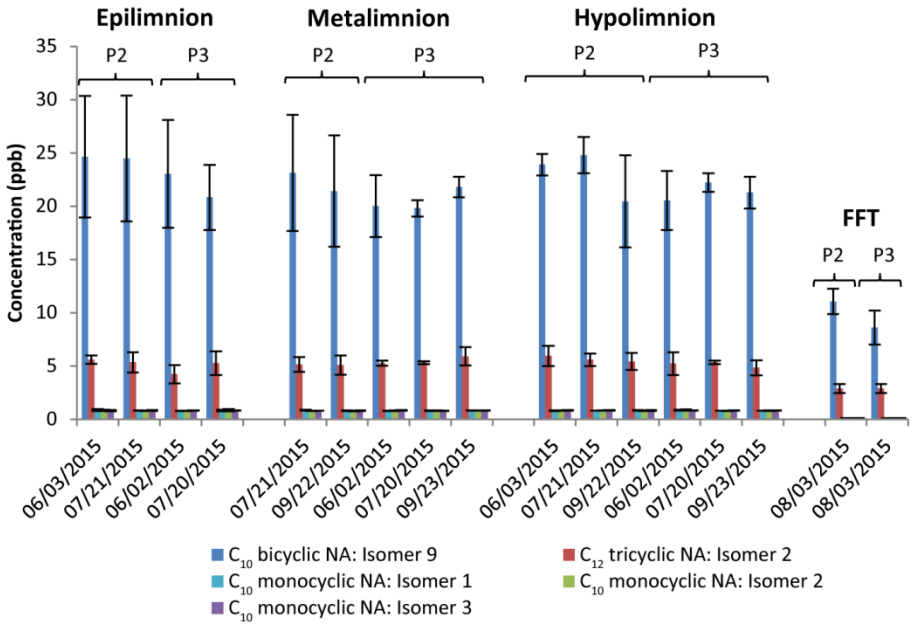

Figure 14. The semi-quantitative concentrations of naphthenic acids (C_{10} bicyclic acids Isomer 9, C_{12} tricyclic carboxylic acid Isomer 2, C_{10} monocyclic carboxylic Isomer 1, C_{10} monocyclic carboxylic acid Isomer 2, C_{10} monocyclic carboxylic acid Isomer 3) which were lower in both of the FFT pore water extracts, relative to the water cap. These naphthenic acids are labelled on the PCA scores plot of Fig. 12 with red diamonds.

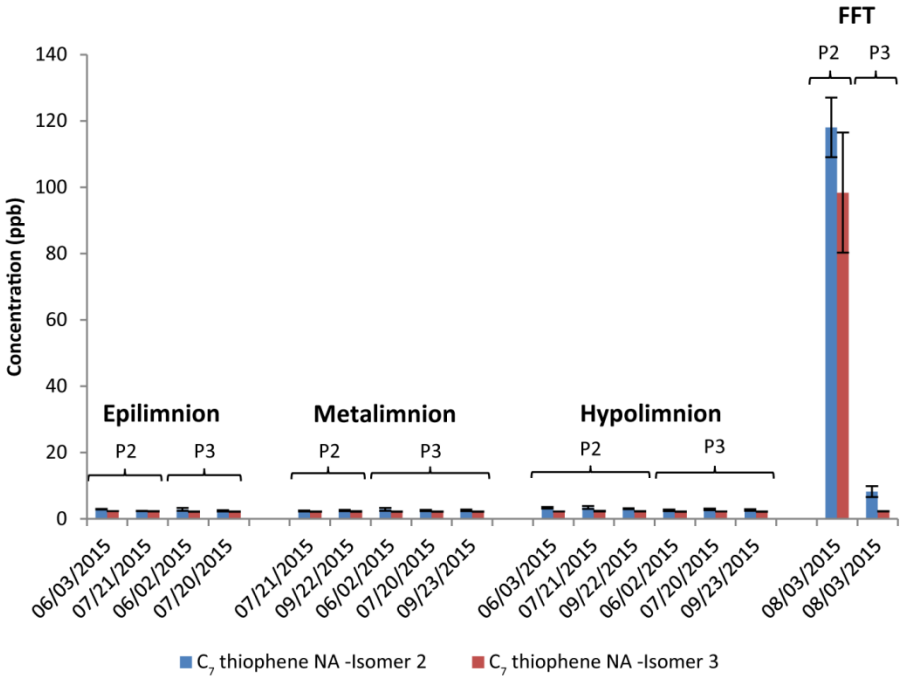

Figure 15. The semi-quantitative concentrations of select naphthenic acids (C_7 thiophene Isomer 2 and C_7 thiophene Isomer 3) which were elevated in the FFT pore water extract from Platform 2. These two naphthenic acids, in addition to others which are not presented in this figure, are labelled on the PCA scores plot of Fig. 12 with a red X.

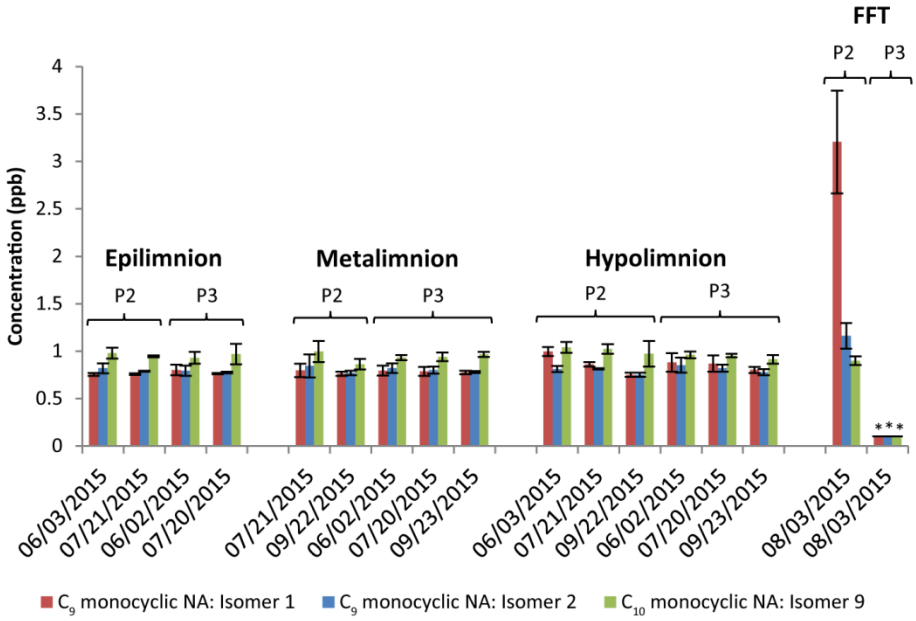

Figure 16. The semi-quantitative concentrations of naphthenic acids (C_9 monocyclic carboxylic acid Isomer 1, C_9 monocyclic carboxylic acid Isomer 2, C_{10} monocyclic carboxylic acid Isomer 9) which were contributed to the differentiation of the samples. The three naphthenic acids were below detection limits in the FFT pore water sample from Platform 3 (indicated by *) and are labelled on the PCA scores plot of Fig. 12 with red squares.

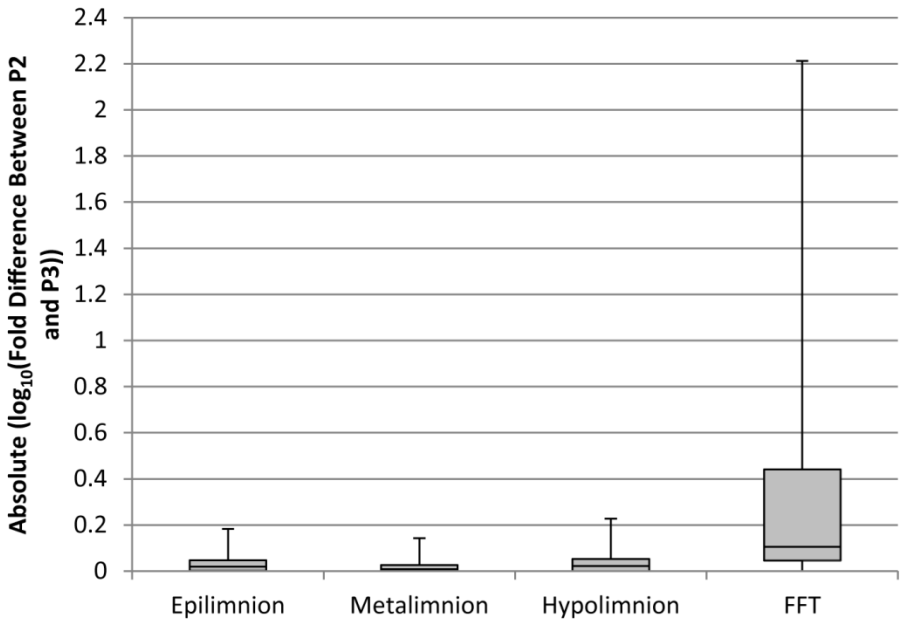

Figure 17. Distribution of NA isomer concentration fold differences between Platforms 2 and 3.

Table 1. List of the sampling dates and depths of the collected samples from the water cap.

Sampling Date	**Water Cap – Platform 2**		
	Epilimnion	**Metalimnion**	**Hypolimnion**
June 3/2015	1.5 m	N.C.	8.25 m
July 21/2015	1.5 m	5.75 m	9 m
September 22/2015	N.C.	5 m	10 m
Sampling Date	**Water Cap – Platform 3**		
	Epilimnion	**Metalimnion**	**Hypolimnion**
June 2/2015	1.5 m	5.5 m	7.25 m
July 20/2015	1.5 m	5 m	7 m
September 23/2015	N.C.	5 m	8.5 m

N.C.= Not collected

Table 2. Reference standards used for the semi-quantitation of NAs in this study.

Calibration Standard	Quantification Mass Ion (*m/z*)	Linearity (R^2)	IDL (pg/µL)	MDL (pg/µL)
adamantane-1-carboxylic acid, methyl ester	194	0.997	31	0.16
1-methylcyclohexane-1-carboxylic acid, methyl ester	156	0.991	35	0.18
trans-4-ethylcyclohexane carboxylic acid, methyl ester	170	0.995	43	0.22
1-pentalenecarboxylic acid, octahydro-3-methyl-, methyl ester	182	0.997	24	0.12
5-ethyl-thiophene-2-carboxylic acid, methyl ester	170	0.998	36	0.18

IDL = Instrument detection limit; MDL = Method detection limit

Table 3. The number of isomers detected within each zone of BML for each targeted NA class.

Structural Moiety	Carbon Number	Number of Isomers Detected		
		Water Cap	Fluid Fine Tailings (Platform 2)	Fluid Fine Tailings (Platform 3)
Monocyclic NAs	C_8	3	5	3
	C_9	10	18	12
	C_{10}	17	24	18
Bicyclic NAs	C_8	6	6	6
	C_9	14	14	14
	C_{10}	14	14	14
	C_{11}	17	17	17
Tricyclic NAs	C_{11}	9	9	9
	C_{12}	12	12	12
Thiophene NAs	C_7	3	3	3

Table 4. List of reference standards which were used for the semi-quantitation of specific NAs.

Structural Moiety	Carbon Number	Calibration Standard
Monocyclic NAs	C_8	1-methylcyclohexane-1-carboxylic acid, methyl ester
	C_9	*trans*-4-ethylcyclohexane carboxylic acid, methyl ester
	C_{10}	*trans*-4-ethylcyclohexane carboxylic acid, methyl ester
Bicyclic NAs	C_8	1-Pentalenecarboxylic acid, octahydro-3-methyl-, methyl ester
	C_9	1-Pentalenecarboxylic acid, octahydro-3-methyl-, methyl ester
	C_{10}	1-Pentalenecarboxylic acid, octahydro-3-methyl-, methyl ester
	C_{11}	1-Pentalenecarboxylic acid, octahydro-3-methyl-, methyl ester
Tricyclic NAs	C_{11}	Adamantane-1-carboxylic acid, methyl ester
	C_{12}	Adamantane-1-carboxylic acid, methyl ester
Thiophene NAs	C_7	5-ethyl-thiophene-2-carboxylic acid, methyl ester

Table 5. Mean and standard deviation (given in parentheses) of ∑ semi-quantified concentrations for the targeted naphthenic acids. ∑ Concentration values were calculated by summation of all isomers. "n" represents the number of sampling events at each zone of the site. Each sample was extracted in triplicate.

Platform 2				
	Epilimnion (n = 2)	Metalimnion (n = 2)	Hypolimnion (n = 3)	Fluid Fine Tailings (n = 1)
$\sum C_8$ monocyclic NAs	2.2 (0.2)	2.2 (0.1)	2.3 (0.1)	36.5 (4.8)
$\sum C_9$ monocyclic NAs	8.7 (0.5)	8.5 (0.3)	9.2 (0.8)	57.6 (9.2)
$\sum C_{10}$ monocyclic NAs	15.0 (1.2)	13.2 (0.4)	15.4 (1.3)	30.6 (4.5)
$\sum C_8$ bicyclic NAs	15.6 (1.2)	14.4 (0.6)	15.3 (1.0)	27.7 (2.4)
$\sum C_9$ bicyclic NAs	35.5 (2.2)	33.4 (1.5)	37.4 (3.6)	90.8 (9.2)
$\sum C_{10}$ bicyclic NAs	84.4 (10.7)	72.9 (10.7)	84.8 (9.7)	118.9 (7.5)
$\sum C_{11}$ bicyclic NAs	205.7 (12.9)	175.5 (22.6)	227.6 (25.8)	229.8 (43.6)
$\sum C_{11}$ tricyclic NAs	28.5 (1.8)	25.1 (1.8)	30.5 (2.4)	79.4 (9.0)
$\sum C_{12}$ tricyclic NAs	108.4 (4.8)	97.4 (7.5)	115.2 (9.4)	128.8 (14.7)
$\sum C_7$ thiophene NAs	7.1 (0.4)	7.1 (0.3)	8.4 (1.1)	218.8 (27.1)
Platform 3				
	Epilimnion (n = 2)	Metalimnion (n = 3)	Hypolimnion (n = 3)	Fluid Fine Tailings (n = 1)
$\sum C_8$ monocyclic NAs	2.4 (0.1)	2.4 (0.1)	2.5 (0.1)	2.4 (0.2)
$\sum C_9$ monocyclic NAs	8.6 (0.4)	8.5 (0.4)	8.8 (0.6)	9.6 (0.9)
$\sum C_{10}$ monocyclic NAs	14.3 (0.7)	14.1 (0.5)	14.6 (0.9)	19.0 (1.8)
$\sum C_8$ bicyclic NAs	14.7 (1.2)	14.6 (1.0)	14.8 (1.0)	16.3 (1.8)
$\sum C_9$ bicyclic NAs	34.3 (2.4)	34.3 (2.0)	34.5 (1.6)	40.2 (2.3)
$\sum C_{10}$ bicyclic NAs	79.1 (10.1)	75.1 (4.4)	74.2 (6.9)	72.7 (8.9)
$\sum C_{11}$ bicyclic NAs	172.1 (11.1)	201.9 (16.3)	191.5 (24.3)	236.2 (25.5)
$\sum C_{11}$ tricyclic NAs	26.2 (1.1)	27.3 (1.9)	27.4 (1.8)	75.6 (8.0)
$\sum C_{12}$ tricyclic NAs	97.4 (8.5)	109.7 (9.3)	107.9 (12.3)	146.1 (17.1)
$\sum C_7$ thiophene NAs	7.1 (0.4)	7.1 (0.3)	7.4 (0.9)	12.8 (1.6)

Table 6. The *p*-values from univariate statistical analyses assessing the temporal variations within each zone of the water cap. [a]Student`s t-test was performed. [b]One-way ANOVA was performed. "n" represents the number of sampling events at each zone of the site. Each sample was extracted in triplicate.

Platform 2			
	Epilimnion[a] (n = 2)	Metalimnion[a] (n = 2)	Hypolimnion[b] (n = 3)
$\sum C_8$ monocyclic NAs	0.810	0.656	0.179
$\sum C_9$ monocyclic NAs	0.637	0.949	0.011
$\sum C_{10}$ monocyclic NAs	0.317	0.217	0.030
$\sum C_8$ bicyclic NAs	0.840	0.354	**0.003**
$\sum C_9$ bicyclic NAs	0.534	0.456	**0.006**
$\sum C_{10}$ bicyclic NAs	0.742	0.459	0.105
$\sum C_{11}$ bicyclic NAs	0.752	0.480	0.111
$\sum C_{11}$ tricyclic NAs	0.486	0.158	0.294
$\sum C_{12}$ tricyclic NAs	0.692	0.367	0.594
$\sum C_7$ thiophene NAs	0.015	0.484	0.613
Platform 3			
	Epilimnion[a] (n = 2)	Metalimnion[b] (n = 3)	Hypolimnion[b] (n = 3)
$\sum C_8$ monocyclic NAs	0.736	0.810	0.522
$\sum C_9$ monocyclic NAs	0.959	0.430	0.452
$\sum C_{10}$ monocyclic NAs	0.876	0.703	**0.001**
$\sum C_8$ bicyclic NAs	0.469	0.682	0.279
$\sum C_9$ bicyclic NAs	0.128	0.316	0.788
$\sum C_{10}$ bicyclic NAs	0.452	0.728	0.038
$\sum C_{11}$ bicyclic NAs	0.446	0.534	0.066
$\sum C_{11}$ tricyclic NAs	0.408	0.203	0.017
$\sum C_{12}$ tricyclic NAs	0.669	0.532	0.365
$\sum C_7$ thiophene NAs	0.294	0.574	0.401

Table 7. The *p*-values from univariate statistical analyses assessing the spatial variations of ∑ NA concentrations between Platform 2 and Platform 3. Student`s t-test was used to compare means.

	Epilimnion	Metalimnion	Hypolimnion	FFT
$\sum C_8$ monocyclic NAs	0.392	0.0113	**0.00329**	**6.78E-06**
$\sum C_9$ monocyclic NAs	0.718	0.928	0.585	**7.25E-05**
$\sum C_{10}$ monocyclic NAs	0.222	0.794	0.170	**0.00582**
$\sum C_8$ bicyclic NAs	0.213	0.718	0.284	**0.00253**
$\sum C_9$ bicyclic NAs	0.280	0.815	0.0227	**0.000262**
$\sum C_{10}$ bicyclic NAs	0.430	0.819	0.0237	**0.00367**
$\sum C_{11}$ bicyclic NAs	0.437	0.724	0.0162	0.839
$\sum C_{11}$ tricyclic NAs	0.0264	0.270	**0.00618**	0.607
$\sum C_{12}$ tricyclic NAs	0.0405	0.0480	0.178	0.246
$\sum C_7$ thiophene NAs	0.706	0.423	**0.000365**	**1.08E-05**

Table 8. The *p*-values from univariate statistical analyses assessing the spatial variations of ∑ NA concentrations between the zones of the water cap (epilimnion vs metalimnion vs hypolimnion) at Platform 2 and Platform 3. The concentrations from each sampling events were averaged within each zone of the water cap. Welch's test was used to compare the mean concentrations between the epilimnion, metalimnion, and hypolimnion.

	Platform 2	Platform 3
$\sum C_8$ monocyclic NAs	0.6100	0.152
$\sum C_9$ monocyclic NAs	0.3250	0.469
$\sum C_{10}$ monocyclic NAs	0.1060	0.542
$\sum C_8$ bicyclic NAs	0.5150	0.938
$\sum C_9$ bicyclic NAs	0.1250	0.961
$\sum C_{10}$ bicyclic NAs	0.3730	0.534
$\sum C_{11}$ bicyclic NAs	0.0170	**0.004**
$\sum C_{11}$ tricyclic NAs	0.0100	0.248
$\sum C_{12}$ tricyclic NAs	0.0170	0.118
$\sum C_7$ thiophene NAs	**0.0010**	0.959

Table 9. The number of NAs which showed statistically significant temporal differences ($p < 0.01$) between the sampling events within each zone of the water cap at Platform 2 and Platform 3. [a]Student`s t-test was performed. [b]One-way ANOVA was performed.

Naphthenic Acid	Platform 2			
	Total Number of Isomers Detected in Water Cap	Epilimnion[a] (n = 2)	Metalimnion[a] (n = 2)	Hypolimnion[b] (n = 3)
C_8 monocyclic NAs	3	0	0	1
C_9 monocyclic NAs	10	0	0	4
C_{10} monocyclic NAs	17	0	0	3
C_8 bicyclic NAs	6	0	0	1
C_9 bicyclic NAs	14	1	0	7
C_{10} bicyclic NAs	14	0	0	1
C_{11} bicyclic NAs	17	0	1	3
C_{11} tricyclic NAs	9	0	0	0
C_{12} tricyclic NAs	12	0	0	0
C_7 thiophene NAs	3	1	0	0
Total NAs	**105**	**2**	**1**	**20**

Naphthenic Acid	Platform 3			
	Total Number of Isomers Detected in Water Cap	Epilimnion[a] (n = 2)	Metalimnion[b] (n = 3)	Hypolimnion[b] (n = 3)
C_8 monocyclic NAs	3	0	0	0
C_9 monocyclic NAs	10	0	0	0
C_{10} monocyclic NAs	17	0	1	5
C_8 bicyclic NAs	6	0	0	0
C_9 bicyclic NAs	14	1	0	1
C_{10} bicyclic NAs	14	0	1	4
C_{11} bicyclic NAs	17	1	0	2
C_{11} tricyclic NAs	9	0	0	2
C_{12} tricyclic NAs	12	1	0	0
C_7 thiophene NAs	3	0	0	0
Total NAs	**105**	**3**	**2**	**14**

Table 10. The number of isomers which displayed significant spatial differences (Student's *t*-test, $p < 0.01$) between Platform 2 and Platform 3. The concentrations from each sampling events were averaged at each platform.

Naphthenic Acids	Total Number of Isomers Detected in Water Cap	Number of isomers which significantly differed between P2 and P3			
		Epilimnion	Metalimnion	Hypolimnion	FFT
C_8 monocyclic NAs	3	1	1	1	2
C_9 monocyclic NAs	10	0	0	0	9
C_{10} monocyclic NAs	17	1	1	2	9
C_8 bicyclic NAs	6	1	0	0	2
C_9 bicyclic NAs	14	0	0	3	7
C_{10} bicyclic NAs	14	0	0	4	3
C_{11} bicyclic NAs	17	5	0	2	0
C_{11} tricyclic NAs	9	2	0	5	0
C_{12} tricyclic NAs	12	1	1	2	0
C_7 thiophene NAs	3	1	0	1	3
Total NAs	**105**	**12**	**3**	**20**	**35**

Table 11. The number of isomers which displayed significant spatial differences between the three zones of the water cap. The concentrations from each sampling events were averaged within each zone. Welch's test was used to compare the mean concentrations between the epilimnion, metalimnion, and hypolimnion.

Naphthenic Acids	Total Number of Isomers Detected in Water Cap	Number of isomers which significantly differed between zones of water cap	
		Platform 2	Platform 3
C_8 monocyclic NAs	3	0	0
C_9 monocyclic NAs	10	0	0
C_{10} monocyclic NAs	17	1	0
C_8 bicyclic NAs	6	0	0
C_9 bicyclic NAs	14	1	1
C_{10} bicyclic NAs	14	1	0
C_{11} bicyclic NAs	17	1	2
C_{11} tricyclic NAs	9	1	0
C_{12} tricyclic NAs	12	0	0
C_7 thiophene NAs	3	1	0
Total NAs	**105**	**6**	**3**

Chapter Five: Improved coverage of naphthenic acid fraction compounds by comprehensive two-dimensional gas chromatography coupled with high resolution mass spectrometry

David T. Bowman[1], Karl J. Jobst[1,2], Xavier Ortiz[2], Eric J. Reiner[2,3], Lesley A. Warren[4,5], Brian E. McCarry[1], Greg F. Slater[1,4]

The work in this chapter has been published in: "D.T. Bowman *et al.*, Improved coverage of naphthenic acid fraction compounds by comprehensive two-dimensional gas chromatography coupled with high resolution mass spectrometry, J. Chromatogr. A (2017), http://dx.doi.org/10.1016/j.chroma.2017.07.17"

Author Affiliations:

[1] Department of Chemistry and Chemical Biology, McMaster University, 1280 Main Street West, Hamilton, Ontario, Canada, L8S 4M1
[2] Laboratory Services Branch, Ontario Ministry of the Environment and Climate Change, 125 Resources Road, Toronto, Ontario, Canada, M9P 3V6
[3] Department of Chemistry, University of Toronto, 80 St. George Street, Toronto, Ontario, Canada, M5S 3H6.
[4] School of Geography and Earth Sciences, McMaster University, 1280 Main Street West, Hamilton, Ontario, Canada, L8S 4K1
[5]Department of Civil Engineering, University of Toronto, 35 St. George Street, Toronto, ON, Canada, M5S 1A4

Author Contributions:

Study conceived by BEM and DTB. Study designed by DTB, GFS, KJJ, XO, and EJR. DTB performed sample extraction. DTB and KJJ performed GC×GC/HRMS analysis. DTB performed data analysis. DTB wrote manuscript, with editorial comments from GFS, KJJ, LAW, and XO.

Abstract:

This study reports the first application of comprehensive two-dimensional gas chromatography coupled to a high-resolution quadrupole time-of-flight mass spectrometer (GC×GC/HRQTOF-MS) for the characterization of naphthenic acid fraction compounds (NAFCs) from the Alberta Oil Sands Region. High resolution mass spectrometry (HRMS) significantly increased the coverage of NAFCs in the mixture and allowed the differentiation of NAFCs from several chemical classes. Mass defect plots were useful for visualizing the complex datasets generated by GC×GC/HRQTOF-MS and led to the identification of 1105 chemical species with unique elemental compositions (<5 ppm mass accuracy). It was demonstrated that GC×GC/HRQTOF-MS could distinguish chemical species with the C_3 vs SH_4 mass split. Mass defect plots were shown to be a powerful screening tool and enabled the detection of extensive isomer series from the SO_2 chemical class, some of which have not been previously reported in oil sands related samples. The GC×GC/HRQTOF-MS approach is expected to improve NAFC monitoring programs since the technique allows the qualitative analysis of individual NAFCs and provides unique fingerprints via isomer distributions which may assist in future fingerprinting studies.

1. Introduction:

The Athabasca oil sands are the third largest oil reserve in the world.[1] The caustic hot water extraction of bitumen from oil sands material results in the production of tailings.[2,3] The aqueous component of tailings, referred to as oil sands process-affected water (OSPW), has shown acute and chronic toxicity towards a variety of aquatic organisms. This toxicity is widely attributed to the presence of a complex mixture of organic compounds referred to as naphthenic acids (NAs).[4–10] In accordance with Alberta's zero discharge policy, OSPW must be stored on site in tailing ponds and settling basins.[2] Since NAs are somewhat soluble in water, they have the potential to migrate into the greater environment via leakage into groundwater.[11] Therefore, it is critical that suitable analytical techniques are developed to not only monitor NAs, but also differentiate industrial NA sources from natural sources.

Naphthenic acids are one of the most complex organic mixtures in the world, and their characterization poses a tremendous challenge to analytical chemists.[12] The term "naphthenic acids" was originally used to define the complex mixture of aliphatic and alicyclic monocarboxylic acids ($C_nH_{2n+Z}O_2$ where n = number of carbons, Z = hydrogen deficiency, by formation of rings), but in light of recent studies[13–15], the definition has been expanded to include compounds with sulphur and/or nitrogen heteroatoms, mono- and polyoxygenated species, and a variety of mixed oxygen-/nitrogen-/sulfur-containing species (e.g. NO_x, SO_x). For each chemical class, a range of double bond equivalents (DBEs) and carbon numbers (degree of alkylation) exist[16], in addition to a large number of structural isomers for each n- and Z-values[17–20]. In order to accommodate this broader definition of NAs, the mixture of chemicals present in the acidified fraction of OSPW is generally referred to as acid extractable organics (AEOs), or, more commonly, naphthenic acid fraction compounds (NAFCs).[12]

Advances in analytical techniques, such as ultrahigh resolution mass spectrometry, have greatly improved our ability to detect and characterize NAFCs in environmental samples. Fourier transform ion cyclotron mass spectrometry (FTICR MS) coupled to negative electrospray ionization (ESI)[13,15,21,22] has contributed to the unambiguous assignment of elemental compositions to thousands of features in OSPW due to its ultrahigh mass resolution (~500,000 resolution at *m/z* 400) and high mass accuracy (<1 ppm)[23,24]. Direct infusion FTICR MS has also been coupled with atmospheric pressure photoionization (APPI)[15] to provide complementary data for nonpolar compounds with poor ESI efficiencies. However, direct infusion does not allow the distinction of structural isomers, which have been shown to be useful in NA fingerprinting applications[25–28]. Derivatized extracts containing NAFCs have been analyzed by gas chromatography (GC) coupled to FTICR MS with electron ionization (EI), chemical ionization with methane (CI-CH_4) and ammonia (CI-NH_3)[17], and atmospheric pressure chemical ionization (APCI).[18] The mass resolution of FTICR MS is sufficient to resolve multiple

heteroatom classes, but the selected ion chromatograms (SICs) were consistent with an unresolved complex mixture of structural isomers.[17] When NAFCs are separated by high performance liquid chromatography (HPLC), structural isomers also typically co-elute as one peak[29] The chromatographic resolution of NAFCs has been significantly improved by packed column supercritical fluid chromatography (SFC), where the authors showed that the technique could partially and fully resolve many isobaric naphthenic acids.[29]

Comprehensive two-dimensional gas chromatography mass spectrometry (GC×GC/MS) has also significantly improved the chromatographic resolution of NAFCs, and allowed the separation of structural isomers. The structures of individual naphthenic acids with cyclohexane-[19], alicyclic bicyclic-[20,30], adamantane-[19,31], diamantane-[32], indane-[19,33], tetralin-[19,33], and naphthalene-[33] chemical moieties ("O_2" class) have been firmly identified in previous studies by comparison to reference standards. In addition, the structures of a few naphthenic acids from "non-traditional" chemical classes have been confirmed with reference standards, such as thiophene carboxylic acids[19] ("SO_2" class) and diamondoid dicarboxylic acids[34] ("O_4" class). However, a large proportion of the chemical species within naphthenic acid mixtures still remain unidentified. The structural elucidation of unknown NAFCs by GC×GC is challenging due to the extreme complexity of NA mixtures, lack of available standards and absence of NAFC mass spectra in mass spectral libraries. Complete chromatographic separation of NAFCs has yet to be achieved, especially in the latter part of the chromatogram. Coupling GC×GC with a high resolution mass spectrometer has been shown to significantly improve the non-targeted analysis of complex environmental mixtures[35–42]. Such techniques are advantageous since they can not only resolve structural isomers and produce isomer profiles, but also provide information on chemical classes, double bond equivalents, and carbon numbers based on mass accuracy.

The work described in this study illustrates the application of coupling comprehensive two-dimensional gas chromatography with APCI and a high resolution quadrupole time-of-flight mass spectrometer for the characterization of NAFCs. The combination of multidimensional chromatography and high resolution mass spectrometry was shown to significantly improve NAFC monitoring efforts since it can readily distinguish chemical classes, and also resolve and monitor the presence of individual structural isomers.

2. Experimental

2.1 Sample collection and preparation

The fluid fine tailings (FFT) sample was collected from Base Mine Lake (BML), which is an end pit lake established at the Mildred Lake Mine, located approximately 35 km north of Fort

McMurrary, Alberta, Canada. A more in-depth description of the site can be found elsewhere in literature.[43,44] The sample was collected at a depth of 18 m from Platform 2 using a non-commercial pneumatic piston sampling device, as described in a previous study[43]. Following collection, the sample was stored in a pre-cleaned Nalgene plastic bottle (1 L volume) at -20°C and was thawed prior to extraction.

The FFT sample was centrifuged at 3100 rpm for 60 minutes and the supernatant was removed. The supernatant was filtered by a 0.45 µm syringe filter (Gelman Sciences, Ann Arbor, MI, USA), acidified to pH 2, and extracted with dichloromethane (4 x 15 mL). The extracts were combined and concentrated to 1 mL by rotary evaporation. The extract was quantitatively transferred to a glass vial and concentrated to 30 µL by blowing gently with nitrogen. The NAFCs with carboxylic acid moieties were converted to methyl ester derivatives by treatment with diazomethane in dichloromethane. Diazomethane was added until the yellow colour persisted, which indicates an excess of derivatizing reagent. Prior to analysis, pyrene-d_{10} dissolved in toluene (final concentration: 1 ppm) was added to the sample as an internal standard. The extraction efficiency of the sample preparation procedure was evaluated by calculating the percent recovery of two recovery surrogate standards (4-tertbutylcyclohexane-1-carboxylic acid, 83% ± 3; 2-hexyldecanoic acid, 87% ± 14), which were added following centrifugation.

2.2 Instrumentation

GC×GC/HRQTOFMS analysis was performed using an Agilent 7890B gas chromatograph (Agilent Technologies, Santa Clara, CA, USA) fitted with a Zoex ZX2 GC×GC thermal modulator (Zoex, Houston, TX, USA) and interfaced to a Waters Xevo G2-XS quadrupole time-of-flight mass spectrometer (Waters Corporation, Milford, MA, USA). The first-dimension column was a DB-17ms 30 m x 0.25 mm x 0.15 µm film followed by a Restek Siltek deactivated guard column 1 m x 0.25 mm in the modulator loop. The second-dimension column was a DB-5ms 1 m x 0.10 mm x 0.10 µm film, and was placed in a secondary oven. The secondary column was then connected to a Custom MXT tubing (sulfinert treated) 0.8 m x 0.18 mm, which was inserted into the transfer line. Helium was used as the carrier gas, and the flow was set at 1 mL/min. The injector temperature was set at 280 °C. The initial oven temperature was held at 40 °C for 1 minute, and then ramped at a rate of 3 °C/min to 310 °C, and held for 10 minutes. The secondary oven was set at a 10 °C offset, relative to the primary oven. The modulator was set at a 15 °C offset, relative to the primary oven, and a modulation period of 3 seconds was used. The transfer line was set to 340 °C. The cone gas at a flow rate of 100 L/hr and the auxiliary gas flow set at 150 L/hr. The source temperature was 150 °C, with the detector run in TOF mode using an acquisition range of 50 to 1200 amu with an acquisition rate of 30 Hz. The mass spectrometer was operated at a resolving power of > 20 000 (FWHM), and internal mass calibration was performed by using a lock mass ion (1185.9452) from a reference compound,

tris(perfluoroheptyl)-s-triazine. Data processing was conducted using GC Image HRMS R2.5 (Zoex).

A Pegasus 4D system (LECO Corp., St. Joseph, MI, USA) was used to collect nominal mass electron ionization (EI) mass spectra for this study. The system utilized DB-17ms (30 m x 0.25 mm x 0.15 μm film) as the primary column and DB-5ms (1 m x 0.10 mm x 0.10 μm film) as the secondary column. The primary oven was programmed to hold at 40°C for 1 minute, ramp to 310°C at 2.5°C/min, and hold at 310°C for 20 minutes. The secondary oven and modulator oven offset were set to +5 and +20°C relative to the primary oven, respectively. A modulation period of 3 seconds was used. The ion source and transfer line temperature were set to 200 and 280°C, respectively. The time-of-flight mass spectrometer was operated with an acquisition rate of 200 spectra/second, and an acquisition range set to 50 – 500 Da. Data processing was performed by ChromaTOF version 4.50.8.0 (LECO).

2.3 Kendrick mass defect plots

A composite mass spectrum was created using the GC Image software by generating a 'blob' mass spectrum for the entire chromatogram. The software combined the centroid mass spectral data for all of the chromatographic time points using a bin of 0.002 Da. The ions from the composite mass spectrum were converted to the Kendrick mass scale by multiplying the International Union of Pure and Applied Chemistry (IUPAC) mass by 14.00000 and dividing by 14.01565. The Kendrick mass scale gives CH_2 an exact mass of 14.000, so homologous series will share a unique mass defect. Mass defects were calculated by subtracting the Kendrick exact mass from the Kendrick nominal mass. Kendrick mass defect (KMD) plots were constructed using Microsoft Excel by plotting the exact mass (x-axis) against its mass defect (y-axis). Elemental compositions were assigned based on mass accuracy using a combination of custom macros for Microsoft Excel and Elemental Composition Calculator (Varian Inc., Walnut Creek, CA) [17,45]. For the assignments, 0-100 of the elements C, H, N, O and S were considered, and all assignments were made within 5 ppm of the theoretical values. Ions which could not be identified with the above criteria, such as column bleed and other siloxanes, were removed from the dataset.

3. Results and Discussion

3.1 Ionization of naphthenic acids

In this study, naphthenic acid fraction compounds were ionized by an atmospheric pressure chemical ionization (APCI) source, operated in positive mode. The ionization of NAFCs by APCI generally occurred by protonation. APCI was advantageous in this study since it

minimized fragmentation and enhanced the relative abundance of the (pseudo)molecular ions. Similar observations were reported for the ionization of petroleum biomarkers (such as steranes, diasteranes, and petacyclic triterpanes) in crude oil by APCI. [46] A comparison of APCI and EI mass spectra for the methyl esters of adamantane-1-carboxylic acid and adamantane-2-carboxylic acid (Figure S1 in the supplementary information) showed that when ionized by APCI, both isomers were observed to form intense protonated $[M+H]^+$ molecular ions. The 100% relative abundance of the protonated molecular ions produced by APCI are significantly higher than the relative abundances of the molecular ions produced by EI (Figure S1).

3.2 Differentiation of chemical classes by GC×GC/HRMS

The two-dimensional total ion current (TIC) chromatogram for a typical fluid fine tailings pore water extract is shown in Figure 1. Despite the increased resolving power of GC×GC, the NAFCs elute as an unresolved complex mixture and very few individual components are chromatographically resolved in the TIC chromatogram. The addition of accurate mass measurements of the high resolution mass spectrometer (HRMS) allowed for the differentiation of chemical classes and significantly improved the profiling of NAFCs. When examined at nominal mass resolution, numerous clusters of isobaric NAFCs are observed, as illustrated in Figure 2a, which displays a selected ion chromatogram (SIC) with a mass window of 199 ± 0.5. Narrowing the mass window of the SIC enables isobaric species belonging to different chemical classes to be distinguished and elemental compositions to be assigned. This is illustrated in Figures 2b-f which show the chromatographic resolution of NAFCs from five different chemical classes found within one nominal mass unit: SO_2 class ($C_{10}H_{15}SO_2$, -0.5 ppm), O class ($C_{15}H_{15}O$, -2.0 ppm), O_3 class ($C_{11}H_{19}O_3$, -1.0 ppm), HC class ($C_{15}H_{19}$, -1.0 ppm), and O_2 class ($C_{12}H_{23}O_2$, -0.5 ppm). Generally, it was observed that the chemical species with higher double bond equivalences (DBE) possessed later first dimension retention times. The NAFCs within the O_2 chemical class were observed to elute first, followed by the O_3 and SO_2 chemical classes. The NAFCs from the HC and O chemical classes showed the longest retention times. The necessity of high resolution mass spectrometry is apparent since the HC and O chemical classes co-elute in the nominal mass SIC (Figure 2a). A resolving power of 5000 is required to distinguish the co-eluting isobars and the two chemical classes are clearly differentiated by the SICs in Figures 2c and 2e.

3.3 Differentiation of the C_3 vs SH_4 mass split by GC×GC/HRMS

Sulfur-containing compounds are components of petroleum, and their characterization is important due to regulatory requirements for sulfur content in petroleum. [47] However, identifying the presence of sulfur-containing compounds can be challenging due to the very small mass difference between compounds with the C_3 vs SH_4 mass split (Δm = 0.0034 Da). Ultrahigh

resolution mass spectrometry is typically required to resolve this mass split. For instance, at *m/z* 250, the full width half maximum (FWHM) resolving power required to separate two masses with the C_3 vs SH_4 mass split is 73 000. High resolution chromatographic techniques can lower the resolving power requirements of the mass analyzer for the differentiation of such mass splits. This was recently shown by Byer *et al.*, who coupled GC×GC to a high resolution time-of-flight mass spectrometer (~25,000 mass resolution) to resolve C_3 vs SH_4 mass splits and other common mass splits within a crude oil sample. [42]

The combination of GC×GC and high resolution MS in this study enabled the differentiation of numerous instances where this mass split occurred (Figure 3). In order to differentiate such isobars by GC×GC/HRMS, there are two requirements: (1) the isobars must be chromatographically resolved, and (2) the ions must be measured by the mass spectrometer with high mass accuracy. Since many isomers are typically found for each elemental composition, the mass measurements for all structural isomers must be recorded with high precision. The resolution of C_3 vs SH_4 isobars in the NAFC mixture in this study is illustrated in Figure 3. The selected ion chromatogram for masses 191.0705 ± 0.003 ($C_{11}H_{11}O_3$) and 191.0742 ± 0.003 ($C_8H_{15}SO_3$) shown on the left column of Figure 3a demonstrate that the chromatographic resolution of the isobars is achieved. The portion of the composite mass spectrum shown on the right of Figure 3a is a plot of the centroid mass spectral data collected at each chromatographic time point with a bin of 0.0001 Da. The spread of the centroid data is less than 0.0025 Da for each mass, demonstrating the high precision and accuracy of the instrument, and the two masses are clearly differentiated. In a similar vein, Figure 3b shows a SIC chromatogram and composite mass spectrum which shows the differentiation of $C_{18}H_{23}O_3$ and $C_{15}H_{27}SO_3$. At half height, the distribution of the centroid peaks of each isobar are less than 0.003 Da and the two chemical species are differentiated. Similarly, the differentiation of $C_{11}H_{13}O_2$ and $C_8H_{17}O_2S$ is illustrated in Figure S2. The use of GC×GC is advantageous in this example since the two isobars possess similar first dimension retention times, and are only chromatographically resolved in the second dimension. Without the use of multidimensional chromatography, the isobars would have possessed the same time domain and the masses would not have been independently distinguished. A FWHM resolving power of over 52 000, 57 000, 85 000 is theoretically required to resolve the mass splits in Figures S2, 3a, 3b, respectively. A key factor enabling the resolution of these mass splits with a QTOF-MS is the chromatographic resolution of the isobars achieved via GC×GC separation. In cases where co-elutions of isobars occur, different combinations of GC column stationary phases can be explored to achieve chromatographic resolution and facilitate the differentiation of C_3 vs SH_4 isobars.

3.4 Exploring GC×GC/HRMS data via Kendrick mass defect plots and chemical class histogram plots

Data mining of GC×GC datasets can be a laborious and time-consuming task due to the large number of peaks resolved in GC×GC chromatograms. Mass defect filtering has been shown to be an effective non-targeted approach to simplify the datasets generated by the GC×GC/HRMS experiments and to provide an overview of the elemental compositions within environmental samples. [35] In this study, a Kendrick mass defect (KMD) plot (See Figure 4) was used to clearly differentiate species with different heteroatoms, carbon numbers, and double bond equivalences. An advantage of GC×GC/HRMS is that the high resolution chromatograms produced by the technique provide complementary isomer specific information for each elemental composition on the KMD plot. In this sample, 77 isomer peaks were resolved for four selected NAFCs from the O_2 class (DBE = 2) with the following elemental composition: $C_9H_{17}O_2$, $C_{10}H_{19}O_2$, $C_{11}H_{21}O_2$, and $C_{12}H_{23}O_2$. While it has been previously shown that GC/FTICR MS is able to differentiate and chromatographically resolve numerous chemical classes, the technique was not able to resolve structural isomers[17,18], presumably due to lower peak capacity of the one-dimensional GC column and the slower acquisition rate of the mass analyzer.

As a result of the extreme complexity of NAFC mixtures, and the lack of available mass spectra in library databases, the identification of 'unknown' NAFCs is a challenging and cumbersome task. In previous studies[19,30–32], the structures of unknown NAFCs have been primarily identified using GC×GC/MS (nominal mass) by (1) interpretation of 'unknown' EI mass spectra from first principles, and (2) confirmation of structural proposal by comparing the GC×GC retention times and EI mass spectra of unknowns with that of commercially available or synthesized reference standards. However, by utilizing the accurate mass measurements of the QTOF-MS, the process is simplified, and it is possible to assign elemental compositions to unknowns in the sample, and generate tentative structure proposals. The KMD plot enabled the identification of three families of SO_2 NAFCs with DBE values of 4, 7, and 10 (Figure 5). As a result of the structured nature of the two-dimensional chromatogram (See Figure 5), it is possible to identify trends related to the chemical structures of the compounds. It is well known that when complex mixtures are separated by GC×GC, chemically similar analytes elute in similar regions based on their chromatographic behavior[48]. As shown in Figure 5, an increase in unsaturation leads to an increase in the first dimension retention times of the homologous series. Furthermore, within a homologous series, an increase in alkylation leads to a slight increase in both the first and second dimension retention times. Many structural isomers were resolved for each elemental composition, further exemplifying the complexity of NAFC isomer series. Structural isomers were observed to elute in bands with similar second dimension retention times. For additional clarity, Figures S4, S5, and S6 in the supplementary information document present individual SICs for each elemental composition.

The NAFCs from the SO_2 class with DBE values of 4 were observed as protonated cations and were previously confirmed as the methyl esters of alkylated thiophene carboxylic acids by comparison to reference standards. [19] The structures of the NAFCs from the SO_2 class with DBE values of 7 and 10 were not confirmed with reference standards, but are speculated to be methyl esters with a benzothiophene and dibenzothiophene chemical moiety, respectively. The detection of NAFCs from the SO_2 class are worthy of note since it has been previously reported that sulphur-containing NAFCs may be important for the distinction of oil sands impacted waters from natural waters[18,49]. The isomer distributions of SO_2 NAFCs are not well understood and may aid in the differentiation of OSPW sources.

Figure 6 presents the histogram for the relative abundances of each compound class identified in the NAFC mixtures, calculated from the composite mass spectrum. The O_2 class was the most abundant chemical class in the sample, representing 57.6% of the total ion intensity. The O_2 class contains derivatized classical naphthenic acids, but as a result of the extraction method used in this study, it may also include other acidic and neutral chemical species from the sample (possessing hydroxyl, ketone, aldehyde, ether, and/or ester substituents). The HC class was the second most abundant compound class (20.8%), followed by the O (8.7%), O_3 (6.9%), and O_4 (2.0%) chemical classes. When summed, the mono- and polyoxygenated NAFCs represented over 75.2% of the total ion intensity. Sulfur-containing NAFCs (SO_x) were detected in the sample and represented 3.4% of the total ion current intensity. The most abundant chemical class with a sulfur heteroatom was the SO_2 class (1.1%), followed by the SO_3 class (0.7%). Nitrogen-containing NAFCs were also identified in the sample, but their summed abundance was minor (0.6%) compared to the other classes. The relatively high abundance of compounds from the HC class in the extracts indicates that there is some fragmentation of NAFCs occurring within the APCI source. The presence of hydrocarbons with low DBEs confirms this since they are known to possess extremely low water solubilities. However, since it is possible that during the fragmentation of methyl esters, the charge may remain localized on the polar fragment, the fragmentation rate may in fact be higher. Nevertheless, it should be noted that APCI was useful for minimizing the relative contribution of the HC class. Ortiz *et al*. reported that the HC class was the most abundant chemical class when NAFCs were ionized by EI.[17]

4. Conclusion

In this study, GC×GC/HRQTOFMS utilizing APCI was used for the characterization of NAFCs in a fluid fine tailings pore water extract. . Selected ion chromatograms with narrow mass windows (±0.003 *m/z*) were useful for simplifying complex nominal mass chromatograms and resolving NAFCs from different chemical classes. It was demonstrated that GC×GC/HRQTOFMS could distinguish chemical species with the C_3 vs SH_4 mass split, which

traditionally has only been resolved by ultrahigh resolution mass spectrometry. KMD plots were shown to be a powerful visualization tool for complex GC×GC datasets and are expected to improve efforts focused on the identification of NAFCs. KMD plots allowed the detection of numerous baseline resolved NAFCs from the SO_2 chemical class, some of which have not been previously reported in oil sands related samples. This technique is expected to improve NAFC monitoring efforts since it can not only provide a global overview of the elemental compositions within complex NAFC mixtures, but also allow for the monitoring of specific individual naphthenic acids.

Acknowledgements

This article is dedicated to the memory of Dr. Brian E. McCarry (1946-2013). Funding for this work was provided by NSERC Canada and Syncrude Canada (Grant: CRDPJ 488301-15). The authors would like to thank Dr. Matthew Lindsay, Tara Colenbrander-Nelson, Daniel Arriaga, Patrick Morris, and Florent Risacher for collecting the fluid fine tailings sample, Syncrude Canada Limited Reclamation and Closure Research Group for field sampling support, and the Centre for Microbial Chemical Biology (CMCB) at McMaster University for access to the Pegasus 4D instrument.

References:

(1) Government of Alberta. Alberta Energy: Oil Sands http://www.energy.alberta.ca/OurBusiness/oilsands.asp (accessed Sep 18, 2016).

(2) Giesy, J. P.; Anderson, J. C.; Wiseman, S. B. Alberta oil sands development. *Proc. Natl. Acad. Sci.* **2010**, 107 (3), 951–952.

(3) Headley, J. V; Mohamed, M. H.; Frank, R. A.; Martin, J. W.; Hazewinkel, R. R. O.; Humphries, D.; Gurprasad, N. P.; Hewitt, L. M.; Muir, D. C. G.; Lindeman, D.; et al. Chemical fingerprinting of naphthenic acids and oil sands process waters — A review of analytical methods for environmental samples. *J. Environ. Sci. Heal. Part A.* **2013**, 48 (10), 1145–1163.

(4) Frank, R. A.; Kavanagh, R.; Kent Burnison, B.; Arsenault, G.; Headley, J. V.; Peru, K. M.; Van Der Kraak, G.; Solomon, K. R. Toxicity assessment of collected fractions from an extracted naphthenic acid mixture. *Chemosphere* **2008**, 72 (9), 1309–1314.

(5) Anderson, J.; Wiseman, S. B.; Moustafa, A.; Gamal El-Din, M.; Liber, K.; Giesy, J. P. Effects of exposure to oil sands process-affected water from experimental reclamation ponds on Chironomus dilutus. *Water Res.* **2012**, 46 (6), 1662–1672.

(6) Kavanagh, R. J.; Frank, R. A.; Burnison, B. K.; Young, R. F.; Fedorak, P. M.; Solomon, K. R.; Van Der Kraak, G. Fathead minnow (Pimephales promelas) reproduction is impaired when exposed to a naphthenic acid extract. *Aquat. Toxicol.* **2012**, 116–117, 34–42.

(7) Peters, L. E.; MacKinnon, M.; Van Meer, T.; van den Heuvel, M. R.; Dixon, D. G. Effects of oil sands process-affected waters and naphthenic acids on yellow perch (Perca flavescens) and Japanese medaka (Orizias latipes) embryonic development. *Chemosphere* **2007**, 67 (11), 2177–2183.

(8) Nero, V.; Farwell, A.; Lee, L. E. J.; Van Meer, T.; MacKinnon, M. D.; Dixon, D. G. The effects of salinity on naphthenic acid toxicity to yellow perch: Gill and liver histopathology. *Ecotoxicol. Environ. Saf.* **2006**, 65 (2), 252–264.

(9) Marentette, J. R.; Frank, R. A.; Bartlett, A. J.; Gillis, P. L.; Hewitt, L. M.; Peru, K. M.; Headley, J. V.; Brunswick, P.; Shang, D.; Parrott, J. L. Sensitivity of walleye (Sander vitreus) and fathead minnow (Pimephales promelas) early-life stages to naphthenic acid fraction components extracted from fresh oil sands process-affected waters. *Environ. Pollut.* **2015**, 207, 59–67.

(10) Reinardy, H. C.; Scarlett, A. G.; Henry, T. B.; West, C. E.; Hewitt, L. M.; Frank, R. A.; Rowland, S. J. Aromatic naphthenic acids in oil sands process-affected water, resolved by GCxGC-MS, only weakly induce the gene for vitellogenin production in zebrafish (danio rerio) larvae. *Environ. Sci. Technol.* **2013**, 47 (12), 6614–6620.

(11) Roy, J. W.; Bickerton, G.; Frank, R. A.; Grapentine, L.; Hewitt, L. M. Assessing Risks of Shallow Riparian Groundwater Quality Near an Oil Sands Tailings Pond. *Groundwater* **2016**, 54 (4), 545–558.

(12) Headley, J. V.; Peru, K. M.; Barrow, M. P. Advances in Mass Spectrometric Characterization of Naphthenic Acids Fraction Compounds in Oil Sands Environmental Samples and Crude Oil - A Review. *Mass Spectrom. Rev.* **2015**, 35 (2), 311–328.

(13) Grewer, D. M.; Young, R. F.; Whittal, R. M.; Fedorak, P. M. Naphthenic acids and other acid-extractables in water samples from Alberta: What is being measured? *Sci. Total Environ.* **2010**, 408 (23), 5997–6010.

(14) Headley, J. V.; Peru, K. M.; Armstrong, S. A.; Han, X.; Martin, J. W.; Mapolelo, M. M.; Smith, D. F.; Rogers, R. P.; Marshall, A. G. Aquatic plant-derived changes in oil sands

naphthenic acid signatures determined by low-, high-, and ultrahigh-resolution mass spectrometry. *Rapid Commun. Mass Spectrom.* **2009**, 23, 515–522.

(15) Barrow, M. P.; Witt, M.; Headley, J. V.; Peru, K. M. Athabasca oil sands process water: Characterization by atmospheric pressure photoionization and electrospray ionization Fourier transform ion cyclotron resonance mass spectrometry. *Anal. Chem.* **2010**, 82 (9), 3727–3735.

(16) Barrow, M. P.; Headley, J. V; Derrick, P. J. Data visualization for the characterization of naphthenic acids within petroleum samples. *Energy Fuels* **2009**, No. 12, 2592–2599.

(17) Ortiz, X.; Jobst, K. J.; Reiner, E. J.; Backus, S.; Peru, K. M.; McMartin, D. W.; O'Sullivan, G.; Taguchi, V. Y.; Headley, J. V. Characterization of naphthenic acids by gas chromatography-fourier transform ion cyclotron resonance mass spectrometry. *Anal. Chem.* **2014**, 86 (15), 7666–7673.

(18) Barrow, M. P.; Peru, K. M.; Headley, J. V. An added dimension: GC atmospheric pressure chemical ionization FTICR MS and the Athabasca oil sands. *Anal. Chem.* **2014**, 86 (16), 8281–8288.

(19) Bowman, D. T.; Slater, G. F.; Warren, L. A.; McCarry, B. E. Identification of individual thiophene-, indane-, tetralin-, cyclohexane-, and adamantane-type carboxylic acids in composite tailings pore water from Alberta oil sands. *Rapid Commun. Mass Spectrom.* 2014, 28 (19), 2075–2083.

(20) Wilde, M. J.; Rowland, S. J. Structural Identification of Petroleum Acids by Conversion to Hydrocarbons and Multidimensional Gas Chromatography-Mass Spectrometry. *Anal. Chem.* **2015**, 87 (16), 8457–8465.

(21) Mapolelo, M. M.; Rodgers, R. P.; Blakney, G. T.; Yen, A. T.; Asomaning, S.; Marshall, A. G. Characterization of naphthenic acids in crude oils and naphthenates by electrospray ionization FT-ICR mass spectrometry. *Int. J. Mass Spectrom.* **2011**, 300 (2–3), 149–157.

(22) Rowland, S. M.; Robbins, W. K.; Corilo, Y. E.; Marshall, A. G.; Rodgers, R. P. Solid-Phase Extraction Fractionation To Extend the Characterization of Naphthenic Acids in Crude Oil by Electrospray Ionization Fourier Transform Ion Cyclotron Resonance Mass Spectrometry. *Energy Fuels* **2014**, 28, 5043–5048.

(23) Rodgers, R. P.; Schaub, T. M.; Marshall, A. G. Petroleomics: MS Returns to Its Roots. *Anal. Chem.* **2005**, 77 (1), 20 A-27 A.

(24) Marshall, A. G.; Rodgers, R. P. Petroleomics: Chemistry of the underworld. *Proc. Natl. Acad. Sci*. 2008, 105 (47), 18090–18095.

(25) Rowland, S. J.; West, C. E.; Scarlett, A. G.; Ho, C.; Jones, D. Differentiation of two industrial oil sands process-affected waters by two-dimensional gas chromatography/mass spectrometry of diamondoid acid profiles. *Rapid Commun. Mass Spectrom.* **2012**, 26 (5), 572–576.

(26) Frank, R. A.; Roy, J. W.; Bickerton, G.; Rowland, S. J.; Headley, J. V.; Scarlett, A. G.; West, C. E.; Peru, K. M.; Parrott, J. L.; Conly, F. M.; et al. Profiling oil sands mixtures from industrial developments and natural groundwaters for source identification. *Environ. Sci. Technol.* **2014**, 48 (5), 2660–2670.

(27) Lengger, S. K.; Scarlett, A. G.; West, C. E.; Frank, R. A.; Hewitt, L. M.; Milestone, C. B.; Rowland, S. J. Use of the distributions of adamantane acids to profile short-term temporal and pond-scale spatial variations in the composition of oil sands process-affected waters. *Environ. Sci. Process. Impacts* **2015**, 17 (8), 1415–1423.

(28) Frank, R. A.; Milestone, C. B.; Rowland, S. J.; Headley, J. V.; Kavanagh, R. J.; Lengger, S. K.; Scarlett, A. G.; West, C. E.; Peru, K. M.; Hewitt, L. M. Assessing spatial and temporal variability of acid-extractable organics in oil sands process-affected waters. *Chemosphere* **2016**, 160, 303–313.

(29) Pereira, A. S.; Martin, J. W. Exploring the complexity of oil sands process-affected water by high efficiency supercritical fluid chromatography/orbitrap mass spectrometry. *Rapid Commun. Mass Spectrom.* **2015**, 29 (8), 735–744.

(30) Wilde, M. J.; West, C. E.; Scarlett, A. G.; Jones, D.; Frank, R. A.; Hewitt, L. M.; Rowland, S. J. Bicyclic naphthenic acids in oil sands process water: Identification by comprehensive multidimensional gas chromatography–mass spectrometry. *J. Chromatogr. A* **2015**, 1378, 74–87.

(31) Rowland, S. J.; Scarlett, A. G.; Jones, D.; West, C. E.; Frank, R. a. Diamonds in the rough: Identification of individual naphthenic acids in oil sands process water. *Environ. Sci. Technol.* **2011**, 45 (7), 3154–3159.

(32) Rowland, S. J.; West, C. E.; Scarlett, A. G.; Jones, D.; Frank, R. a. Identification of individual tetra- and pentacyclic naphthenic acids in oil sands process water by comprehensive

two-dimensional gas chromatography/mass spectrometry. *Rapid Commun. Mass Spectrom.* **2011**, 25 (9), 1198–1204.

(33) West, C. E.; Pureveen, J.; Scarlett, A. G.; Lengger, S. K.; Wilde, M. J.; Korndorffer, F.; Tegelaar, E. W.; Rowland, S. J. Can two-dimensional gas chromatography/mass spectrometric identification of bicyclic aromatic acids in petroleum fractions help to reveal further details of aromatic hydrocarbon biotransformation pathways? *Rapid Commun. Mass Spectrom.* **2014**, 28 (9), 1023–1032.

(34) Lengger, S. K.; Scarlett, A. G.; West, C. E.; Rowland, S. J. Diamondoid diacids ('O4' species) in oil sands process-affected water. *Rapid Commun. Mass Spectrom.* **2013**, 27 (23), 2648–2654.

(35) Ubukata, M.; Jobst, K. J.; Reiner, E. J.; Reichenbach, S. E.; Tao, Q.; Hang, J.; Wu, Z.; Dane, a. J.; Cody, R. B. Non-targeted analysis of electronics waste by comprehensive two-dimensional gas chromatography combined with high-resolution mass spectrometry: Using accurate mass information and mass defect analysis to explore the data. *J. Chromatogr. A* **2015**, 1395, 152–159.

(36) Zushi, Y.; Hashimoto, S.; Fushimi, A.; Takazawa, Y.; Tanabe, K.; Shibata, Y. Rapid automatic identification and quantification of compounds in complex matrices using comprehensive two-dimensional gas chromatography coupled to high resolution time-of-flight mass spectrometry with a peak sentinel tool. *Anal. Chim. Acta* **2013**, 778, 54–62.

(37) Ieda, T.; Ochiai, N.; Miyawaki, T.; Ohura, T.; Horii, Y. Environmental analysis of chlorinated and brominated polycyclic aromatic hydrocarbons by comprehensive two-dimensional gas chromatography coupled to high-resolution time-of-flight mass spectrometry. *J. Chromatogr. A* **2011**, 1218 (21), 3224–3232.

(38) Hashimoto, S.; Takazawa, Y.; Fushimi, A.; Tanabe, K.; Shibata, Y.; Ieda, T.; Ochiai, N.; Kanda, H.; Ohura, T.; Tao, Q.; et al. Global and selective detection of organohalogens in environmental samples by comprehensive two-dimensional gas chromatography-tandem mass spectrometry and high-resolution time-of-flight mass spectrometry. *J. Chromatogr. A* **2011**, 1218 (24), 3799–3810.

(39) Hashimoto, S.; Zushi, Y.; Fushimi, A.; Takazawa, Y.; Tanabe, K.; Shibata, Y. Selective extraction of halogenated compounds from data measured by comprehensive multidimensional gas chromatography/high resolution time-of-flight mass spectrometry for non-target analysis of environmental and biological samples. *J. Chromatogr. A* **2013**, 1282, 183–189.

(40) Zushi, Y.; Hashimoto, S.; Tamada, M.; Masunaga, S.; Kanai, Y.; Tanabe, K. Retrospective analysis by data processing tools for comprehensive two-dimensional gas chromatography coupled to high resolution time-of-flight mass spectrometry: A challenge for matrix-rich sediment core sample from Tokyo Bay. *J. Chromatogr. A* **2014**, 1338, 117–126.

(41) Myers, A. L.; Watson-Leung, T.; Jobst, K. J.; Shen, L.; Besevic, S.; Organtini, K.; Dorman, F. L.; Mabury, S. a; Reiner, E. J. Complementary nontargeted and targeted mass spectrometry techniques to determine bioaccumulation of halogenated contaminants in freshwater species. *Environ. Sci. Technol.* **2014**, 48 (23), 13844–13854.

(42) Byer, J. D.; Siek, K.; Jobst, K. Distinguishing the C3 vs SH4 Mass Split by Comprehensive Two-Dimensional Gas Chromatography–High Resolution Time-of-Flight Mass Spectrometry. *Anal. Chem.* **2016**, 88 (12), 6101–6104.

(43) Dompierre, K. A.; Lindsay, M. B. J.; Cruz-Hernández, P.; Halferdahl, G. M. Initial geochemical characteristics of fluid fine tailings in an oil sands end pit lake. *Sci. Total Environ.* **2016**, 556, 196–206.

(44) Dompierre, K. A.; Barbour, S. L. Characterization of physical mass transport through oil sands fluid fine tailings in an end pit lake: a multi-tracer study. *J. Contam. Hydrol.* **2016**, 189, 12–26.

(45) Sühring, R.; Ortiz, X.; Pena-Abaurrea, M.; Jobst, K. J.; Freese, M.; Pohlmann, J.-D.; Marohn, L.; Ebinghaus, R.; Backus, S.; Hanel, R.; et al. Evidence for High Concentrations and Maternal Transfer of Substituted Diphenylamines in European Eels Analyzed by Two-Dimensional Gas Chromatography− Time-of-Flight Mass Spectrometry. *Environ. Sci. Technol.* **2016**, 50, 12678–12685.

(46) Lobodin, V. V.; Maksimova, E. V.; Rodgers, R. P. Gas chromatography/atmospheric pressure chemical ionization tandem mass spectrometry for fingerprinting the Macondo oil spill. *Anal. Chem.* **2016**, 88, 6914–6922.

(47) Ávila, B. M. F.; Pereira, V. B.; Gomes, A. O.; Azevedo, D. A. Speciation of organic sulfur compounds using comprehensive two-dimensional gas chromatography coupled to time-of-flight mass spectrometry: A powerful tool for petroleum refining. *Fuel* **2014**, 126, 188–193.

(48) Murray, J. A. Qualitative and quantitative approaches in comprehensive two-dimensional gas chromatography. *J. Chromatogr. A* **2012**, 1261, 58–68.

(49) Headley, J. V.; Barrow, M. P.; Peru, K. M.; Fahlman, B.; Frank, R. A.; Bickerton, G.; McMaster, M. E.; Parrott, J.; Hewitt, L. M. Preliminary fingerprinting of Athabasca oil sands polar organics in environmental samples using electrospray ionization Fourier transform ion cyclotron resonance mass spectrometry. *Rapid Commun. Mass Spectrom.* **2011**, 25 (13), 1899–1909.

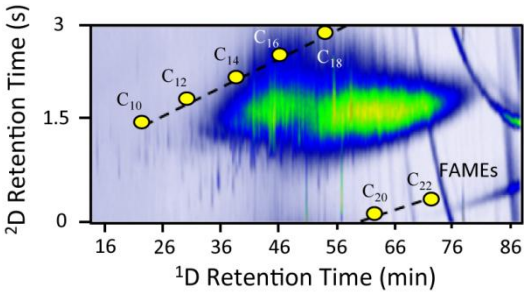

Figure 1. Two-dimensional total ion current (TIC) chromatogram of a methylated fluid fine tailings pore water extract. Fatty acid methyl esters (FAMEs) are labelled on the chromatogram as a reference point for relative retention times.

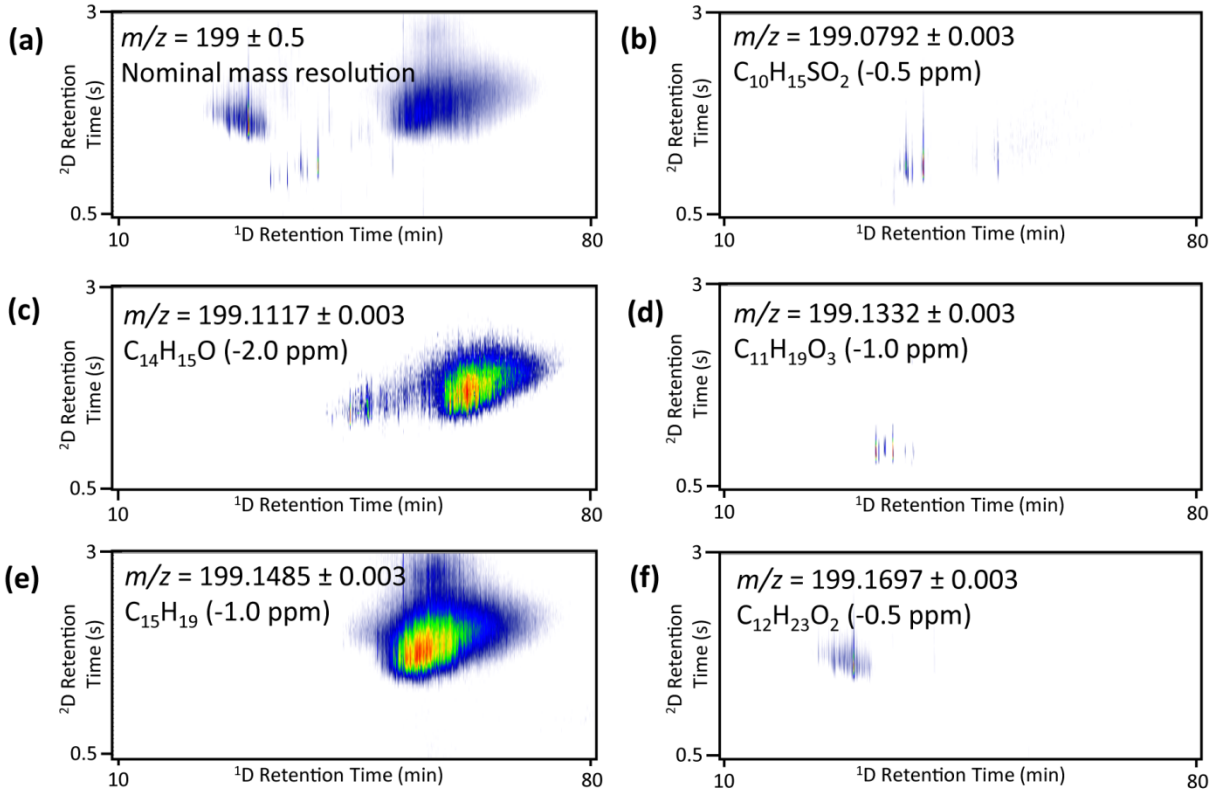

Figure 2. Examples of SICs showing the chromatographic resolution of NAFC with the same nominal mass: *m/z* 199. (a) Nominal mass resolution: *m/z* 199 ± 0.5, (b) *m/z* 199.0792 ± 0.003 (SO_2 class) (c) *m/z* 199.1117 ± 0.003 (O class) (d) *m/z* 199.1332 ± 0.003 (O_3 class) (e) *m/z* 199.1485 ± 0.003 (HC class) and (f) 199.1697 ± 0.003 (O_2 Class).

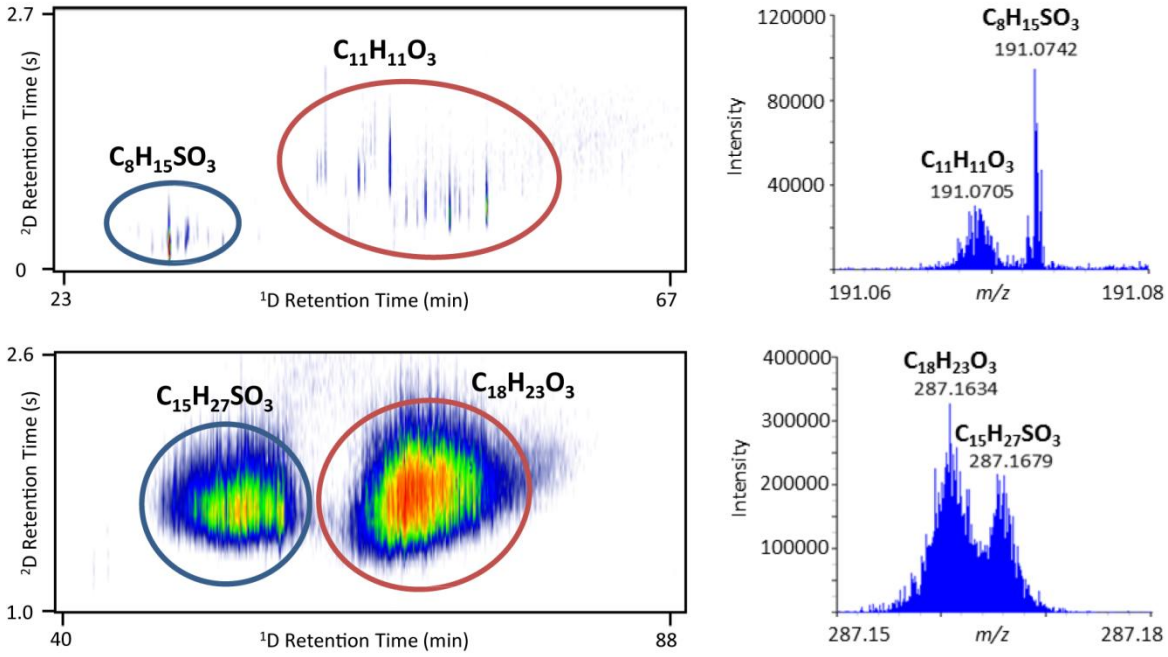

Figure 3. Selected ion chromatogram and composite mass spectrum demonstrating the differentiation of the following elemental compositions with the C_3 vs SH_4 mass split: (a) $C_{11}H_{11}O_3$ and $C_8H_{15}SO_3$ and (b) $C_{18}H_{23}O_3$ and $C_{15}H_{27}SO_3$.

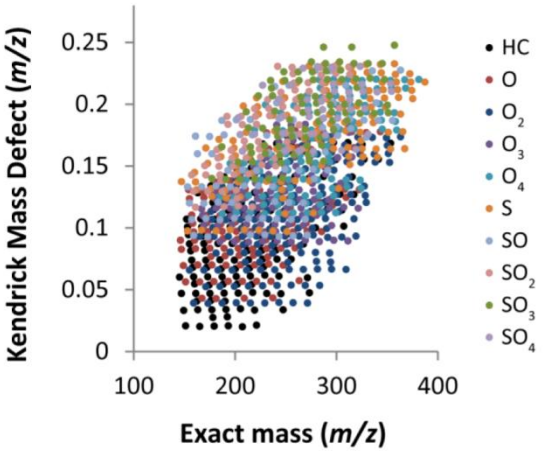

Figure 4. Kendrick mass defect plot generated from the composite mass spectrum.

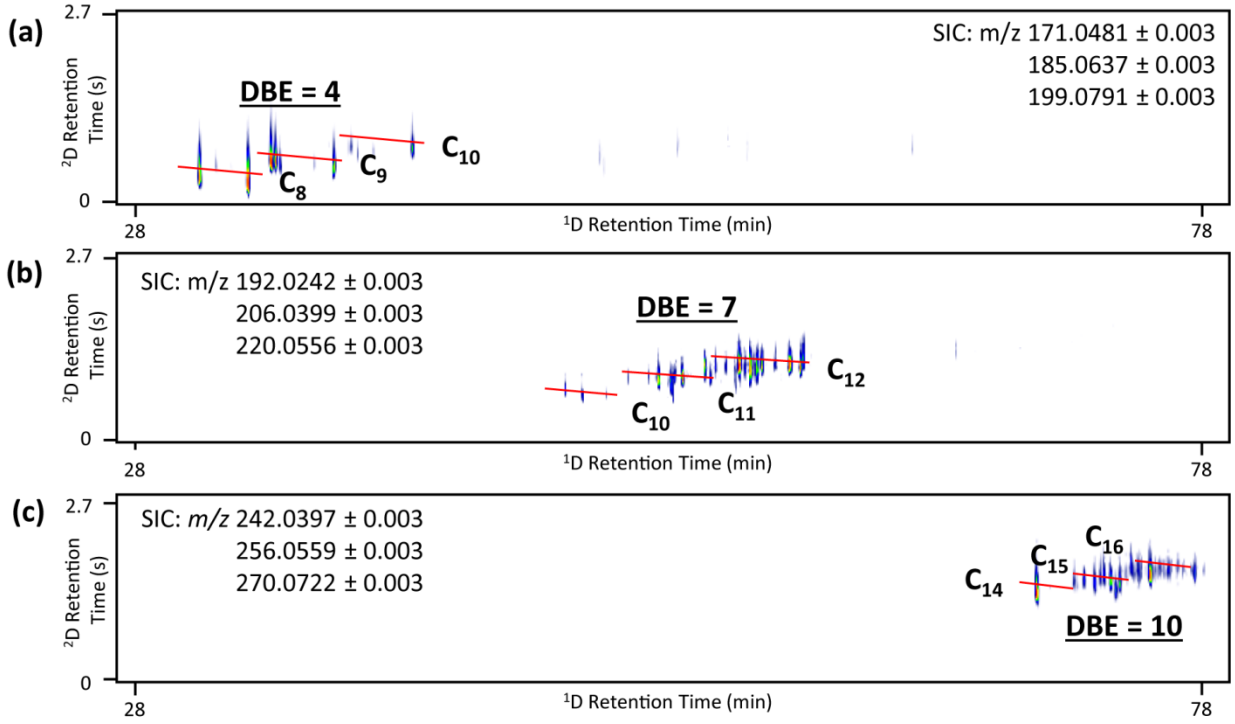

Figure 5. Chromatographic resolution of three homologous series from the SO_2 chemical class: (a) DBE = 4, $C_8 – C_{10}$,(b) DBE = 7, $C_{10} – C_{12}$, and (c) DBE = 10, $C_{14} – C_{16}$.

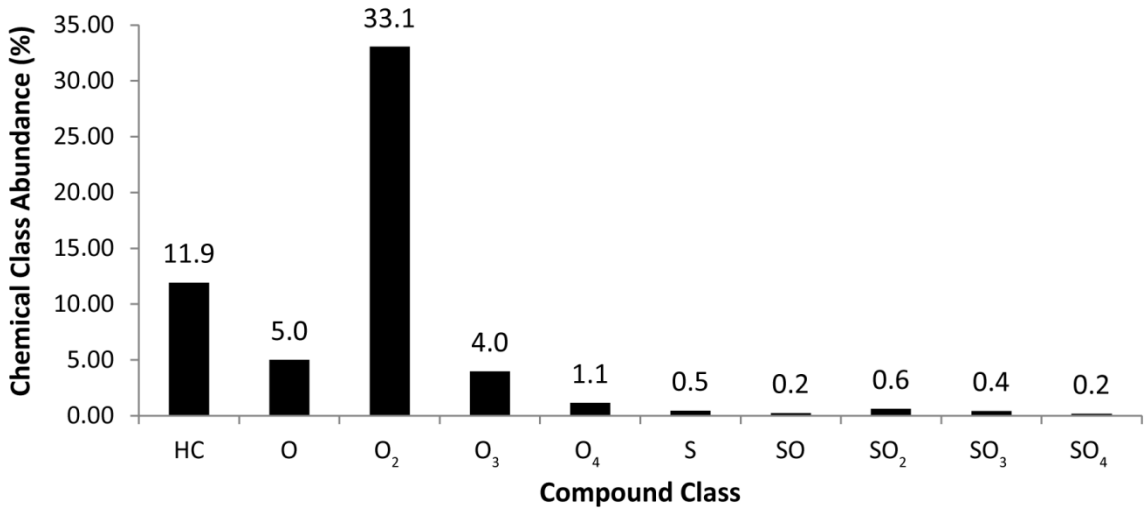

Figure 6. Compound class abundance histogram summarizing the identified NAFCs. The percentage abundance of each chemical class was calculated from the total counts of all identified chemical species within its class, relative to the total counts of all identified chemical classes.

Supporting Information

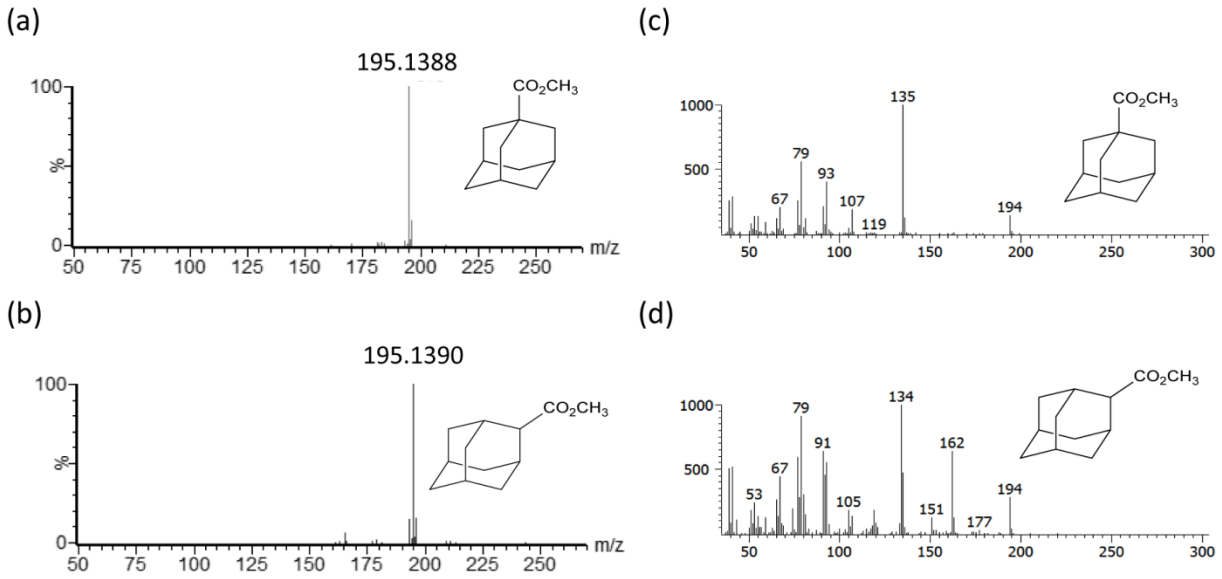

Figure S1. Atmospheric pressure chemical ionization (APCI) mass spectra of (a) adamantane-1-carboxylic acid, methyl ester and (b) adamantane-2-carboxylic acid, methyl ester. Electron ionization (EI) mass spectra of (c) adamantane-1-carboxylic acid, methyl ester and (d) adamantane-2-carboxylic acid, methyl ester.

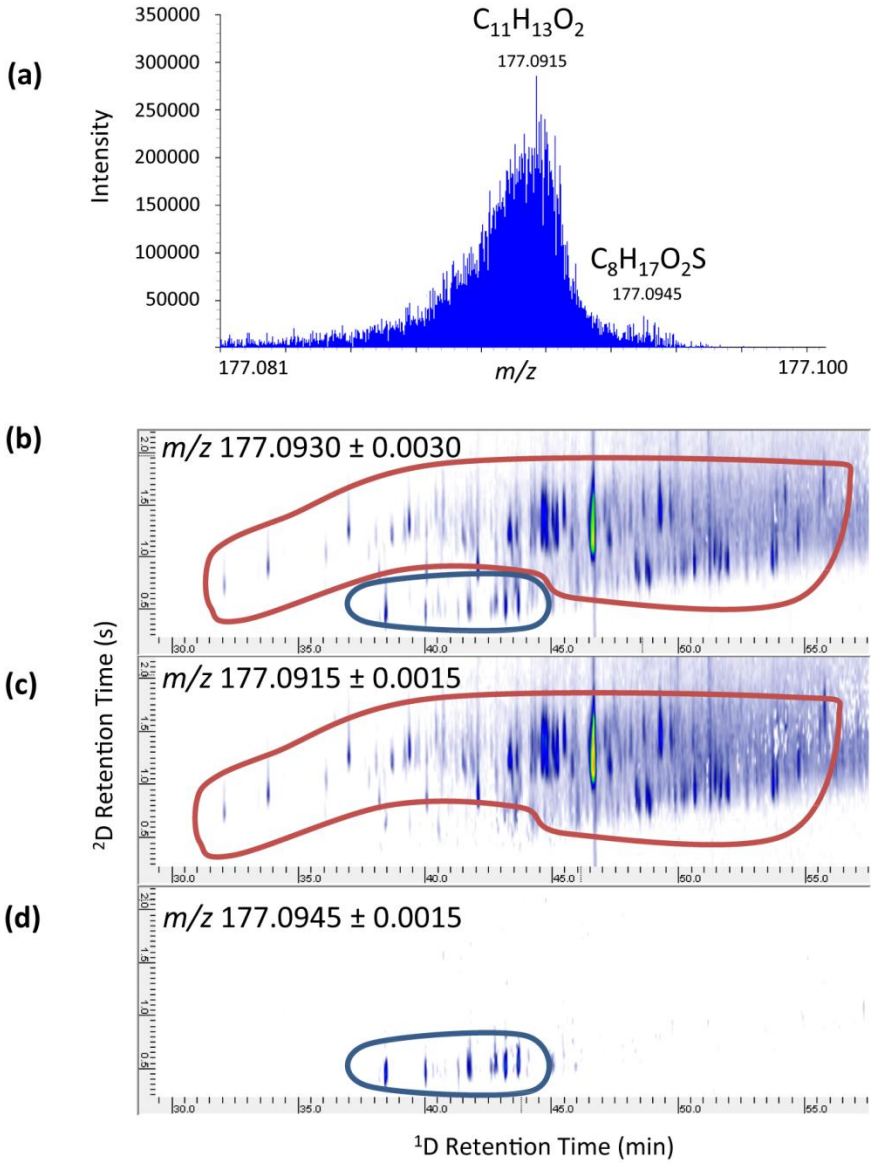

Figure S2. Differentiation of $C_{11}H_{13}O_2$ and $C_8H_{17}O_2S$ by GC×GC/HRQTOF-MS. (a) Composite mass spectrum, and SIC of (b) *m/z* 177.0930 ± 0.0030, (c) *m/z* 177.0915 ± 0.0015, (d) *m/z* 177.0945 ± 0.0015.

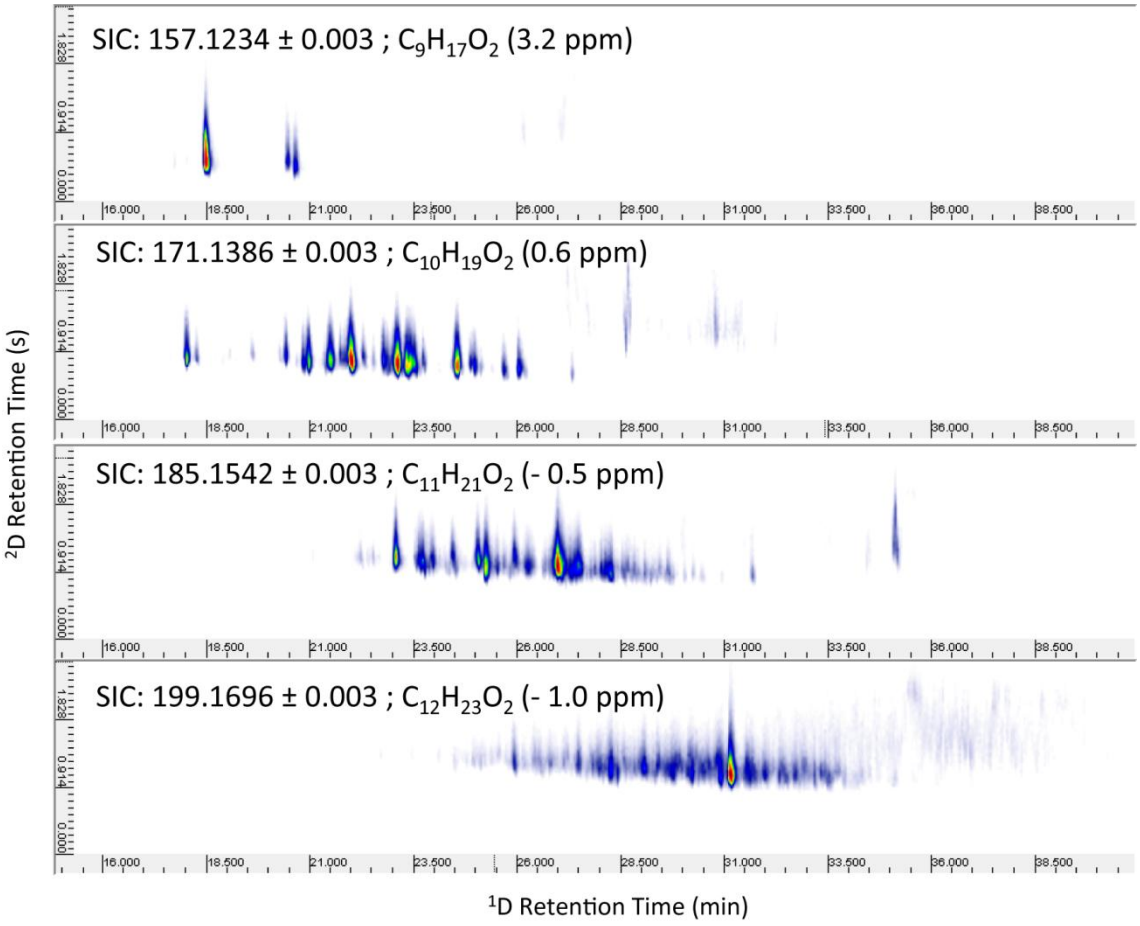

Figure S3: Chromatographic separation of structural isomers from the O_2 class (DBE = 1.5) with the following elemental compositions: (a) $C_9H_{17}O_2$, (b) $C_{10}H_{19}O_2$, (c) $C_{11}H_{21}O_2$, (d) and $C_{12}H_{23}O_2$.

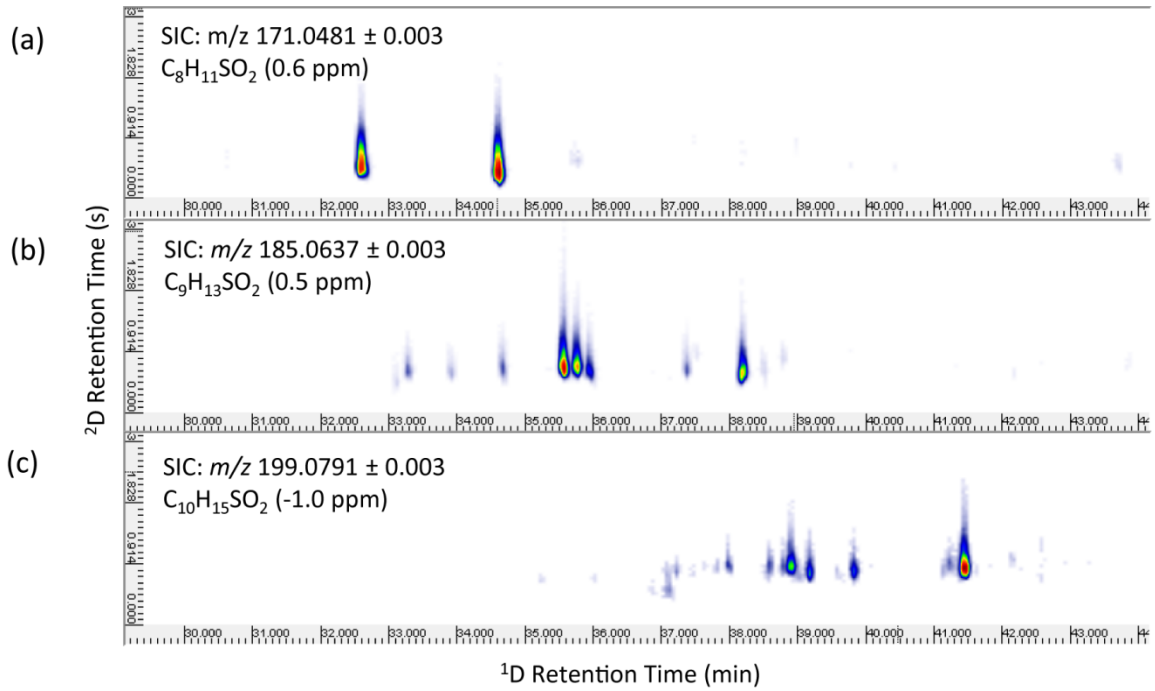

Figure S4. Selected ion chromatograms of NAFCs from the SO_2 class with DBE = 4: (a) $C_8H_{11}SO_2$, (b) $C_9H_{13}SO_2$, and (c) $C_{10}H_{15}SO_2$.

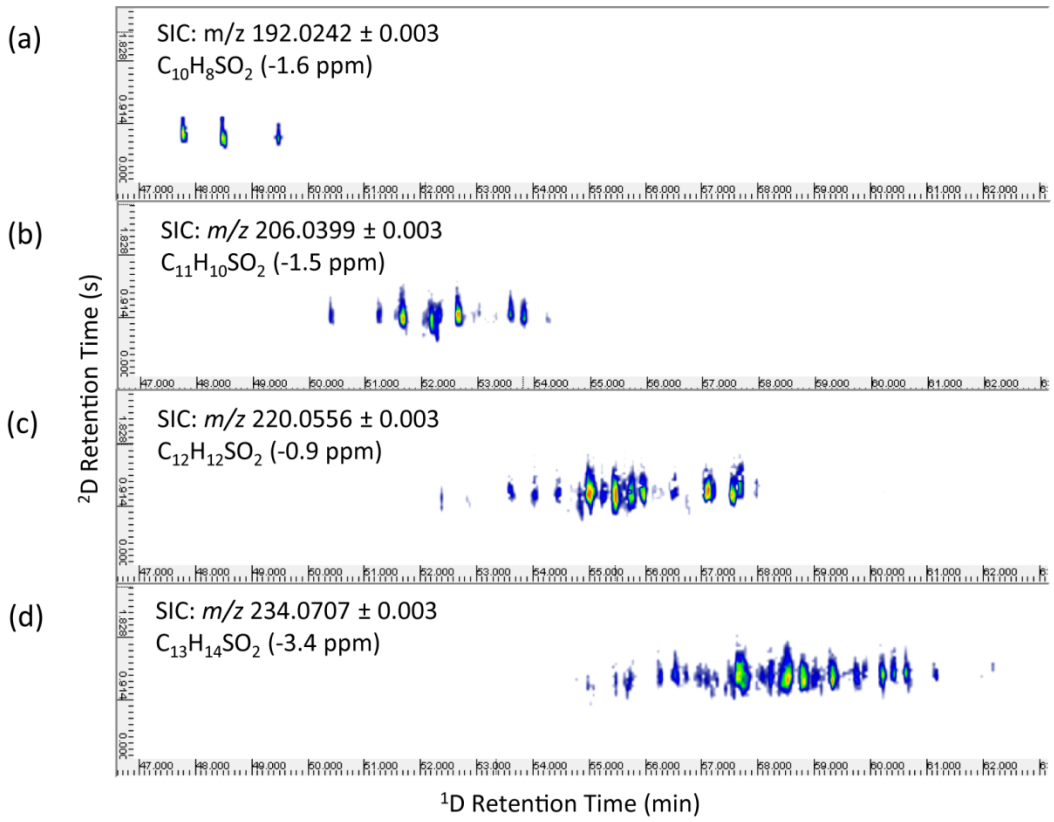

Figure S5. Selected ion chromatograms of NAFCs from the SO_2 class with DBE = 7: (a) $C_{10}H_8SO_2$, (b) $C_{11}H_{10}SO_2$, (c) $C_{12}H_{12}SO_2$, and (d) $C_{13}H_{14}SO_2$.

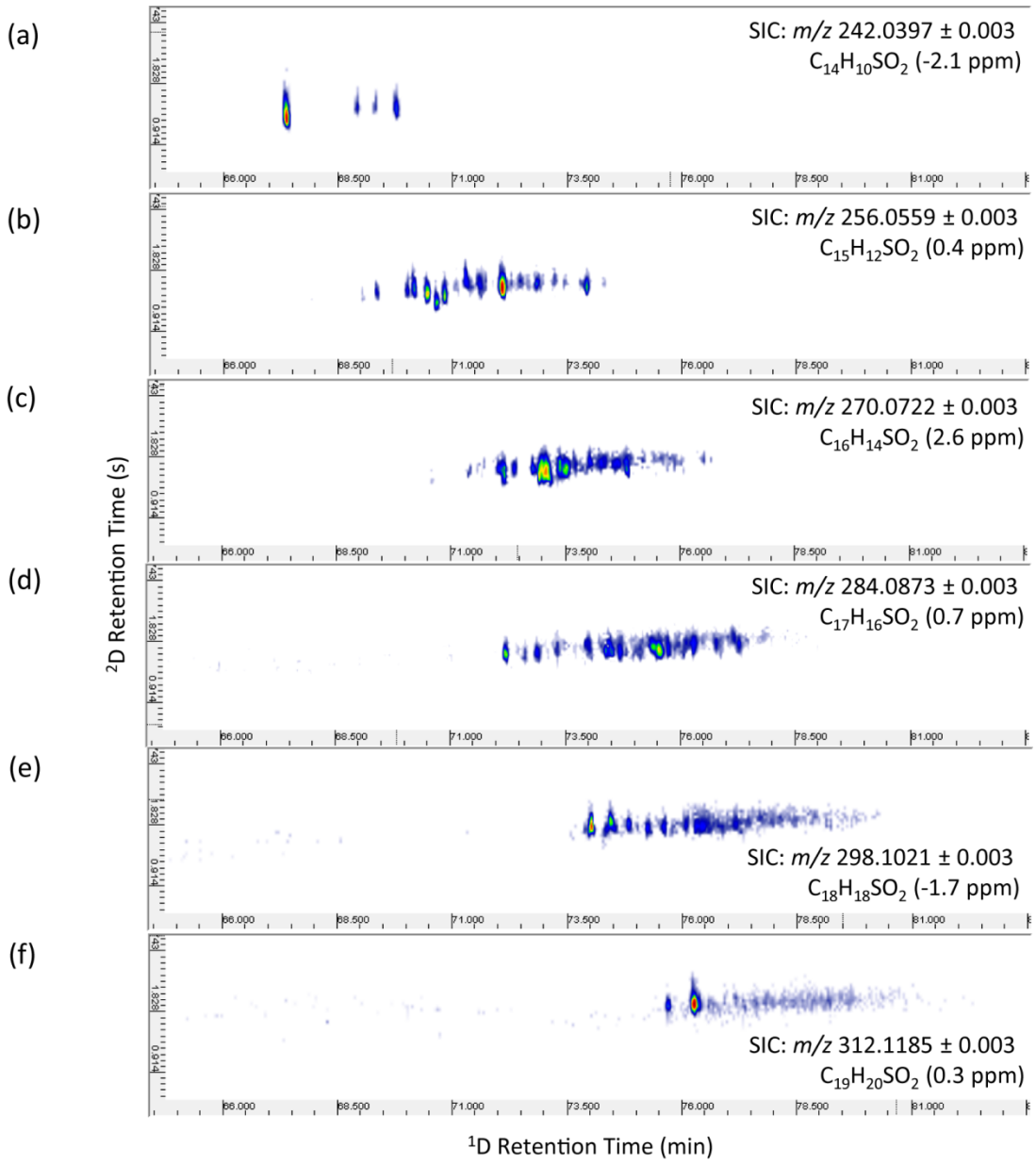

Figure S6: Selected ion chromatograms of NAFCs from the SO_2 class with DBE = 10: (a) $C_{14}H_{10}SO_2$, (b) $C_{15}H_{12}SO_2$, (c) $C_{16}H_{14}SO_2$, and (d) $C_{17}H_{16}SO_2$, (e) $C_{18}H_{18}SO_2$, and (f) $C_{19}H_{20}SO_2$.

Chapter Six: Conclusions and future research

6.1 Summary of research

This dissertation explores the use of multidimensional chromatography mass spectrometry for the chemical fingerprinting of NA mixtures at reclamation sites in the Athabasca oil sands region to improve our understandings of their composition and environmental fate.

Chapter two presents an analytical methodology which utilizes GC×GC/TOFMS (LECO Pegasus 4D) for the analysis of (methylated) naphthenic acids (NAs) from a sand cap pore water sample from Syncrude's Sandhill Fen reclamation site. Multidimensional chromatography significantly improved the chromatographic separation of NAs and facilitated the resolution of diverse isomer distributions. The structured nature of the two-dimensional chromatogram was useful for identifying isomers and alkylated homologues. The structures of resolved NAs were elucidated through interpretation of their electron ionization (EI) mass spectra and, when available, confirmed by comparison with the retention times and mass spectra of reference standards. This study presents the first identification of a sulfur-containing naphthenic acid via the elucidation of the methyl ester derivatives of alkyl-substituted thiophene carboxylic acids. The identification of thiophene-type carboxylic acids is notable since sulfur-containing NAs have been reported as being useful for distinguishing sources of OSPW[1,2], and knowledge of such structures could help improve monitoring programs. In addition, although indane-, tetralin-, and cyclohexane-type carboxylic acids had been previously identified in petroleum and commercial NA mixtures[3,4], this study confirmed for the first time that NAs with the aforementioned structural moieties were also present within an environmental sample derived from the processing of bitumen. In addition, this study also identified the presence of adamantane-type carboxylic acids (observed as methyl esters) within composite tailings pore water, which have been reported as constituents of various OSPW samples.[5–7] In Chapter two, the same method was used to identify a number of bicyclic carboxylic acids and sulfur-containing alicyclic monocyclic carboxylic acids (speculated to possess a thiacyclohexane and/or tetrahydrothiophene chemical moiety) within pore water extracts from the sand cap and CT deposit of Sandhill Fen. These studies were useful for underlining the complexity of NA isomer distributions within pore water from Sandhill fen, and enlarged the inventory of known individual NAs which can be used in future monitoring efforts, or in studies related to the degradation and/or toxicity of individual NAs.

Chapter three explores the application of GC×GC/TOFMS for the monitoring of individual naphthenic acids at Syncrude's Sandhill Fen reclamation site. NA profiles (comprised of the suite of identified NAs) were normalized within each sample to the C_{11} tricyclic NAs

(adamantane-1-carboxylic acid and adamantane-2-carboxylic acid), and the relative abundances of each individual isomer were used to assess the spatial and temporal variabilities at the site. In addition, percentage compositions were calculated for each set of structural isomers, and the variability of the resulting fingerprints were evaluated. In general, significant compositional differences were observed between the four monitoring wells. Fingerprints by percentage compositions were able to distinguish the sand cap from the CT deposit. Moreover, Chapter three revealed that significant temporal differences could be detected by monitoring the changes in the relative abundances of isomers. A subset of NAs from Well 6A underwent significant decreases, which was attributed to the downward movement of freshwater from the fen. The other monitoring wells generally did not display temporal differences, relative to the first sampling date. A number of isomer sets (C_{10}-, and C_{11}- bicyclic NAs; C_{11}-, and C_{12}-tricyclic NAs) displayed consistent relative proportions between the four monitoring wells and could potentially be used as markers for Sandhill Fen.

In Chapter four, the spatial and temporal variabilities of NA profiles were evaluated within the water cap of Syncrude's Base Mine Lake (BML), which is the first demonstration end pit lake in the Athabasca oil sands region (AOSR). Demonstrated for the first time in this study, individual NAs were semi-quantified by external calibration using the closest available reference standard. Total concentrations were calculated for each NA class by summation of all structural isomers, and, in general, very little spatial and temporal variations were detected, even with a turnover event occurring before the last sampling event. In addition, NA profiles from the water cap were compared to profiles within two samples from the FFT; significant compositional differences were observed between the water cap and the FFT, and between the two FFT samples. Evaluations of the concentrations of the individual NAs revealed that the concentration differences were driven by only a few isomers within each isomer series. Subsequent statistical analyses demonstrated that the profiling of individual isomers could reveal additional compositional differences, which were masked by the comparison of total concentrations. As a result, the benefit of the high resolving power of GC×GC/TOFMS is clearly demonstrated, and this study shows that the profiling of individual NAs can provide complementary data to established fingerprinting techniques (such as HPLC/Orbitrap-MS and FTICR-MS), to improve the characterization of NAs within environmental samples.

Chapter five presents the development of a methodology which couples comprehensive two-dimensional gas chromatography to a high resolution quadrupole-time-of-flight mass spectrometer for the characterization of (methylated) naphthenic acid fraction compounds (NAFCs). The combination of multidimensional chromatography and high resolution mass spectrometry was advantageous since it not only allowed the resolution of diverse isomer profiles, but also allowed the distinction of NAFCs from different chemical classes (including chemical species with the C_3 vs SH_4 mass split). Kendrick mass defect (KMD) plots were useful

for providing a global overview of the elemental compositions within NAFC mixtures (assigned based on mass accuracy). KMD plots are expected to improve efforts focused on the identification of 'unknown' NAFCs, and in this study, allowed the identification of a number baseline resolved 'sulfur-containing' NAs.

6.2 Future directions of research

The identifications of individual NAs from Chapter two and three presents a large inventory of NAs with elucidated structures. While the toxicities of classical and aromatic NAs from the O_2 chemical class have been studied previously[8,9], very few studies have investigated the toxicities of sulfur-containing NAs[10], thus demonstrating a gap in the literature. The identification of sulfur-containing NAs can allow future studies to explore the potential acute and chronic effects that sulfur-containing NAs might exert upon aquatic biota, via toxicity testing with reference standards or predicted toxicities via computational studies. Moreover, the elucidation of structures from the SO_2 chemical class provides candidates for potential degradation studies of model compounds. Such studies would provide a glimpse into the susceptibility of sulfur-containing NAs to degradation and would help elucidate degradation pathways, which could be useful for directing strategies for the reclamation of tailings.

Chapters three and four demonstrated the advantages that multidimensional chromatography offers to the monitoring of NAs, and following this work, there are a number of follow-up studies which could be performed to answer site-specific questions at Sandhill Fen and BML. A potential issue at Sandhill fen is the transfer of pore water from the sand cap or CT deposit to the overlying fen. To investigate this, pond water samples from the overlying fen could be analyzed by GC×GC/TOFMS to investigate whether NAs are present in the fen, and whether GC×GC can determine their source. This proposed study would require a more detailed survey of the sand cap wells to further assess spatial variabilities at the site. In addition, surface water samples from nearby creeks, which were used to establish the wetland at Sandhill Fen, would be analyzed to characterize the profiles of background NAs which occur within natural waters. Our preliminary analyses from Sandhill fen revealed that the percentage compositions of isomers from a number of classes (such as C_{11}-, C_{12}-tricyclic NAs, and C_{10}-,C_{11}-bicyclic NAs) were consistent between the four monitoring wells. As a result, such NAs may be useful for the sourcing of NAs from both the CT deposit and the sand cap. In Chapter four, GC×GC/TOFMS analyses provided semi-quantitative concentrations for monocyclic, bicyclic, tricyclic, and thiophene carboxylic acids within the water cap for three sampling campaigns. Follow-up studies should continue to semi-quantify at BML to determine whether concentrations will decrease over time. The primary strategy for the remediation of NAs within end pit lakes is by microbial degradation via indigenous microbial communities, therefore, it would be important to determine whether this process is occurring at the site. Furthermore, since the two FFT samples displayed

high compositional differences, future sampling campaigns should target a range of depths at the site to further investigate the heterogeneity of the FFT deposit. Since the de-watering of FFT is expected to contribute pore water into the water cap, it would be advantageous to understand the composition of such mixtures.

The non-targeted approach of GC×GC/HRMS and mass defect filtering has the potential to significantly enhance the environmental monitoring of not only naphthenic acids, but also other persistent and toxic contaminants. The natural next step would involve applying the GC×GC/QTOF-MS method to further investigate variations at oil sands reclamation sites. Kendrick mass defect plots provide a global overview of the elemental compositions within a GC×GC data set (assigned based on mass accuracy), and conveniently distinguish compounds based on chemical class, carbon number, and DBE. Furthermore, the examination of trends within chemical classes, such as the relative abundances of DBE versus carbon number, may allow the detection of global differences within samples which are not observed by the comparison of single families of isomers. Alternatively, in a similar vein to recent oil sands forensics studies[11,12], GC×GC/QTOF-MS can be used to analyze a number of other sources from the AOSR, such as OSPW samples from tailings ponds (of different oil operators) and bitumen-influenced ground and surface water samples. The comparison of NA isomer distributions, in combination with chemical class histograms and Kendrick mass defect plots, has to potential to significantly improve the characterization of NAs and may provide useful fingerprints for source differentiation. Lastly, Kendrick mass defect plots can simplify data mining and significantly improve efforts focused on the identification of NAs. Collision induced dissociation (CID) experiments can be performed to further probe the structures of compounds within OSPW and related samples. It is possible that in addition to compounds which possess carboxylic acid substituents, there are chemical species within the samples which possess other functional groups. The identities of such compounds are of interest, since they may contribute the overall toxicity and recalcitrance of OSPW and related samples.

References:

(1) Headley, J. V.; Barrow, M. P.; Peru, K. M.; Fahlman, B.; Frank, R. A.; Bickerton, G.; McMaster, M. E.; Parrott, J.; Hewitt, L. M. Preliminary fingerprinting of Athabasca oil sands polar organics in environmental samples using electrospray ionization Fourier transform ion cyclotron resonance mass spectrometry. *Rapid Commun. Mass Spectrom.* **2011**, *25* (13), 1899–1909.

(2) Barrow, M. P.; Peru, K. M.; Headley, J. V. An added dimension: GC atmospheric pressure chemical ionization FTICR MS and the Athabasca oil sands. *Anal. Chem.* **2014**, *86* (16), 8281–8288.

(3) Rowland, S. J.; West, C. E.; Scarlett, a. G.; Jones, D.; Boberek, M.; Pan, L.; Ng, M.; Kwong, L.; Tonkin, a. Monocyclic and monoaromatic naphthenic acids: Synthesis and characterisation. *Environ. Chem. Lett.* **2011**, *9* (4), 525–533.

(4) West, C. E.; Pureveen, J.; Scarlett, A. G.; Lengger, S. K.; Wilde, M. J.; Korndorffer, F.; Tegelaar, E. W.; Rowland, S. J. Can two-dimensional gas chromatography/mass spectrometric identification of bicyclic aromatic acids in petroleum fractions help to reveal further details of aromatic hydrocarbon biotransformation pathways? *Rapid Commun. Mass Spectrom.* **2014**, *28* (9), 1023–1032.

(5) Rowland, S. J.; Scarlett, A. G.; Jones, D.; West, C. E.; Frank, R. a. Diamonds in the rough: Identification of individual naphthenic acids in oil sands process water. *Environ. Sci. Technol.* **2011**, *45* (7), 3154–3159.

(6) Rowland, S. J.; West, C. E.; Scarlett, A. G.; Ho, C.; Jones, D. Differentiation of two industrial oil sands process-affected waters by two-dimensional gas chromatography/mass spectrometry of diamondoid acid profiles. *Rapid Commun. Mass Spectrom.* **2012**, *26* (5), 572–576.

(7) Lengger, S. K.; Scarlett, A. G.; West, C. E.; Frank, R. A.; Hewitt, L. M.; Milestone, C. B.; Rowland, S. J. Use of the distributions of adamantane acids to profile short-term temporal and pond-scale spatial variations in the composition of oil sands process-affected waters. *Environ. Sci. Process. Impacts* **2015**, *17* (8), 1415–1423.

(8) Scarlett, A. G.; West, C. E.; Jones, D.; Galloway, T. S.; Rowland, S. J. Predicted toxicity of naphthenic acids present in oil sands process-affected waters to a range of environmental and human endpoints. *Sci. Total Environ.* **2012**, *425*, 119–127.

(9) Jones, D.; Scarlett, A. G.; West, C. E.; Rowland, S. J. Toxicity of individual naphthenic acids to Vibrio fischeri. *Environ. Sci. Technol.* **2011**, *45* (22), 9776–9782.

(10) West, C. E.; Scarlett, A. G.; Tonkin, A.; O'Carroll-Fitzpatrick, D.; Pureveen, J.; Tegelaar, E.; Gieleciak, R.; Hager, D.; Petersen, K.; Tollefsen, K.-E.; et al. Diaromatic sulphur-containing "naphthenic" acids in process waters. *Water Res.* **2014**, *51*, 206–215.

(11) Frank, R. A.; Roy, J. W.; Bickerton, G.; Rowland, S. J.; Headley, J. V.; Scarlett, A. G.; West, C. E.; Peru, K. M.; Parrott, J. L.; Conly, F. M.; et al. Profiling oil sands mixtures from industrial developments and natural groundwaters for source identification. *Environ. Sci. Technol.* **2014**, *48* (5), 2660–2670.

(12) Ross, M. S.; Pereira, A. dos S.; Fennell, J.; Davies, M.; Johnson, J.; Sliva, L.; Martin, J. W. Quantitative and qualitative analysis of naphthenic acids in natural waters surrounding the Canadian oil sands industry. *Environ. Sci. Technol.* **2012**, *46* (23), 12796–12805.